An investigation into the function of SUMOylation of Nse2 and PCNA in *S. pombe*

Lauren Small

2014

A thesis submitted for the degree of Doctor of Philosophy at the University of Sussex

Candidates declaration

I declare that this thesis has not been and will not be submitted in whole or in part to another University for the award of any other degree. The work described is my own work except where otherwise stated.

Signed: 

Date: 12/12/2014

Acknowledgements

I would like to thank Felicity Watts for the opportunity to work in her lab, for teaching me and for providing so much helpful feedback.

Thanks to all members of the Watts lab past and present, including Mai and Robbie and particularly Brenda, who was a huge help and support whilst she was in the lab, and has continued to be a friend throughout my PhD. I would also like to thank all of the members of the GDSC who have given me help and advice over the years. Particularly in the last couple of years Sarah, Suzi, Catrina, Dom and Pete, who have been great company and great friends.

Special thanks goes to my family and friends for their constant love and support and for keeping me smiling over the years! In particular my mum Janet has provided unwavering friendship, love and support in every form not only throughout my PhD but for my whole life and I can't thank her enough, she is an inspiration to me.

Finally I'd like to thank Joe, without whom I absolutely wouldn't have got this far. Your love and support, encouragement and belief in me has been invaluable. You gave me the confidence to get this far and to follow my heart to the next chapter of my career and our lives.

I have been incredibly lucky to have such amazing friends and family to support me and share this journey with.

University of Sussex

Lauren Small

An investigation into the function of SUMOylation of Nse2 and PCNA in *S. pombe*

SUMMARY

Small ubiquitin like modifier (SUMO) is post-translationally attached to target proteins, forming a covalent bond between its C-terminal glycine and one or more lysine residues on the target protein. SUMO modification of target proteins can affect protein-protein interactions, protein activity, localisation and stability. This study set out to develop an efficient *in vitro* SUMOylation system to enable the identification of target lysine residues in *S. pombe* proteins by mass spectrometry. This involved incorporating a trypsin cleavage site adjacent to the SUMO di-glycine motif to improve peptide coverage during mass spectrometry. Several SUMOylated target proteins were identified here, including the E2 SUMO conjugating enzyme Hus5, the E3 SUMO ligase Nse2 and PCNA.

The second part of this study focused on the characterisation of unSUMOylatable E3 SUMO ligase *nse2* mutants. Integration of lysine to arginine mutations into the genome did not result in any mutant phenotypes and a function for auto-SUMOylation of Nse2 was not identified. During this study, human patients with mutations in the *nse2* gene were reported and the equivalent mutations were integrated into the *S. pombe nse2* gene to investigate the effect of the mutations.

The final part of this work involved the analysis of the SUMOylation of *S. pombe* PCNA. Using the *in vitro* system, four target lysine residues for SUMO were identified. SUMOylation of PCNA was also observed *in vivo* following pull-down studies and 2D gel analysis of wild type and unSUMOylatable mutants. Extensive epistasis analysis was undertaken using these mutants to investigate the role of SUMOylation of *S. pombe* PCNA.

Aims

The aim of the work in this thesis was primarily to develop an efficient *in vitro* system to identify modified lysine residues on SUMO target proteins using mass spectrometry. The subsequent aims were firstly, to identify the modified lysine residues in the Smc5/6-associated SUMO ligase Nse2 and the trimeric sliding clamp PCNA and secondly, to analyse the role of SUMOylation in each case.

ABBREVIATIONS

A	Alanine
Ade	Adenine
APS	Ammonium persulphate
ATP	Adenosine triphosphate
AMP	Adenosine monophosphate
BER	Base excision repair
bp	Base pair
BSA	Bovine serum albumin
CDK	Cyclin-dependent kinase
CPD	Cyclobutane pyrimidine dimer
CPT	Camptothesin
CPK	Creatine phosphokinase
Cre	Cre recombinase
Da	Dalton
DAPI	4, 6-amino-2-phenylindole
DMSO	Dimethylsulphoxide
DNA	Deoxyribonucleic acid
dNTP	Deoxyribonucleotide triphosphate
DSB	Double strand break
DTT	Dithiothreitol
E. coli	Escherichia coli
ECL	Enhanced chemi-luminescence
EDTA	Ethylenediaminetetraacetic acid
ELN	Extremely low nitrogen
g	Gram
G418	Geneticin
Gy	Gray
HR	Homologous recombination
H. s	*Homo sapiens*
HU	Hydroxyurea
IPTG	Isopropyl-β-D- thiogalactopyranoside
IR	Ionizing Radiation
J/m^2	Joules per meter squared
K	Lysine

kb	Kilobase
kDa	Kilodalton
l	Litre
leu	Leucine
LiOAc	Lithium acetate
M	Molar
MCS	Multiple cloning site
ml	Milliliter
MMS	Methylmethane-sulphonate
MS	Mass spectrometry
µg	Microgram
µl	Microlitre
µM	Micromolar
NAT	Nourseothricin sulfate
NER	Nucleotide excision repair
NHEJ	Non-homologous end joining
OD	Optical density
ORF	Open reading frame
PBS	Phosphate buffered saline
PCR	Polymerase chain reaction
PEG	Polyethylene glycol
PIP	PCNA interacting protein
PMSF	Phenylmethylsulphonyl fluoride
Pol	Polymerase
PRR	Post Replicative Repair
R	Arginine
RPM	Revolutions per minute
S. cerevisiae	*Saccharomyces cerevisiae*
SDS-PAGE	Sodium dodecyl sulphate polyacrylamide gel electrophoresis
SIM	SUMO interacting motif
TBE	Tris borate
TCA	Trichloroacetic acid
TE	Tris aminomethane
TEMED	N, N, N', N'-tetramethyl-ethylenediamine
Ura	Uracil
UV	Ultra-violet

UVER	UV-excision repair
YE	Yeast extract
YEA	Yeast extract plus agar
YNB	Yeast nitrogen base
X-gal	5-bromo-4-chloro-3-indol-β-D galactopyranoside

Contents

List of Figures

List of tables

1 Introduction

The maintenance of genome stability by successful replication of DNA and repair of damage is necessary for the life of all organisms. DNA damage can accumulate from both endogenous and exogenous sources, and can result in DNA modifications, replication fork stalling and DNA strand breaks. Successful repair of this damage by highly regulated DNA damage response pathways is critical to maintain cell viability. Errors in replication and repair can result in insertions, deletions and mis-paired nucleotide bases. If these errors are not repaired efficiently, the permanent integration of mutations into the genome can result in genomic instability, unregulated cell growth or cell death.

1.1 *S. pombe* as a model organism

The fission yeast *S. pombe* is widely used as a model organism for studying the cell cycle, DNA replication and repair. It is a unicellular eukaryote and proliferates with a doubling time of approximately 2.5 hours. Cells are uniformly rod shaped, growth extends from the tips and cells divide by medial fission. *S. pombe* has three chromosomes and exists as a haploid. The sequence of the *S. pombe* genome was published in 2002 (Wood et al. 2002), and this facilitates genetic manipulation to allow processes such as the creation of strains with gene deletions, or integration of mutant alleles. Biochemical and genetic techniques can be readily undertaken to investigate the effects of mutations or gene deletions at the molecular level, as well on the organism as a whole. The conservation of cell cycle control as well as DNA replication and repair pathways between yeast and mammals make *S. pombe* a favourable model organism for biochemical and genetic analysis. The organism has been used in landmark studies that have important implications for understanding processes in higher eukaryotes. For example, the identification of *cdc* genes in the Nurse lab and the observation of their functional conservation between yeast and humans (Nurse et al, 1976). The Nobel prize winning work of Paul Nurse, Lee Hartwell and Tim Hunt using *S. pombe*, *S. cerevisiae* and sea urchins respectively, demonstrates the importance of model organisms in discovering the basis of fundamental systems such as cell cycle control. More recently, DNA

damage response genes have also been described to be modified by SUMO. (Albuquerque et al, 2013; Cremona et al, 2012; Dou et al, 2010) *S. pombe* is used in this study to investigate the role of SUMOylation in DNA damage repair.

1.2 Ubiquitin

Ubiquitin is a post-translational modifier protein which is very highly conserved from yeast to humans. It is a small, stable protein of approximately 10kDa in size. Structurally, ubiquitin forms a ββαββαβ fold, and has a flexible, unstructured C-terminal tail (Vijay-Kumar et al, 1987). It is attached to target proteins via an isopeptide bond which is formed between its C-terminal glycine residue and a lysine residue on the target protein. Ubiquitination occurs following a three step ATP-dependent conjugation pathway which requires specific E1 ubiquitin activating enzymes, E2 ubiquitin conjugating enzymes and E3 ligases. Whilst only two E1 ubiquitin activating enzymes have been identified in mammals, over 50 E2 ubiquitin conjugating enzymes and hundreds of E3 ubiquitin ligases have been identified, and these provide substrate specificity (Komander & Rape, 2012).

1.2.1 The ubiquitin conjugation pathway

Before entering the conjugation pathway, precursor ubiquitin needs to be cleaved at the C-terminus by specific de-ubiquitinating enzymes (DUBs) called ubiquitin C-terminal hydrolases (UCHs) (Larsen et al, 1998). This exposes two glycine residues, of which the C-terminal glycine is covalently attached to substrate proteins. In an ATP-dependent reaction, the E1 activating enzyme adenylates the C-terminus of ubiquitin, before a thioester bond is formed between the C-terminal carboxyl group of ubiquitin and the catalytic cysteine residue of the E1 activating enzyme. Ubiquitin is then passed to the E2 conjugating enzyme, where again it forms a thioester bond between ubiquitin and the catalytic cysteine residue (Haas & Rose, 1982). Ubiquitin can then be transferred directly to a target protein where an isopeptide linkage is formed between the C-terminal glycine residue and the ε-amine group of a lysine residue on the target protein. E3 ubiquitin ligases are recruited to facilitate the transfer of ubiquitin to the target protein. Ubiquitination is a reversible

modification and ubiquitin can be removed by one of a number of DUBs, some of which are linkage specific (Komander & Rape, 2012).

1.2.2 Ubiquitin chains

Ubiquitin can be attached to target proteins in the form of monomers or poly-ubiquitin chains. Different types of chains can be formed, depending on which lysine residue within ubiquitin is used. The most commonly studied ubiquitin chains contain K48-linked chains. These target the modified protein for degradation mediated by the 26S proteasome (Chau et al, 1989; Thrower et al, 2000), as do K11-linked ubiquitin chains, which have a specific confirmation and are particularly prevalent during mitosis (Jin et al, 2008; Matsumoto et al, 2010a; Matsumoto et al, 2010b). K6- K27- K29- and K33-linked ubiquitin chains have been detected *in vivo* (Meierhofer et al, 2008; Peng et al, 2003), however due to a lack of identification of specific E2 or target proteins for these linkages, their roles have yet to be determined (Komander & Rape, 2012). The primary role of ubiquitin chains formed using K63 is not to target proteins for degradation, but to alter protein-protein interactions (Deshaies & Joazeiro, 2009; Komander & Rape, 2012). Mixed ubiquitin chains have also been observed, which result in proteasomal degradation of the target protein (Kirkpatrick et al, 2006). Branched ubiquitin chain structures are formed when two different lysine residues are used to extend a chain from the same molecule, however the function of these structures has yet to be described. Ubiquitin chains are recognised by proteins containing ubiquitin-binding domains (UBD), which can include multiple ubiquitin interacting motifs (UIMs) (Komander, 2009). UIM-containing proteins are able to distinguish between K48-linked chains, which have a closed conformation (Eddins et al, 2007; Tenno et al, 2004; Varadan et al, 2002) and K63-linked ubiquitin chains, which have an open and flexible conformation (Datta et al, 2009; Komander et al, 2009; Weeks et al, 2009).

1.2.3 Ubiquitin targets

As well as targeting proteins for degradation, ubiquitination can serve as a regulator of protein activity and is involved in co-ordinating several important

DNA repair processes. One of the ways by which ubiquitin can regulate protein activity is by targeting inhibitor proteins for degradation. A well-documented example of this is the regulation of the mammalian transcription factor NF-κB, which is required for the inflammatory response (Hayden & Ghosh, 2008). NF-κB is bound by its inhibitor IκBα (inhibitor of NF-κB) under normal conditions. Poly-ubiquitination of IκBα with K48-linked ubiquitin chains targets it for proteasomal degradation. This releases NF-κB, allowing transcription of its target genes (Iwai, 2014).

Ubiquitination can affect the cellular localisation of its target proteins. For example mono-ubiquitination of the transcription factor p53 signals its export from the nucleus, and this can be reversed by de-ubiquitinating enzyme USP10 in human cells (Yuan et al, 2010). p53 is also poly-ubiquitinated, which targets it for degradation. p53 modification ensures that it is maintained at low levels in unchallenged cells. Detection of DNA damage results in the inhibition of the ubiquitin E3 ligase responsible for p53 ubiquitination. This prevents degradation of p53, which can then promote the transcription of DNA repair genes, as well as genes required for checkpoint arrest or apoptosis (Brooks & Gu, 2011; Hock et al, 2011). Ubiquitination can also regulate protein-protein interactions. This is demonstrated by its important role in PCNA modification, which defines which pathway is taken during Post Replicative Repair (PRR) (see section 1.8.2).

1.3 SUMO

The Small ubiquitin like modifier SUMO is covalently attached to target proteins following a conjugation pathway similar to that of the ubiquitination pathway (described in section 1.3.1). The structure of SUMO closely resembles that of ubiquitin, despite the low sequence homology between the proteins (~18%), except for an extended and unstructured N-terminus which is unique to SUMO (Bayer, 1998). SUMO is highly conserved and is expressed in all eukaryotes studied. It was initially identified in *S. cerevisiae* (Meluh & Koshland, 1995) where it is encoded by the *SMT3* gene. In *S. pombe*, as in budding yeast, *Drosophila* and *C. elegans*, SUMO is encoded by a single gene. In *S. pombe*, SUMO is encoded by the *pmt3* gene (Tanaka et al, 1999). Higher eukaryotes including

humans and plants contain several SUMO genes. (Kurepa et al, 2003; Lois et al, 2003). Four SUMO proteins, SUMO-1 to 4 have been described in humans (Guo, 2004; Melchior, 2000). SUMO-2 and SUMO-3 share significant sequence homology (~95%) and are referred to as SUMO-2/3 as it is difficult to separate their function (Saitoh & Hinchey, 2000; Su & Li, 2002; Vertegaal et al, 2006a). SUMO-4 is not ubiquitously expressed and mutant isoforms have been implicated in type 1 diabetes (Guo, 2004), however its role remains largely elusive.

Disruption or deletion of SUMO in organisms which carry a single SUMO gene results in lethality. The exception to this is the *pmt3-d* null mutant in *S. pombe*, which is extremely sick and displays significant sensitivity to several stresses and toxins (Tanaka et al, 1999). SUMO pathway mutants cause defects in chromosome structure and segregation in several organisms, including *S. pombe* (al-Khodairy et al, 1995; Tanaka et al, 1999; Xhemalce et al, 2004a), *S. cerevisiae* (Strunnikov et al, 2001) and *Drosophila* (Hari et al, 2001). Disruption or deletion of SUMO in higher eukaryotes results in developmental defects including cleft lip and pallet formation. This has been observed for a haplo-insufficient patient, as well as heterozygous mice (Alkuraya et al, 2006). Embryonic lethality of mice is observed in response to disruption of the SUMOylation pathway, with cells displaying aberrant nuclear envelope structures and defects in chromosome condensation (Nacerddine, 2005).

1.3.1 The SUMO conjugation pathway

As is the case with ubiquitin, SUMO is produced as a precursor protein which requires proteolytic processing into a mature form. Unlike ubiquitin however, there is only one E1 SUMO activating enzyme, one E2 SUMO conjugating enzyme and two E3 SUMO ligases currently identified in *S. pombe* (See Figure 1.1 B). SUMO is activated by the formation of a thioester bond between its C-terminal glycine residue and a subunit of the E1 SUMO activating enzyme which is a heterodimer comprising Rad31 and Fub2. It is then transferred to the E2 SUMO conjugating enzyme Ubc9/Hus5, which can facilitate attachment to target proteins in the presence or absence of a SUMO E3 ligase. Several SUMO moieties can be conjugated to a target protein to form SUMO chains, the role of which is

discussed in section 1.3.2. A cartoon representation of the SUMO conjugation pathway can be seen in Figure 1.1 (A).

1.3.1.1 SUMO proteases

S. pombe and *S. cerevisiae* contain two SUMO proteases, Ulp1 and Ulp2, both of which are able to remove SUMO from target proteins. Ulp1 is localised at the nuclear pore complex (NPC) and is primarily responsible for the processing of mature SUMO, as demonstrated by an accumulation of unconjugated SUMO in *ulp1* null *S. pombe* cells (Li, 1999; Taylor et al, 2002). Ulp2 is localised within the nucleus and is thought to have a major role in the de-conjugation of SUMO and SUMO chains from nuclear proteins. This is supported by an accumulation of SUMO chains in the *S. cerevisiae ulp2-d* mutant (Bylebyl et al, 2003). SUMO processing and de-conjugation is carried out by sentrin-specific proteases (SENPs) in humans. Six SENPs have so far been characterised in humans, of which SENP1, 2, 3 and 5 have C-terminal domains which are related to Ulp1. SENP6 and 7 have C-terminal domains related to Ulp2. The N-terminal domains of SENPs determine their cellular localisation (Hay, 2007).

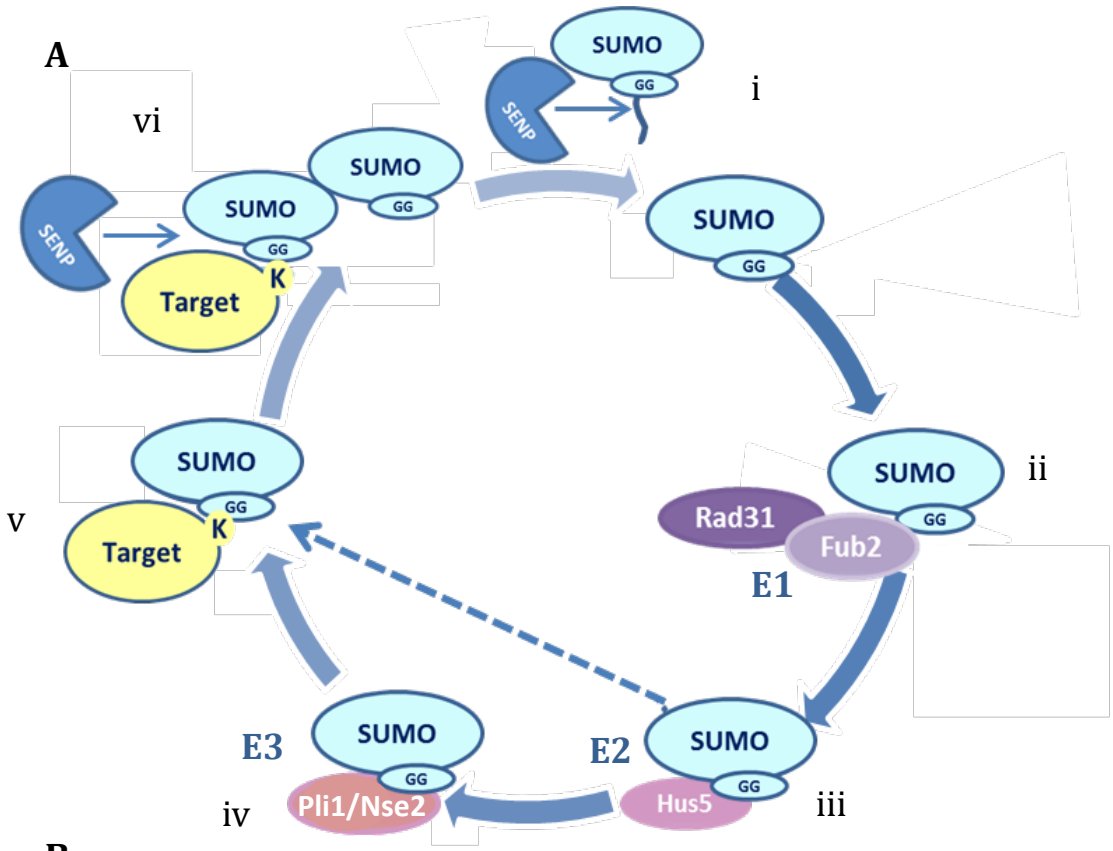

Species	SUMO	E1	E2	E3
S.p	*pmt3*	*rad31-fub2*	*hus5*	*nse2, pli1*
S.c	*SMT3*	*AOS1-UBA2*	*UBC9*	*SIZ1, SIZ2, MMS21* (*S.p. nse2*), *ZIP3*
H.s	*SUMO-1* *SUMO-2* *SUMO-3* *SUMO-4*	*AOS1-UBA2*	*UBC9*	*MMS21, PIAS-1-4, PC2, RANBP2, HDAC4, TOPORS, KAP1*

Figure 1.1 The SUMO conjugation pathway.

(A) i) SUMO is cleaved by proteases to reveal the C-terminal di-glycine motif. ii) A thioester bond is formed between the SUMO C-terminus and the E1 activating enzyme. iii) SUMO is transferred to the E2 conjugating enzyme which can facilitate its attachment to a specific lysine residue on the target protein. iv) In some cases an E3 ligase is required. v) SUMO can be attached to target proteins as a monomer or in the form polySUMO chains, which are detected by STUbls and subsequently targeted for degradation by the proteasome. vi) SUMO specific proteases remove SUMO from the target protein. (B) Genes encoding SUMO pathway components in *S.pombe* (*S.p*) *S.cerevisiae* (*S.c*) and humans (*H.s*).

1.3.1.2 E1 SUMO activating enzyme

The SUMO E1 activating enzyme exists as a heterodimer and was first identified in *S. cerevisiae* as Aos1/Uba2 (Johnson et al, 1997) The *S. pombe* SUMO E1 heterodimer is formed of Rad31, which was identified in a screen of radiation sensitive mutants, and Fub2 (Ho et al, 2001; Shayeghi et al, 1997; Tanaka et al, 1999). The N-terminal domain of Rad31 and the C-terminal domain of Fub2 together resemble the ubiquitin E1 monomer (Johnson et al, 1997). The E1 activating enzyme facilitates the formation of a thioester bond between the C-terminal SUMO glycine residue and a cysteine in the Fub2 subunit, in an ATP-dependent reaction. The C-terminal glycine residue is first adenylated. This results in a conformational change bringing the conserved catalytic cysteine of the E1 closer to SUMO, which then attacks the adenylated intermediate and releases AMP forming a thioester bond (Schulman & Wade Harper, 2009). Thioester bond formation causes a conformational change which results in the rotation of the E1 catalytic cysteine domain away from the thioester catalytic site, reforming the adenylation active site (Olsen et al, 2010). The E1-bound SUMO is next transferred to the E2 SUMO conjugator.

1.3.1.3 E2 SUMO conjugating enzyme

The *S. pombe* E2 SUMO conjugating enzyme Ubc9/Hus5 was identified in a screen aimed at identifying checkpoint proteins (al-Khodairy et al, 1995; Ho et al, 2001). Studies into the *S. cerevisiae* and human homologue Ubc9 demonstrated that SUMO is transferred from the E1 activating enzyme to form a thioester bond with the catalytic cysteine residue of the E2 (Desterro, 1997; Johnson & Blobel, 1997; Schwarz et al, 1998). This transfer requires an interaction between the catalytic domains of the E1 and E2 proteins (Wang et al, 2007). Ubc9/Hus5 is able to facilitate the attachment of SUMO to the ε-amine group of a lysine residue on target proteins without the aid of an E3 SUMO ligase. SUMO modification of target proteins can occur at lysine residues that are part of a SUMO consensus motif. This consensus sequence is defined as ΨKxE, where Ψ is a large hydrophobic amino acid e.g. I, V or L, and x can be any amino acid. This sequence is present in some but not all target proteins (Hay, 2005; Rodriguez et al, 2001).

The non-covalent interactions of Ubc9/Hus5 have been the subject of several studies in recent years and are suggested to be involved in the regulation of SUMOylation. Non-covalent interactions between Ubc9 and a SUMO-like domain (SLD) in Rad60 have been proposed to play a role in promoting the modification of proteins involved in DNA repair, facilitated by the E3 ligase Nse2. Conversely, non-covalent interactions between Hus5 and SUMO are suggested to promote global SUMOylation, facilitated by the E3 SUMO ligase Pli1 (Prudden et al, 2011).

1.3.1.4 E3 SUMO ligases

E3 SUMO ligases facilitate the transfer of SUMO from the E2 conjugating enzyme to a specific lysine residue on target protein which may or may not be part of the SUMO consensus sequence described above. Several E3 SUMO ligases have been identified and these are classified into three groups, the largest of which is the SP-RING class of SUMO ligases. The SP-RING motif is similar to a motif found in some ubiquitin E3 ligases and is essential for ligase function (Hochstrasser, 2001). SP-RING ligases are able to interact with the E2 conjugating enzyme, as well as SUMO, via SUMO interacting motifs (SIMs). SIMs consist of a hydrophobic core flanked by acidic residues. The binding of the acidic residues to a basic area on the surface of SUMO positions the ligase for efficient transfer of SUMO to target proteins (Hannich et al, 2005; Minty et al, 2000; Reverter & Lima, 2005; Song et al, 2004).

SP-RING proteins include the PIAS (protein inhibitor of activated STAT) subgroup. Included in the PIAS family are *S. cerevisiae* Siz1 and Siz2 (Hochstrasser, 2001) as well as five mammalian proteins, PIAS1, PIAS3 and three PIAS variant proteins. PIAS proteins are able to interact with DNA via a SAR, Acinus and PIAS (SAP) motif, as well as with SUMO via SIMs (Rytinki et al, 2009). SP-RING proteins Nse2 and Pli1 are the only two SUMO ligases identified to date in *S. pombe*. Cells deficient in the Pli1 ligase do not display a severe mutant phenotype. However, deletion of *pli1* results in sensitivity to the microtubule inhibitor TBZ, as well as elevated levels of mini-chromosome loss, suggesting a role in kinetochore function (Xhemalce et al, 2004a). Synthetic lethality is observed in *pli-d* cells in combination with homologous

recombination mutants, and a loss of Pli1 also affects telomere length, demonstrating roles for Pli1-dependent SUMOylation in recombination and genome stability (Xhemalce et al, 2004a). Nse2 is associated with the Smc5/6 complex and is important for genome stability. This will be discussed further in section 1.7.1.1

The second class of SUMO ligase includes RanBP2, which is part of the nuclear pore complex. RanBP2 does not contain a RING finger-like domain and interacts with the SUMO E2 conjugating enzyme Ubc9 at a surface distinct from the catalytic site (Tatham et al, 2005). It associates with the SUMO E2 via an unfolded catalytic site, positioning SUMO to facilitate its attachment to its target protein, RanGAP1 (Pichler et al, 2002).

The third E3 ligase classified is human Pc2 (Kagey et al, 2003), which promotes SUMOylation and transport of CtBP (C terminal binding protein) to the nucleus (Lin et al, 2003), as well as co-localisation of CtBP to PcG bodies (Kagey et al, 2003).

1.3.1.5 SUMO chains

Human SUMO-2 and SUMO-3 contain the ΨKxE consensus sequence in the extended N-terminus, as does the *S. cerevisiae* homologue SMT3. Poly-SUMO chains are formed by covalent attachment of SUMO to lysine residues within this motif. SUMO-1 shares only 50% sequence homology with SUMO-2/3 and lacks the N-terminal consensus sequence which is required for SUMO chain formation (Tatham et al, 2001). Thus, SUMO-1 likely acts as a chain terminator (Matic et al, 2008). Proteomic screens have revealed that SUMO-1 and SUMO-2/3 conjugate to both separate and overlapping subsets of target proteins, indicating that the different isoforms have distinct as well as overlapping functions (Vertegaal et al, 2006b). K11- and K15- linked SUMO chains have been observed in humans and *S. cerevisiae,* respectively (Bencsath et al, 2002; Tatham et al, 2001).

S. pombe SUMO does not contain an N-terminal SUMO consensus motif. However poly-SUMO chains are formed via two N-terminal lysine residues at positions 14 and 30 (Skilton et al, 2009). SUMO chain formation is implicated in

several processes involving DNA damage repair, chromatin regulation and replication stress (Srikumar et al, 2013; Ulrich, 2008).

SUMO targeted ubiquitin ligases (STUbLs) contain single or multiple SIMs which recognise SUMO chains and target poly-SUMOylated proteins for proteasome-mediated degradation. Mutation of STUbLs results in an accumulation of high molecular weight SUMO species, and sensitivity to DNA damage (Sriramachandran & Dohmen, 2014). Rnf4 is the best characterised STUbL in human cells. It is a RING finger protein and recognises SUMO chains via several SIMs (Tatham et al, 2008). In particular, Rnf4 recognises poly-SUMOylated PML and ubiquitinates the PML protein as well as the poly-SUMO chains attached to it, targeting PML for proteasomal degradation (Tatham et al, 2008). *S. pombe* Rfp1 and Rfp2 share sequence homology with Rnf4 and also contain RING finger domains. Both of these proteins form a complex with Slx8 and act to label poly-SUMOylated targets for ubiquitin-mediated proteasomal degradation. Rfp1 was shown to interact with E3 SUMO ligase Pli1 and Rad60 in yeast two hybrid screens (Sun et al, 2007). Recent research has suggested that Slx8 is required for the removal of potentially harmful Top1 cleavage complexes in the absence of Tdp1 (Heideker et al, 2011; Steinacher et al, 2013). STUbL complexes are important in maintaining genome stability, as demonstrated by the presence of Rad52 foci in cells containing Slx8 temperature sensitive mutant alleles (Prudden et al, 2007).

1.3.2 The role of SUMO modification

Post-translational modification of proteins by SUMO (SUMOylation) has been observed to affect several important cellular processes including regulation of the cell cycle, chromosome segregation, transcription and the DNA damage response. At the molecular level SUMO modification affects protein-protein interactions, cellular localisation and protein-DNA interactions (Johnson, 2004). RanGAP1 was the first protein reported to be covalently modified by SUMO-1. Rather than targeting proteins for degradation, the consequence of this reversible SUMO modification is cellular re-localisation. SUMOylation of RanGAP1 results in its transport from the cytoplasm to the nuclear pore

complex, as well as enhancing its interaction with RanBP2 (M J Matunis, 1996; Mahajan et al, 1997).

Many DNA repair proteins are SUMOylated, and this can affect the activity, substrate specificity and recruitment of the target protein. An example of this is the E3 ubiquitin ligase BRCA1 (breast cancer 1, early onset), which is a SRUbL. In human cells, BRCA1 and 53BP1 (tumor protein p53 binding protein 1) are SUMOylated at sites of DNA damage, mediated by the E3 SUMO ligases PIAS1 and PIAS4 (Galanty et al, 2009; Morris et al, 2009). SUMOylation enhances BRCA1's E3 ubiquitin ligase activity towards histones H2A and H2AX (Morris et al, 2009), and the recruitment of BRCA1 to DNA damage sites is decreased in the absence of PIAS1 or PIAS4 (Galanty et al, 2009).

SUMOylation can also regulate target proteins by inducing conformational changes which affect their activity. For example the activity of the base excision repair (BER) factor thymidine DNA glycosylase (TDG) is regulated by SUMOylation. TDG binds to the abasic site (AP) which is formed following the excision of an incorrectly inserted nucleotide with high affinity, protecting the DNA ends from being converted into double strand breaks (DSBs) before the recruitment of endonucleases (Hardeland et al, 2002). SUMOylation of AP-bound TDG causes a conformational change which decreases the affinity of TDG for the AP site and results in its dissociation from the DNA. SUMO proteases subsequently remove the SUMO modification, recycling TDG for further rounds of BER (Hardeland et al, 2002).

SUMO and ubiquitin modification of the same protein is being increasingly observed and can have opposing effects, acting as a switch between different pathways. For example, whilst ubiquitination of IκBα promotes its degradation and the subsequent activation of NF-κB as mentioned above, SUMOylation of IκBα stabilises the protein, acting in contrast to ubiquitin and inhibiting NF-κB (Desterro et al, 1998). Another example of cross-talk between ubiquitin and SUMO is the modification of PCNA by both PTM's, which occurs on the same lysine residue (See section 1.8.2-1.8.3).

1.4 *S. pombe* cell cycle

The cell cycle is a highly regulated process involving DNA replication and cell division and is essential for proliferation. Four phases make up the cell cycle, G1, S, G2 and M. Entrance into and progression through the cell cycle is a highly ordered and regulated process governed by the accumulation and inhibition of sequential cyclin-Cdk (cyclin- dependent kinase) complexes. Cdk proteins are expressed constitutively and are present at constant concentrations throughout the cell cycle. The *cdc2* gene encodes the Cdk protein, Cdc2 (equivalent to human Cdk1) which controls the cell cycle in *S. pombe* (Brizuela et al, 1987; Nurse & Bissett, 1981). Cdc2 is activated by four cyclins in *S. pombe* that are expressed and degraded in a controlled manner throughout the cell cycle (Evans et al, 1983). Irreversible and robust feedback loops commit the cell to cell cycle events, meaning that regulation must be tightly controlled. Cell cycle checkpoints exist which can halt the cell cycle and co-ordinate repair pathways before cells can progress to the next phase. Cell cycle checkpoints are discussed in section 1.5. Below is a brief description of cell cycle control in *S. pombe.*

1.4.1 G1/S phase

Extracellular signals and environmental factors induce a cell to enter the cell cycle and begin proliferation. For proliferating cells to enter the cell cycle at G1, all S and G2 cyclin-Cdk complexes must be repressed. The Anaphase Promoting Complex (APC) suppresses G2 cyclin complex formation by targeting the G2 cyclin Cdc13 for proteasomal degradation (Tyson et al, 2002). Rum1 inhibits the S and G2 cyclin–Cdk complexes during mitosis and at the beginning of G1. The G1 cyclins Puc1 and Cig1 are not affected by Rum1 and their accumulation results in the phosphorylation and subsequent proteasomal degradation of Rum1 (Benito et al, 1998; Correa-Bordes et al, 1997). The Skp1 Cullin and F box (SCF) complex acts as a ubiquitin E3 ligase and targets G1/S Cdk1 inhibitors for degradation by the proteasome (Harper, 2001). G1/S cyclin production is increased and cyclin-Cdk complexes inactivate the APC and phosphorylate target proteins involved in replication to promote entry into S phase.

Replication is initiated in G1 by the assembly of the origin recognition complex (ORC) at replication origins, which are located throughout the DNA. The ORC comprises six subunits, ORC 1-6 and serves to mark replication origins and recruit components of the replisome. It remains associated with chromatin at all stages of the cell cycle (Lygerou & Nurse, 1999; Moon et al, 1999; Ogawa et al, 1999)

Both budding and fission yeast chromosomes contain ~400 origins of replication (ORIs) (Segurado et al, 2003). These are best characterised in *S. cerevisiae,* where ORIs are approximately 150bp in length and include autonomous replicating sequence (ARS) repeats which are required for ORC binding (Broach et al, 1983; Newlon & Theis, 1993). In *S. pombe*, origins of replication are defined as AT-rich sequences which range from 0.5-1.5 Kb, and they can be utilised in research for use as replication origins in plasmids.

1.4.1.1 Initiation of DNA replication

The ORC recruits Cdc18, Cdt1 and the MCM complex, which comprises Mcm2-7. The MCM complex is loaded onto the DNA by Cdc18 and Cdt1 in an ATP-dependent manner during G1 (Kearsey et al, 2000; Neuwald et al, 1999). The MCM complex is highly conserved between species and is essential for replication (Li et al, 2011). It acts as the core of a replicative helicase and is required to unwind the DNA double helix so that single stranded template DNA is accessible to replicative polymerases. Two MCM complexes are loaded onto each origin of replication to allow bi-directional replication to take place (Labib et al, 2000; Lei & Tye, 2001). An MCM-bound origin forms the 'pre-replication complex' (Pre-RC), and these are referred to as 'licenced' replication origins (Kearsey et al, 2000; Nishitani et al, 2000). *S. cerevisiae* and human protein homologues involved in replication are shown in Table 1.1.

	S.p	S.c	H.s	Role
Pre-RC	Orc1-6	Orc1-6	ORC1-6	Marks replication origins
	Cdc18	Cdc6	Cdc6	Loads MCM complex to replication origins
	Cdt1	Cdt1	Cdt1	
	MCM complex			
	Mcm2	Mcm2	Mcm2	Core of replicative helicase
	Mcm3	Mcm3	Mcm3	
	Cdc21	Mcm4	Mcm4	
	Mcm5	Mcm5	Mcm5	
	Mcm6	Mcm6	Mcm6	
	Mcm7	Mcm7	Mcm7	
Pre-IC	Cdc23	Mcm10	Mcm10	Pol-α recruitment. *S.p* Cdc23 reported to have primase activity
	Cdc45	Cdc45	Cdc45	Required for MCM helicase activity
	Rad4	Dpb11	TOPBP1	Checkpoint mediator
	Drc1	Sld1	-	Aids Rad 4 loading
	Sld3	Sld3	-	Required for Cdc45 loading
	Mrc1	Mrc1	CLASPIN	Checkpoint mediator
	Mcl1	Ctf4	AND1	Couples MCM complex to pol-α
	GINS complex			
	Sld5	Sld5	Sld5	Scaffold for MCM and Cdc45
	Psf1	Psf1	Psf1	
	Psf2	Psf2	Psf2	
	Psf3	Psf3	Psf3	
FPC	Swi3	Csm3	TIPIN	Regulatory role, Fork stabilisation, checkpoint activation
	Swi1	Tof1	TIM1	

Table 1.1. *S.pombe* (*S.p*), *S.cerevisiae* (*S.c*) and human (*H.s*) homologues involved in replication initiation and continuation.

1.4.2 S phase

The onset of S phase promotes the assembly of the pre-initiation complex (Pre-IC), which precedes origin firing. Inactivation of the APC allows for the accumulation of the DDK (Dbf4-dependent kinase) complex (Hsk1-Dfp1), which acts together with Cdc2 to recruit several other proteins to form the Pre-IC (Diffley, 2004) (See Table 1.1). The Pre-IC includes Cdc45 and the GINS complex, which together with MCM1-7 are known as the CMG complex and form an active helicase (Moyer et al, 2006). The DDK complex is inactivated following origin firing, and components of the pre-replication complex dissociate from the DNA, adding to the robust prevention of further replication origin firing (Baum et al, 1998; Takeda et al, 1999).

Several additional proteins form the replication progression complex (RPC), which remains associated with the replication fork. These include the replication factor C (RFC) complex, which is a clamp loader, and proliferating cell nuclear antigen PCNA. PCNA acts as a homo-trimeric sliding clamp which docks the DNA polymerases at the DNA and interacts with a host of other proteins involved in replication. PCNA enhances the activity of the replicative polymerases (Pol δ and Pol ε) and is loaded onto the DNA by the RFC complex at 3' template-primer junctions (Moldovan et al, 2007). The structure and roles of PCNA are discussed in more detail in section 1.8. Other factors associated with the RPC include the 'connector protein' Mcl1 (*H.s*. AND1) which interacts with several replication fork components, topoisomerases, polymerases, DNA ligase and the endonucleases Rad2 (*H.s*. FEN-1) and Dna2. Swi1 and Swi3 (*H.s.* TIM1/TIPIN) form the fork protection complex (FPC), that interacts with many replisome proteins and acts to promote replication fork stability. The FPC interacts with checkpoint mediator protein Mrc1, linking the polymerase and helicase (Bando et al, 2009; Katou et al, 2003) as well as cohesin, to stabilise sister chromatid cohesion (Errico et al, 2009; Leman & Noguchi, 2013). Swi3 also interacts with Rad11. RPA is made up of three subunits, the largest of which (*S. pombe* Rad11) binds to single stranded DNA. It recruits checkpoint proteins required for activation of the intra-S checkpoint (Leman & Noguchi, 2013; Noguchi et al, 2004) (See section 1.5.2).

Activation of the MCM helicase results in the unwinding of the DNA ahead of the replication fork in an ATP-dependent manner, allowing bi-directional replication to begin. DNA unwinding is preceded by the dissociation of Cdc18 and Cdt1 (Yanow et al, 2001).

1.4.2.1 Replication

Replication can only occur 5' to 3', resulting in the two new DNA strands being synthesised in opposite directions. A short RNA primer is synthesised by polymerase α. This is extended by polymerase ε for continuous replication on the leading strand. Discontinuous replication occurs on the opposite strand which is known as the 'lagging strand' (Figure 1.2). Here, polymerase δ synthesises 100-200 base DNA fragments called Okazaki fragments (Okazaki R et al, 1967). Okazaki fragments displace the previous RNA primer as well as several nucleotides upstream of the primer. This results in a 'flap' which is cleaved by the endonuclease Rad2 (*H.s FEN1*), or processed by Dna2, and ligated by DNA ligase I (Goulian et al, 1990). Single stranded DNA which is exposed during lagging strand synthesis is protected by RPA binding. Replication continues in both directions until two replication forks moving in opposite directions converge, or until a fork-blocking lesion is encountered.

1.4.3 G2/M phase entry and progression

S. pombe cells spend approximately 70% of their cell cycle in G2. The M phase cyclin-Cdk complex is formed following an increase in Cdc13 cyclin levels during S phase. Cdc2 associated with Cdc13 is phosphorylated on Tyr 15 by Mik1 during S phase and by Wee1 in G2 (Christensen et al, 2000). An increase in the levels of Cdc13 and its association with Cdc2 promotes the phosphorylation and activation of Cdc25. Cdc25 de-phosphorylates Cdc2, resulting in high levels of Cdc2 activity and promoting entry into mitosis (Morgan, 1997). During metaphase, the APC is activated by Cdc2-Cdc13.

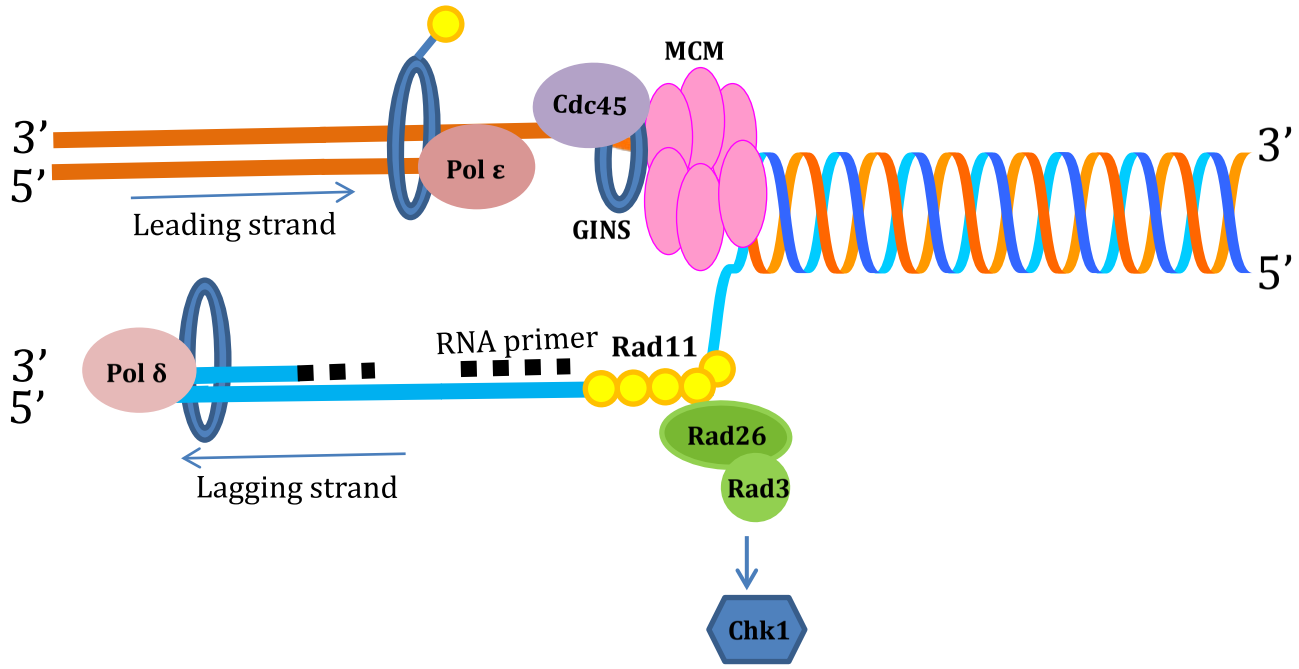

Figure 1.2 Replication fork structure

The DNA double helix is unwound by the MCM helicase complex which requires the GINS complex and Cdc45 for activity. DNA polymerase-α synthesises RNA primers which are extended by Pol δ in the 5’ to 3’ direction to form Okazaki fragments on the lagging strand. Exposed ssDNA is protected by Rad11 (RPA) binding. DNA synthesis on the leading strand requires DNA polymerase-ε. Blockage to replication by DNA damage or stalling of the replication fork results in an increase in exposed ssDNA, which is bound by Rad26-Rad3 (H.s ATRIP-ATR). This results in checkpoint activation and recruitment of DNA damage repair proteins through activation of Chk1. Several other proteins are associated with the replisome to co-ordinate and regulate DNA synthesis. Some of these factors are shown on the left for simplicity.

1.5 Cell cycle checkpoints

Completion of DNA replication and the repair of any endogenously or exogenously acquired DNA damage is essential for the maintenance of genome stability. Cell cycle checkpoints halt the cell cycle following detection of damage, stabilise the replication fork and activate DNA damage response pathways to repair any damage before the cell cycle can continue. There are three major checkpoints throughout the cell cycle. These are at G1/S, intra-S and G2/M. The checkpoint response is co-ordinated by a range of well conserved proteins, which can be divided into sensors, mediators, and effectors. Table 1.2 shows the *S. pombe*, *S. cerevisiae* and human checkpoint protein homologues.

Checkpoint activation is co-ordinated by two proteins in eukaryotes. These are phosphatidyl inositotide-3' kinase (PI3K) – related kinases Ataxia telangiectasia mutated (ATM) (*S. pombe* Tel1) and ATM-and Rad3-related (ATR) (*S. pombe* Rad3) (Carr, 1997). In higher eukaryotes, ATR is an essential gene (de Klein et al, 2000). Mutations in the ATM gene in humans or mice cause ataxia telangiectasia (AT). AT is a progressive disorder, characteristics of which include ataxia, radiation sensitivity and pre-disposition to cancers (Barlow et al, 1996; Lavin & Shiloh, 1997). ATM and ATR are required in response to specific types of damage. ATM is recruited to the sites of double strand breaks by the Mre11, Rad50, Nbs1 (MRN) complex, which also recruits further DNA repair proteins. ATR is recruited with ATR interacting protein (ATRIP) to stalled replication forks, where RPA covered single stranded DNA is present, and in response to UV induced DNA damage (Cliby et al, 1998; Wright et al, 1998; Zou & Elledge, 2003). The *S. pombe* ATR homologue Rad3 (N J Bentley et al, 1996) is required for checkpoint activation in response to both replication fork stalling and DNA damage, along with Rad26 (homologue of *H.s.* ATRIP), which is phosphorylated by Rad3 and required for Rad3 function (Edwards et al, 1999).

S.p	*S.c*	*H.s*
Sensor proteins		
Rad3	Mec1	ATR
Tel1	Tel1	ATM
Rad26	Ddc2	ATRIP
9-1-1 Complex		
Rad9	Ddc1	Rad9
Hus1	Mec3	Hus1
Rad1	Rad17	Rad1
Rad17-RFC complex		
Rad17	Rad24	Rad17
Rfc2-5	Rfc2-5	Rfc2-5
MRN complex		
Mre11	Mre11	Mre11
Rad50	Rad50	Rad50
Nbs1	Xrs2	Nbs1
Mediator proteins		
Crb2	Rad9	53BP1
Mrc1	Mrc1	Claspin
Rad4	Dpb11	TOPBP1
Effector kinases		
Chk1	Chk1	Chk1
Cds1	Rad53	Chk2

Table 1.2. *S.pombe* (*S.p*), *S.cerevisiae* (*S.c*) and human (*H.s*) homologues involved in checkpoint activation and signalling.

1.5.1 G1/S phase checkpoint

Double strand breaks are detected by ATM in higher eukaryotes. ATM phosphorylates the effector kinase Chk2 (*S. pombe* Cds1), which in turn phosphorylates and inactivates Cdc25. This results in inhibition of Cdk2, which is subsequently unable to activate Cdc45 and initiate the assembly of replication machinery (Bartek & Lukas, 2001).

Rad17-RFC and the PCNA-related clamp, the 9-1-1 (Rad9-Rad1-Hus1) complex, are recruited to ssDNA (Caspari et al, 2000; Thelen et al, 1999). Rad17-RFC is an alternative clamp loader which is required to load the damage-specific 9-1-1 clamp onto the DNA (Bermudez et al, 2003). TopBp1 (*S. pombe* Rad4) binds Rad9 and ATR (*S. pombe* Rad3), which phosphorylates and inactivates Chk1 (Furuya et al, 2004). Subsequent Cdc25 inactivation results in G1 arrest. *S. pombe* spend very little time in G1, making G1/S checkpoint studies challenging.

1.5.2 Intra-S phase checkpoint

DNA damage encountered during S phase in *S. pombe* results in checkpoint mediator protein Mrc1-facilitated activation of the effector kinase Cds1, by Rad3 (Boddy et al, 1998; Brondello et al, 1999; Lindsay et al, 1998). Cds1 phosphorylates and inactivates Cdc25 (Alao & Sunnerhagen, 2008), leading to cell cycle arrest. Cds1 activation also results in an accumulation of tyrosine kinase Mik1, which promotes ubiquitin-mediated degradation of Cdc25 and also phosphorylates and inhibits Cdc2 (Boddy et al, 1998). DNA damage encountered during S phase can cause replication forks to stall (described in section 1.6.5.3). Cds1 inhibits late origin firing and acts to stabilise stalled replication forks by phosphorylating the Mus81-Eme1 endonuclease (Furuya & Carr, 2003).

1.5.3 G2/M checkpoint

The G2/M checkpoint is the most important checkpoint for *S. pombe* and cells must have reached a critical size, have fully replicated their DNA and repaired any DNA damage before progressing to mitosis. Cdc25 removes the inhibitory phosphate from Cdc2 when cells have reached a critical size, allowing mitotic

entry (Dunphy & Kumagai, 1991; Kumagai & Dunphy, 1991; Rupeš, 2002; Russell & Nurse, 1986). DNA damage is detected by the MRN complex and Rad3 is recruited with Chk1 mediator protein Crb2 and Rad4, resulting in the activation of the effector kinase Chk1 (Saka et al, 1997). Rad4 is required to act as a scaffold protein which interacts with Rad17, Crb2 and the phosphorylated Rad9 subunit of the 9-1-1 complex and is required for Rad3-dependent phosphorylation of Chk1 (Qu et al, 2013). Chk1 causes cell cycle arrest by activating Wee1, which phosphorylates and inhibits Cdc25, preventing the activation of Cdc2, and therefore entry into mitosis (Raleigh & O'Connell, 2000). Cdc25 is also bound and inactivated by 14-3-3 proteins Rad24 and Rad35, and is subsequently exported from the nucleus (Lopez-Girona et al, 1999).

1.6 DNA damage response pathways

Endogenous sources of DNA damage include stalled or collapsed replication forks (section 1.6.5.3-1.6.5.4) and oxidative damage resulting from metabolism. Oxidative damage also occurs as a result of exposure to ionising radiation. Exposure to DNA damaging agents such as UV irradiation or methyl methanesulfonate (MMS) can cause a range of lesions which must be repaired to maintain genomic stability. The main DNA repair pathways are outlined briefly below. This work focuses on recombination-mediated repair and post-replicative repair, which are discussed in section 1.6.5.3 and 1.8.2 respectively.

1.6.1 Nucleotide excision repair (NER)

NER is required for the removal of DNA helix-distorting bulky lesions caused by UV irradiation. These include cyclobutane pyrimidine dimers (CPDs) and 6-4 photoproducts. It is also utilised for the repair of endogenously formed oxidative legions and bulky adducts which can be caused by drugs used for chemotherapy (Schärer, 2013). The NER pathway is conserved between prokaryotes, eukaryotes and mammals and consists of global genome repair (GGR) and transcription coupled repair (TCR). In GGR, DNA damage is recognised by XPC-HR23b (*S. pombe* Rhp41/42 and Rhp23) and DDB1/2 (*S. pombe* Ddb1). In TCR damage recognition requires CSB and CSA (*S. pombe* Rhp26 and Rhp28) (Batty & Wood, 2000).

XPA (*S. pombe* Rhp14), RPA and TFIIH are recruited to the site of damage. The TFIIH complex, which includes the 3'-5' helicase XPB (*S. pombe* Rhp25) and the 5'-3' helicase XPD (*S. pombe* Rhp3), is recruited to unwind the DNA surrounding the lesion (de Laat et al, 1999). XPG (*S. pombe* Rad13) and XPF-ERCC1 (*S. pombe* Rad16-Swi10) are recruited and cleave 3' and 5' of the damage respectively, in an ATP-dependent reaction (Mu et al, 1996; O'Donovan et al, 1994). This results in the excision of a 24-32 nucleotide fragment containing the lesion (Huang et al, 1992). The resulting gap is filled in by replicative polymerases Pol δ or Pol ε and sealed by DNA ligase I (Wood & Shivji, 1997).

Mutations in NER genes result in genetic disorders including Xeroderma pigmentosum (XP), Cockayne syndrome (CS) and trichothiodystrophy (TTD) (Lehmann, 2003).

1.6.2 Base excision repair (BER)

The BER pathway recognises non-bulky DNA lesions including alkylation and oxidised nucleotides. DNA glycolsylases recognise and excise damaged bases. This results in an apurinic or apyrimidinic (AP) abasic site, which can also occur spontaneously as a result of hydrolysis (Robertson et al, 2009). AP sites are cleaved either by AP endonucleases or DNA glycosylases which possess AP-lyase activity (Aspinwall et al, 1997; Nash et al, 1997; Sun et al, 1995; Wallace, 2013). Cleavage 3' of the AP site results in short patch BER. Here, the single damaged base is removed and the gap filled by Polβ and then ligated by DNA ligase (Podlutsky et al, 2001). Cleavage 5' of the AP site results in long patch BER, where several bases are removed. These are replaced by the replicative polymerases polδ or polε, which produce a flapped structure. This is processed by Rad2 and sealed by DNA ligase (Fortini & Dogliotti, 2007; Memisoglu & Samson, 2000).

1.6.3 UV damage excision repair (UVER)

S. pombe cells possess an alternative pathway for the removal of UV photoproducts. This became apparent when UV lesions could be repaired in cells which were defective in the NER pathway (McCready et al, 1993). The UVER pathway requires Uve1, which is not conserved in *S. cerevisiae* or higher eukaryotes (Bowman et al, 1994; Yonemasu et al, 1997). This alternative pathway was confirmed when *S. pombe* cells deleted for Rad13 (*H.s* XPG) and Uve1 lost the ability to repair UV-induced damage (Yonemasu et al, 1997). Uve1 recognises several UV-induced lesions including 6-4 photoproducts and CPDs as well as nucleotide mismatches, and acts as an endonuclease to cleave DNA 5' of the damage, in an ATP-independent reaction (Bowman et al, 1994). Rad2 processes the resulting DNA flap by cleaving 3' of the damage, which releases it. DNA polδ fills the gap aided by PCNA and the RFC complex, and the nick is sealed by DNA ligase (Alleva et al, 2000; Yonemasu et al, 1997). A Rad2-independent pathway for the repair of UV damage has also been suggested, likely involving recombination (Kunz & Fleck, 2001; McCready et al, 2000; Yonemasu et al, 1997).

1.6.4 Mismatch repair (MMR)

The mismatch repair pathway recognises incorrectly incorporated bases and small loops which can form as a result of replication slippage. In bacteria, MutH recognises newly synthesised DNA, which is not methylated. A MutH homologue has not yet been described in eukaryotes. In human cells, MutSα (MSH2-MSH6) and MutSβ (MSH2-MSH3) are associated with PCNA and the replisome (Iyama & Wilson Iii, 2013). MutSα (*S. pombe* homologue Msh2-Msh6) recognises single mismatched bases as well as DNA loops (Rudolph et al, 1999; Tornier et al, 2001). MutLα (MLH1-PMS2) is one of three Mut homologues in humans and has endonuclease activity. MutLα is conserved in *S. pombe* (Mlh1-Pms1) (Schär et al, 1997) and is the major MutL heterodimer. It interacts with MutS and PCNA and makes a nick in the DNA (Pluciennik et al, 2010), which is used by the 5' to 3' exonuclease Exo1 to excise the damaged base. This is subsequently repaired by DNA polδ and DNA ligase I (Iyama & Wilson Iii, 2013).

1.6.5 Double strand break repair

Double strand breaks can arise endogenously, as a result of single strand break processing or replication fork stalling and collapse. Programmed DSB's are also formed as a controlled intermediate in meiosis and V (D) J recombination, and during mating type switching in *S. cerevisiae* to initiate gene conversion (Li et al, 2012). Exogenous causes of DSBs include exposure to ionising radiation (IR) or MMS. Two well-defined pathways exist for the repair of DSBs, NHEJ and HR, described briefly below.

1.6.5.1 Non-homologous end joining (NHEJ)

In mammals, the majority of DSB repair is carried out via NHEJ in G1 and G2 phase (Beucher et al, 2009). NHEJ repairs DSBs by ligating together two DNA ends, regardless of their sequence homology. In mammals, The DSB ends are first bound by a heterodimer formed of Ku70 and Ku80, which encircles the DNA (Walker et al, 2001). This provides competition with the MRN complex and Exo1 for the binding of DNA ends (Tomita et al, 2003). DNA-PK catalytic subunits (DNA-PKcs) are then recruited to the break through interactions with the C-terminus of Ku80, and become auto-phosphorylated. This results in an active ring complex and translocation of the Ku complex away from the break to allow access to the DNA PKcs (Yoo & Dynan, 1999). Processing of the DNA ends is often required before re-ligation can take place. This can be carried out by Artemis, which has both 3' and 5' endonuclease activity (Kurosawa & Adachi, 2010). Polynucleotide kinase phosphatase (PNKP) is also involved in end processing. It generates 5'-phosphate ends and removes 3' phosphates to allow for ligation or nucleotide insertion (Claire Chappell, 2002). DNA ligase IV is required for end-joining and its activity is dependent on an interaction with XRCC4 (Bryans et al, 1999; Riballo et al, 2009). XRCC4 also interacts with XLF which may be required for the alignment of DNA ends (Andres et al, 2012). As well as the Ku proteins, DNA ligase IV is conserved in *S. pombe* and an Xlf homologue has also been identified (Cavero et al, 2007). However DNA-PKcs and XRCC4 homologues have not yet been identified in this organism. If DSB repair is not efficiently completed by NHEJ in G2, DNA resection promotes repair by homologous recombination (Goodarzi & Jeggo, 2013).

1.6.5.2 Homologous recombination (HR)

Homologous recombination uses the sister chromatid as a template for the repair of DSBs. This means that HR is active during S and G2 phase (Beucher et al, 2009). HR initially involves resection of the DNA, followed by invasion of the homologous sequence and resolution of intermediate structures. The path chosen to resolve intermediate HR structures including Holliday junctions, determines whether or not there is crossover between homologous DNA sequences (Krejci et al, 2012).

The first step in HR is 5' to 3' end resection of the broken DNA to expose 3' single stranded overhangs (Figure 1.3A-B). This requires the MRN complex and CtIP (*S. pombe* Ctp1) (Sartori et al, 2007), as well as Exo1 (Garcia et al, 2011). The exposed ssDNA is bound by the large subunit of RPA (Brill & Stillman, 1989; Erdile et al, 1991) (*S. pombe* Rad11) (Parker et al, 1997). RPA is subsequently displaced by Rad51, which forms pre-synaptic filaments (Kurokawa et al, 2008). Rad51 recruitment is facilitated by several mediator proteins, predominantly BRCA2 in humans, as well as Rad52 and Rad54. Rad52 is the main mediator protein in *S. pombe,* which contains two Rad52 homologues, Rad52 (previously Rad22) and Rti1. Rad54 (previously Rhp54) is also conserved (Raji & Hartsuiker, 2006). Rad51 binding is also mediated by additional proteins Rad55-Rad57 *S. pombe* (Li & Heyer, 2008).

Rad51 filament formation is stabilised by the Rad55/Rad57 heterodimer (Akamatsu et al, 2007) as well as by Sfr1/Swi5 in *S. pombe* (Haruta et al, 2006). Rad51 filament formation and stabilisation catalyses the invasion and displacement of the homologous strand. This results in the formation of a D-loop in an ATP-dependent reaction, which is promoted by Rad54. The 3' strand is extended by DNA pol δ or ε, extending the D-loop (Holmes & Haber, 1999; Krejci et al, 2012; Sung, 1994) (Figure 1.3C).

Synthesis dependent strand annealing (SDSA) occurs when the D-loop is unwound and the newly synthesised DNA strand is displaced and anneals back to the 3' resected ssDNA (Figure 1.3D). DNA polymerases undertake gap filling and the DNA ends are ligated. SDSA therefore does not result in cross-over events (Ferguson & Holloman, 1996; Nassif et al, 1994)

Double Holliday junctions are formed following 'capture' of the 3' overhang on the other side of the DSB (Figure 1.3E). These must be either dissolved or resolved by endonucleases. Dissolution of double HJ's is non-recombinogenic and requires the BLM helicase and Top3-Rmi1-Rmi2 (*S. pombe* homologues Rqh1, Top3 and Rmi1) to de-catenate and unlink the crossed-over strands (Svendsen & Harper, 2010; Wu & Hickson, 2003) (Figure 1.3F).

Resolution of double Holliday junctions can result in either cross-over or non-crossover events. When the displaced stands at both of the Holliday junctions are cleaved, (facilitated by GEN-1/Yen1 in human/*S. cerevisiae* cells respectively), the result is a non-crossover product (Figure 1.3G) (Ip et al, 2008). An *S. pombe* GEN-1/Yen1 homologue has not been identified. Alternatively, one Holliday junction is resolved as described above, whilst the non-displaced strands at the other HJ are cleaved. This results in cross-over/recombination. The exact mechanism by which this takes place is not well defined. Mus81-Eme1 is the main resolvase in *S. pombe,* which efficiently cleaves nicked HJ's and can also cleave a range of recombination structures (Hope et al, 2007; Wallace, 2013). Other resolvases include XPF/ERCC1 (*S. pombe* Swi9/Swi10) (Carr et al, 1994; Rodel et al, 1997) and Slx1-Slx4 (Coulon et al, 2004).

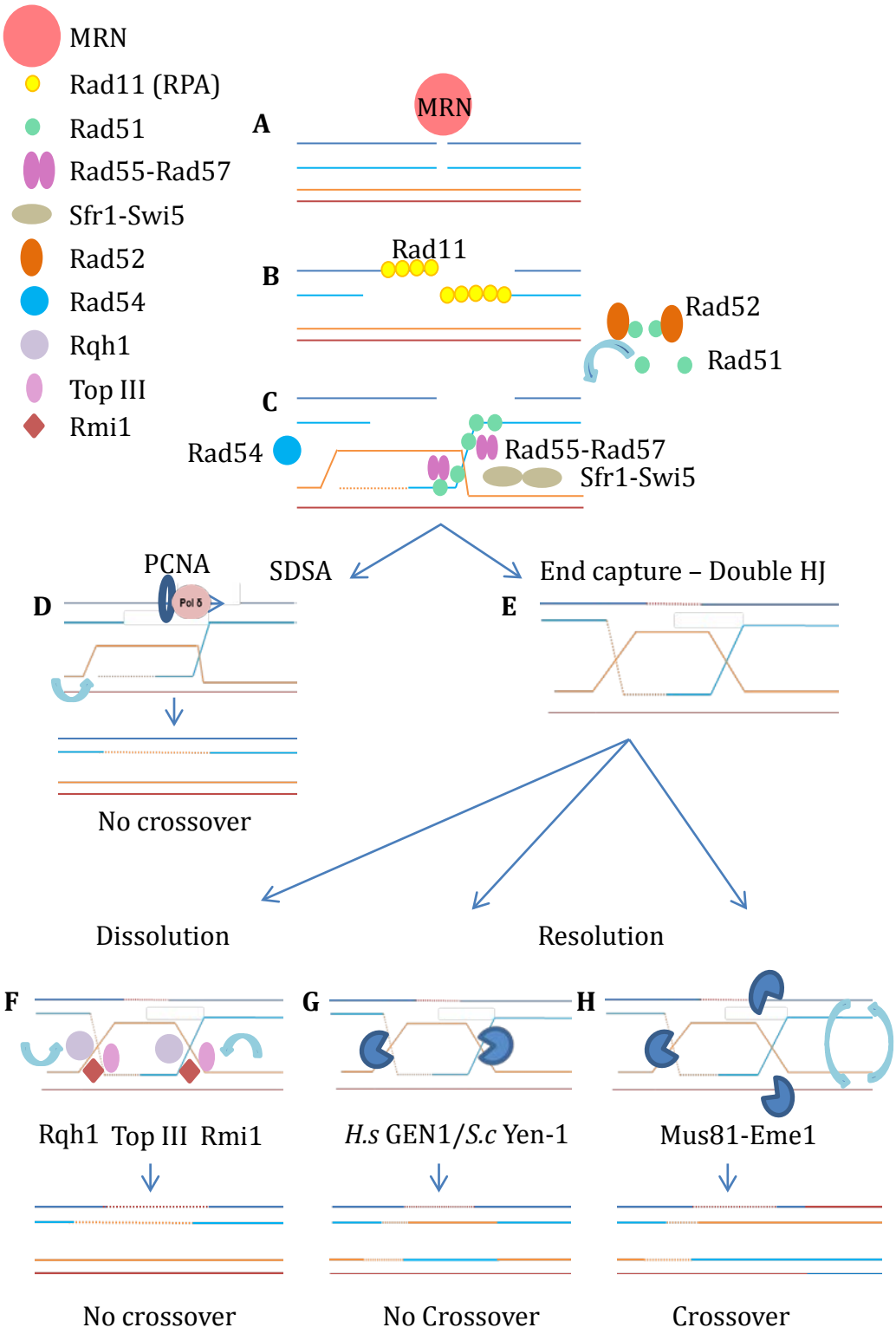

Figure 1.3 Homologous recombination

Figure 1.3 Homologous recombination

(**A-B**) Double strand DNA breaks are detected and the 3' ends resected by the MRN complex and Exo1. Rad11 (*H.s*. RPA) binds to the ssDNA before being replaced by Rad51, which is recruited via mediator proteins including Rad52. (**C**) Rad51 filament formation is stabilised by Rad55-Rad57 or Sfr1-Swi5. This stimulates invasion of the homologous DNA duplex and displacement of the DNA to form a D-loop and is promoted by Rad54. (**D**) SDSA occurs when the invading strand is displaced and ligates back to the 3' resected DNA end, avoiding cross-over. (**E**) 'capture' of the ssDNA on the other side of the DSB results in the displaced strand being used as a template. Re-joining of the invading strand results in the formation of a double Holliday Junction. (**F**) DHJ's can be resolved by dissolution, where Rqh1, Top3 and Rmi1 facilitate de-catenation, resulting in non-crossover products. (**G-H**) DHJ Resolution can result in either cross-over or non-crossover products. In humans and *S. cerevisiae*, GEN-1/Yen1 facilitate non-crossover products. Cleavage by the structure-specific endonuclease Mus81-Eme1 results in crossover formation. DHJ = double Holliday junction.

1.6.5.3 Replication fork stalling

A stalled replication fork is described as a stable fork structure which is still associated with the replisome, and which can resume replication following removal of the fork-blocking lesion. Alternatively stalled forks remain stable until they are encountered by a converging replication fork with which they can merge (Lambert & Carr, 2013).

Replication forks can stall as a result of replicative stress. This could arise from the replication fork encountering proteins associated with DNA, secondary structures in DNA or sites of DNA damage. Treatment of cells with hydroxyurea (HU) or (MMS), cause fork stalling either due to the depletion of dNTP's through inhibition of the ribonuclease reductase (RNR), or the formation of bulky DNA adducts, respectively. MMS also induces DSBs which can lead to fork collapse (Groth et al, 2010; Zegerman & Diffley, 2009). Controlled stall sites are present in the genome, for example at the mating type locus in *S. pombe*, where replication fork progression on one side of the Mat locus is inhibited by Rtf1 (Mirkin & Mirkin, 2007). Additionally some regions of the DNA, for example the ribosomal DNA, are more prone to fork stalling. Stalling is particularly prevalent where there are repeated sequences and AT-rich regions. These are called fragile sites (Leman & Noguchi, 2013).

Stalled replication forks must be stabilised whilst the checkpoint response is activated and DNA repair pathways are co-ordinated. This is necessary to

prevent fork collapse, which can result in one-ended DSBs and recombination events. When replication forks stall, the helicase can continue to unravel the DNA double helix, exposing long stretches of ssDNA (Byun et al, 2005; Sogo et al, 2002). RPA-bound ssDNA activates the intra-S ATR-dependent checkpoint. Subsequent inhibition of cell cycle progression and late origin firing stabilises the replication fork and allows time for repair or to resolve the cause of replicative stress by other mechanisms (Zeman & Cimprich, 2014). Swi1 and Swi3 (part of the FPC) are required at stalled forks and programmed stall sites to prevent an accumulation of aberrant DNA structures in *S. pombe* (Noguchi et al, 2004).

Lesions encountered on the leading strand can be overcome by trans-lesion synthesis (TLS) or template switching (TS). These mechanisms of damage avoidance are discussed further in section 1.8.2. If the fork-stalling lesion cannot be removed or bypassed, replication fork re-start can occur downstream of a lesion which affects only one strand of DNA, following re-priming. However it is unclear whether this is a frequent event (Atkinson & McGlynn, 2009; Zeman & Cimprich, 2014).

Stalled replication forks can also be rescued by the firing of dormant replication origins, or by fork reversal. Fork reversal is thought to involve 'unwinding' of the blocked fork and the formation of a four stranded DNA structure similar to a Holliday junction. The physiological role of this structure is unclear and seems to occur more frequently when the ATR pathway is impaired (Ragland et al, 2013). Reversed replication forks cause topological constraints and are converted into DSBs. Repair of the damage may subsequently be facilitated by excision repair or damage by-pass mechanisms following the formation of a DSB and recombination mediated repair (Atkinson & McGlynn, 2009; Branzei & Foiani, 2010). 'One ended' DSBs are formed as a result of a replication fork encountering a single strand DNA break. Resection and Rad51 recruitment results in strand invasion and D loop formation, as described in section 1.6.5.2. The DNA synthesis that is continued by the invading strand is much more extensive than in HR repair, and is error prone. This is known as break induced replication (BIR) (Carr & Lambert, 2013; Yang et al). The use of recombination

for replication re-start can also occur in the absence of a DSB and can result in the newly synthesised DNA strand using an inappropriate template sequence. This has been observed in *S. pombe* in response to fork stalling at protein-DNA complexes and can result in major chromosomal re-arrangements (Iraqui et al, 2012; Lambert et al, 2010; Lambert et al, 2005)

1.6.5.4 Replication fork collapse

Prolonged stalling of replication forks, a failure to re-start forks or failure to overcome fork stalling lesions can result in replication fork collapse. This is thought to involve dissociation of the replisome, particularly in the absence of the ATR pathway (Carr et al, 2011). However the structures which occur at stalled and collapsed replication forks have not been identified. Replisome disengagement has been proposed to occur in mouse cells (Ragland et al, 2013), but this has not yet been observed in human cells (Zeman & Cimprich, 2014). Disassembly of the replisome has been observed in *S. pombe* cells lacking Cds1 (Meister et al, 2007), and in this case the replisome would need to be re-recruited and re-activated to continue replication. DSBs are often formed at collapsed forks, and these require NHEJ or recombinational repair which can lead to genome re-arrangements. The Smc5/6 complex is thought to be involved in the stabilisation of stalled or collapsed replication forks and the resolution of structures resulting from recombination.

1.7 SMC complexes

The SMC family of proteins are typically 100 – 170 kDa in size and contain N - and C-terminal globular regions, separated by two coiled coil domains which fold back on each other via a central hinge region. This brings together the globular head regions to form an active ATPase domain. SMC proteins form heterodimers through interactions between their hinge regions and are associated with a number of non-SMC proteins (Harvey et al, 2002).

The SMC family comprises Smc1 and 3, part of the cohesin complex, Smc2 and 4, part of the condensin complex and Smc5 and 6, which are required in recombination and repair processes. Related to the Smc proteins is Rad50, which is part of the MRN complex (Murray & Carr, 2008).

Cohesin is associated with sister chromatids, and prevents them from separating before anaphase. It contains two non-SMC proteins, Scc1 and Scc3 in budding yeast (*S. pombe* Rad21 and Psc3) which form a bridge between the globular heads of Smc1 and Smc3 (*S. pombe* Psm1 and Psm3). Rad21 is a member of the kleisin family, which is a family of proteins that interact with Smc proteins. It is cleaved by separase to release sister chromatids at anaphase so that they can be separated (Nasmyth & Haering, 2005).

Condensin consists of Smc2 and Smc4 (*S. pombe* Cut14 and Cut3), and three non-SMC proteins. Of these, CAP-D and CAP-G contain HEAT repeats, which encode two α- helices separated by a turn. CAP-H is a member of the kleisin family (Hirano et al, 1997; Kranz et al, 2013) and bridges the ATPase domains of Smc2 and Smc4, as well as mediating the interaction between the CAP-D and CAP-G subunits. Condensin forms a flexible structure which acts as a scaffold for interacting proteins (Neuwald & Hirano, 2000). It is associated with chromosomes and acts to form supercoiled structures to condense the chromatin for mitosis (Murray & Carr, 2008).

The MRN complex is structurally similar to the SMC protein complexes and is formed from a homodimer of Rad50. Two molecules of Mre11 and Nbs1 bridge the ATPase domains (Williams et al, 2010) .

1.7.1 The Smc5/6 complex

The Smc5/6 complex is essential for cell viability and is implicated in several DNA damage dependent processes including homologous recombination, recovery of stalled replication forks and telomere elongation.

Smc6 (previously called Rad18) was the first eukaryotic SMC protein to be described. It was identified in a study of the *S. pombe* DNA damage sensitive mutant *rad18-x* (Lehmann et al, 1995). Along with Smc5, it forms a complex with six non-SMC proteins Nse1-6, each of which is described briefly below. Deletion of the genes encoding all components of the Smc5/6 complex, except for *nse5* and *nse6,* is lethal in *S. pombe,* indicating that the complex is essential for viability. This is likely due to a requirement for Smc5/6 complex function in DNA replication (Ampatzidou et al, 2006). As is the case with other SMC

proteins, Smc5 and Smc6 interact non-covalently via their central hinge regions. The globular heads at the C- and N- termini of both Smc5 and Smc6 form ATPase domains that are bridged by Nse4 (a member of the kleisin family) and Nse3 (Palecek et al, 2006a).

Nse1 is thought to associate with Nse3 and Nse4 to stabilise their interaction (Palecek et al, 2006a; Sergeant, 2005). It contains a RING finger domain typical of E3 ubiquitin ligases. Human Nse1 was observed to facilitate ubiquitination *in vitro* in the presence of Nse3 (Doyle et al, 2010; Pebernard et al, 2008). Nse1 is also proposed to bridge and stabilise the interaction between Nse3 and Nse4 (Hudson et al, 2011) and is required for Smc5/6 function in DNA repair (Pebernard et al, 2008). Nse2 is a SUMO ligase and is described in more detail in section 1.7.1.1.

Nse3 (MAGE-G1) contains a MAGE domain. Several MAGE family proteins have been found to bind to and stimulate E3 ubiquitin ligases (Doyle et al, 2010). Nse3 binds to the Smc5/6 head domains (Palecek et al, 2006b). Nse4 has a kleisin domain at its C terminus which is required for binding to the Smc5 head domain in yeast and humans (Palecek et al, 2006b; Pebernard et al, 2008; Sergeant, 2005). Additionally, the N-terminus of Nse4 contains an Nse3-binding domain (Guerineau et al, 2012).

In *S. pombe*, Nse5 has been reported to bind close to the head domains of Smc5/6, and to form a heterodimer with Nse6 (Duan et al, 2009b), which contains HEAT repeats. The roles of Nse5 and Nse6 are not well defined. There are no currently identified human homologues of Nse5 and Nse6 and neither protein is essential for viability in *S. pombe* (Palecek et al, 2006b; Pebernard et al, 2006). Nse5 interacts non-covalently with SUMO as well as Hus5/Ubc9, and is reported to influence the cellular localisation of the Smc5/6 complex (Bustard et al, 2012).

1.7.1.1 Nse2

Nse2 contains an SP-RING domain at its C-terminus and is known to function as a SUMO-ligase. The fact that a ligase dead mutant is viable while the Nse2 null strain is not indicates that the SUMO ligase function of Nse2 is not essential for

viability (Andrews et al, 2005; Potts & Yu, 2005; Sergeant, 2005). The N-terminus of Nse2 is associated with the coiled coil region of Smc5. Disruption of this interaction leads to defects in cell growth and DNA damage repair, the severity of which depends on the level of disruption (Duan et al, 2009b) .

Nse2 does not contain the SAR, Acinus and PIAS (SAP) motif which is required for DNA binding in other PIAS proteins. However as the Smc5/6 complex is associated with chromatin, Nse2 could be targeted to the DNA through its interaction with Smc5 (Lindroos et al, 2006; Stephan et al).

Several substrates of Nse2 have been identified in *S. pombe*, including Nse2 itself. Nse2 has also been shown to facilitate SUMOylation of Nse3 *in vitro* and Smc6 both *in vitro* and *in vivo* (Andrews et al, 2005). Nse2 target proteins identified in other organisms include Smc5 and Ku70 in *S. cerevisiae* (Zhao & Blobel, 2005) and Trf1 and Trf2, which are involved in telomere maintenance, as well as the cohesin subunits in humans (Potts et al, 2006; Potts & Yu, 2007)

nse2-SA mutants which are ligase dead and thus unable to facilitate SUMOylation are highly sensitive to a range of DNA damaging agents, including HU, UV and MMS (Andrews et al, 2005). *mms21* mutants defective in the *S.cerevisiae* homologue are similarly sensitive to DNA damage and also display defects in mitosis (Prakash & Prakash, 1977) indicating an important role for Nse2-mediated SUMOylation in the DNA damage response and repair of double strand breaks. Functional Nse2 is also required for the resolution of Rad51-dependent X-shaped DNA structures which can arise at stalled replication forks (Branzei et al, 2006; Chavez et al, 2010).

The viability of *nse2-SA* mutants suggests that the stability of the Smc5/6 complex as a whole is not adversely affected by mutation in the SP-RING domain (Andrews et al, 2005). The *nse2-SA* mutant is synthetically lethal with two Smc6 mutants, *rad18-x* and *rad18-74*, which have mutations close to the hinge region and the ATP binding site, respectively (Andrews et al, 2005; Irmisch et al, 2009). This suggests that the stability of Smc6 may be affected in the absence of Nse2-mediated SUMOylation (Andrews et al, 2005).

The *nse2-SA* mutant is hyper-sensitive to DNA damage and *nse2* deletion is lethal (Andrews et al, 2005). This is in contrast to the other SUMO ligase Pli1 , which is not essential and not sensitive to genotoxins when deleted (Xhemalce et al, 2004a). *nse2-SA* mutants have wild type levels of high molecular weight SUMO chains, whereas *pli1.d* cells show drastically reduced SUMO chain formation (Watts et al, 2007). Taken together, and considering the range of Nse2 target proteins identified so far, it appears that Nse2-mediated SUMOylation in association with the Smc5/6 complex and Rad60 is required for a discrete range of DNA repair processes and cellular functions, including DSB repair, telomere maintenance and cohesin functions, whereas Pli1-dependent SUMOylation functions in global SUMOylation and SUMO chain formation (Albuquerque et al, 2013; Prudden et al, 2011).

1.7.2 Smc5/6 functions

The Smc5/6 complex is associated with chromatin predominantly during S phase in *S. pombe*. It is also observed at centromeres and telomeres in both *S. pombe* and *S. cerevisiae*, indicating its requirement for accurate centromere separation (Lindroos et al, 2006; Pebernard et al, 2008). The complex is also recruited to ribosomal DNA (rDNA) which is prone to replication fork stalling, and this is increased following HU treatment (Pebernard et al, 2008). In both *S. cerevisiae* and human cells, the Smc5/6 complex is recruited to artificially induced DNA DSBs, and this is facilitated by the MRN complex (De Piccoli et al, 2006; Lindroos et al, 2006; Potts et al, 2006). These observations suggest a role for the complex in the response to replication stress and repair of DSBs.

Genetic analysis of mutants defective in the Smc5/6 complex proteins indicates epistasis with mutants defective in proteins involved in HR. Smc6 mutants are sensitive to genotoxins including UV and IR, and deletion of *S. pombe* Rad51/Rad55 homologues (previously called Rhp51/Rhp55) alleviates this sensitivity (Ampatzidou et al, 2006; Lehmann et al, 1995). Analysis of two well-characterised Smc6 mutants, *smc6-x* and *smc6-74* showed an accumulation of recombination intermediates. This is similar to the *S. cerevisiae mms2* mutant mentioned above, suggesting a role for the complex in HR repair. In addition to this, both *smc6* mutants were reported to show ‘cut’ phenotypes, consistent

with unresolved structures impeding mitosis (Ampatzidou et al, 2006; Irmisch et al, 2009). The severity of *smc5/6* mutant phenotypes is enhanced in combination with *sgs1-d* or *mus81-d*, which have helicase and endonuclease activity respectively, and are involved in crossover resolution (Kegel & Sjögren, 2010).

When replication forks are stalled (following HU treatment), Rad52 and RPA recruitment requires Smc6. Rad51 recruitment however, does not require the Smc5/6 complex (Irmisch et al, 2009). Rad52 has been shown to form Rad51-independent foci in response to replication stress, and its recruitment may act to protect nascent DNA ends and stabilise the stalled fork using its strand annealing ability (Bass et al, 2012). Rad52 recruitment to stalled replication forks is abolished in the *smc6-74* mutant, but not in the *smc6-x* mutant. Rad52 recruitment to collapsed replication forks however, is unaffected in both *smc6* mutants. This lead to the suggestion of an 'early' role for the Smc5/6 complex in HR, which involves facilitating Rad52 and RPA recruitment, perhaps by stabilising the stalled fork structure. This role is only defective in the *smc6-74* mutant, which is impaired in ATP binding (Irmisch et al, 2009).

The complex is also required at a 'late' stage of HR, following fork collapse. This is apparent by the accumulation of recombination structures in both *smc6-74* and *smc6-x* mutants, as well as in *smc5* and *nse2* mutants. This points to a role in the resolution of HR-dependent structures, which is required for DNA repair and replication re-start. Loss of this function results in aberrant and potentially fatal mitosis (Irmisch et al, 2009).

The *smc6-74* mutant phenotype is suppressed by the BRCT domain-containing protein Brc1. This suppression is dependent on several other proteins, including structure specific nucleases (Sheedy et al, 2005; Verkade et al, 1999). Brc1 is homologous to *S. cerevisiae* Esc4, which is required in response to MMS and HU treatment (Sheedy et al, 2005). Brc1 is required at stalled replication forks and has been suggested to act as a scaffold for repair proteins during replication. Brc1 could act to promote non-homologous repair pathways that do not require Smc5/6 function, such as lesion bypass by TLS, or to process intermediates in

the absence of the complex (Bass et al, 2012; Irmisch et al, 2009; Murray & Carr, 2008).

Whilst loss of Smc5/6 complex function is lethal in *S. pombe*, loss of the HR pathway is not, suggesting additional roles for the complex, outside of DNA repair (Ampatzidou et al, 2006). These might involve regulation of chromatin structure, through Nse2-mediated SUMOylation of the Cohesin subunits, and an involvement in the relief of topological stress, indicated by synthetic lethality between the *smc6-74* mutant and a Top2 mutant (Verkade et al, 1999).

In higher eukaryotes the Smc5/6 complex is also implicated in telomere elongation via the ALT pathway by Nse2-induced SUMOylation of telomeric regulatory proteins. As mentioned above, Nse2-dependent SUMOylation of Trf1 and Trf2 promotes HR dependent elongation of telomeres (Potts & Yu, 2007).

The exact mechanisms by which the Smc5/6 complex and the Nse proteins facilitate the stabilisation of stalled replication forks and recovery of replication intermediates are still unclear. The non-Smc proteins have been suggested to act to recruit the complex to specific sites. Two *nse5* mutants characterised in *S. cerevisiae* suggested a potential role for Nse5 in the localisation of the Smc5/6 complex. One mutant was also implicated in the resolution of X-shaped structures that are formed as a result of replication fork stalling and collapse, however the mechanisms behind this have yet to be described (Bustard et al, 2012).

1.7.3 Rad 60

Rad60 is a member of the RENi family of proteins, which are SLD-containing proteins conserved from yeast to humans (Novatchkova et al, 2005). It was initially identified in a screen for HR mutants, which display phenotypes similar to Smc5/6 mutants (Morishita et al, 2002). Rad60 is associated physically and functionally with the Smc5/6 complex and is delocalised from the nucleus in response to HU treatment and S phase checkpoint activation. It is also required for recovery from replication arrest (Boyd et al, 2010; Morishita et al, 2002; Prudden et al, 2009).

Rad60 was immunoprecipitated with Smc5 in non-stoichiometric amounts and may be involved in regulation of Smc5/6 at stalled replication forks. It has been proposed to act as a scaffold to bring pathway components to SUMO targets (Irmisch et al, 2009).

Rad60 has an acidic and disordered N-terminus which contains a SIM that is required in response to replicative stress (Raffa et al, 2006). The C-terminus contains two C terminal SLDs (Boddy et al, 2003; Novatchkova et al, 2005). SLD1 has a SIM binding site and is essential for viability (Boyd et al, 2010). SLD1 interacts with the Fub2 subunit of the SUMO E1 activator heterodimer, SUMO E3 ligase Pli1, and the STUbL (SUMO targeted ubiquitin ligase) Slx8 in *S. pombe* (Prudden et al, 2009). SLD2 is not essential for viability, however deletion of this domain results in destabilisation of the Rad60 protein and increased sensitivity to DNA damage (Boyd et al, 2010). SLD2 is known to non-covalently interact with the SUMO E2 conjugator Ubc9/Hus5 as mentioned in section 1.3.1.3. It is suggested that Rad60 acts with the Smc5/6 complex to facilitate Nse2 dependant SUMOylation in response to DNA damage, whereas SUMO bound Ubc9 facilitates Pli1-dependent global SUMOylation (Prudden et al, 2011).

It is likely that Rad60 also has a role independent of SUMOylation. Rad60 is required for recovery from replication arrest, and may be involved in the regulation of Smc5/6 at stalled replication forks, implicated by its phosphorylation by checkpoint kinase Cds1 (Boddy et al, 2003; Miyabe et al, 2009; Raffa et al, 2006).

1.8 PCNA

PCNA (Proliferating cell nuclear antigen) was named after its discovery in humans as an antigen during a study of autoantibodies (Miyachi et al, 1978). It forms a homo-trimeric ring which encircles DNA during replication and can move in both directions, acting as a docking station for the DNA polymerases and a wide range of proteins involved in replication and repair (Moldovan et al, 2007). Hundreds of PCNA-interacting proteins have been identified to date and PCNA and its interacting proteins are involved in a variety of processes,

including cell cycle regulation, chromosome cohesion, MMR, BER and NER (Strzalka & Ziemienowicz, 2011). Several interacting proteins possess a PIP (PCNA interacting protein) motif (Gulbis et al, 1996; Jonsson et al, 1998), which is a conserved peptide sequence of QxxΨ (Ψ being a hydrophobic residue). Non-conancial PIP boxes are described as having an N terminal KAx sequence (Xu et al, 2001). For example XPG (*S. pombe* Rad13) the NER endonuclease, contains a C-terminal PIP box. This is necessary for NER activity as well as PCNA binding, although the mechanisms underlying these interactions are unclear (Gary et al, 1997). PCNA is post-translationally modified by SUMO and ubiquitin and this determines the choice of post replicative repair pathways.

1.8.1 PCNA structure

PCNA consists of three identical monomers. Each monomer contains two globular domains which are separated by an inter-domain connecting loop (IDCL). The crystal structure of the *S. cerevisiae* homologue of PCNA (POL30) indicates that it is extremely similar to that of the β subunit of bacterial DNA polymerase III, despite a lack of sequence homology, suggesting a similar function (Krishna et al, 1994). It is possible to distinguish between a front 'C' side and back side of the PCNA trimer, due to the subunits interacting in a directional 'head to toe' manner. It is the 'C' surface with which polymerases and other replication proteins interact, and this ensures directionality of replication. The inner surface of the ring, which interacts with DNA, contains α-helices and is positively charged, whilst the outer surface is formed from β-sheets and is negatively charged (Gulbis et al, 1996; Krishna et al, 1994). A hydrophobic pocket is located underneath the IDCL of each monomer, which accommodates the structure formed by the PIP motif on some PCNA-interacting proteins. Any changes in the PIP motif sequence or flanking sequence can dramatically alter the binding affinity (Bruning & Shamoo, 2004; Gulbis et al, 1996). Homotrimeric PCNA has the ability to bind three proteins at the same time via PIP motifs, with one binding to each monomer. This is observed with the RFC complex where the different PCNA subunits bind different RFC monomers, and FEN1 (*S. pombe* Rad2), a copy of which can occupy each of the three PCNA monomers (Bowman et al, 2004; Sakurai et al, 2005). The crystal structure of both ubiquitinated and

SUMOylated PCNA confirms that these modifications occur on the 'back' face of PCNA, opposite to where the DNA polymerases interact. These structures also demonstrated that SUMO and ubiquitin modifications do not alter the conformation of PCNA (Freudenthal et al, 2011).

1.8.2 PCNA ubiquitination and PRR

Post replicative repair (PRR) pathways or 'damage tolerance' pathways are employed to allow replication to continue past a site of DNA damage. There are two types of PRR, error-prone translesion synthesis (TLS), and error-free template switch (TS). The path taken to overcome the lesion is dependent on PCNA ubiquitination by members of the Rad6 epistasis group (Jentsch et al, 1987; Ulrich, 2005; Xiao et al, 1999). Rad6 is a ubiquitin E2 conjugating enzyme and part of a group of proteins which result in the mono- or poly-ubiquitination of PCNA at a stalled replication fork (Hoege et al, 2002) (Figure 1.4).

TLS is activated in response to replication fork blocking lesions, following PCNA mono-ubiquitination at K164. Stalling of the replication fork results in the exposure of ssDNA which is subsequently bound by RPA. This recruits the E3 ubiquitin ligase Rhp18 which acts with the ubiquitin E2 conjugating enzyme Rad6 to mono-ubiquitinate PCNA on K164 (Hoege et al, 2002). This is a highly conserved modification which has been observed in all eukaryotes studied so far. Y family polymerases (except for Rev1), including Polη and Polζ (Rev3/Rev7) contain PIP motifs. In addition, all of the TLS polymerases have an increased affinity for mono-ubiquitinated PCNA due to the presence of ubiquitin binding domains called UBM or UBZ domains. (Sale et al, 2012) TLS polymerases are able to accommodate damaged bases in their active site and insert a nucleotide opposite to the lesion. Replication is continued past the lesion by a TLS polymerase before the replicative DNA polymerase is switched back. This allows the damage to remain undetected by the replicative polymerase, which has 3' to 5' proof- reading activity (Sale et al, 2012) (Friedberg, 2005). Translesion synthesis is error-prone and can lead to permanent mutations.

PCNA mono-ubiquitination on K164 can be extended to form K63-linked ubiquitin chains. This is facilitated by the ubiquitin E2 heterodimer Ubc13-Mms2 and E3 ubiquitin ligase Rad5. Poly-ubiquitination promotes the bypass of damage by template switching (TS), an apparently error-free process which is not well defined, but possibly involves recombination (Hoege et al, 2002; Parker & Ulrich, 2009). Recently, human ZRANB3 was shown to interact with poly-ubiquitinated PCNA. This protein has nuclease and helicase domains which could aid stalled replication fork resolution (Zeman & Cimprich, 2012).

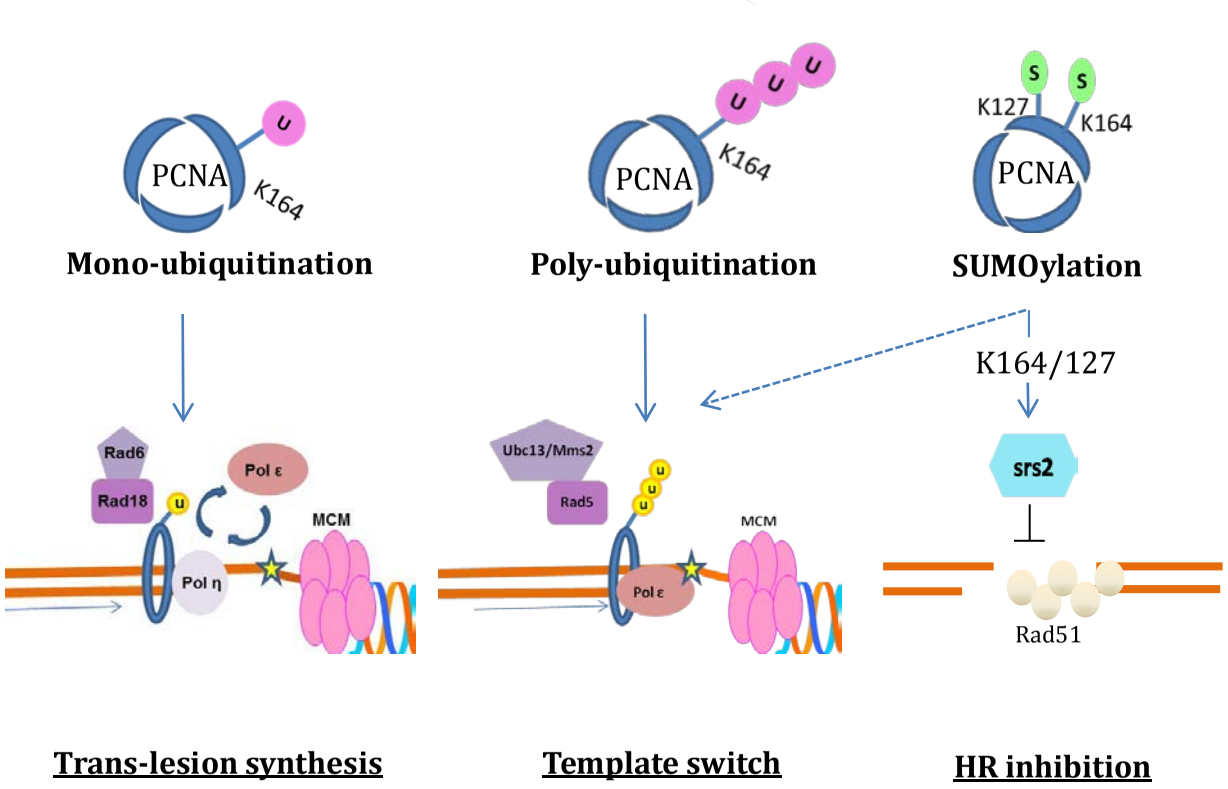

Figure 1.4 PCNA modification by ubiquitin and SUMO

Mono-ubiquitination on K164 is facilitated by ubiquitin E2 conjugating enzyme Rad6 and E3 ligase. Rad18. Mono-ubiquitination results in polymerase switching from the replicative polymerase to a TLS polymerase which can accommodate a lesion in the active site. The lesion is bypassed and the replicative polymerase is switched back to continue replication. Poly-ubiquitination on K164 is facilitated by ubiquitin E2 conjugating enzyme heterodimer Ubc13/Mms2 and E2 ligase Rad5. This results in lesion bypass by template switching, a mechanism that involves recombination. In *S.cerevisiae,* SUMOylation of PCNA on K164 recruits helicase Srs2. Srs2 inhibits Rad51 nucleofilament formation which inhibits inappropriate recombination during S phase. A similar mechanism for HR inhibition occurs in humans, involving PARI.

Whilst the general PRR pathway is conserved between organisms, some differences exist in *S. pombe*. PCNA is ubiquitinated in response to DNA damaging agents or replication stress in budding yeast and humans (Hoege et al, 2002). However, PCNA ubiquitination is also detected in S phase in unchallenged cells in *S. pombe*, and this is increased in response to DNA damage (Frampton et al, 2006). In contrast to *S. cerevisiae*, *S. pombe* PCNA ubiquitination is also observed in G2 in response to DNA damage including ionising radiation (Frampton et al, 2006)

1.8.3 SUMOylation of PCNA

As well as being ubiquitinated, *S. cerevisiae* PCNA is also SUMOylated, predominantly on K164. This requires the SUMO E2 conjugating enzyme Ubc9 and the E3 SUMO ligase Siz1. SUMO modification is also observed on K127, albeit to a lesser extent (Hoege et al, 2002). K127 is part of a SUMO consensus site which likely allows interaction with Ubc9. SUMOylation at this site has been suggested to block the interaction with PCNA-interacting proteins (Moldovan et al, 2006). PCNA SUMOylation in *S. cerevisiae* occurs constitutively during normal S phase, and is increased in response to replication stress. This results in the recruitment of a helicase called Srs2, via its C-terminal SIM and PIP motifs (Shaheen et al, 2010). Srs2 is an anti-recombinogenic helicase which inhibits Rad51 filament formation in the early stages of HR. It does so by stimulating ATP hydrolysis of Rad51 which reduces its affinity for DNA (Papouli et al, 2005; Pfander et al, 2005b). The predominant role of PCNA SUMOylation in *S. cerevisiae* appears to be the inhibition of inappropriate recombination. It has been suggested that this prevents unwanted sister chromatid recombination that could result in deletions and gross chromosomal rearrangements (Moldovan et al, 2007). The inhibition of recombination allows time for ubiquitin-dependent repair by the Rad6 error-prone or error-free pathways.

PCNA SUMOylation has more recently been reported in chicken DT40 cells, *Xenopus laevis* and human cells (Arakawa et al, 2006; Gali et al, 2012a; Leach & Michael, 2005a). Two PCNA SUMOylation sites were identified on human PCNA *in vitro*, K164 and K254. A C-terminal fusion of SUMO to PCNA resulted in a decrease in recombination resulting from induced DSBs and an increased

resistance to replication fork-blocking lesions. Over-expression of a *PCNA-K254R* mutant resulted in elevated γH2AX foci and suggested that SUMOylation of K254 reduces DSB formation. The authors concluded that in the presence of SUMO-modified PCNA, replication forks encountering DNA lesions are less likely to be converted to DSBs (Gali et al, 2012a). An Srs2 ortholog recently identified in human cells called PARI may act to inhibit recombination in a similar manner to Srs2. PARI also contains C-terminal SIM and PIP motifs and preferentially interacts with SUMOylated PCNA. It also interacts with Rad51 and disrupts Rad51 filament formation, removing Rad51 from DNA. PARI does not possess ATPase or helicase activity and acts in stoichiometric amounts however, suggesting different modes of action to Srs2 (Moldovan et al, 2012).

Several proteins interact with SUMOylated PCNA via PIP and SIM motifs. For example *S. cerevisiae* Rad18 recruitment is greatly enhanced by the presence of a SIM, however this SIM is not conserved in other organisms {Parker, 2012 #573. Elg1 forms an alternative clamp loader with RFC 2-5. The *S. cerevisiae* Elg1 sequence also contains SUMO interacting motifs (SIMs) as well as a PIP box (Kubota et al, 2013). *S. cerevisiae* Elg1 interacts with both unmodified and modified PCNA (Parnas et al, 2010). Yeast two hybrid assays and IPs have suggested that Elg1 interacts preferentially with SUMOylated PCNA. It was also found that in the absence of Elg1, SUMOylated PCNA and Srs2 accumulated on the chromatin. These results led researchers to propose that Elg1-RFC may have a role in the unloading of SUMOylated PCNA from chromatin (Parnas et al, 2010). It was noted that whilst Elg1 appears to play a role in PCNA unloading, it is possible that the accumulation of SUMOylated PCNA observed in *elg1* mutants in *S. cerevisiae* is the result of PCNA being SUMOylated in S phase when it is associated with the chromatin (Ulrich, 2013). The human homologue of Elg1, ATAD5 also contains SIMs, and these enable recruitment of a de-ubiquitinating complex which targets ubiquitinated PCNA (Ahmad & Stewart, 2005).

1.9 Aims

The aim of the work in this thesis was to primarily develop and efficient *in vitro* system to identify SUMO modified lysine residues on SUMO target proteins. Further, to utilise this system to identify novel SUMO target proteins *in vitro*, before investigating the effect of lysine to arginine mutants of target proteins integrated into the *S. pombe* genome. Following the identification of SUMO E3 ligase Nse2 mutants in human patients, this work set out to investigate the effect of the equivalent Nse2 mutations in *S. pombe*. A third aim of the work described here was to confirm the SUMOylation of PCNA in *S. pombe*, and to investigate the biological function of this modification compared to that in other organisms.

2 Materials and methods

2.1 DNA methods

2.1.1 Agarose gel electrophoresis

300ml agarose gels at 0.8% were generally used to analyse DNA samples, however 1-1.5% gels were used to analyse DNA fragments smaller than 500bp. To make 300ml 0.8% gels, 2.4g agarose (Melford) was dissolved in 300ml of 1 X TBE buffer by heating in a microwave. Once cooled slightly, ethidium bromide was added to a final concentration of 0.25µg/ml and the agarose solution was poured into a gel cast to set. Gels were placed in a gel tank filled with 1 X TBE buffer. 6 X loading buffer was added to DNA samples to a final concentration of 1 X, and water added to give a 20µl sample volume. In some cases, 20-30µl of DNA was loaded into a gel for gel purification. 5µl of a 1Kb ladder (Invitrogen) was run alongside samples for size comparison. Gel electrophoresis was carried out at 150V for approximately 30 minutes and DNA bands visualised using a UV transilluminator.

2.1.2 Gel purification

DNA was visualised on and excised from an electrophoresis gel using a sterile scalpel. DNA was purified from agarose gels using QIAquick Gel Extraction Kit (QIAGEN), as per the manufacturer's instructions.

2.1.3 Restriction digest

Restriction digests were carried out using NEB restriction enzymes. A typical 50µl reaction would be set up as described below:

10 x NEB buffer	5µl
0.5 - 1µg DNA	2µl
Restriction enzyme	1µl
Sterile H_2O	43µl
Total volume	50µl

Digests were incubated at 37°C for 1 hour and 1µl analysed by gel electrophoresis (see section 2.1.3). Plasmids being digested were subsequently PCR purified. DNA fragments being digested for ligation into a plasmid were either PCR purified or gel purified prior to ligation.

2.1.4 Ligation

Ligation reactions were carried out using either Quick ligase (NEB), or T4 DNA ligase (Roche) as per manufacturer's instructions. A 3 fold molar excess of insert was used in most cases. Quick ligase reactions were incubated for 5 minutes at room temperature. T4 ligase reactions were incubated overnight at 16°C. Ligated products were subsequently transformed into NM522 *E. coli* cells. A typical reaction is described below:

Quick ligase reaction

2 x Quick Ligation buffer	10µl
50ng plasmid DNA	1µl
3 x molar excess insert DNA	3µl
Quick ligase	1µl
Sterile H_2O	5µl
Total volume	20µl

T4 DNA ligase reaction

10 x T4 ligase buffer	2µl
50ng plasmid DNA	2 µl
3 x molar excess insert DNA	3µl
T4 DNA ligase	1µl
Sterile H_2O	12µl
Total volume	20µl

2.1.5 Plasmid DNA isolation and purification

Individual bacterial colonies were inoculated in 5ml LB broth (See section 2.2.2) with appropriate selective antibiotics (eg. 100µg/ml ampicillin). Cultures were incubated at 37°C with shaking (180rpm) for a minimum of 4 hours to overnight. For screening colonies for positive ligations, the DISH miniprep method was used. When the DNA was required for subsequent sequencing, digest or transformation the QIAprep Spin Miniprep Kit was used (QIAGEN).

2.1.5.1 DISH minipreps

1ml of bacterial culture grown as mentioned above was transferred to a 1.5ml eppendorf tube and harvested using a table top centrifuge at 13,000 rpm for one minute. Supernatant was discarded and the pellet resuspended in 100µl DISH I solution. 200µl DISH II solution was added and mixed by inverting. 150µl of ice

cold DISH III was then added and mixed by inverting, before centrifuging at 13,000 rpm for five minutes. The supernatant was collected and put into a fresh tube. 200µl of phenol chloroform was then carefully added and mixed by inverting before centrifuging at 13,000 for 5 minutes. The top layer of solution was transferred to a fresh eppendorf tube containing 1ml of 100% ethanol and mixed well. Samples were then centrifuged at 13,000 rpm for five minutes and the supernatant discarded. The pellet was dried using a desiccator and then re-suspended in 30µl of 1XTE containing 20µg/ml RNAse. 2 -5µl was analysed by electrophoresis gel.

DISH I
9g/l Glucose
3g/l Tris-base
3.72g/l EDTA

DISH II
0.2M NaOH
1% SDS

DISH III
3M KOAc
11.5% Galacial acetic acid

2.1.5.2 QIAprep Spin Miniprep

5ml of bacterial culture was used for QIAprep Spin Miniprep kit (QIAGEN) as per manufacturer's instructions.

2.1.6 PCR amplification of DNA

PCR amplification was carried out using either KOD hot start polymerase (Merck Millipore) as per manufacturer's instructions, or *pfu* polymerase which was purified from BL21 *E. coli* cells (See section 2.3.7). Where *pfu* was used, a typical reaction set up was as follows:

10 x pfu buffer containing MgSO4	5µl
2.5mM dNTP mix	2µl
10µM Primers (Forward + Reverse)	1µl +1µl
DNA (50ng)	1µl
Pfu	1µl
Distilled H_2O	39µl
Total volume	50µl

A typical PCR cycling programme was as follows:

Step	Temperature	Time
Lid heating	94°C	1 min
Initial denature	94°C	30s
Denature	94°C	30s
Annealing	45-55°C (5°C below primer Tm)	30s
Extension	68°C	1min/Kb
20-30 cycles		
Final extension	68°C	2 min
Hold	6°C	infinite

1-5 µl of PCR products were analysed on agarose gel. (See section 2.1.1)

2.1.7 Site directed mutagenesis

Two methods of site directed mutagenesis were used. Complementary primers were designed, which contained the mutagenic sequence flanked on either side by 15 nucleotides which complement the template sequence. In one method, *pfu* polymerase was used in a 50µl reaction as described above, to amplify around the entire plasmid. PCR products were analysed on a 0.8% agarose gel as above. In order to digest the methylated DNA template and leave only mutagenized plasmid, 1µl of *Dpn*I enzyme was added to the reaction. This was incubated at 37°C for 1 hour and then subject to PCR purification (QIAGEN) as per manufacturer's instructions. Plasmids were sequenced by GATC.

In the second method, based on Horton et al., 1989, two PCR fragments are generated with overlapping ends, both of which contain the desired mutation (See diagram 1A). These fragments were gel purified (QIAGEN, see part 2.1.5) and used in a subsequent PCR in equimolar amounts. In this reaction, the external primers were used to fuse and amplify the mutagenic fragment (See diagram 1B). This was then be PCR purified, digested and ligated into the vector of choice. (See section 2.1.7, 2.1.3 and 2.1.4 respectively).

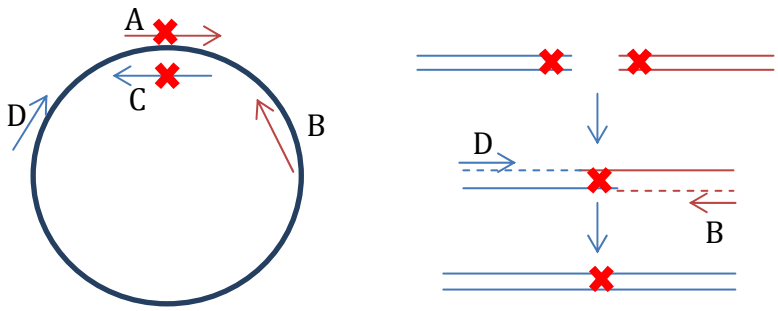

Figure 2.1 PCR mutagenesis

Primer pairs A and B, and C and D were used in two separate reactions. This generated two fragments containing the desired mutation, with overlapping ends A. These two fragments were subsequently used as the template for a third PCR using primers D and B, which fused and amplified the mutagenic fragment B.

2.1.8 PCR purification

PCR products and restriction digests were purified using QIAquick PCR Purification Kit (QIAGEN), as per the manufacturer's instructions.

2.1.9 Sequencing

Sequencing was carried out by GATC-biotech, and results uploaded to a server. Sample requirements were 5µl of 30-100ng/µl DNA and 5µl of 30pmol/µl primer per sample.

2.1.10 Ethanol precipitation

2 sample volumes of 100% ethanol and 1/10 volume of 3M NaOH were added to PCR products. Samples were incubated at -20°C for a minimum of 1 hour to overnight. Samples were centrifuged at 13,000 rpm for 5 minutes and the supernatant discarded. The pellet was resuspended in 500µl of 70% ethanol and centrifuged at 13,000 rpm for 5 minutes. The supernatant was discarded and the pellet was dried using a desiccator. The pellet was resuspended in 30µl of sterile H_2O. 1µl was run on an electrophoresis gel.

2.1.11 Linker annealing

Two complementary oligonucleotides were designed, with *Nde*I compatible overhangs and diluted to 100nmol. 5µl of each was added to 40µl of sterile H_2O in an eppendorf tube and heated to 95°C in a water bath to anneal the linker. The water bath was then switched off and cooled to room temperature. 2µl of the heated and cooled solution was used in a ligation reaction with 50ng of digested vector in a 20µl ligation reaction (see section 2.1.4). Following ligation, 90µl of sterile H_2O was added and the sample was heated to 80°C for 5 minutes before cooling quickly. 20µl of the ligation mixture was then used for an *E. coli* transformation (see section 2.2.4)

2.1.12 Primers used in this study

2.1.12.1 Primers used in chapter 3

Primer name	Sequence 5' to 3'	Purpose
Sorf F sphI	GCATGCATTATATACCACATTACGCTATTCTTGCTTCAAACAATCACAACAGTCATTCCT	Amplify SUMO ORF for cloning into pAW8
Sorf R spe I	ACTAGTCTAAAGGCATAGATGGGTGCAACCACCTAACTGTTCTAAGACAGCCTC	
pAW41 Forward	AGTAAACGTAGTAAGCAAATAATTAACGTAGCTTTAAGACACAACTAAACAAAATAGTGGAGTAGATTTATACACGTTATTAGAATACTCAAGCTTGGAC	Integrate Ura4 and LoxP
pAW41 Reverse	GGGGTACAATCAAATTCTCATAGATCAGGAATGACTGTTGTGATTGTTTGAAGCAAGAATAGCGTAATGTGGTATATAATTTCACCACCCCCGCCGCCCG	
pAW12 F STOP	TTTAGCTTGATATGGAAGATGGCGATCAAATTGAGGCTGTCTTAGAACAGTTAGGTGGTTGCACCCATCTATGCCTTTAGAAGCTTAGCTACAAATCCCA	Integrate Ura4 and LoxM
pAW12 R stop	GATGCTGGAGATGATAAACGTATTGGCAAAATCAAAATATTAGTTTTGAGTATATGAAACAGCTTAAAAATACTTGTACTGAATTCGAGCTCGTTTAAAC	
LoxM check R	CTACCACAATTCGCCGATTAGAAGCCG	Sequence across LoxM site
sumo R seq	CTAAAGGCATAGATGGGTG	Sequence across trypsin cleavage site
PAW41 F seq	TGGAGTAGATTTATACACG	Sequence across LoxP site
Mut arg F	GCTGTCTTAGAACAGCGAGGTGGTTGCACCCATCTATGCC	Introduce trypsin cleavage site before GG
Mut arg R	AAGGCATAGATGGGTGCAACCACCTCGCTGTTCTAAGACAGC	
paw8 nde mut 1 F	CGGTAAGTAAATTGGACACATGATTTAACAAAGCG	Mutate Nde1 site in pAW8
paw8 nde mut 1 R	CGCTTTGTTAAATCATGTGTCCAATTTACTTACCG	
paw8 nde mut 2 F	CCTCTATCCTTTTGCTCACATGTTTATGAG	Mutate second Nde1 site in pAW8
paw8 nde mut 2 R	CTCATAAACATGTGAGCAAAAGGATAGAGG	

Primer name	Sequence 5' to 3'	Purpose
Nde mut1 check new	CCGGTTATTCAACTTGCACC	Sequence first Nde1 mutation
Nde mut 2 check F	GGCTCATGGCGTTAAAGAG	Sequence second Nde1 mutation
sumo bs Nde mut F	TATAGTATCTGAGAACATATGTCTGAATCACCATC	Mutate end of promoter to form Nde1 site with start codon
sumo bs Nde mut R	GATGGTGATTCAGACATATGTTCTCAGATACTATA	
sumo bs HIS linker F	TATGGGTAGCAGCCACCATCATCACCATCATCA	HIS_6 Linker for SUMO base strain
sumo bs HIS linker R	TATGATGATGGTGATGATGGTGGCTGCTACCCA	
pREP His linker F	CATGGGTAGCAGCCACCATCATCACCATCATCA	HIS_6 Linker for pREP vector
pREP His linker R	TATGATGATGGTGATGATGGTGGCTGCTACC	

2.1.12.2 Primers used in chapter 4

Primer name	Sequence 5' to 3'	Purpose
Nse2 pAW8 F (sph)	GCATGCTGCCATTCTTCATAAAAACG TACTGGAGGTTA	Amplify SUMO ORF for cloning into pAW8
Nse2_pAW8 R (spe)	ACTAGTCTAAGCTTCTTTTAAATTCG TTATTTCCTGAGCGC	
Nse2_pAW41 F	CCAAATGAGAATATTTCATAACCCAT TCATTTGTATTAAACGTGACAGTAAA TAAGAATTTATTTAGTCTTTATACAT ATAGAATACTCAAGCTTGGAC	Integrate Ura4 and LoxP
Nse2_pAW41 R	AAAGAATGTTTTTTAAGCAAGGGTA ATAACCACGTTTTAAAATTTAAACTC CAGTACGTTTTTATGAAGATTGATGG CATTCACCACCCCCGCCGCCCG	
Nse2_pAW12 F	GTCTTTACTTAAGAAAGATGAGATTC TTGAACGCAGATTACGCCGCGCTCAG GAATTAAGTAATTTAAAAGAAGCTTA GAAGCTTAGCTACAAATCCAA	Integrate Ura4 and LoxM
Nse2_pAW12 R	ATAAACAAATACATTAAATATAATAA TAATAATAATAATAATAAATCCGGATC AGTACTACAATGTAAATAGAAAAGGA GAATTCGAGCTCGTTTAAAC	
Nse2_loxPcheck F	CCAAATGAGAATATTTCATAACCCAT TCATTT	Sequence across LoxP site
Nse2_loxPcheck R	TCCCAAAGGTAAACCAACTTCTTTGA GGCCTTCTA	Sequence across LoxP site
Nse2_loxMcheck F	GCGCTCAGGAAATAAGTAATTTTAAA AGAAGCTTAG	Sequence across LoxM site
Nse2_LoxMcheck R	TAGGAACCAGTAGCCAAAGAGCCTTT GGAAGACAT	
Nse2_K134R_F	GGCACACAAGGAGAATACATTGAATT TAGAAAAACCATATGGCATGAGC	K134R mutagenesis
Nse2_K134R_R	GCTCATGCCATATGGTTTTTCTAAAT TCAATGTATTCTCCTTGTGTGCC	
Nse2_K229R_F	CAAAGGTCTTTACTTAGGGAAGATGA GATTCTT	K229R mutagenesis
Nse2_K229R_R	AAGAATCTCATCTTCCCTAAGTAAAG ACCTTTG	

Primer name	Sequence 5’ to 3’	Purpose
Nse2_K248R_F	GAAATAAGTAATTTAAGAGAAGCTTAGTCCTT	K248R mutagenesis
Nse2_K248R_R	AAGGACTAAGCTTCTCTTAAATTACTTATTTC	
A234_Stop F	CGCAGATTACGCCGCCTCAGGAAATAAGTAATTTAAAAG	A234 mutagenesis
A234_Stop R	CTTTTAAATTACTTATTTCCTGAGGCGGCGTAATCTGCG	
T172A F	GATAACAGATGCCCTTTAGCTTTACAACCAATTGTTC	T172 mutagenesis
T172A R	GAACAATTGGTTGTAAAGCTAAAGGGCATCTGTTATC	
Nse2 S223X F	5' GCTCGTTTACAAAGGTGATTACTTAAGGAAGATG 3'	S223X mutagenesis
Nse2 S223X R	5' CATCTTCCTTAAGTAATCACCTTTGTAAACGAGC 3'	
K135X (S116) F	GAATACATTGAATTTAAATAAACCATATGGCATGAGC	K135X mutagenesis
K135X (S116) R	GCTCATGCCATATGGTTTATTTAAATTCAATGTATTC	
pAW8 external F	TGCGCCTGCTGGAAGATG	Sequencing primers
pAW8 external R	GAGCGCAGCGAGTCAGTG	

2.1.12.3 Primers used in chapter 5

Primer name	Sequence 5' to 3'	Purpose
Pcn1 LoxM chkR	CAAGTTTTTCTACCCTTCAG TTTGTTGGTTCT	Sequence across LoxM site
PCN1 CHK2	CAATGACAACGGTATCTCTCT GCA	Sequencing primer
PCNA bs lox P check F	GCGTATTACGTAGTGTATGG	Sequence across LoxP site
PCNA K13R F	CAGGCTGCTTTGTTGAGAAA GCTTCTCGATGCC	Lysine to arginine mutagenesis primers
PCNA K13R R	GGCATCGAGAAGCTTTCTCA ACAAAGCAGCCTG	
PCNA K164R F	ACTAGCATTGATTGTAGAGA GGGTGTTCGTTTTAG	
PCNA K164R R	CTAAAACGAACACCCTCTCTA CTAGCATTGATTGT	
PCNA K172R F	GTTCGTTTTAGCTGCAGGGG AGATATTGGTAATG	
PCNA K172R R	CCATTACCAATATCTCCCCTG CAGCTAAAACGAAC	
PCNA K253R F	TTTTATCTTGCCCCAAGAAT TGGTGAGGAGGATG	
PCNA K253R R	CATCCTCCTCACCAATTCTTG GGGCAAGATAAAA	
PCNA stop R	CTCCTCATCCTCCTCACC	Sequencing primer
PCNA Nde1 mut F	GCTTGTATAAAATATAATTAC GCATATGCTTGAAGCTAG	Nde1 mutagenesis at start codon
PCNA Nde1 mut R	CTAGCTTCAAGCATATGCGTA ATTATATTTTATACAAGC	
HIS linker F	TATGGGTAGCAGCCACCATCA TCACCATCATCA	HIS linker for PCNA base strain
HIS linker R	TATGATGATGGTGATGATGG TGGCTGCTACCCA	

2.2 BACTERIAL METHODS

2.2.1 *E. coli* strains

NM522

NM522 competent cells were used for expression and purification of plasmid DNA. NM522 contains a lacZ mutation which can be complemented with plasmids encoding lac-α to allow for blue-white screening.

BL21

BL21 competent cells were used for expression and purification of recombinant tagged proteins. BL21 strains contain the λ-DE3 lysogen which encodes for the lacI repressor gene and the T7 RNA polymerase under the control of an inducible lac-UV5 promoter. The lac repressor binds the lac operator, preventing transcription and thus repressing expression of the T7 RNA polymerase. IPTG is a compound which can bind the lac repressor. This prevents the repressor from binding to the lac operator, inducing expression of the T7 RNA polymerase. This strain can therefore provide inducible expression of gene products cloned into expression vectors which contain the T7 promoter, following addition of IPTG (life technologies). The BL21 cells used here are chloramphenicol resistant.

2.2.2 Bacterial media

LB broth was used to grow bacterial cultures. Components are as follows:

Tryptone	10g/l
Yeast extract	5g/l
NaCl	5g/l

8g/l agar was added to make solid media.

Antibiotics were added to solid or liquid media to select for cells containing plasmids with antibiotic resistant markers. Antibiotics were used at the following concentrations:

Ampicillin	100µg/ml
Kanamycin	50µg/ml
Chloramphenicol	34µg/ml

2.2.3 Preparation of competent *E. coli* cells

A single colony was inoculated in 5ml LB media and incubated overnight at 37°C with shaking (180rpm) (BL21 cultures were supplemented with 24µg/ml chloramphenicol). This pre-culture was diluted with 1 litre of pre-warmed LB media and incubated at 37°C with shaking (180rpm) for 2 – 4 hours until OD_{600} 0.5-0.6. The culture was then chilled on ice for 30 minutes to 1 hour before being centrifuged at 5000rpm for 5 minutes at 4°C . The supernatant was discarded and the pellet resuspended in 25ml ice cold TRNS 1 solution. This was incubated in ice for 30 to 60 minutes. Cells were harvested by centrifugation at 5000 rpm for 5 minutes at 4°C. The pellet was resuspended in 12ml of TRNS 2 solution and incubated on ice for one hour. The cells were snap frozen using in eppendorf tubes in 300µl aliquots using liquid nitrogen.

TRNS 1

RbCl	12g/l
$MnCl_2.4H_2O$	9.9g/l
$CaCl.2H_2O$	1.5g/l
CH_3COON_a	2.88g/l
Glycerol	66ml/l
pH adjusted to 5.8 using 0.2M acetic acid	

TRNS 2

RbCl	6g/l
$CaCl.2H_2O$	11g/l
MOPS	2.1g/l
Glycerol	66ml/l
pH adjusted to 6.8 using KOH	

2.2.4 *E. coli* transformation

Competent cells were thawed on ice for 10 to 15 minutes. 100-200ng of plasmid DNA was added to 100µl of thawed cells and incubated on ice for 20 to 30 minutes. The cells were heat shocked at 37°C for 90 seconds. 1 ml of LB media was added and the cells incubated at 37°C to allow expression of the antibiotic resistance gene. Cells were centrifuged at 3000rpm for 5 minutes. The supernatant was discarded and the cells resuspended in the remaining supernatant (approximately 100µl). Cells were spread onto solid LB media containing the appropriate antibiotics and incubated at 36°C overnight.

2.2.5 Blue-white selection

Blue-white selection was used to select for recombinant *E. coli* containing plasmids with insertional inactivation of the lacZ gene. Where blue-white selection as used, X-GAL and IPTG were added to solid media to a final concentration of:

X-GAL	100µg/ml
IPTG	0.5mM

2.2.6 Bacterial vectors

pGEM-T Easy (Promega)

The pGEM-T easy vector was used as a cloning vector prior to sub-cloning into subsequent vectors. pGEM-T easy is a linearised vector with 3' thymidine overhangs. This allows for efficient ligation with PCR products where deoxyadenosine overhangs which are added by some *taq* polymerases. The multiple cloning site is located within the α-peptide coding region of β-galactosidase. Successful ligations result in insertional inactivation of this coding region, allowing for blue-white screening of recombinant vectors. T7 and SP6 RNA polymerase promoters flanking the multiple cloning site were used for sequencing with complementary universal primers SP6 and Y7 which are provided by GATC.

pET15b

The pET15b expression vector was used to fuse N-terminal 6xHIS tags to proteins of interest. This allows for purification of affinity tagged proteins using Ni^{2+} agarose beads (QIAGEN, see section 2.3.5). A thrombin cleavage site allows for cleavage of the HIS tag following expression and purification if required. Expression is under control of the T7 RNA polymerase promoter and thus inducible by addition of IPTG. pET15b also encodes an ampicillin resistance gene.

pGEX KGH

pGEX KGH expression vector was used to express N-terminally GST tagged proteins. Following expression proteins were purified using glutathione sepharose beads (Pierce). A thrombin cleavage site allows for cleavage of the GST tag following expression and purification if required. Expression is under control of the tac promoter, which is a hybrid of two bacterial promoters, *trp* and l*ac (SIGMA Aldrich).* This allows for IPTG induced expression of the recombinant protein. pGEX contains an ampicillin resistance gene.

2.3 PROTEIN METHODS

2.3.1 SDS-PAGE

Biorad Mini Protean II kits were used for SDS-PAGE gel preparation. Proteins were resolved on 10 or 12.5% separating gels. 100µl of 10% ammonium persulphate (APS) and 10 µl of TEMED was added to 10ml of separating buffer solution. The separating solution was poured between 1mm Biorad glass plates which had been previously cleaned using IMS. 500µl of isobutanol was added on top of the solution which was left to set at room temperature for 20 minutes. Once set, the isobutanol layer was poured off and distilled water was used to remove any traces of isobutanol. Whatman 3mm filter paper was used to extract residual water. 50µl of 10% APS and 10µl of TEMED was added to 5ml of 6% stacking gel solution. The stacking gel was poured on top of the separating gel and a 1mm 10 or 15 well gel comb placed in between the plates. The stacking gel was left to set at room temperature for approximately 20 minutes. The gel comb was removed and gels assembled using a Bio-rad kit. 5X SDS sample buffer was added to protein samples. Samples were denatured at 90°C for 5 minutes. 10-20 µl of samples were loaded into each well. 8 µl of *Colourplus 17-175 kDa protein ladder* (Invitrogen) was loaded into the first lane for size comparison. Gels were covered with 1 x SDS running buffer and run at 150 V for approximately 45 minutes or until the dye front reached the bottom of the gel.

4X Separating gel buffer

Tris HCl, pH 8.8	1.5 M
SDS	0.4%

4X stacking gel buffer

Tris HCl, pH 6.8	0.5 M
SDS	0.4%

Separating gel solution (to make 2 gels)

	10%	**12.5%**
Protogel	3.3ml	4.2ml
4 x separating gel buffer	2.5ml	2.5ml
Distilled H_2O	5.0ml	3.3ml
10% APS	100 µl	100 µl
TEMED	10 µl	10 µl

Stacking gel solution (to make 2 gels)

	6%
Protogel	1.0 ml
4 x separating gel buffer	1.3 ml
Distilled H_2O	2.8 ml
10% APS	50 µl
TEMED	10 µl

2.3.2 Gel staining

SDS-PAGE gels were stained using either Coomassie stain or *Instantblue* (Expedion). For Coomassie staining, SDS-PAGE gels were placed in a clean dish and approximately 10ml of Coomassie gel stain added. Gels were incubated at room temperature for 1 hour or at 4°C overnight with gentle shaking. Gels were then rinsed with water before being placed in approximately 10ml of destain solution overnight with gentle shaking. For *Instantblue* staining, SDS-PAGE gels were placed in a clean square petri dish and 10ml of *Instantblue* (Expedeon) stain added. Gels were incubated with gentle shaking at room temperature for 30 minutes to allow protein bands to become visible. Sterile H_2O was used to rinse gels before protein gel extraction for analysis by mass spectrometry

Coomassie gel stain

Coomassie Brilliant Blue (Sigma)	1g/l
Methanol	45%
Glacial acetic acid	10%

Destain solution

Methanol	10%
Glacial acetic acid	10%

SDS-PAGE gels were placed in a clean square petri dish and 10ml of *Instantblue* (Expedeon) stain added. Gels were incubated with rocking at room temperature for 30 minutes to allow protein bands to become visible. Sterile H_2O was used to rinse gels before protein gel extraction for analysis by mass spectrometry

2.3.3 Western blotting

Whatman 3mm filter paper was cut to slightly larger than an SDS-PAGE gel, and twelve pieces per gel were soaked in 1 X semi-dry transfer buffer. One piece of PVDF membrane (Millipore) per gel was also cut to the size of an SDS-PAGE gel and soaked in methanol. 6 pieces of Whatman paper were stacked and placed on an Electroblotter (Biorad). A 50ml tube was used to roll over the paper and remove any air bubbles. A piece of PVDF membrane was then placed on top of the stack. The SDS-PAGE gel was laid on top of the membrane and 6 pieces of Whatman paper soaked in semi-dry transfer buffer were placed on top of the gel. Bubbles were removed by again using a 50ml tube to roll over the stack. The Electroblotter was run at 150mA for 35 minutes per gel. The top stack of filter paper and the SDS-PAGE gel were discarded, and the PVDF membrane was transferred to a clean container and covered with 4% milk (in PBS containing 0.1% tween-20). The membrane was blocked by incubating for a minimum of 30 minutes at room temperature or overnight at 4^{o}C with gentle shaking.

Appropriate primary antibodies were added to blocked PVDF membranes at a concentration of 1:2000, unless stated otherwise. Membranes were incubated with primary antibody for 1 hour or overnight at 4°C with gentle shaking.

Membranes were washed with 3 x 5 minute changes of PBS containing 0.1% Tween-20. 10 ml of 4% milk (in PBS containing 0.1% tween-20) was added to membranes and an HRP-conjugated secondary antibody was added to a final concentration of 1:2,000. Membranes were incubated at room temperature for 1 hour with gentle shaking. Membranes were washed using 2 x 5minute changes of PBS containing 0.1% tween and a 1 x 5 minute incubation with PBS.

2.3.4 Enhanced Chemi-luminescence (ECL)

Proteins were visualised by incubating membranes with *Pierce* ECL Western Blotting Substrate as per manufacturer's instructions for approximately two minutes. Membranes were placed between two sheets of projector film and exposed to X-ray film (Kodak) in a dark room for 30 seconds to 1 hour, depending on strength of the antibodies. X-ray film was developed using an x-ray developer machine.

2.3.5 Ni^{2+}affinity purification

A single colony of BL21 *E. coli* containing the appropriate expression vector was inoculated in 10ml of LB media containing the appropriate antibiotics. The culture was incubated overnight at 37^{o}C with shaking (180rpm). The pre-culture was added to 1-litre of pre-warmed LB media containing the appropriate selective antibiotic. The culture was incubated at 37°C for approximately 4 hours to OD_{600} 0.6. Protein expression was induced by addition of 1mM IPTG. The culture was incubated either for 4 hours at 37°C or overnight at 16°C with shaking (180rpm). The cells were harvested by centrifugation at 5,000 rpm for 5 minutes and the supernatant discarded. The cell pellet was stored at –20^{o}C for 1 – 24 hours, before being re-suspended in 20 ml ice-cold binding buffer freshly supplemented with 0.1mM PMSF or one protease inhibitor tablet (Roche) per 50ml buffer. The cells were sonicated on ice at 27% amplitude for 5 x 15 seconds, with 30 second intervals. The cells were centrifuged at 15,000 rpm for 15 minutes at 4^{o}C. The supernatant was decanted into a clean 15ml polypropylene tube and kept on ice. 500µl of Ni^{2+}-agarose beads were added to a 5ml chromatography column (NEB) at 4°C. 6ml of binding buffer were added to the column and allowed to flow through to

equilibrate the beads. The cell lysate was applied to the column and allowed to pass through the column by gravity. The beads were then washed by adding 10ml of binding buffer, followed by 10ml of wash buffer. Elution buffer was added to the column and 6 x 0.5 ml fractions were collected and placed on ice. The protein concentration of each elution was determined by Bradford assay and 10µl samples were analysed by SDS-PAGE as described above. The elution fractions containing the highest concentrations of protein were snap frozen using liquid nitrogen and stored at -80°C.

Binding buffer

Tris-HCl pH 7.5	20mM
NaCl	200mM
Imidazole	30mM

Wash buffer

Tris-HCl pH 7.5	20mM
NaCl	200mM
Imidazole	60mM

Elution buffer

Tris-HCl pH 7.5	20mM
NaCl	200mM
Imidazole	500mM

2.3.6 GST purification

A single colony of BL21 *E. coli* containing the appropriate expression vector was inoculated in 10ml of LB media containing the appropriate antibiotics. The culture was incubated overnight at 37^{o}C with shaking (180rpm). The pre-culture was added to 1-litre of pre-warmed LB media containing the appropriate selective antibiotic. The culture was incubated at 37°C for approximately 4 hours to OD_{600} 0.6. Protein expression was induced by addition

of 1mM IPTG. The culture was incubated either for 4 hours at 37°C or overnight at 16°C with shaking (180rpm). The cells were harvested by centrifugation at 5,000 rpm for 5 minutes and the supernatant discarded. The cell pellet was stored at –20°C for 1 – 24 hours, before being re-suspended in 15ml NETN + freshly supplemented with 0.1mM PMSF or one protease inhibitor tablet (Roche) per 50ml buffer. The cells were sonicated on ice at 27% amplitude for 5 x 15 seconds, with 30 second intervals. The cells were centrifuged at 15,000 rpm for 15 minutes at 4°C to clear cell debris. The supernatant was decanted into a clean 15ml polypropylene tube and kept on ice. 500µl of glutathione sepharose (GST) beads were added to a 5ml chromatography column. 3 bed volumes of NETN buffer freshly supplemented with protease inhibitors was added to the column and allowed to flow through by gravity to equilibrate the beads. The cell lysate was added to the beads. A cap was placed on the bottom of the column and the beads and lysate were incubated at 4°C for an hour on a roller. The beads were washed four times by adding 5 bed volumes of NETN, followed by 5 bed volumes of wash buffer. To elute bound proteins, 1 bed volume of elution buffer was added to the beads. A cap was placed onto the column and the sample was incubated on a roller at 4°C for 30 minutes to one hour. 6 x 0.5 ml fractions were collected and placed on ice. The protein concentration of each elution was determined by Bradford assay and 10µl samples were analysed by SDS-PAGE as described above. The elution fractions containing the highest concentrations of protein were snap frozen using liquid nitrogen and stored at -80°C.

NETN buffer

Tris-HCl pH 8.0	20mM
NaCl	100mM
EDTA	1mM
NP-40	0.5%

Wash buffer

Tris-HCl pH 8.0	100mM
NaCl	120mM

Elution buffer

Tris-HCl pH 8.0	100mM
NaCl	120mM
Glutathione	20mM

2.3.7 *pfu* purification

Following transformation with pGEX-pfu, BL21 cells were inoculated in 10ml LB with kanamycin at 37°C overnight. This pre-culture was used to inoculate 500ml of LB supplemented with kanamycin and incubated at 37°C with shaking (180rpm) until they reached OD_{600} 0.6. Protein expression was induced by adding 1mM IPTG and incubating for a further 4 hours. Cells were pelleted by centrifugation at 3000 rpm for 5 minutes. The cell pellet was resuspended in PBS300. Cells were lysed by sonicating at 27% amplitude for 5 seconds three times. The lysed cells were centrifuged at 15,000 rpm for 30 minutes. The supernatant was decanted into a fresh 15ml tube and incubated at 75°C for 30 minutes. The sample was centrifuged at 15,000 rpm for 15 minutes and the supernatant transferred to a fresh tube. 0.5ml of Ni^{2+} agarose was added to a 15ml chromatography column (New England Biolabs). The beads were equilibrated with 10ml PBS300 (PBS + 150mM NaCl). The heat treated supernatant was then applied to the column. The beads were washed with 20ml of PBS300 + 15mM imidazole, and then with 3ml PBS300 + 25mM imidazole. 5 x 1ml elution fractions were collected after addition of 5ml PBS300 + 500mM imidazole. 5µl of each elution fraction was visualised on a 7.5% SDS PAGE gel (see section 2.3.1). Peak fractions were combined and an equal volume of storage buffer added. Samples were dialysed against 2 changes of 1l of storage buffer at 4°C for 12 hours. Samples were aliquoted and stored at -80°C. Serial

dilutions of the enzyme were prepared in storage buffer and used to compare to commercially available pfu in order to determine an appropriate dilution factor.

Pfu storage buffer

Tris pH8.0	50mM
EDTA	0.1mM
DTT	1mM
NP-40	0.1%
Tween-20	0.1%
Glycerol	50%

2.3.8 Bradford assay

To determine the protein concentration of a sample, 1ml of Bradford assay reagent (Biorad) was diluted with 4ml of H_2O. 1µl protein sample was added to 1 ml of diluted Bradford reagent. 1ml of diluted Bradford reagent was used as a blank control and the OD_{595} of the sample was measured using a spectrophotometer. Protein concentration of the sample was determined by comparing the sample reading against a BSA standard curve.

2.3.9 *In vitro* sumoylation assays

DNA encoding components of the SUMOylation pathway had previously been cloned into the expression vectors described below.

Component	**Plasmid**	**Tag**	**Antibiotic resistance**
SUMO.GG	pET15b	His	Ampicillin
Rad31 (E1 subunit)	pET28a	His	Kanamycin
Fub2 (E1 subunit)	pGEX	GST	Ampicillin
Hus 5 (E2)	pGEX	GST	Ampicillin
Pli1 (E3)	pET15b	His	Ampicillin

Recombinant proteins were expressed and purified as described above. Plasmid DNA containing the Rad31 and Fub2 was co-transformed into BL21 competent cells, expressed and co-purified using Ni^{2+} agarose as described above. The eluate was applied to 100µl GST beads and purified as described.

Typically, a 20µl reaction contained 2µl 10x SUMO reaction buffer, approximately 1.5µg GST-Ubc9, 10µg HIS-SUMOGG.tr , 2µg HIS-Rad31 – GST-Fub2, 3.5U Creatine phosphokinase, 0.12U pyrophosphatase and 1µg of the protein of interest, with or without 1µg GST_Pli1. Reactions were incubated at 30°C for two hours, and analysed by SDS-PAGE and *Instantblue* staining. Where mass spectrometry was used for analysis, 40µl reactions were set up. In this case 30µl was used for staining and 10µl for analysis by western blot.

10 x SUMO reaction buffer

Tris-HCl	500mM
$MgCl_2$	50mM
ATP	50mM
Creatine phosphate	100mM

2.3.10 TCA extraction of proteins from *S. pombe*

Overnight cultures of *S. pombe* were diluted to OD 0.2 and incubated at 30°C for 3 – 4 hours. $4x10^7$ cells of exponentially growing *S. pombe* cultures were pelleted by centrifugation at 3000 rpm for 5 minutes. Pellets were resuspended in 500µl H_20 and placed on ice. 75µl NaOH/BME was added and samples were vortexed and incubated on ice for 15 minutes. 75µl of 50% TCA was added to and samples were vortexed before incubating on nice for a further 10 minutes. Samples were centrifuged at 13,000 rpm for 10 minutes at 4°C. Supernatant was aspirated and the pellets were resuspended in 30µl HU buffer. If the sample turned yellow, 1µl of 1.5M Tris-HCl pH8.8 was added. Samples were denatured at 90°C for 10 minutes before being centrifuged at 13,000 rpm for 5 minutes. Samples were analysed by SDS-PAGE.

2.3.11 Denaturing *in vivo* pull down using Ni^{2+} beads

10^9 cells of exponentially growing *S. pombe* were pelleted by centrifuging at 3,000 rpm for 5 minutes. Pellets were resuspended in 5ml ice cold H_2O and placed on ice. 0.8ml of freshly made NaOH/BME was added and samples were vortexed and then incubated on ice for 20 minutes. 0.8ml of 50% TCA was added to samples which were then centrifuged and incubated on ice for 20 minutes. Samples were centrifuged at 10,000 rpm for 20 minutes at 4°C.

Supernatant was discarded and the pellets resuspended in 1ml of buffer A. Samples were transferred to a clean eppendorf tube and incubated at room temperature for 1 hour on a rotating wheel. Samples were centrifuged at 13,000 rpm for 10 minutes at 4°C. The supernatant was transferred to a fresh eppendorf tube. 30µl aliquots of Ni^{2+} agarose beads per sample were washed three times using 500µl of buffer A + 0.05% tween-20. The cell extract (supernatant) was applied to the equilibrated Ni^{2+} agarose beads. 15µl of 10% tween-20 and 15mM imidazole was added to each sample. Samples were incubated overnight at room temperature on a rotating wheel. Samples were centrifuged for 2,000 rpm for 30 seconds and the pellet washed twice with 1ml buffer A + 0.05% tween-20. Samples were then washed four times with 1ml of buffer C containing 0.05% tween. Samples were centrifuged at 200 rpm for 30 seconds and supernatant discarded. The beads were resuspended in 30µl HU buffer. Samples were denatured at 90°C for 5 minutes before being centrifuged at 13,000 rpm for 5 minutes. Samples were analysed by SDS-PAGE.

NaOH/BME

NaOH	1.85M
2-mercaptoethanol	7.5% w/v

Buffer A

Guanidinium HCl	6M
NaH_2PO_4 pH8.0	0.4M
Tris-HCl pH8.0	1M

Buffer C

Urea	8M
NaH_2PO_4 pH6.3	0.4M
Tris-HCl pH6.3	1M

Tween-20

Tween	10% w/v

HU buffer

Urea	8M
EDTA	1mM
Tris-HCl pH6.8	200mM
SDS	5% w/v
DTT	1.5% w/v
Bromophenol blue	0.1%

2.3.12 In-gel digestion of *Instantblue* stained proteins

Protein bands were excised from SDS-PAGE gels using a sterile scalpel and placed in low protein binding eppendorf tubes. A sterile micro-pipette tip was used to break the gel into small pieces. 50µl of acetonitrile was added to the gel pieces and the sample was vortexed briefly. The sample was centrifuged at 3,000 rpm for 30 seconds and the supernatant discarded. 50µl of acetonitrile was added and the sample incubated at room temperature for 15 minutes. The sample was centrifuged at 3,000 rpm for 30 seconds and the supernatant discarded. 50µl of 10mM DTT/25mM NH_4HCO_3 (ammonium bicarbonate) was added to the sample which was then vortexed briefly. The sample was heated at 90°C for 15 minutes to reduce the proteins. The sample was cooled to room temperature and then centrifuged at 3,000 rpm for 30 seconds. The supernatant was discarded. 50µl of 55mM iodoacetamide/25mM NH_4HCO_3 was added and the sample was vortexed briefly. The sample was centrifuged as above and supernatant removed. The gel pieces were washed with 50µl of 25mM NH_4HCO_3 for 10 minutes. 50µl of acetonitrile was added and the sample was briefly vortexed before being centrifuged as above. The supernatant was discarded. The sample was washed by again adding 50µl 25mM NH_4HCO_3 and incubating at room temperature for 5 minutes. The sample was centrifuged and supernatant discarded as above. The gel pieces were dried in a speedvac for approximately 30 minutes. 5µl of 25ng/µl trypsin and 45 µl of 25mM NH_4HCO_3 was added and the sample was incubated on ice for 45 minutes. The sample was then incubated overnight at 37°C.

The supernatant was removed from the sample and placed in a fresh eppendorf tube. 50mM of 20mM NH_4HCO_3 was added to the remaining gel pieces. These

were vortexed briefly and incubated at room temperature for 20 minutes before being centrifuged at 3 000 rpm for one minute. The supernatant was added to the fresh eppendorf tube. This step was repeated twice using 50µl of 5% formic acid/50% acetonitrile. The pooled supernatant was concentrated to approximately 20µl using a speedvac. Samples were stored at -20°C until required for analysis by mass spectrometry, which was carried out by other members of the lab.

2.3.13 2D gel analysis

2.3.13.1 Protein extraction

Approximately $2x10^8$ cells from exponentially growing *S. pombe* culture were harvested by centrifugation at 3,000 rpm for 5 minutes. Pellets were resuspended in 1ml of 20% TCA and transferred to a clean eppendorf tube. Samples were centrifuged at 13,000 rpm for 1 minute and supernatant discarded. Pellets were resuspended in 200µl of 20% TCA and transferred to screw cap tubes. An equal volume of glass beads was added and samples were ribolysed 3 times for 20 seconds. A sterile needle was used to pierce the bottom of the tubes and these were placed on top of a clean eppendorf tube, inside of a 15ml polypropylene tube. 400µl of 5% TCA was added and samples were centrifuged at 1,000 rpm for 1 minute. The sample collected in the eppendorf tubes was centrifuged at 13,000 rpm for 5 minutes at 4°C and the supernatant was discarded. Samples were again centrifuged at 13,000 rpm for 1 minute at 4°C and any remaining supernatant removed by pipetting. Pellets were resuspended in 1ml of ice cold acetone. Samples were incubated on ice for 30 minutes with agitation. Samples were centrifuged at 13 000 rpm for 30 minutes at 4°C. Supernatant was discarded and pellets were dried using a dessicter for 10 minutes. Pellets were resuspended in 200µl of resuspension buffer freshly supplemented with IPG buffer and DTT and were incubated at room temperature for 60 minutes on a rotating wheel. Samples were centrifuged at 13,000 rpm for 15 minutes. The supernatant was transferred to a clean 1.5ml eppendorf tube. A Bradford assay was performed to determine the protein concentration of the samples. 50µg of proteins were diluted with 125µl of rehydration buffer freshly supplemented with IPG buffer and DTT.

2.3.13.2 Rehydration

The samples were pipetted in a line along the edge of a channel of an IPG strip holding tray. The cover sheet of an IPG strip (Bio-Rad pH3-10) was peeled off and the strip placed face down on top of the protein sample, ensuring that no bubbles were present. 1 – 2ml of mineral oil was pipetted on top of the strips to prevent drying out. A plastic lid was placed over the tray and samples were incubated overnight at room temperature.

2.3.13.3 First Dimension

The next day, strips were removed and held over tissue paper to remove excess mineral oil. Strips were placed face up into a lane on an Ettan IPGphor isoelectric focusing machine as per manufacturer's instructions. The first dimension was run using the settings outlined below:

Step	**Voltage**	**kV/h**
Step and hold	300	0.2
Gradient	1000	0.3
Gradient	5000	4.0
Step and hold	5000	2.0

2.3.13.4 Second dimension

Strips were placed face up in an IPG strip holding tray and 2.5ml of equilibration buffer freshly supplemented with 10mg/ml DTT was added. Samples were incubated for 15 minutes at room temperature with gentle shaking. Samples were rinsed using sterile H_2O and then incubated for a further 15 minutes with 2.5ml of equilibration buffer freshly supplemented with 25mg/ml iodoacetamide. 10% 1mm SDS-PAGE gels were prepared with a 6% stacking gel and an IPG strip comb. IPG strips were dipped in 1 X SDS running buffer and loaded onto the SDS gel, ensuring that the strip is in contact with the stacking gel. Strips were overlayed with 1 x laemmli SDS buffer + 0.5% low melting point agarose. Samples were run next to 10µl of *Colourplus* broad range pre-stained protein ladder (New England Biolabs). SDS-PAGE gels were run at 150V for approximately an hour or until the dye front reached the bottom of the gel. Proteins were visualised by western blotting as described above.

Resuspension buffer

Urea	7M
Thiourea	2M
CHAPS	4%
DTT	60mM
IPG buffer pH 3-10	2%

Rehydration buffer

Urea	6M
Thiourea	2M
CHAPS	2%
DTT	50mM
IPG buffer pH 3-10	0.5%
Bromophenol blue	0.002%

Equilibration buffer

Tris-HCl pH8.8	50mM
Glycerol	30%
Urea	6M
SDS	10%
Bromophenol blue	0.002%

1 X Laemmli SDS buffer

Tris-HCl pH6.8	63mM
Glycerol	10%
SDS	2%
Bromophenol blue	0.002%
Low melting point agarose	0.5%

2.3.14 Phos-tag gel analysis

2.3.14.1 Sample preparation

Whole cell extracts from *S. Pombe* cultures were prepared as described in section 2.3.10, using HU buffer without EDTA, following exposure to either12mM HU or 0.05% MMS.

HU buffer - EDTA

Urea	8M
Tris-HCl pH6.8	200mM
SDS	5% w/v
DTT	1.5% w/v
Bromophenol blue	0.1%

2.3.14.2 SDS-PAGE gel preparation

7.5% SDS-PAGE gels were made as desscribed in section 2.3.1, with 20uM $MnCl_2$ and 10uM phos-tag added to the resolving gel mix immediately before the temed. 6% stacking gel was prepared as described in section 2.3.1. 10µl of each sample was loaded into the gel. No molecular weight marker was used due to the presence of EDTA in the buffers of commercially available markers. Gels were ran at 45V for two to three hours or until the dye reaches the bottom of the gel.

2.3.14.3 Western blotting

PVDF membrane (Millipore) per gel was cut to the size of an SDS-PAGE gel and soaked in methanol for one minute, before being soaked in ‘ transfer buffer B’ for 30 minutes. The SDS PAGE gel was soaked in transfer buffer B + 1mM EDTA for 10 minutes, and then in transfer buffer B - EDTA for 10 minutes with gentle shaking. 6 pieces of Whatman 3mm filter paper were cut to slightly larger than an SDS-PAGE gel. Two Pieces were soaked in ‘transfer buffer A, One piece was soaked in ‘transfer buffer B’ and three pieces were soaked in ‘transfer buffer C’.

The filter papers and membrane were placed in an Electroblotter (Biorad) in the following order : Two layers of filter paper soaked in transfer buffer A (bottom), one layer of filer paper soaked in transfer buffer B, PVDF membrane, SDS-PAGE gel, and finally three layers of filter paper soaked in transfer buffer C on top. Air

bubbles were removed by rolling a 50ml tube on top of the filter paper and gel stack. The gel was transferred at 40mA for 1 hour and 15 minutes.

The top stack of filter paper and the SDS-PAGE gel were discarded, and the PVDF membrane was transferred to a clean container and covered with 5% milk (in PBS containing 0.1% tween-20). The membrane was blocked by incubating for a minimum of 40 minutes at room temperature or overnight at 4°C with gentle shaking. Membranes were incubated with primary antibody for 1 hour or overnight at 4°C with gentle shaking. Membranes were washed with 3 x 5 minute changes of PBS containing 0.1% Tween-20. The membrane was incubated with 10ml of a 1:2000 dilution of α-Cds1 antibody in 0.5% milk-PBST for a minimum of three hours or overnight at 4°C. Secondary antibodies (α-rabbit) were added as described in section 2.3.3 and Proteins were visualised as described in section 2.3.4.

Transfer buffer A

Tris-HCl pH10.4	300mM
Methanol	15%

Transfer buffer B

Tris-HCl pH10.4	30mM
Methanol	15%

Transfer buffer C

Tris-HCl pH9.4	25mM
Methanol	15%
e-aminocaproic acid	40mM

2.4 *S. pombe* methods

2.4.1 *S. pombe* media

S. pombe media was used as follows:

Rich media (YE)

Yeast extract	5g/l
Glucose	20g/l
Adenine	200mg/ml
Leucine, uracil, histidine and arginine	100mg/ml
For solid media (YEA), 25 g/l DIFCO Bactoagarwas added.	

Minimal media (YNB)

Yeast Nitrogen Base	1.9g/l
Glucose	20g/l
Ammonium sulphate	4g/l
For solid media (YNB), 30g/l DIFCO Bactoagar and 0.2 ml/l of 10M NaOH was added to liquid YNB.	

Solid sporulation media (ELN – Extra low nitrogen)

Formedium Edinburgh Minimal Media (EMM)	27.3g/l
Ammonium chloride	50 mg/l
Adenine	200mg/l
Leucine	100mg/l
Uracil	100mg/l
Histidine	100mg/l
Arginine	100mg/l
DIFCO (Bacto) Agar	25g/l

2.4.2 *S. pombe* strains

The strains 501 and 503 used in this study as 'wild type' have the genotype *ade6-704, leu1-32, ura4-D18.* They require adenine, L-leucine and uracil to be added to minimal media for growth. This means that one or a combination of these amino acids can be used as a marker when present on a transformed plasmid, or when integrated into the genome of the wild type strain. Strain used in this study are listed in Table 2.1.

2.4.3 Selective media

A final concentration of 100µg/ml of adenine, uracil or leucine was added to liquid or solid YNB media to make selective media or plates. Fluoroorotic Acid (5'FOA) is converted to a toxic product 5-flurouracil by strains expressing a functional *ura4*$^{+}$ gene. Therefore 5-Fluoroorotic Acid (5'FOA) can be added to YEA or YNBA supplemented with appropriate amino acids to select for strains which do not contain the *ura4*$^{+}$ gene. Antibiotic markers which are either integrated into the genome or located on a plasmid can be selected for by adding the appropriate antibiotic to solid or liquid media. Antibiotic markers used in this study include nourseothricin (NAT) and geneticin. Phloxine B was added to YEA to stain dead cells. Thiamine was added to YNBA media supplemented with appropriate amino acids to repress the *nmt*1 promoter encoded in some expression vectors. The table below shows final concentrations of supplements added to media for selection. Note that G418 is not appropriate for use in minimal media.

Adenine	100µg/ml
L-Leucine	100µg/ml
Uracil	100µg/ml
5'FOA	1mg/ml
NAT	100µg/ml
G418	20mg/ml
Phloxine B	0.5mg/ml
Thiamine	5µg/ml

2.4.4 List of strains used in this study

Strain	Genotype
Wild type (wt)	*ade6-704, leu-32, ura4-D18, h+*
Wild type (wt)	*ade6-704, leu-32, ura4-D18, h-*
SUMO base strain	*(LoxP-SUMO-ura4^{+}-LoxM) ade6-704, leu-32, h+*
SUMO	*(LoxP-SUMO-LoxM) ade6-704, leu-32, h+*
SUMO.tr	*(LoxP-SUMO.tr-LoxM) ade6-704, leu-32, h+*
HIS-SUMO	*(LoxP-HIS$_6$-SUMO-LoxM) ade6-704, leu-32, h+*
HIS-SUMO-tr	*(LoxP-HIS$_6$-SUMO.tr-LoxM) ade6-704, leu-32, h+*
nse2 base strain	*(LoxP-nse2-ura4^{+}-LoxM) ade6-704, leu-32, h+*
nse2	*(LoxP-nse2-LoxM) ade6-704, leu-32, h+*
nse2-K134R	*(LoxP-nse2-K134R-LoxM) ade6-704, leu-32, h+*
nse2-K229R	*(LoxP-nse2-K229R-LoxM) ade6-704, leu-32, h+*
nse2-K248R	*(LoxP-nse2-K248R-LoxM) ade6-704, leu-32, h+*
nse2-K229R K248R	*(LoxP-nse2-K229R K248R-LoxM) ade6-704, leu-32, h+*
nse2-K134R K229R K248R	*(LoxP-nse2-K134R K229R K248R-LoxM) ade6-704, leu-32, h+*
nse2-T172A	*(LoxP-nse2-T172A-LoxM) ade6-704, leu-32, h+*
nse2-S226X	*(LoxP-nse2-S226X-LoxM) ade6-704, leu-32, h+*
nse2-T172A S226X	*(LoxP-nse2-T172A S226X-LoxM) ade6-704, leu-32, h+*
nse2-A234X	*(LoxP-nse2-A234X-LoxM) ade6-704, leu-32, h+*
pcn1 base strain	*(LoxP-pcn1-ura4^{+}-LoxM) ade6-704, leu-32, h+*
pcn1	*(LoxP-pcn1-LoxM) ade6-704, leu-32, h+*
pcn1-K164R	*(LoxP-pcn1-K164R-LoxM) ade6-704, leu-32, h+*
pcn1-K172R	*(LoxP-Pcn1-K172R-LoxM) ade6-704, leu-32, h+*
pcn1-K253R	*pcn1-K253R, ade6-704, leu-32, h+*
pcn1-K13R	*pcn1-K13R, ade6-704, leu-32, h+*
pcn1-K164R K172R	*pcn1-K164R K172R, ade6-704, leu-32, h+*
pcn1-K164R K253R	*pcn1-K164R K253R, ade6-704, leu-32, h+*
pcn1-K172R K253R	*pcn1-K172R K253R, ade6-704, leu-32, h+*

Strain	Genotype
pcn1-3R	*pcn1-K164R K172R K253R, ade6-704, leu-32, h+*
pli1-d	*pli1* : : *ura4*$^{+}$, *ade6-704, leu-32, ura4-D18, h+*
pli1-d, K164R	*pli1* : : *ura4*$^{+}$, *pcn1-K164R, ade6-704, leu-32, ura4-D18, h+*
pli1-d, K3R	*pli1* : : *ura4*$^{+}$, *pcn1-K164R K172R K253R ade6-704, leu-32, ura4-D18, h+*
nse2-SA	*nse2-SA* : : *ura4*$^{+}$, *ade6-704, leu-32, ura4-D18, h+*
nse2-SA, K164R	*nse2-SA* : : *ura4*$^{+}$, *pcn1-K164R, ade6-704, leu-32, ura4-D18, h+*
nse2-SA, 3R	*nse2-SA* : : *ura4*$^{+}$, *pcn1-K164R K172R K253R, ade6-704, leu-32, ura4-D18, h+*
rhp18-d	*rhp18* : : *kanMX6, ade6-704, leu-32, ura4-D18, h+*
rhp18-d, K164R	*rhp18* : : *kanMX6, pcn1-K164R, ade6-704, leu-32, ura4-D18, h+*
rhp18-d, K164R K172R	*rhp18* : : *kanMX6, pcn1-K164R K172R ,ade6-704, leu-32, ura4-D18, h+*
rhp18-d, K164R K253R	*rhp18* : : *kanMX6, pcn1-K164R K253R, ade6-704, leu-32, ura4-D18, h+*
rhp18-d, K172R K253R	*rhp18* : : *kanMX6, pcn1-K172R K253R, ade6-704, leu-32, ura4-D18, h+*
rhp18-d, 3R	*rhp18* : : *kanMX6, pcn1-K164R K172R K253R, ade6-704, leu-32, ura4-D18, h+*
mms2-d	*mms2* : : *natMX6, ade6-704, leu-32, ura4-D18, h+*
mms2-d, K164R	*mms2* : : *natMX6, pcn1–K164R ade6-704, leu-32, ura4-D18, h+*
mms2-d, K164R K172R	*mms2* : : *natMX6, pcn1–K164R K172R, ade6-704, leu-32, ura4-D18, h+*
mms2-d, K164R K253R	*mms2* : : *natMX6, pcn1–K164R K253R, ade6-704, leu-32, ura4-D18, h+*
mms2-d, 3R	*mms2 : : natMX6, pcn1-K164R K172R K253R, ade6-704, leu-32, ura4-D18, h+*
rev1-d	*rev1 : : kanMX6, ade6-704, leu-32, ura4-D18, h+*
rev1-d, K164R	*rev1 : : kanMX6, pcn1-K164R, ade6-704, leu-32, ura4-D18, h+*
rev1-d, K172R	*rev1 : : kanMX6, pcn1-K172R, ade6-704, leu-32, ura4-D18, h+*

Strain	Genotype
rev1-d, K164R K253R	*rev1 : : kanMX6, pcn1-K164R K253R, ade6-704, leu-32, ura4-D18, h+*
rev1-d, K172R K253R	*rev1 : : kanMX6, pcn1-K172R K253R, ade6-704, leu-32, ura4-D18, h+*
rev1-d, 3R	*rev1 : : kanMX6, pcn1-K164R K172R K253R, ade6-704, leu-32, ura4-D18, h+*
rev3-d	*rev3 : : kanMX6, ade6-704, leu-32, ura4-D18, h+*
rev3-d, K164R	*rev3 : : kanMX6, pcn1-K164R, ade6-704, leu-32, ura4-D18, h+*
rev3-d, K172R	*rev3 : : kanMX6, pcn1-K172R, ade6-704, leu-32, ura4-D18, h+*
rev3-d, K164R K253R	*rev3 : : kanMX6, pcn1-K164R K253R, ade6-704, leu-32, ura4-D18, h+*
rev3-d, K172R K253R	*rev3 : : kanMX6, pcn1-K172R K253R, ade6-704, leu-32, ura4-D18, h+*
rev3-d, 3R	*rev3 : : kanMX6, pcn1-K164R K172R K253R, ade6-704, leu-32, ura4-D18, h+*
dinB-d	*dinB : : kanMX6, ade6-704, leu-32, ura4-D18, h+*
dinB-d, K164R	*dinB : : kanMX6, pcn1-K164R, ade6-704, leu-32, ura4-D18, h+*
dinB-d, K172R	*dinB : : kanMX6, pcn1-K172R, ade6-704, leu-32, ura4-D18, h+*
dinB-d, K164R K253R	*dinB : : kanMX6, pcn1-K164R K253R, ade6-704, leu-32, ura4-D18, h+*
dinB-d, K172R K253R	*dinB : : kanMX6, pcn1-K172R K253R, ade6-704, leu-32, ura4-D18, h+*
dinB-d, 3R	*dinB : : kanMX6, pcn1-K164R K172R K253R, ade6-704, leu-32, ura4-D18, h+*
rad13-d	*rad13 : : ura4⁺, ade6-704, leu-32, ura4-D18, h+*
rad13-d, K164R	*rad13 : : ura4⁺, pcn1-K164R, ade6-704, leu-32, ura4-D18, h+*
rad13-d, K3R	*rad13 : : ura4⁺, pcn1-K164R K172R K253R, ade6-704, leu-32, ura4-D18, h+*
rad2-d	*rad2 : : ura4, ade6-704, leu-32, ura4-D18, h+*
rad2-d, pcn1-K164R	*rad2 : : ura4, pcn1-K164R, ade6-704, leu-32, ura4-D18, h+*
rad2-d, pcn1-3R	*rad2 : : ura4, pcn1-K164R K72R K253R, ade6-704, leu-32, ura4-D18, h+*
uve1-d	*uve1 : : LEU2, ade6-704, leu-32, ura4-D18, h+*
uve1-d, pcn1-K164R	*uve1 : : LEU2, pcn1-K164R, ade6-704, leu-32, ura4-D18, h+*
uve1-d, pcn1-3R	*uve1 : : LEU2, pcn1-K164R K172R K253R, ade6-704, leu-32, ura4-D18, h+*
sfr1-d	*sfr1 : : KanMX6, ade6-704, leu-32, ura4-D18, h+*
sfr1-d, pcn1-K164R	*sfr1 : : KanMX6, pcn1-K164R, ade6-704, leu-32, ura4-D18, h+*
sfr1-d, pcn1-3R	*sfr1 : : KanMX6, pcn1-K164R K172R K253R, ade6-704, leu-32, ura4-D18, h+*
mre11-d	*mre11 : : ura4, ade6-704, leu-32, ura4-D18, h+*
mre11-d, rhp18-d	*mre11 : : ura4, rhp18 : : kanMX6, ade6-704, leu-32, ura4-D18, h+*
mre11-d, pcn1-K164R	*mre11 : : ura4, rhp18 : : kanMX6, pcn1-K164R, ade6-704, leu-32, ura4-D18, h+*
mre11-d, pcn1-3R	*mre11 : : ura4, rhp18 : : kanMX6, pcn1-K164R K172R K253R, ade6-704, leu-32, ura4-D18, h+*
cds1-d	*cds1 : : ura4, ade6-704, leu-32, ura4-D18, h+*
cds1-d, pcn1-K164R	*cds1 : : ura4, pcn1-K164R, ade6-704, leu-32, ura4-D18, h+*
cds1-d, pcn1-3R	*cds1 : : ura4, pcn1-K164R K172R K253R ade6-704, leu-32, ura4-D18, h+*

Strain	Genotype
chk1-d	*chk1 : : ura4, ade6-704, leu-32, ura4-D18, h+*
chk1-d, pcn1-K164R	*chk1 : : ura4, pcn1-K164R, ade6-704, leu-32, ura4-D18, h+*
HA-chk1	*chk1 : ep, ade6-704, leu-32, ura4-D18, h+*
HA-chk1, pcn1-K164R	*chk1 : ep, pcn1-K164R, ade6-704, leu-32, ura4-D18, h+*
HA-chk1, pcn1-3R	*chk1 : ep, pcn1-K164R K172R K253R, ade6-704, leu-32, ura4-D18, h+*

2.4.5 *S. pombe* vectors

pREP vectors

pREP vectors are used for overexpression of tagged proteins in *S. pombe*. pREP41 and 42 are derived from the *S. pombe* vectors pREP 1 and pREP2, respectively. Truncations of the TATA box of the *nmt*1 promoter give rise to an intermediate strength promoter, which is weaker than that of pREP 1/2. pREP 41 contains the *LEU2* marker, whilst pREP42 encodes a *ura4*$^+$ marker, allowing for selection of positive colonies with selective media. These vectors can be used for expression of proteins tagged at the N-terminus with either the 2 x myc epitope and 6 x HIS tag (myc_2 HIS_6), or a 3 x HA tag. During this study the myc_2 HIS_6 tag was excised from pREP41 by digesting with *Nde*I and *Nco*I and replaced with a HIS_6 linker to avoid false positive results resulting from SUMOylation of the myc tag.

pAW vectors

pAW vectors were generated for use in the recombination-mediated cassette exchange system (Watson et al, 2008). pAW12 and pAW41 are used as templates for PCR reactions which result in a LoxP site being incorporated upstream of the gene of interest and a *ura4*$^+$ marker and LoxM site being incorporated directly after the stop codon. The exact sequence flanked by loxP and loxM is cloned into the pAW8 vector, where site directed mutagenesis can be carried out. Transformation of a base strain with pAW8 results in integration of a wild type or mutant gene into the genome between the lox sites. This allows for analysis of mutant genes without the need for overexpression and under the control of the endogenous promoter.

pAW41

pAW41 contains a *ura4*+ marker flanked by two half loxP sequences. pAW41 was used as a template for a PCR reaction using primers which include 20 nucleotides of plasmid specific sequence at the 3' end (described in Watson et al) and 100 nucleotides which are complementary to the *S. pombe* wild type genome. The forward primer contains homology to the sequence upstream of the target gene start codon at the 5' end. The reverse primer abuts the forward primer. Transformation with the resulting PCR product results in integration of the *ura4*+ marker and the two half loxP sites upstream of the target gene. Transformants were plated onto YNB supplemented with adenine and leucine to select for *ura4*+ positive colonies.

pAW 5

pAW5 is a cre-recombinase-expressing vector with a *LEU2* marker. Transformation with pAW5 allows for expression of Cre recombinase and recombination between the two half loxP sites to form a full loxP site upstream of the target gene. This results in loss of the *ura4*+ marker which can be selected for using 5'FOA. Transformants were plated onto YNB supplemented with adenine, uracil and thiamine to repress Cre recombinase expression. Positive colonies are then grown overnight in YE media to allow for expression of the cre recombinase. 500 cells were plated onto 5'FOA to select for cells that had lost the *ura4*+ marker.

pAW12

pAW12 contains a *ura4*+ marker and a LoxM site. pAW12 was used as a template for a PCR reaction using primers which include 20 nucleotides of plasmid specific sequence at the 3' end (described in Watson et al. 2008) and 100 nucleotides which are complementary to the *S. pombe* wild type genome adjacent to the stop codon of the target gene. The forward primer contains homology to the gene sequence from 100 bases upstream of the target codon, whilst the reverse primer contains homology to the gene sequence directly downstream of the stop codon. Transformation with the resulting PCR product results in integration of a *ura4*+ marker and a LoxM3 site immediately

downstream of the target gene. Transformants were plated onto YNB supplemented with adenine and leucine to select for *ura4*$^{+}$ positive colonies. This results in a loxP – gene – *ura4*$^{+}$ - loxM strain referred to as the 'base strain'.

pAW8

pAW8 contains a multiple cloning site flanked by LoxP and LoxM sites. The multiple cloning site encodes lac Z and can therefore be used for blue-white screening, as described in section 2.2.1. pAW8 also encodes a selectable *LEU2* marker and Cre recombinase which is under control of an *nmt*1 promoter. The exact sequence flanked by the loxP and loxM sites integrated into the genome to form the 'base strain' was cloned into the pAW8 vector. This construct can be used for site directed mutagenesis to allow for incorporation of mutations into the genome. pAW8 containing either the wild type sequence or mutated sequence of the target gene is transformed into the base strain and the LEU2 marker selected for by plating on YNB supplemented with adenine, uracil and thiamine. Positive colonies were grown overnight in YEA to allow for expression of the Cre recombinase and recombination between the loxP and loxM sites. Successful incorporation of wild type or mutant gene from pAW8 results in a loss of the *ura4*$^{+}$ marker. 500 cells are plated onto 5'FOA plates to select for cells which have lost *ura4*$^{+}$. Colonies are then replica plated onto YNB supplemented with uracil and adenine. Colonies that do not grow on this media have lost the pAW8 plasmid and therefore the *LEU2* marker and were re-streaked onto 5'FOA. Incorporation of mutant genes was confirmed by PCR following genomic DNA extraction or colony PCR (see section 2.4.6 and 2.4.7) and sequencing.

2.4.6 *S. pombe* transformation (Bahler method 1998)

S. pombe cells were inoculated in YE and grown overnight at 30°C. Cells were diluted and grown for a further 4 hours to OD_{600} 0.5 (approximately $4x10^{6}$ cells). 20ml culture was centrifuged at 3,000rpm for 5 minutes. Pellets were washed with sterile water and centrifuged again at 3,000 rpm for 5 minutes. Cells were resuspended in 1ml LiOAc/TE and transferred to a 1.5ml eppendorf before being centrifuged at 3000 rpm for 5 minutes. Cells were resuspended in 100µl LiOAc/TE. 500ng - 1µg plasmid DNA or 10 – 20 µg of purified PCR product was

added and cells were incubated at room temperature for 10 minutes. 260µl PEG/liOAc was added and cells incubated at 30°C for 30 minutes. 43µl DMSO was added before incubating at 37°C for 5 minutes. Samples were centrifuged at 3000 rpm for 5 minutes and the cell pellet washed using 500µl sterile water. Samples were centrifuged at 3,000 rpm for 5 minutes and supernatant discarded. Cells were resuspended in remaining supernatant (approximately 100µl) and plated into appropriate selective solid media. Plates were incubated at 30°C for 3 – 5 days until transformants formed colonies.

10 X TE buffer

Tris-HCl pH 7.5	100mM
EDTA pH 8.0	10mM

LiOAc/TE

LiOAc pH 7.5	100mM
TE buffer	1 X

PEG/liOAc

LiOAc pH7.5	100 mM
TE buffer	1 X
PEG-4000	40%

2.4.7 Genomic DNA extraction from *S. pombe*

S. pombe cells were inoculated in 10ml YE and grown overnight at 30°C. Cells were harvested by centrifugation at 3,000rpm for 5 minutes. The cell pellets were resuspended in 2ml SP1 buffer and 2mg/ml zymolyase added. Samples were incubated at 37°C for 30 to 45 minutes. Cells were checked for spheroplasting my mixing 10µl cells with 1µl 10% SDS on a microscope slide and visualising under a light microscope. Cells were then harvested by centrifuging at 3,000rpm for 5 minutes. Cell pellets were resuspended in 900µl of 5 X TE and 100µl of 10% SDS was added to lyse the cells. Samples were

incubated at room temperature for 5 minutes. 300µl of KAc was then added and samples incubated on ice for 10 minutes before centrifuging at 13,000 rpm for 5 minutes. The supernatant was transferred to a fresh eppendorf tube and an equal volume of isopropanol added before being centrifuged at 13,000 rpm for 5 minutes. The supernatant was discarded and the pellet was washed with 500µl of 70% ethanol. Samples were centrifuged at 13,000 rpm for 5 minutes. Supernatant was discarded and the pellet was dried using a desiccator. Pellets were resuspended in 500µl of 5 x TE and 4µl of 10mg/ml RNase added. Samples were incubated at 37°C for one hour. 4µl of 20mg/ml proteinase K was added and samples incubated at 30°C overnight. An equal volume (approx. 500µl) of 25:24:1 phenol:chloroform:isopropanol was added and samples were centrifuged at 13 000 rpm for 5 minutes. The aqueous phase was transferred to a fresh eppendorf. 2 x the volume of 100% ethanol and 1/10 volume of 3M NaAc was added and samples were stored at -20°C for 1 hour to overnight. Samples were centrifuged at 13,000 rpm for 5 minutes and the pellet was washed using 500µl of 70% ethanol. Samples were centrifuges at 13,000 rpm for 5 minutes and the supernatant discarded. Pellets were dried using a desiccator and resuspended in 30µl of sterile water.

SP1 Buffer:

Sorbitol	1.2M
Sodium citrate	50mM
Sodium phosphate	50mM
EDTA	40mM
Buffer was adjusted to pH 5.6 with NaOH	

5 X TE

Tris-HCl pH 7.5	50mM
EDTA pH 8.0	5mM

2.4.8 Colony PCR

One colony was suspended in 50µl sterile H_2O and incubated at 95°C for 5 minutes. Samples were centrifuged at 13,000 rpm for 30s and 6µl of supernatant was pipetted quickly into PCR tubes containing PCR mix as described in section 2.1.6.

2.4.9 *S. pombe* genetic crosses

S. pombe cells of opposite mating types (h^+ and h^-) were mixed together on a small section of solid extra low nitrogen (ELN) media. These were incubated at 25°C for 2 – 3 days. A sample was examined under a light microscope to check for the presence of asci.

2.4.10 Random spore analysis

A sterile loop was used to inoculate a loop of sporulated cells in 1ml of sterile water with 1µl of *Helix pomatia* juice added. Samples were incubated at room temperature on a rotating wheel overnight. Dilutions of 10^{-2} and 10^{-3} cells were plated onto YEA and incubated at 30°C for 3 – 5 days until colonies were visible. Where selectable markers were different, cells were replica plated onto appropriately supplemented media and double mutants analysed.

2.4.11 Tetrad analysis

A sterile loop was used to streak a small amount of sporulated cells at the side on a YEA plate with 10µl sterile water. This was stored in the fridge for one hour to overnight to allow the cell walls of tetrads to start to break down. The plate was then mounted onto a tetrad dissector. A needle was used to dissect tetrads into four individual spores and place them in a line on the YEA plate. A minimum of 14 tetrads were dissected using tetrad analysis. The spores were incubated at 30°C for 3-5 days or until colonies were formed. Spores were replica plated onto appropriate selective plates and phloxin B containing plates which were subsequently UV irradiated. Replica plates were incubated overnight at 30°C and double mutants were identified and analysed.

2.4.12 Survival analysis

UV irradiation

Cells were grown overnight in YE to saturation. Cultures were then diluted to OD_{600} 0.2 and incubated at 30°C for a further 3 to 4 hours. Cells were counted and diluted to a concentration of 5 x 10^3 cells/ml. 500 cells (10 x more for sensitive strains) were plated onto YEA and irradiated at a range of doses from 30 to 200 Jm^{-2}. Plates were incubated at 30°C for 3 days and percentage survival calculated in comparison to non-treated controls.

IR irradiation

Cells were grown overnight in YE to saturation. Cultures were then diluted to OD_{600} 0.2 and incubated at 30°C for a further 3 to 4 hours. Cells were counted and diluted to a concentration of 5 x 10^3 cells/ml and transferred to eppendorf tubes. Cells were irradiated with γ rays from a ^{137}Cs source at a dose of 7Gy/min for doses ranging from 0-1,000 Gy. 100 μl cells (~500 cells) were plated onto (YEA) plates. Colonies were counted following incubation for 3 days at 30°C and percentage survival calculated in comparison to non-irradiated controls.

Spot tests

Spot tests were used to test the sensitivity of strains to a range of genotoxins. MMS is an alkylating agent which causes a range of damage. MMS (methyl methanesulfonate) was used at a range of concentrations from 0.0005 – 0.005%. HU (hydroxyurea) depletes dNTP's and causes replication fork stalling. HU was used at concentrations ranging from 1-5mM.

Cells were grown overnight in YE to saturation. Cultures were then diluted to OD_{600} 0.2 and incubated at 30°C for a further 3 to 4 hours. Cells were counted and diluted to a concentration of 4x10^6 cells/ml. (10 x more cells were plated for very sensitive strains where indicated). Four 10 fold serial dilutions were made for each strain, and 7μl of each dilution was plated onto YEA plates with varying concentrations of the genotoxins mentioned above. YEA plates with no drug were used as controls. Plates were incubated at 30°C for three days and sensitivity of strains compared to each other. Where new point mutants were

generated in essential genes, an additional spot test on YEA was incubated at 37°C to ensure stability of the proteins was not affected.

2.4.13 Microscopy

2.4.13.1 Visualisation of GFP tagged proteins

Strains containing GFP-conjugated proteins were inoculated in 10 ml YE and were grown overnight at 30°C. Samples were diluted to a concentration of 4 x 10^6 cells/ml and incubated at 30°C for a further 3 to 4 hours. 1ml of cells was centrifuged at 3,000 rpm for 5 minutes and the cell pellet washed in 500µl sterile water. 10 - 15µl of the cells were placed on a microscope slide. A coverslip was placed on top and the cells were visualised immediately.

2.4.13.2 DAPI and Calcofluor staining of *S. pombe* cells

A single colony or small loop of *S. pombe* cells was inoculated in 10ml of YE and incubated overnight at 30°C. Cells were diluted to an OD_{600} of 0.2 and incubated at 30°C for 3 to 4 hours to allow for exponential growth. 1ml of cells were transferred to an eppendorf tubes and pelleted by centrifuging at 3,000 rpm for 5 minutes. Cell pellets were washed with 500µl sterile H_2O and pelleted by centrifuging at 3,000 rpm for 5 minutes. The supernatant was discarded and the cell pellet resuspended in the remaining supernatant (approximately 100µl). 5 - 7µl of the cell suspension was pipette onto a microscope slide. Cells were heat fixed at 70°C by placing the slide onto a hot plate for 30 seconds to one minute. Once cooled, 3-4µl DAPI staining solution was pipetted on top of the cells and a coverslip placed on top. Clear nail polish was used to seal the coverslip. Cells were visualised using a Nikon E400 microscope.

DAPI staining solution
1µg/ml DAPI
50µg/ml Calcofluor
50% glycerol

2.4.14 FACS analysis

1ml samples containing a minimum of $5x10^6$ cells were centrifuged at 3,000 rpm for 5 minutes. Cell pellets were washed with 500µl sterile H_2O and re-suspended in 500µl of 70% ethanol. Samples were stored at 4°C until required. 300µl of sample was centrifuged at 3,000 rpm for 5 minutes. The cell pellet was resuspended in 1ml of 50mM sodium citrate (pH 7.0). 5µl of 10mg/ml RNase was added and samples were incubated at 37°C for 2 hours. 2µl of propidium

iodide was added and samples were transferred to FACS tubes. Samples were analysed using a FACScalibur flow cytometer.

3 Establishment of a system to identify SUMO modified proteins

3.1 Introduction

SUMO modifies target proteins following an enzymatic cascade similar to that of ubiquitination, as described previously. Many proteins involved in the DNA damage response have been shown to be SUMOylated *in vivo,* including the ubiquitin E3 ligase BRCA1 (Morris et al, 2009), the BER factor TDG (Hardeland et al, 2002) and the Smc5/6 subunit Smc6 (Andrews et al, 2005). SUMO modification of target proteins is frequently a transient event however, and only a small pool of protein might be modified at any one time. This raises difficulties in isolating and observing SUMO targets *in vivo* without the need for over-expression. Quantitative proteomic screens have identified SUMOylated proteins which are involved in a range of processes including the DNA damage response. In most cases, the role of SUMOylation has still to be determined (Cremona et al, 2012).

In vitro SUMOylation assays can be used as an initial step to determine whether a protein of interest might be modified. For subsequent assays, mutation of lysine residues on the target protein can help to identify the specific sites of modification. Additionally, mass spectrometry can be used to identify specific residues. An *in vitro* SUMOylation system was previously established in the Watts lab to identify SUMO target proteins and to identify SUMOylation sites (Ho et al, 2001). A mature form of recombinant, N-terminally HIS-tagged SUMO (HIS-SUMOGG) was previously purified in the Watts lab for use in *in vitro* assays. Recombinant SUMO pathway components were also expressed and affinity purified from bacteria and used in reactions with the putative target proteins. In this system, modified target proteins are visualised by Coomassie staining or by the presence of higher molecular weight bands following western blotting of an *in vitro* reaction sample. Specifically, the aim here was to take SUMO modified proteins produced in an *in vitro* assay and analyse them by tandem mass spectrometry (LC-MS/MS) to identify specific target lysine residues. Modified lysine residues could then be mapped to the known or

predicted structure of the target protein. This would give an insight into the relevance of the modification, for example whether it competes with another known modification site such as ubiquitination. Molecular modelling of potentially SUMOylated residues would also help to dismiss residues which are on internal or inaccessible lysines.

Analysis by mass spectrometry requires the digestion of peptides by trypsin or other endoproteases e.g. elastase. Trypsin cleaves at the C-terminal side of both arginine and lysine residues. Cleavage of HIS-SUMOGG by trypsin results in a 23 amino acid fragment remaining attached to the target lysine residue. This often makes modified fragments too large for analysis by MS. This chapter describes the generation of a trypsin cleavable recombinant SUMO, HIS-SUMOGG-tr. The leucine residue N-terminal to the diglycine motif was mutated to arginine (L108R), creating a trypsin cleavage site immediately before the diglycine motif. This results in just two amino acids remaining bound to the target peptide following trypsin digestion, which is thus more readily analysed by mass spectrometry. HIS-SUMOGG-tr was subsequently used to identify target lysine residues on *in vitro* SUMO-modified proteins by mass spectrometry.

A trypsin cleavable SUMO was also integrated into the *S. pombe* genome under the control of the endogenous promoter, following the generation of a SUMO base strain. An N-terminal HIS-tag was added with a view to using this strain to identify and analyse SUMOylated species at wild type levels *in vivo.*

3.2 Aims

At the start of this project, individual SUMOylation sites were identified using systematic mutagenesis of individual lysine residues in the target protein. One of the aims of this project was to establish a more efficient method for the identification of SUMOylation sites *in vitro* and to facilitate the identification of specific modified lysine residues. The second aim of the project was to set up a system to identify SUMO target proteins *in vivo*, with SUMO expressed at endogenous levels.

3.3 *In vitro* purification of components of the SUMOylation pathway from bacteria for use in *in vitro* assays

In order to carry out an *in vitro* SUMOylation assay, all components of the SUMO pathway first need to be purified from bacteria. The ORF's of pathway components had been previously cloned into expression vectors containing either HIS or GST tags. E1 activating enzyme heterodimer subunits HIS-Rad31 and GST-Fub2 were co-transformed into *E. coli* and purified using gluathione sepharose beads (Figure 3.1A). E2 conjugating enzyme GST-Hus5 was also purified using gluathione sepharose beads (Figure 3.1B). E3 ligases HIS-Pli1 and GST-Nse2 were purified using Ni^{2+} agarose. GST-Nse2 is shown in Figure 3.1C. All purifications were carried out under native conditions. Newly purified components were tested in an *in vitro* SUMOylation reaction to assess the appropriate concentration of recombinant protein required to form SUMO chains (Figure 3.1D). Elution fraction 4 (lane 2) was deemed to be at a suitable concentration in this case, as SUMO chains are formed efficiently, avoiding excessive SUMOylation which could lead to false positive results. SUMOylation of target proteins can occur in the absence of an E3 SUMO ligase in *in vitro* assays, where there is an excess of SUMOylation machinery. Whilst target proteins are able to interact directly with the E2 conjugating enzyme *in vivo*, it is not clear how often SUMOylation occurs in the absence of E3 ligases *in vivo*. The viability of a *pli1-d nse2-SA* double mutant however (Steinacher et al. 2013), suggests that either proteins can be SUMOylated in the absence of E3 ligases in *S.pombe*, or that there exists an as yet unidentified third SUMO ligase in *S.pombe*.

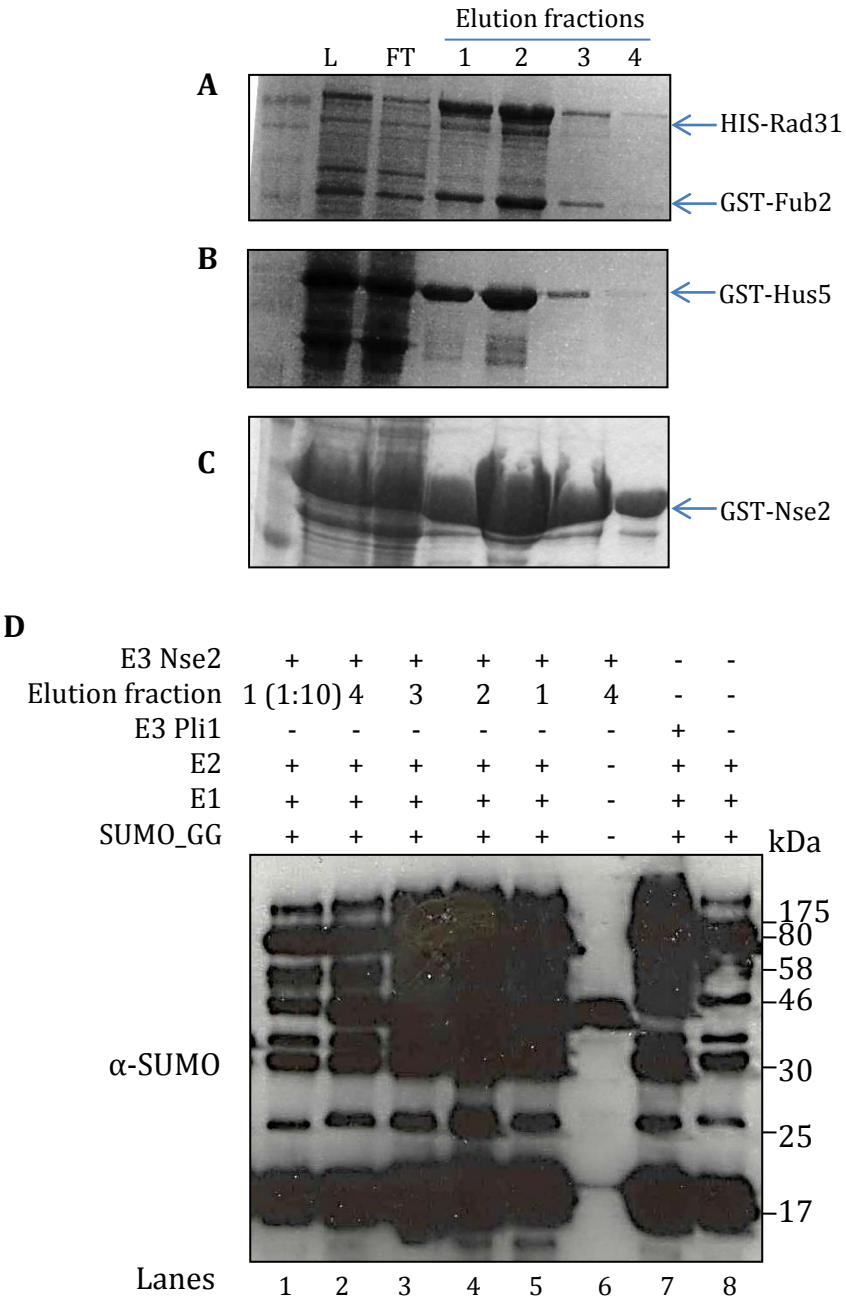

Figure 3.1 Purification of components of the SUMOylation pathway.

(**A**) E1 activating enzyme subunits HIS-Rad31 GST-Fub2 E1 were co-expressed and purified using GST beads. L = cell lysate, FT = flow-through, Elution fractions numbered. (**B**) E2 conjugating enzyme GST-Hus5 purification using GST beads. (**C**) E3 ligase GST-Nse2 purification using Ni^{2+}agarose beads. (**D**) The purified pathway components were used in an *in vitro* assay to confirm their enzymatic activity. The example shown here tests equal volumes of the E3 ligase Nse2 eluates shown in (**C**) in the absence of a specific target protein. *In vitro* assays were analysed by western blot and probed with α–SUMO antibody to visualise SUMOylated species and SUMO chains.

3.4 Creation of a trypsin cleavable SUMO

Mass spectrometry can be used to identify specific target lysine residues which are SUMOylated in an *in vitro* reaction. Incorporation of a trypsin cleavage site into recombinant HIS-SUMOGG adjacent to the diglycine motif increases the probability of identifying modified residues. Site directed mutagenesis was performed on the pET15b-HIS-SUMOGG construct. This resulted in the L108R mutation directly adjacent to the diglycine motif which is conjugated to lysine residues on target proteins (Figure 3.2A). The presence of the mutation was confirmed by sequencing. The mutant will be referred to as HIS-SUMOGG-tr from now on. Expression of HIS-SUMOGG-tr in *E. coli* BL21 cells was induced using 0.1mM IPTG overnight at either 26°C or 37°C in order to identify the optimal conditions for expression (Figure 3.2B). HIS-SUMOGG-tr was purified under native conditions using Ni^{2+} agarose beads following IPTG induction and expression at 26°C overnight, as these conditions produced a higher yield of protein (Figure 3.2B and C). Three eluates were tested for activity in an *in vitro* assay and compared to HIS-SUMO-GG in the presence and absence of E3 ligase Pli1 (Figure 3.2D). HIS-SUMO-GG-tr was able to form SUMO chains *in vitro* at least as efficiently as HIS-SUMO-GG in both the presence (Comparing lanes 6 and 7) and absence (comparing lanes 1 and 2) of the SUMO ligase Pli1.

This trypsin-cleavable SUMO has since been used in several *in vitro* SUMOylation assays, and modified target proteins have been successfully identified and analysed by mass spectrometry following trypsin digestion. The specific modified lysine residues of several target proteins have also been identified (Mercer, B DPhil thesis, University of Sussex). Further examples will be discussed in subsequent chapters. Included in the modified targets identified were SUMOylated forms of some of the components of the SUMO pathway, namely the E1 activating enzyme subunit Fub2 and the E2 conjugator subunit Hus5.

A

SUMOGG DGERIRPDQTPAELDMEDGDQIEAVLEQLGG

SUMOGG-tr DGERIRPDQTPAELDMEDGDQIEAVLEQRGG

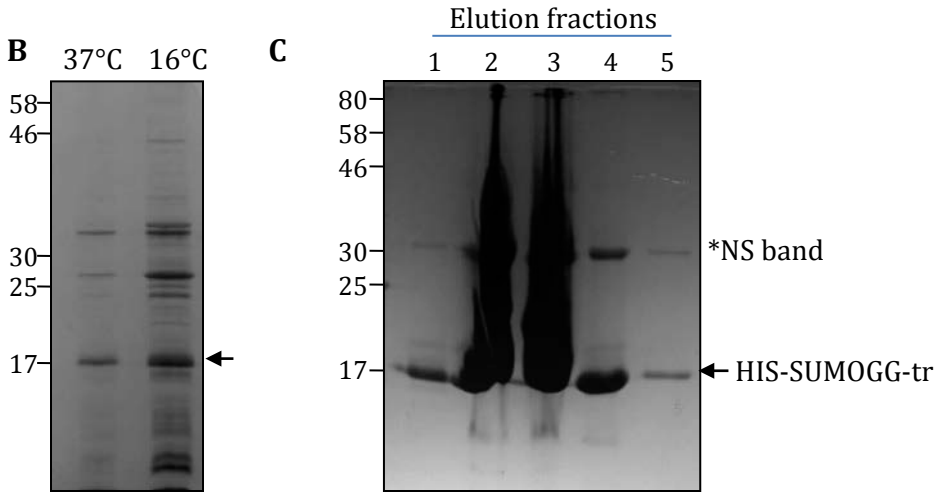

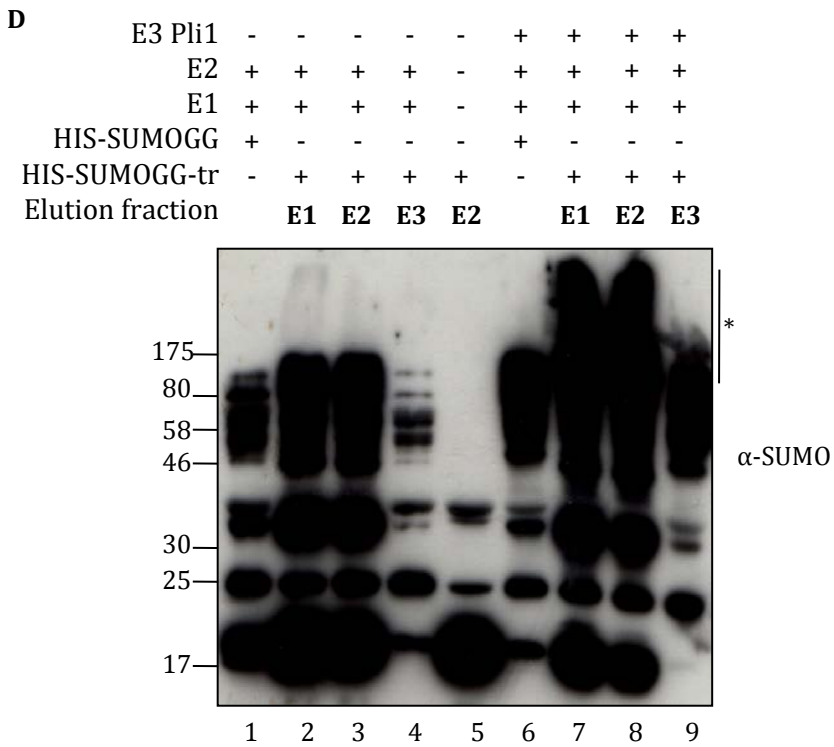

Figure 3.2 Trypsin cleavable SUMO can form SUMO chains *in vitro*.

(A) PCR site directed mutagenesis was used to create a trypsin cleavage site adjacent to the GG motif (L108R). **(B)** Whole cell extract following pET15b-HIS-SUMOGG-tr expression in *E.coli*. induced overnight at either 37°C (lane 1) or 26°C (lane 2). **(C)** HIS-SUMOGG.tr was purified using Ni^{2+} beads. Lane 1, cell lysate; lane 2, flow through; Lanes 3-9, 50µl elution fractions. Both gels are 12.5% SDS-PAGE stained with Coomassie blue staining**.** NS refers to a non-specific band. **(D)** *In vitro* SUMOylation assay comparing the activity of HIS-SUMOGG with HIS-SUMOGG-tr in the presence and absence of E3 SUMO ligase Pli1. Asterisk refers to high molecular weight SUMO chains.

3.5 Identification of SUMO modified Hus5 using trypsin cleavable SUMO

An *in vitro* SUMOylation assay using HIS-SUMOGG-tr was analysed by SDS-PAGE and stained with Coomassie Brilliant Blue to visualise protein bands (Figure 3.3A). The assay was set up in the absence or presence of the E2 conjugating enzyme GST-Hus5. The appearance of higher molecular weight bands suggested that components of the SUMO pathway were themselves being modified. Several bands were sliced from the gel, trypsinized and analysed by mass spectrometry. During mass spectrometry, samples are ionised, fragmented and then fragments are separated by their mass to charge ratio. Fragmentation results in N-terminally or C-terminally charged species, referred to as b ions or y ions, respectively. The difference in mass between adjacent b or y ions allows the identification of specific residues. Therefore the addition of two glycine residues resulting from SUMOylation of a target protein results in a specific mass shift which can be identified by the mass spectrometer. A mass shift confirmed the conjugation of the diglycine motif at Hus5 K50 (Figure 3.3B).

An alignment of the Hus5/Ubc9 sequences from humans, budding and fission yeast and mice can be seen in Figure 3.4A. The lysine residue at position 50 is not conserved between these species. However there is a highly conserved lysine residue two amino acids upstream in all species analysed (K48) (Figure 3.4A). This suggests that this residue might be of biological relevance. The human and mouse Ubc9 K48 residue is identified by SUMO consensus site predicting software 'SUMOplot' as a potential SUMO motif, suggesting that this residue is a candidate for SUMOylation in higher eukaryotes.

K50 can be mapped onto the structure of *S. pombe* Hus5 (Prudden et al, 2011), and is compared to the relative position on the structure of the *S. cerevisiae* ortholog Ubc9 (Duda et al, 2007) (Figure 3.4B). The position of Ubc9 SUMOylation sites in *S. cerevisiae* and humans are also highlighted (Figure 3.4B).

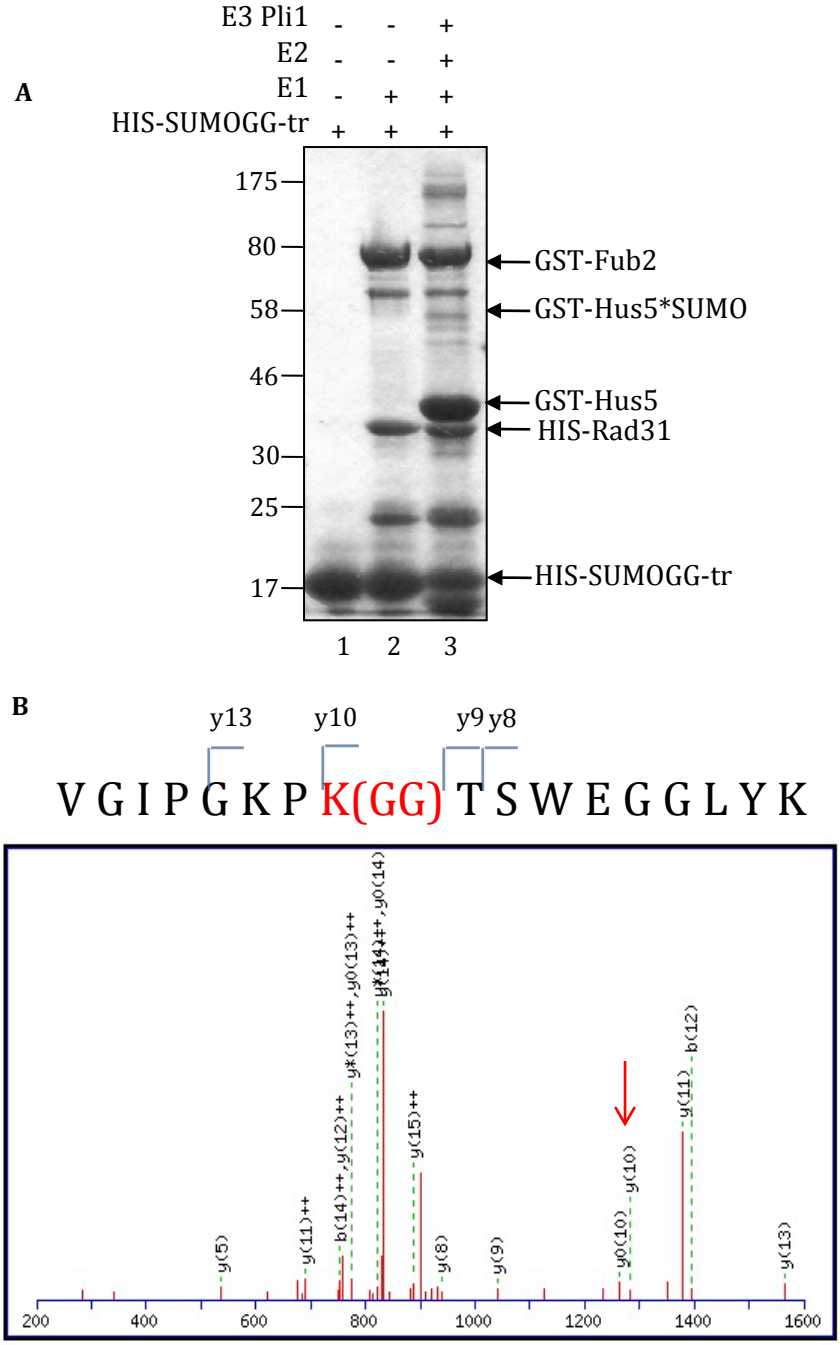

Figure 3.3 Hus5 is SUMOylated *in vitro* at K50

(A) HIS-SUMOGG.tr can be successfully conjugated onto target proteins *in vitro.* Lane 1, HIS-SUMOGG.tr; lane 2, HIS-SUMOGG-tr + E1 activating enzyme HIS-Rad31 GST-Fub2; lane 3, HIS-SUMOGG-tr, HIS-Rad31 GST-Fub2 and E2 conjugating enzyme GST-Hus5. Bands corresponding to SUMOylated Hus5 were sliced from the gel and subject to analysis by mass spectrometry. **(B)** MS/MS data identifying Hus-5 lysine residue K50 conjugated to the SUMO diglycine motif. The red arrow highlights the y10 ion which corresponds to diglycine linked to K50.

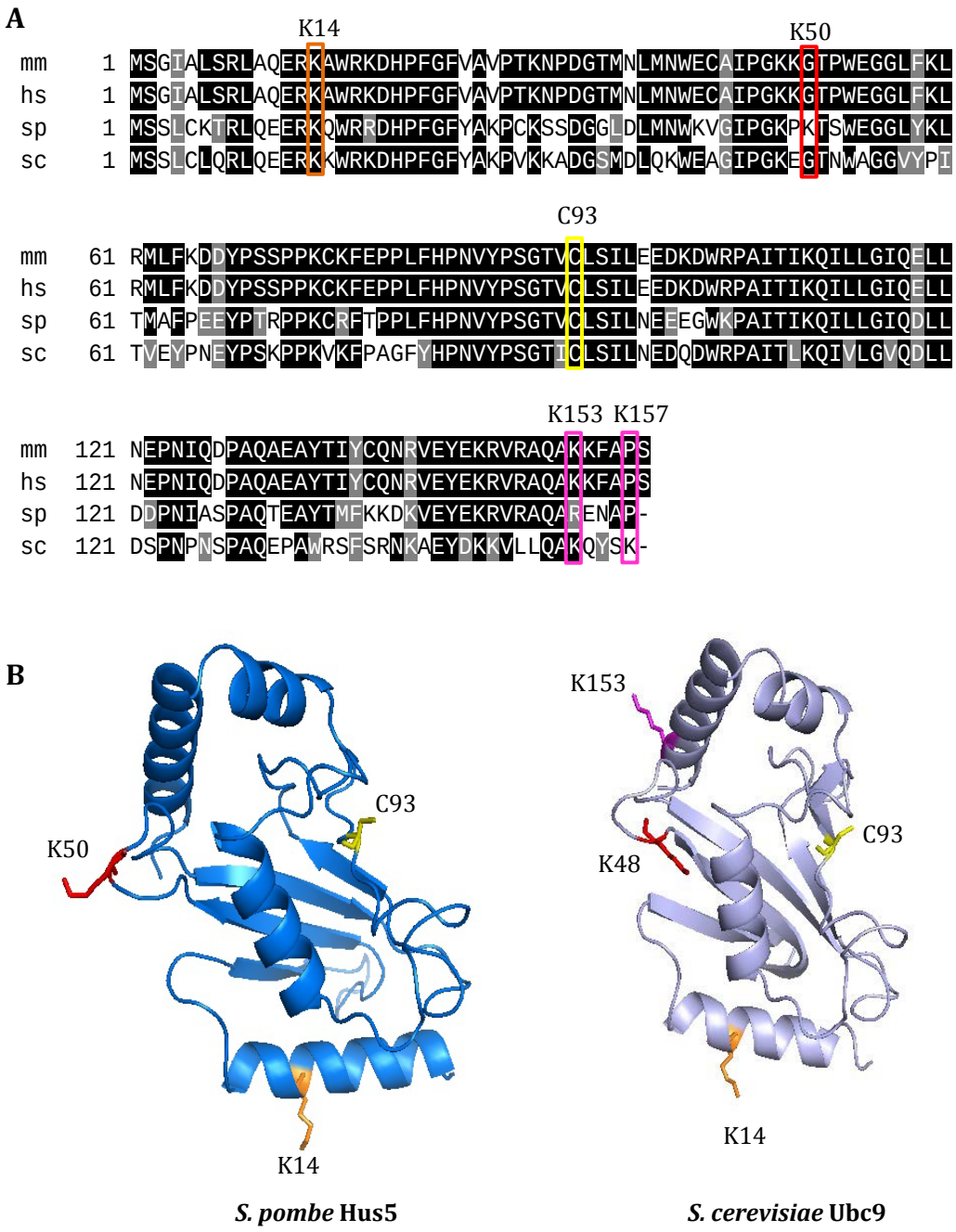

Figure 3.4 Multiple sequence alignment and structure highlighting the position of Hus5 K50

(**A**) Sequence alignment of Hus5/Ubc9 orthologous from mice (*mm*), humans (h*s*), fission (*sp*) and budding (*sc*) yeast. SUMOylated lysines are highlighted in red. (**B**) *S. pombe* Hus5 structure (Prudden et al. 2011), compared to the *S.cerevisiae* Ubc9 structure (Duda, van Waardenburg et al. 2007). The catalytic cysteine residue C93 is highlighted in yellow. The *S. pombe* Hus5 SUMOylation site K50 and the equivalent residue in *S. cerevisiae* (K48) is highlighted in red. Ubc9 is SUMOylated at K153 (R153 in *S. pombe*) and K157 in *S.cerevisiae*, highlighted in pink. K14 is reported to be SUMOylated in humans (highlighted orange).

3.6 Hus5 SUMOylation *in vivo*

In order to investigate whether Hus5 is SUMOylated *in vivo*, the *hus5* gene was cloned into the yeast vector pREP42-HA. Site directed PCR mutagenesis was performed resulting in a K50R mutant (pREP42-HA-Hus5-K50R). The full length SUMO sequence (SUMO-FL) had previously been cloned into pREP41-myc-HIS vector for use in *in vivo* studies (Ho et al, 2011). It has been suggested however, that the myc tag can itself be SUMOylated (Nestoras, K., DPhil thesis, University of Sussex). To prevent the possibility of false positive results, the HIS_6-myc_2 tag was excised from pREP41 by restriction digestion. This was replaced with a linker of two ligated oligonucleotides encoding a HIS_6 tag, resulting in HIS-SUMO-FL (Figure 3.5A). To determine whether K50 is the only lysine residue that is SUMOylated, pREP41-HIS-SUMO-FL was co-transformed into *S. pombe* cells with pREP42-HA-HUS5 or pREP42-HA-HUS5-K50R. HIS-SUMO was pulled down using Ni^{2+} agarose and the eluates subjected to western blot analysis (Figure 3.5B). A band at approximately 50 kDa can be seen when probed with α-HA antibody that is not observed with the K50 mutant. This suggests that Hus5 is SUMOylated *in vivo* on K50 in *S. pombe* and that this is the main, if not the only SUMOylation site. Further investigation is required to determine the role of Hus5 auto-SUMOylation in *S. pombe* and whether K50 modification may have a regulatory role as in other organisms. This line of study was continued by other members of the Watts lab.

A

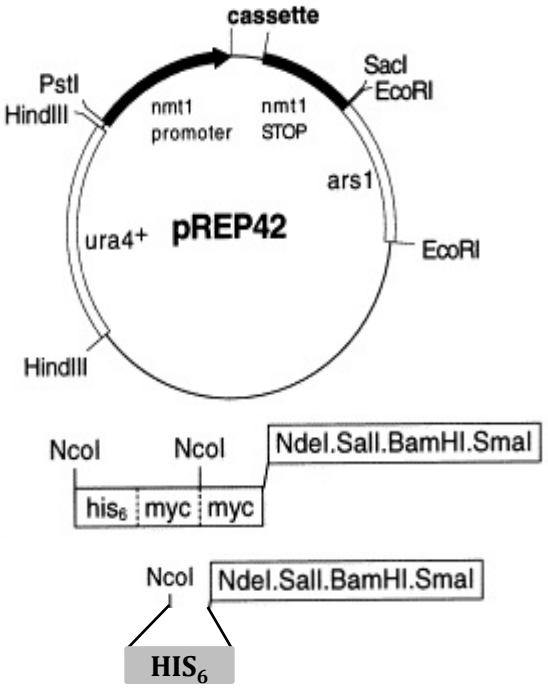
cassette
PstI
HindIII
nmt1
promoter
nmt1
STOP
SacI
EcoRI
ars1
ura4+
pREP42
EcoRI
HindIII
NcoI
NcoI
NdeI.SalI.BamHI.SmaI
his6
myc
myc
NcoI
NdeI.SalI.BamHI.SmaI
HIS6

B

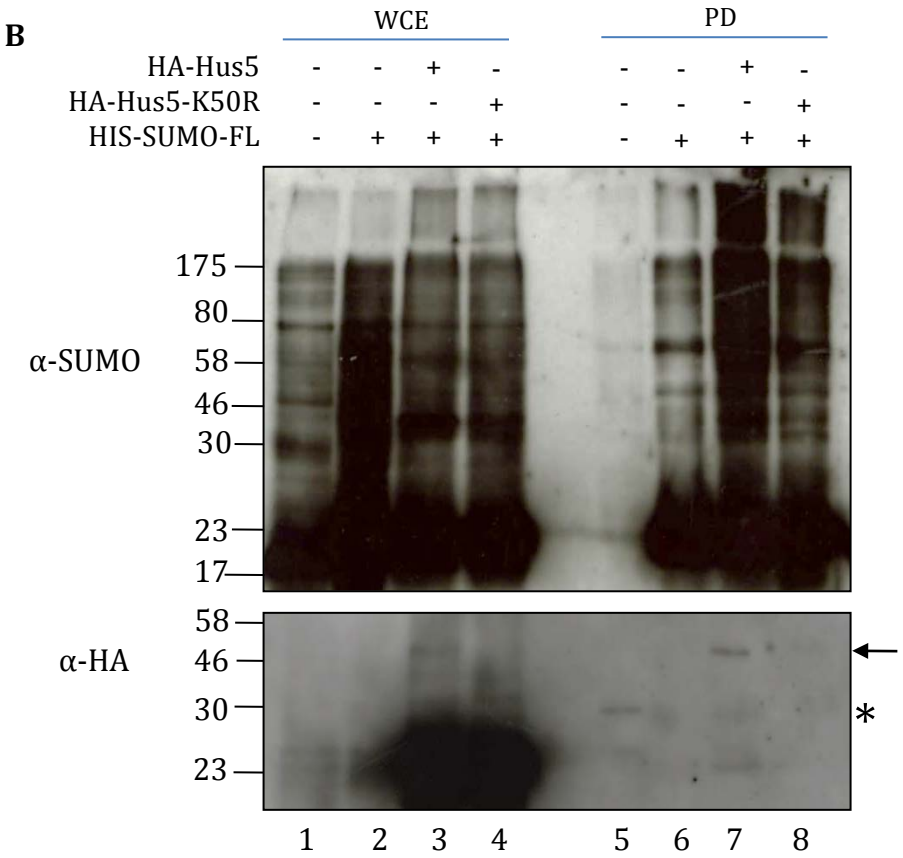
WCE
PD
HA-Hus5 - - + - - - + -
HA-Hus5-K50R - - - + - - - +
HIS-SUMO-FL - + + + - + + +
175
80
α-SUMO 58
46
30
23
17
58
α-HA 46
30
23
*
1 2 3 4 5 6 7 8

Figure 3.5 Hus5 is SUMOylated *in vivo* at K50

(**A**) The myc tag was excised from plasmid pREP41-myc-HIS and replaced with a 6xHIS linker to avoid false positive results resulting from SUMOylation of the myc tag. pREP41-HIS-SUMO-FL was co-transformed into 'wild type' *S. pombe* strain with pREP42-HA-Hus5 or pREP42-HA-Hus5-K50R. HIS-SUMO-FL was purified from whole cell extract and anti-HA antibodies used to detect SUMOylated Hus5. (**B**) Immunoblot using anti-HA antibodies revealed a band corresponding to SUMOylated Hus5 indicated by an arrow. This band is not present when cells are transformed with the Hus5-K50R mutant. Asterisk indicates non-specific band.

3.7 Integration of SUMO-tr into the genome

In order to analyse SUMO targets *in vivo*, without the need for over-expression, a trypsin-cleavable SUMO was inserted into the genome. In order to do this, a SUMO base strain was created. LoxP and LoxM sites were incorporated into the genome flanking the SUMO coding sequence (Figure 3.6), as described by (Watson et al, 2008). This is a two-step process for essential genes. The plasmids pAW41 and pAW12 (Figure 3.6A) were used to incorporate loxP and loxM sites flanking the SUMO sequence in the genome. The first loxP site was incorporated approximately 200 bases upstream of the SUMO start codon so as not to interfere with any overlapping ORFs (Figure 3.6B i). Incorporation of LoxP half sites and the *ura4*$^{+}$ marker was confirmed by PCR (Figure 3.6Bi and C i). Transformation with a Cre-expressing plasmid excised the *ura4*$^{+}$ marker, resulting in formation of a full loxP site. This was confirmed by PCR across the loxP site, using the same primers as in Figure 3.6Bi. Loss of the *ura4*$^{+}$ marker results in an ~ 2 Kb reduction in size of the PCR product (Figure 3.6B ii and C ii). A *ura4*$^{+}$ marker and LoxM sequence was then integrated directly downstream of the SUMO stop codon. This insertion was verified by PCR (Figure 3.6Biii and C iii) and the surrounding genome was sequenced to ensure correct recombination. The resultant strain LoxP-SUMO-*ura4*$^{+}$-LoxM is referred to as the 'base strain'.

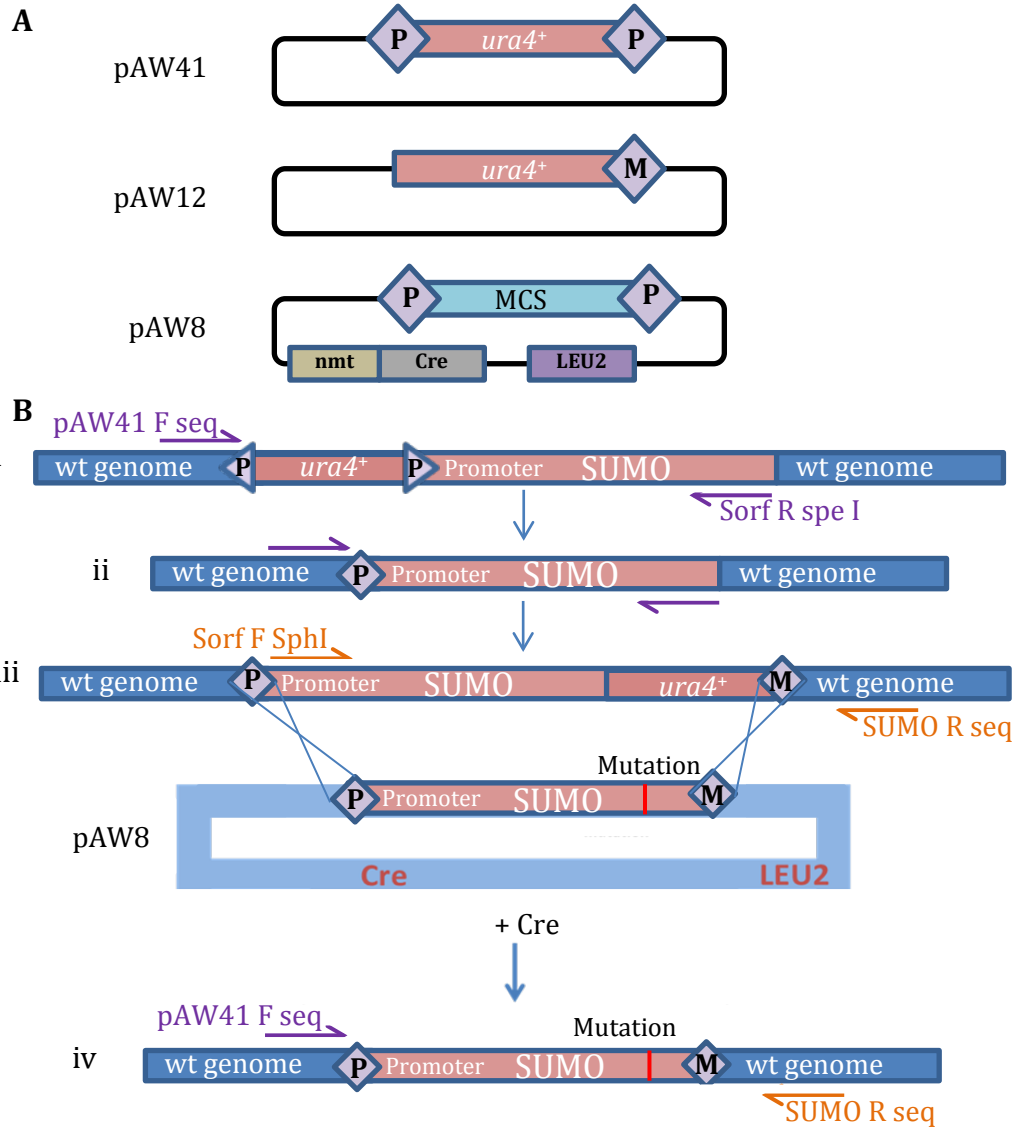
A
pAW41
P
ura4+
P
pAW12
ura4+
M
pAW8
P
MCS
P
nmt
Cre
LEU2
B
i
pAW41 F seq
wt genome
P
ura4+
P
Promoter
SUMO
wt genome
Sorf R spe I
ii
wt genome
P
Promoter
SUMO
wt genome
iii
Sorf F SphI
wt genome
P
Promoter
SUMO
ura4+
M
wt genome
SUMO R seq
Mutation
pAW8
P
Promoter
SUMO
M
Cre
LEU2
+ Cre
iv
pAW41 F seq
Mutation
wt genome
P
Promoter
SUMO
M
wt genome
SUMO R seq
C
i LoxP + ura4+
ii LoxP – ura4+
iii LoxM + ura4+
iv LoxM – ura4+
Kb
4
3
2
1.5
1
0.5
1 2

Figure 3.6 Integration of SUMO-tr into the genome.

(A) Plasmids pAW41, pAW12 and pAW8 (adapted from Watson *et al.* 2008). pAW41 and pAW12 are used as templates for PCR. Transformation of *S.pombe* cells with the PCR products induces recombination and integration of LoxP and loxM sites flaking the SUMO gene. nmt = no message in thiamine promoter. Cre = Cre recombinase encoding gene. Leu = Leucine marker. **(B)** Diagram of recombination between loxP and loxM sites. **i)** Integration of half LoxP sites and *ura4.* **ii)** Excision of *ura4* and formation of full LoxP site. **iii)** Integration of *ura4* and Lox M site. **iv)** Integration of wild type or mutant gene sequence following transformation with pAW8, replacing the wild type DNA and resulting in loss of the *ura4* marker. **(C)** PCR from genomic DNA confirming integration of Lox sites and recombination between pAW8 and the base strain. The PCR products in C (i-iv) are equivalent to the steps outlined in B (i-iv). Primers used in each step are represented by blue or orange arrows

The exact sequence between the new LoxP and LoxM sites in the genome was simultaneously cloned into the pAW8 vector, resulting in pAW8-SUMO. Site directed mutagenesis was used as before, to incorporate a trypsin cleavage site directly upstream of the diglycine motif, resulting in pAW8-SUMO-tr. The base strain was transformed with either pAW8-SUMO or pAW8-SUMO-tr, resulting in recombination between the loxP and loxM sites. The wild type SUMO sequence or the mutant sequence SUMO-tr was consequently incorporated into the genome in place of the wild type SUMO sequence and *ura4*$^{+}$ marker (Figure 3.6B iii-iv). This resulted in loss of the *ura4*$^{+}$ marker which was verified by PCR and sequencing (Figure 3.6 B iv and C iv). These strains will be referred to as SUMO-wt and SUMO-tr, respectively.

3.8 Integration of a HIS-SUMO-tr into the genome

In order to pull down and analyse SUMOylated species *in vivo*, under endogenous conditions, an N-terminal HIS tag was incorporated into the genome using the SUMO base strain. To do this, two *Nde*I restriction sites present in the pAW8 vector were mutated (Figure 3.7A). The first was mutated using site directed mutagenesis, and the second by digesting and incubating with Klenow and then re-ligating the blunt ends. The SUMO and SUMO.tr ORF sequences were then sub-cloned from pAW8 into the *Nde*I-mutated pAW8 vector. Site directed mutagenesis was used to mutate three bases 5' of the SUMO start codon to form an *Nde*I restriction site for both the pAW8-SUMO and pAW8-SUMO.tr constructs. Two oligonucleotides were synthesised and

annealed to form a linker encoding a HIS_6 tag with *Nde*I-compatible overhangs (Figure 3.7B). The pAW8-SUMO and pAW8-SUMO-tr constructs were digested with *Nde*I and ligated with the annealed linker to incorporate a HIS_6 tag directly 5' of the SUMO start codon. This resulted in pAW8-HIS-SUMO and pAW8-HIS-SUMO-tr (Figure 3.7C). Transformation of the SUMO base strain with these constructs resulted in recombination between the Lox sites, incorporating the HIS tagged SUMO or HIS tagged SUMO-tr into the genome, in place of the wild type SUMO ORF.

3.9 Incorporation of a HIS tagged trypsin cleavable SUMO into the genome does not result in a mutant phenotype

The SUMO base strain, SUMO-wt, SUMO-tr, HIS-SUMO and HIS-SUMO-tr strains were tested for sensitivity to DNA damaging agents. None of the strains were sensitive to the DNA replication inhibitor hydroxyurea, or MMS as shown in spot tests (Figure 3.8A). Additionally none of the strains showed a mutant phenotype in response to UV irradiation or ionising radiation (Figure 3.8B). This means that incorporation of the Lox sites, a trypsin cleavage site and HIS tag into the *S. pombe* genome at the SUMO locus does not affect cell viability or response to DNA damaging agents. Therefore these strains can be used for further studies.

A

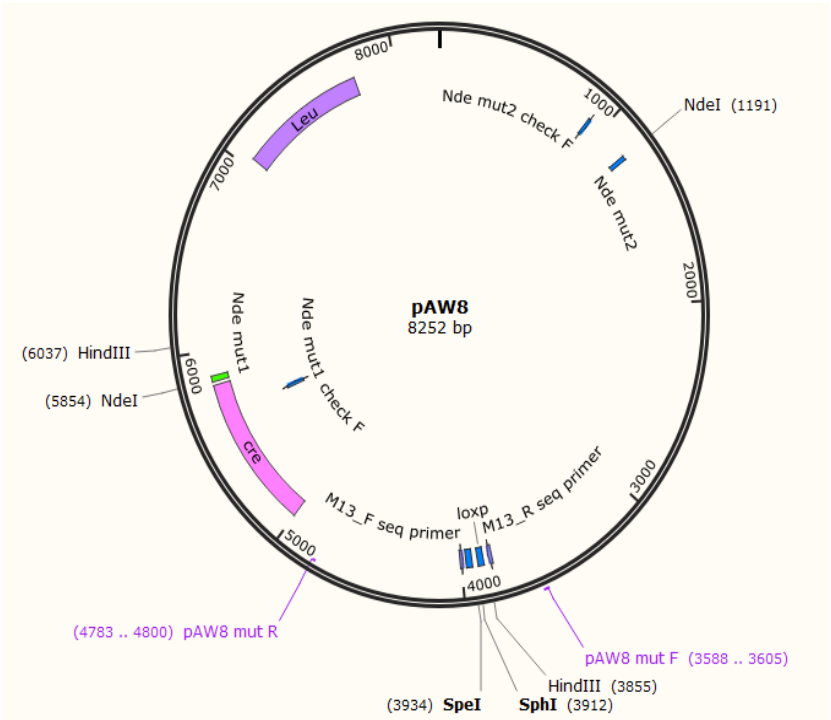

B

Linker F 5' TATGGGTAGCAGCCACCATCATCACCATCATCA 3'

Linker R 5' ACCCATCGTCGGTGGTAGTAGTGGTAGTAGTAT 3'

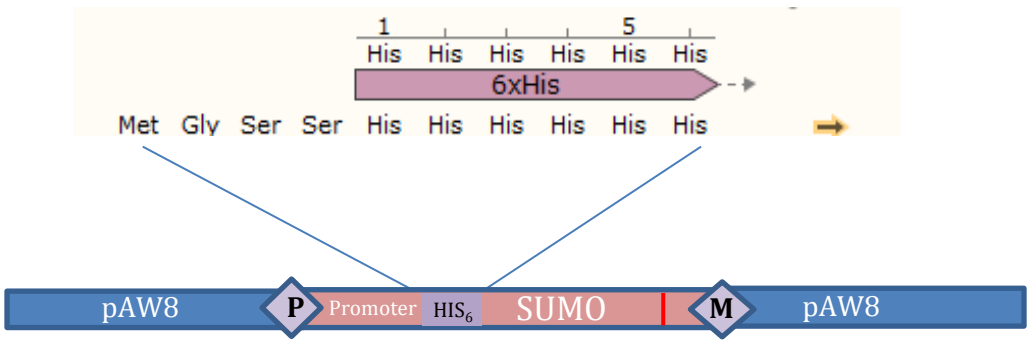

Figure 3.7 Integration of a 6xHIS tag into the SUMO base strain.
(**A**) Plasmid map of the pAW8 plasmid. Two *Nde*I sites in pAW8 were mutated using PCR mutagenesis and SUMO and SUMO-tr were sub-cloned into the MCS. An *Nde*I site was then created at the SUMO start codon for both pAW8-SUMO and pAW8-SUMO-tr. (**B**) Two oligonucleotides were generated and annealed to form a linker encoding a 6xHIS tag with *Nde*I compatible overhangs. This was ligated into the *Nde*I site resulting in HIS-SUMO or HIS-SUMO-tr.

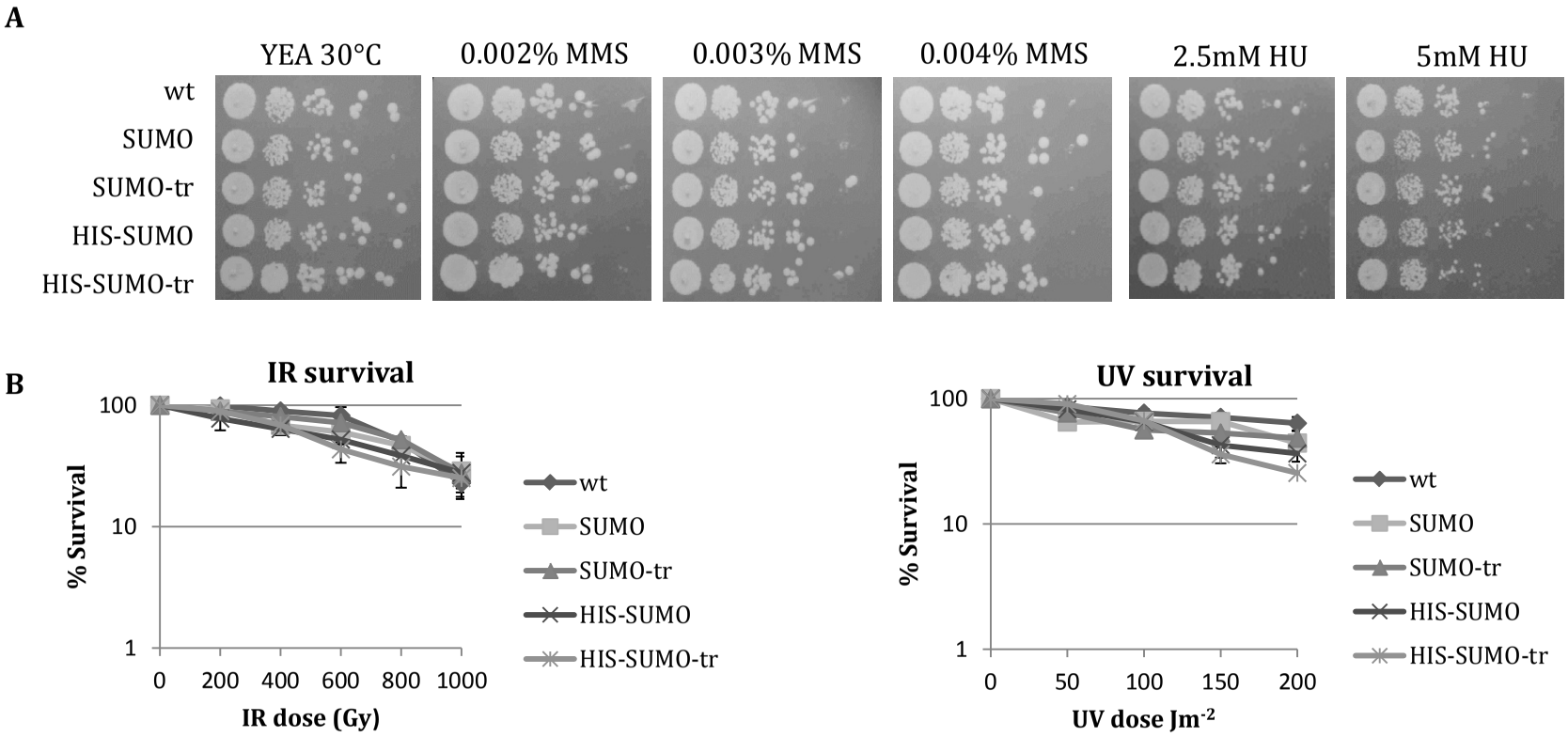

Figure 3.8 Integration of HIS-SUMO-tr into the genome does not result in a mutant phenotype

(A) 10 fold serial dilutions of wild type (wt), SUMO base strain (SUMO) SUMO-tr, HIS-SUMO and HIS-SUMO-tr plated onto YEA plates containing, 2.5mM HU and 5mM HU. None of the tagged or trypsin cleavable SUMO strains is sensitive to HU or MMS. **(B)** UV and IR survival assays for SUMO base strain, SUMO-tr, HIS-SUMO and HIS-SUMO-tr. Integration of a trypsin cleavage or HIS tag site does not result in sensitivity to UV or IR irradiation. Note that whilst an MMS sensitive control is not included here, independent assays confirmed these results and that the plates containing MMS were effective.

3.10 Using HIS-SUMO to pull down SUMOylated species *in vivo*

Ni^{2+} agarose was used to pull down HIS-SUMO under normal growth conditions and following a 200Gy dose of ionising radiation. The incorporation of a HIS tag results in a small band shift which can be seen when probing total cell extract with α-SUMO antibody (Figure 3.9A). High molecular weight SUMOylated species can be seen following a pull-down using HIS-SUMO. Samples probed with α-Nse2 antibody and α-Pcn1 (PCNA) antibody and also revealed the presence of higher molecular weight species, indicating that these proteins are likely to be SUMOylated at endogenous levels in response to DNA damage caused by ionising radiation. (Figure 3.9B). Unmodified PCNA and Nse2 are also detected following treatment with ionising radiation (Figure 3.9B, asterisks). It is unclear why the unmodified forms are pulled down in this assay. One possible explanation is that the SUMO has somehow become detached from the target proteins during purification. This is unexpected as the pull-down was done under denaturing conditions that should have inactivated SUMO specific proteases. However the absence of unmodified protein in lane 4 (HIS-SUMO – IR) suggests that unmodified protein is not binding to the Ni^{2+} agarose beads in untreated samples.

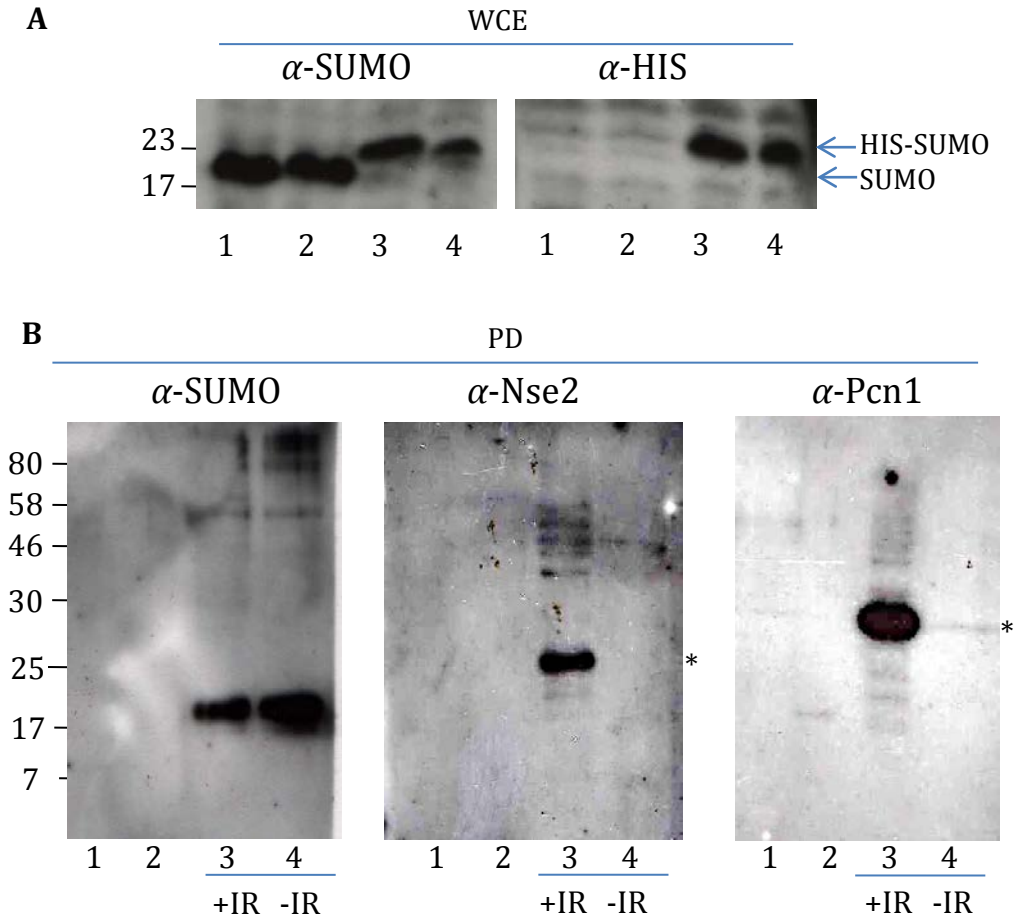

Figure 3.9 HIS-SUMO can be used to pull down SUMOylated species *in vivo*

(**A**) Whole cell extracts. 1, wt; 2, SUMO base strain; 3, HIS-SUMO isolate 1; 4, HIS-SUMO isolate 2. Band shift correlates with HIS tag integration. (**B**) HIS-SUMO pull down using Ni^{2+} agarose beads, + or - 200Gy irradiation. 1, wt; 2, SUMO-wt; 3, HIS-SUMO + IR; 4, HIS-SUMO – IR. Asterisks indicate unmodified protein.

3.11 Discussion

Components of the SUMOylation pathway were successfully expressed and purified from bacteria for use in *in vitro* assays. In order to identify the specific lysine residues which are SUMOylated following an *in vitro* assay, a trypsin-cleavable mutant version of SUMO was created called SUMOGG-tr. Previously, trypsin cleavage of modified proteins resulted in 23 amino acids of the SUMOGG protein remaining bound to the target. In many cases, these fragments would be expected to be too large for mass spectrometry analysis and would result in poor coverage of peptides. The integration of an arginine residue adjacent to the diglycine motif means that trypsin cleavage leaves only two amino acids bound to the target residue. The HIS-tagged trypsin-cleavable SUMO was purified from *E. coli* cells and shown to be proficient in the formation of SUMO chains *in vitro*. This resulted in successful analysis by mass spectrometry and the identification of specific SUMO target sites on a range of proteins. Several SUMO pathway components were identified as being SUMOylated from *in vitro* assays, including Hus5. In an *in vivo* study where Hus5 and SUMO were overexpressed, a band of the expected size of a SUMOylated Hus5 was identified in the strain transformed with wild type Hus5 that was not present when K50 was mutated. This is consistent with K50 being the sole SUMOylation site on Hus5. Ubc9 has been reported to be SUMOylated in both *S. cerevisiae* and humans, where in both cases it is suggested that it has regulatory roles. SUMOylation of mammalian Ubc9 on K14 has been reported to affect target specificity by providing an additional SIM binding surface (Knipscheer et al, 2008). Ubc9 SUMOylation in *S. cerevisiae* has been observed at two sites, K153 and K157, and has been shown to negatively regulate SUMOylation of septins as well as global SUMOylation (Ho et al, 2011). Another report demonstrated a requirement for SUMOylation of *S. cerevisiae* Ubc9 in meiosis, and suggested that auto-sumoylation switches Ubc9 from an active enzyme to a scaffold involved in SUMO chain formation (Klug et al, 2013). The role of Hus5 SUMOylation in *S. pombe* is as yet unknown and these studies were continued by other members of the lab.

A trypsin-cleavable, HIS-tagged SUMO was integrated into the genome following the construction of a SUMO base strain. The replacement of wild type SUMO

with either HIS-SUMO or HIS-SUMO-tr did not result in any mutant phenotype, and so this strain was used to pull-down SUMOylated species *in vivo*. A small scale pull-down using HIS-SUMO resulted in higher molecular weight bands being detected following ionising radiation, when probed with antibodies raised against both PCNA and Nse2. These results will be investigated further in subsequent chapters. This implies that the HIS-SUMO-tr strain can be used in further studies to identify and analyse SUMOylated proteins.

In ongoing and future work, the HIS-SUMO-tr strain could be used to pull down and identify known and novel SUMO targets. The advantage of using this strain is that all proteins are expressed at endogenous levels, reducing possible false positive results arising from the over-expression of tagged constructs. Large scale pull-downs may be required to identify proteins which are modified at low levels. The HIS-SUMO strain could be crossed with mutant strains to investigate the effect of global SUMOylation or the SUMOylation of a specific target protein under a range of conditions. It could also be used in combination with SILAC to identify and analyse levels of SUMOylated proteins *in vivo*. This research could lead to further understanding the role of SUMOylation of proteins involved in several pathways including the DNA damage response.

4 Investigation into Nse2 auto-SUMOylation in S.pombe and analysis of Nse2 mutations found in humans

4.1 Introduction

Unlike the ubiquitin pathway, which features hundreds of E3 ligases, only two SUMO ligases have been identified to date in *S. pombe*. Nse2 is a SUMO ligase which is classified as a member of the PIAS family (Andrews et al, 2005; McDonald et al, 2003; Sergeant, 2005). Members of this class of ligases have a C-terminal SP-RING finger motif similar to but distinct from those in ubiquitin ligases. RING finger domains form a globular structure capable of binding E2 conjugating enzymes, by co-ordinating Cystine and Histidine residues (Borden, et al. 2000). Siz/PIAS (SP-RING) domains have conserved sequences similar to the RING domain observed in ubiquitin E3 ligase proteins, with the exception of two conserved cysteine residues (Hochstrasser, 2001).

Nse2 is thought to play a regulatory role within the Smc5/6 complex, although how this occurs remains to be determined. This chapter investigates three Nse2 auto-SUMOylation sites identified *in vitro*, two of which two have been previously identified in the lab (Andrews, E, DPhil thesis, Univ. of Sussex). The role of Nse2 auto-SUMOylation is also currently unknown. *nse2* lysine to arginine (K to R) mutants were integrated into the genome to investigate the effect of an inability of Nse2 to auto-SUMOylate *in vivo*.

It has been suggested that whilst the other SUMO ligase Pli1 is involved in global SUMOylation, Nse2 targets a specific subset of proteins for SUMOylation, mediated by an interaction between Ubc9 and Rad60 (Prudden et al, 2011). Nse2 is associated with the Smc 5/6 complex, and physically interacts with the coiled coil of Smc5 (Duan et al, 2009b). Nse2 is auto-SUMOylated and SUMOylates other members of the Smc5/6 complex *in vitro*, including Nse3 and Nse2 as well as Smc6, which is also SUMOylated *in vivo* (Andrews et al, 2005).

Recently, two patients have been identified who each carry two mutations in the *mms21* (*nse2*) gene. The patients are not cancer-prone but present with primordial dwarfism and resistance to insulin. The first pair of mutations results in a premature stop codon and a base change within the SP-RING catalytic domain, these are S223X and T172A. These mutations result in reduced SUMO ligase activity of Nse2 in human cells. The second pair of mutations are frame-shift mutations, both resulting in premature stop codons. These are S116fsX132 and A234fsX236. For simplicity, these mutations will be referred to as S116X and A234X from now on. Cells containing these mutations were noted to have a defect in recovery following HU treatment. Bi-nucleate cells were also observed, indicating that these mutations result in a defect in chromosome segregation.

4.2 Aims

The aims of this work were firstly to investigate the role of Nse2 auto-SUMOylation in *S. pombe*, and secondly to create and analyse *S. pombe* strains containing the equivalent *mms21* mutations that were found in patients.

4.3 Nse2 is SUMOylated *in vitro* at residues K134, K229 and K248

An *in vitro* SUMOylation assay was carried out using the trypsin cleavable SUMO protein (SUMO-tr) generated as described previously (see chapter 3.4) using GST-tagged Nse2 as a substrate (Figure 4.1) (Mercer, B DPhil thesis, Univ. of Sussex). Gel slices were analysed by LC-MS/MS and three lysine residues were identified as being SUMOylated. These were K134, K229 and K248 (Figure 4.2 A, B and C, respectively). Two of these residues, K229 and K248, had previously been identified as SUMOylated *in vitro* (Andrews, E, DPhil thesis, Univ. of Sussex). A sequence alignment between *S. pombe* Nse2 and the human and *S. cerevisiae* homologues (Mms21) shows a low level of overall sequence homology between the species at the N terminus. However the catalytic C terminal domain is more highly conserved. The SUMO modified residues identified from this and previous studies are conserved between the *S. pombe* and human sequences (Figure 4.3). The structure of the SP-RING domain of the

human homologue Mms21 is available (He F, 2007) and the structure of *S. cerevisiae* Mms21 with part of the Smc5 protein has also been published (Duan et al, 2009a). There are currently no structural data available for *S. pombe* Nse2. Protein structure modelling software '*phyre2*' was therefore used to generate a predicted structure of *S. pombe* Nse2. The phyre2 server uses 'template-based homology modeling and fold-recognition' (Kelley & Sternberg, 2009) to predict the structure of a protein based on sequence homology and the published structures of homologous proteins or motifs. A results page is generated which includes information about secondary structure prediction, and protein models with a score of confidence (Kelley & Sternberg, 2009). Structures can be opened as a .pdb file using the 'PYMOL Molecular Graphics System'. Using this programme, 3D structures can be highlighted, coloured and manipulated. Further information about the download and use of PYMOL can be found at www.pymol.org. The lysine residues identified as SUMOylated from the *in vitro* SUMOylation assay were mapped to each of these structures (Figure 4.4). K248 is located at the extreme C-terminus of Nse2, which has been shown to interact with Smc5 (Duan et al, 2009b). SUMO modification of this residue could therefore potentially disrupt this interaction, de-stabilising the Smc5/6 complex. K229 is in the SP-RING domain (Figure 4.4, highlighted with a blue box) which is required for SUMO ligase activity, and K134 is positioned in the middle of an α-helix C-terminal to the SP-RING domain.

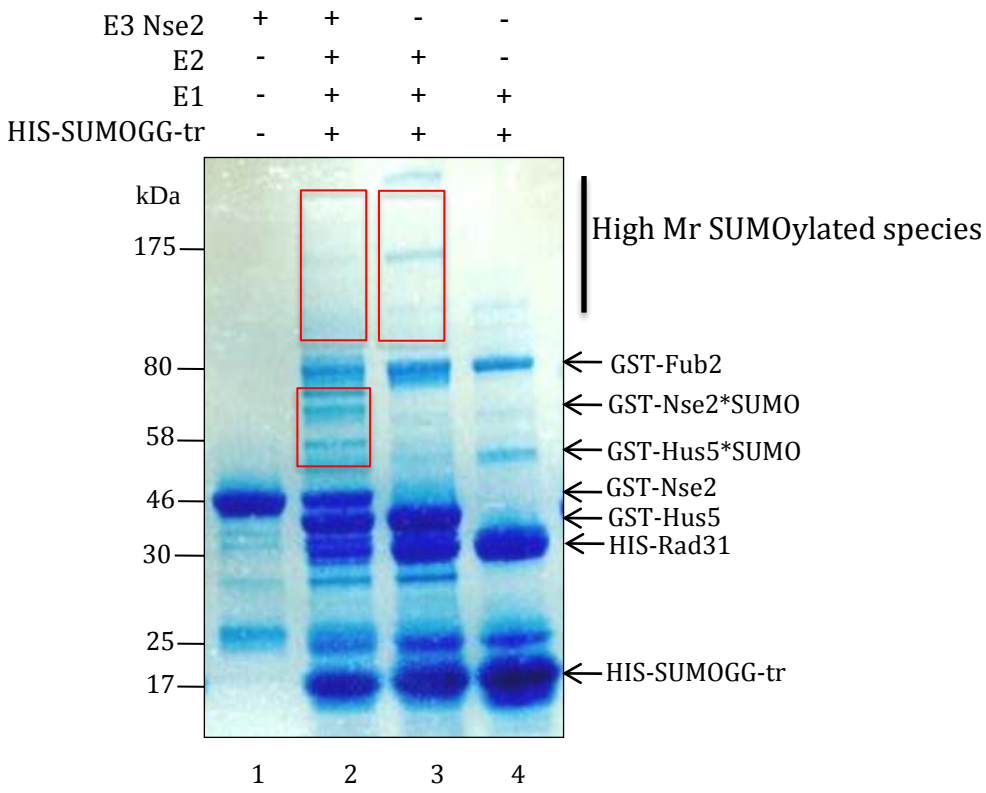

Figure 4.1 Nse2 is auto-SUMOylated *in vitro*.

Colloidal blue staining of SDS-PAGE gel of an *in vitro* SUMOylation assay containing HIS-SUMOGG.tr, E1 activating enzyme, E2 conjugating enzyme and E3 ligase Nse2. Lane 1, GST-Nse2; lane 2, HIS-SUMOGG-tr, E1 activating enzyme HIS-Rad31 GST-Fub2, E2 conjugating enzyme GST-Hus5 and E3 ligase GST-Nse2; lane 3, HIS-SUMOGG-tr, HIS-Rad31 GST-Fub2 and GST-Hus5.; Lane 4, HIS-SUMOGG.tr and HIS-Rad31 GST-Fub2. Red boxes highlight gel slices which were excised and analysed by MS/MS. Bands corresponding to SUMO machinery and SUMOylated proteins are highlighted with arrows (Mercer, B DPhil thesis, Univ. of Sussex). Mr = molecular weight.

A

y8 y2 y1

Y G T Q G E Y I E F K^{134} (GG) K

b11

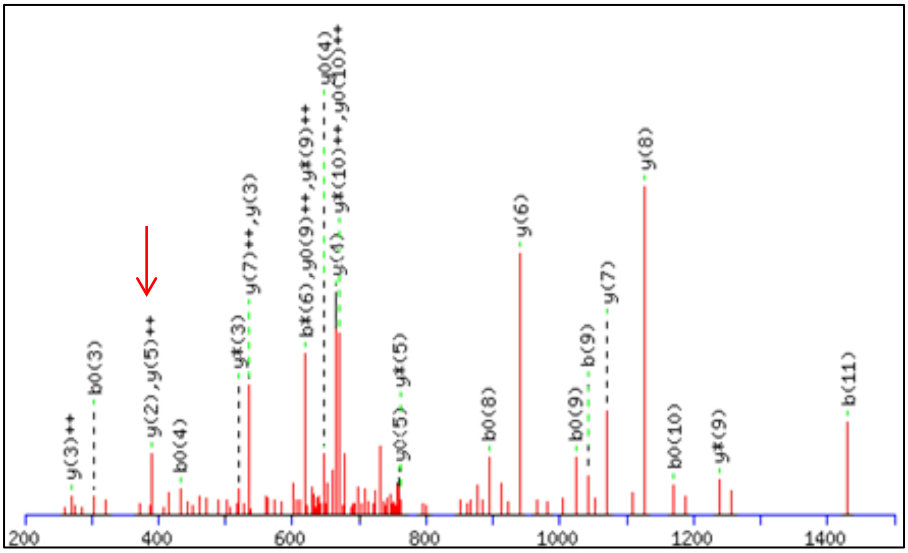

B

y8 y6 y1

S L L K^{229} (GG) E D E I L E R

b4

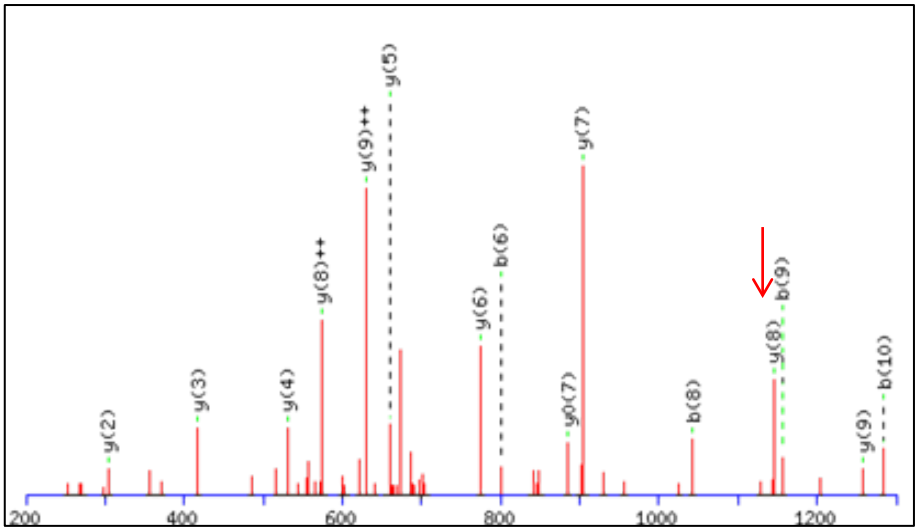

C

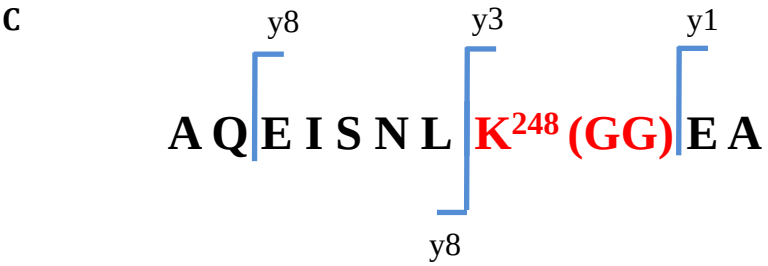

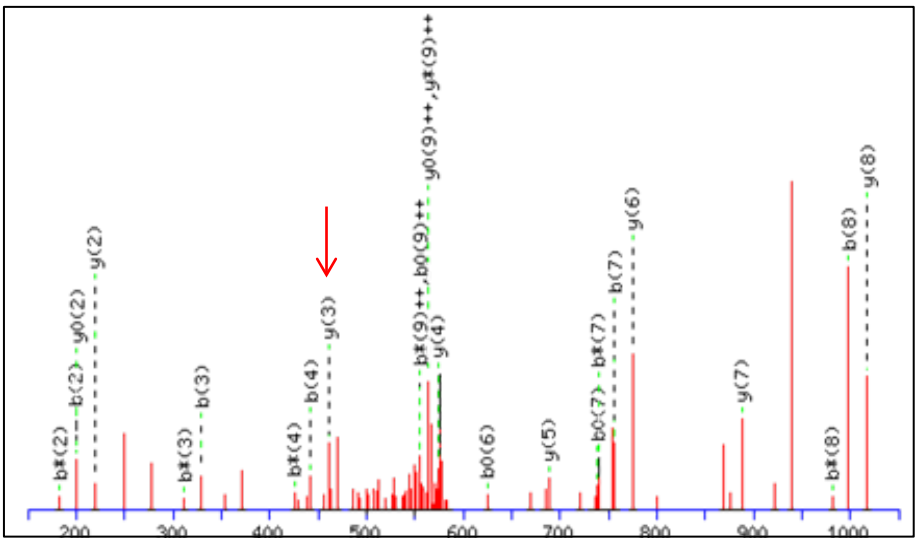

Figure 4.2 Nse2 is SUMOylated *in vitro* at K134, K229 and K248

Nse2 is can be auto-SUMOylated *in vitro.* (**A**) MS/MS data identifying Nse2 lysine residue K134 conjugated to the SUMO diglycine motif. The red arrow highlights the y2 ion which corresponds to diglycine linked to K134. (**B**) MS/MS data identifying Nse2 lysine residue K229 conjugated to the SUMO diglycine motif. (**C**) MS/MS data identifying Nse2 lysine residue K248 conjugated to the SUMO diglycine motif.

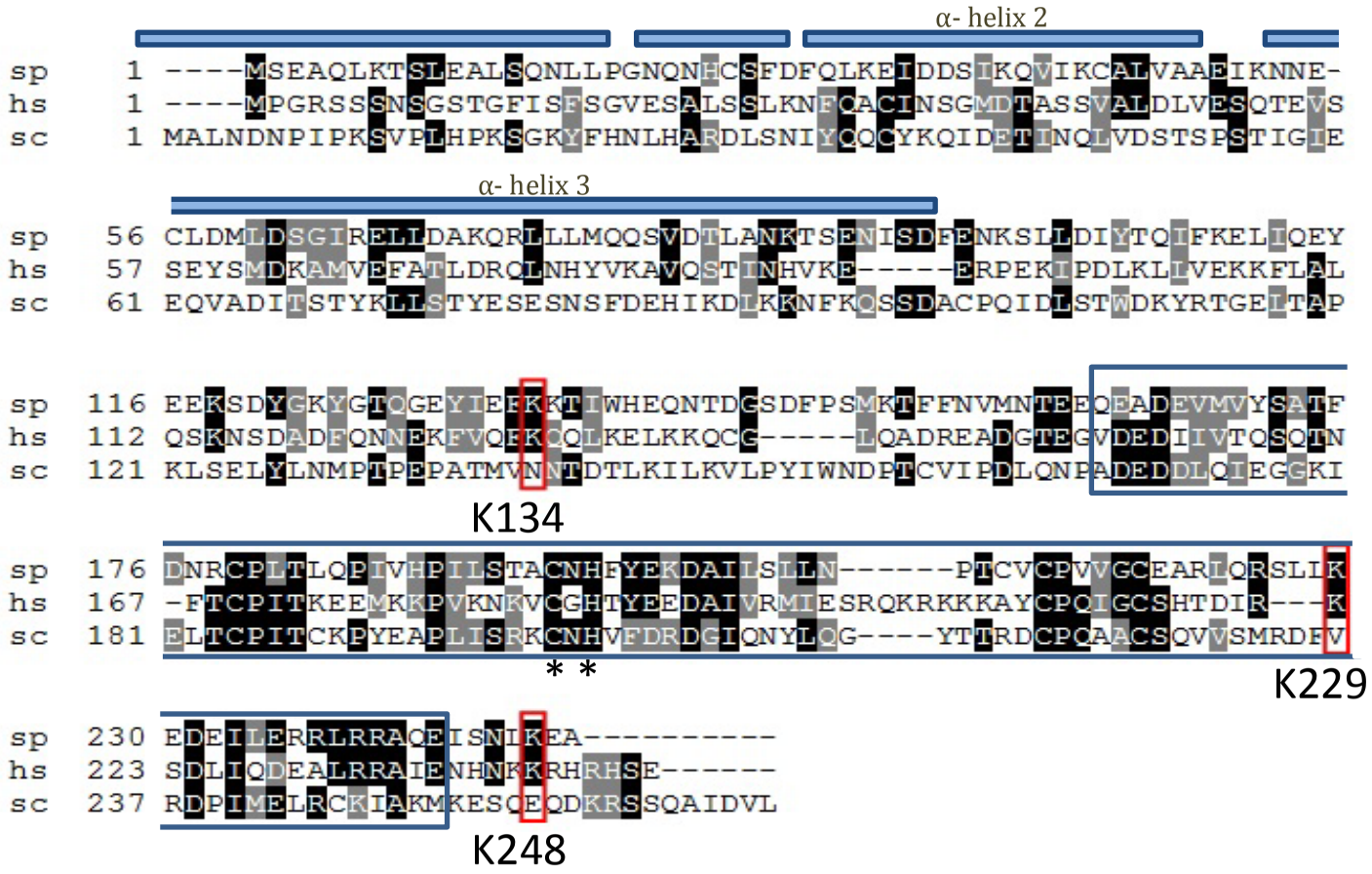

Figure 4.3 Sequence alignment of *S.pombe* Nse2 and *S.cerevisiae* and human homologues Mms21. Lysine residues identified as sumoylated *in vitro* are highlighted with a red box. The SP-RING domain is highlighted with a blue box. * indicates conserved catalytic cysteine and histidine residues. Light blue boxes indicate four areas required for interaction with Smc5 in *S.cerevisiae* which include two α-helices and two N-terminal sequences (Duan, Sarangi et al. 2009 sp = *S.pombe*, hs = human, sc = *S.cerevisiae*

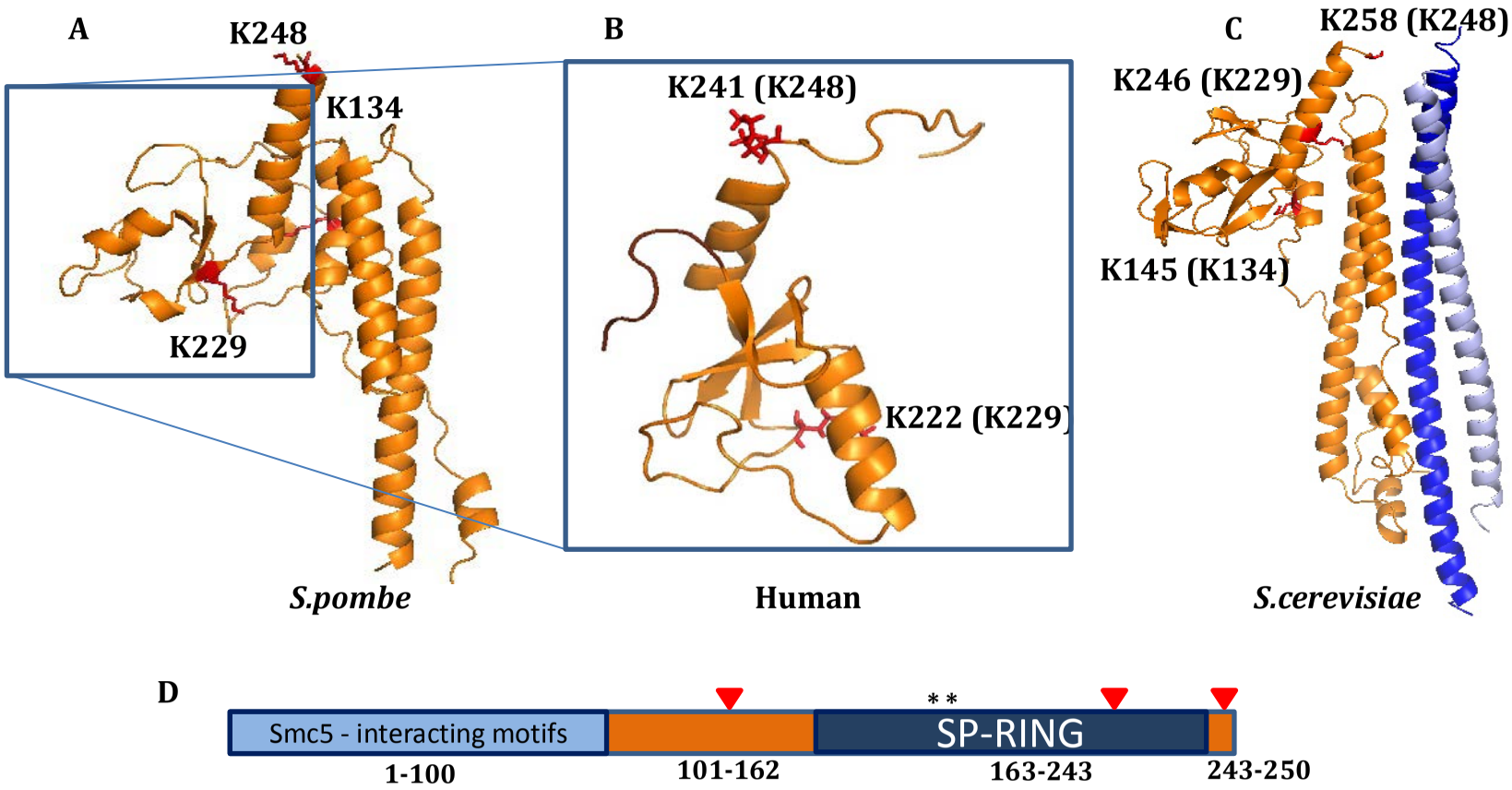

Figure 4.4. Pymol structures of Nse2/Mms21.

(A) Phyre2 predicted structure of *S.pombe* Nse2 with position of SUMOylated residues identified *in vitro* highlighted. **(B)** Human Mms21 SP-RING domain structure (aa 168-247) (He F 2007). The position of the conserved lysine residues are highlighted in red. (**C**) Structure of *S.cerevisiae* Nse2 homologue Mms21 (Duan, Sarangi et al. 2009). The Smc5 arm is highlighted in blue. Mms21 is shown in bronze. The lysine residues closest to those conserved in *S.pombe* and humans are highlighted in red.**(D)** Schematic map of Nse2 highlighting the N –terminal regions involved in Smc5 binding in the S.cerevisiae Mms21 homologue. SUMOylation sites are highlighted with red triangles. Catalytic Cys and His residues highlighted with asterisks.

4.4 Generation of an *nse2* base strain

Previous analysis of *nse2* lysine to arginine mutants in the Watts lab have given conflicting results and it was unclear whether the lysine residues identified as auto-SUMOylated are required for Nse2 SUMO ligase activity. In order to analyse *nse2* K to R mutants *in vivo*, a base strain for *nse2* was generated to allow incorporation of K to R mutations into the genome in place of the wild type *nse2* ORF. LoxP and LoxM sites were incorporated into the genome flanking the *nse2* coding sequence, where LoxP was integrated immediately upstream of the *nse2* promoter, and LoxM directly adjacent to the stop codon, using the method described in chapter 3 (Watson et al, 2008) (Figure 4.5A). This was a two-step process as *nse2* is an essential gene in *S. pombe*. The resultant LoxP-*nse2*-*ura4*$^{+}$-LoxM strain is referred to as the *nse2* base strain. The *nse2* coding sequence flanked by LoxP and LoxM sites was simultaneously cloned into the pAW8 vector to generate pAW8-*nse2*. Transformation of the *nse2* base strain with pAW8-*nse2* resulted in the wild type *nse2* sequence replacing the original sequence and the *ura4*$^{+}$ marker. This strain is referred to as *nse2*. Survival assays using the *nse2* base strain and *nse2* strain were carried out following treatment with ionising radiation and UV irradiation (Figure 4.5B). Neither strain showed increased sensitivity to these damaging agents compared to wild type *S. pombe* cells. The absence of a mutant phenotype means that the *nse2* base strain can be used for the integration of novel *nse2* mutations.

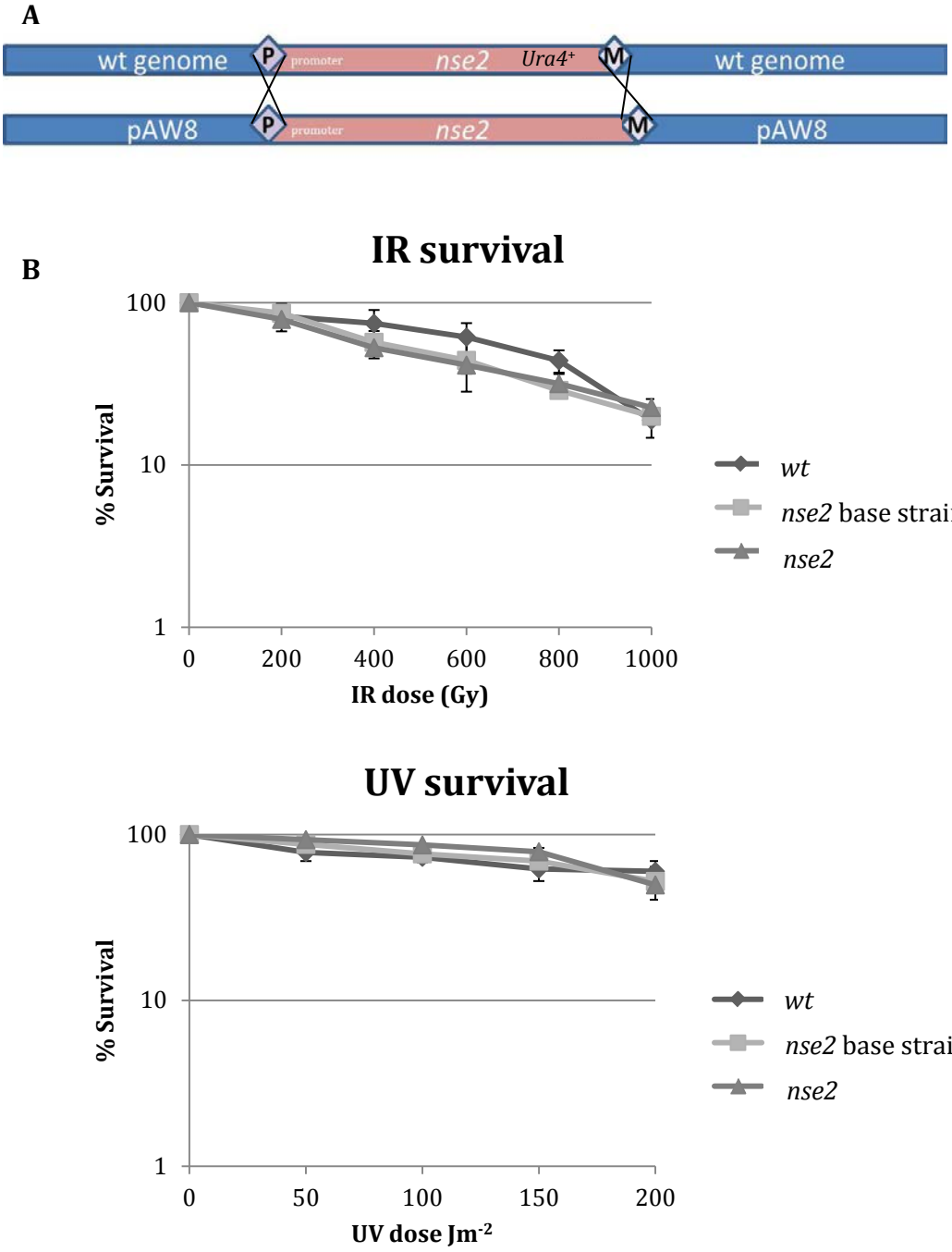

Figure 4.5. The *nse2* base strain has no mutant phenotype.
(**A**) A base strain for nse2 was created and the exact sequence flanked by the LoxP and LoxM sites cloned into the pAW8 plasmid as described previously. Site directed mutagenesis was used to create lysine to arginine mutations at *K134*, *K229* and *K248*. (**B**) Survival curves were plotted following exposure to increasing doses of UV or IR irradiation. *nse2* bs = *nse2* base strain (LoxP-*nse2*-*ura4*-LoxM). Integration of wild type *nse2* into the *nse2* base strain shows no mutant phenotype following UV or IR treatment.

4.5 *nse2* K to R mutants do not have a mutant phenotype

In order to investigate the role of SUMOylation of Nse2 *in vivo*, a series of lysine to arginine mutants were generated. Site directed mutagenesis was used on pAW8-*nse2* to generate *K134R*, *K229R* and *K248R* single mutants, as well as double and triple lysine mutant constructs. These were transformed into the *nse2* base strain and integrated into the genome following recombination between the LoxP and LoxM sites. If Nse2 is not modified at any additional sites other than those identified in the *in vitro* SUMOylation assay, the triple mutant, *nse2*-K*134R K229R K248R*, should be unable to be SUMOylated. None of the lysine mutants showed a notable increase in sensitivity to ionising radiation (Figure 4.6 A). Only the triple lysine mutant showed a very slight increase in sensitivity to high doses of UV irradiation (Figure 4.6 B). None of the lysine to arginine mutants showed an increased sensitivity to hydroxyurea or MMS compared to wild type (Figure 4.7). A ligase dead nse2 mutant has previously been shown to be sensitive to MMS and HU (Andrews et al, 2005), as well as mildly sensitive to ionising radiation and UV irradiation. It has been demonstrated that SUMOylation of target proteins including Smc6 is important for the DNA damage response (Andrews et al, 2005). The lysine mutants created here show no sensitivity to these DNA damaging agents, suggesting that the mutations do not affect the ability of Nse2 to SUMOylate target proteins or interaction of Nse2 with the Smc5/6 complex.

A

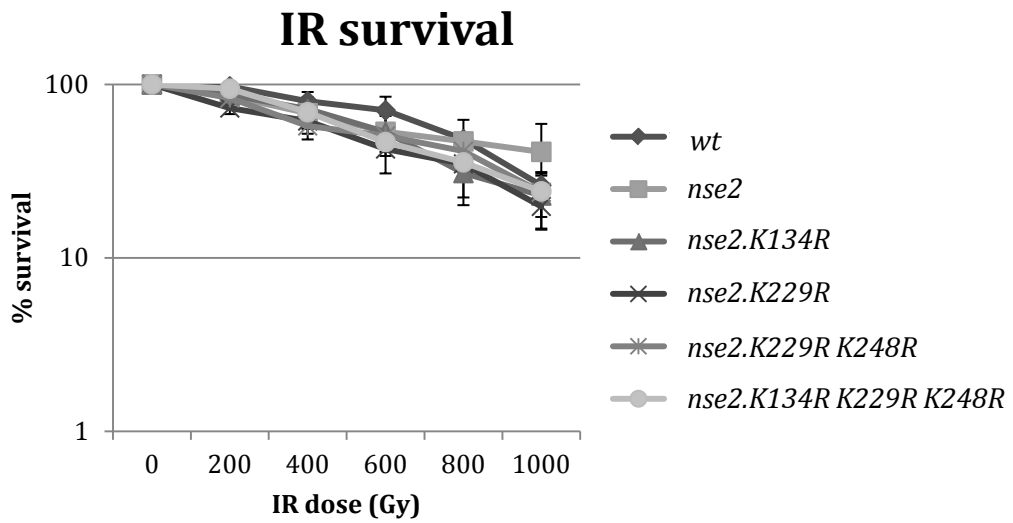

B

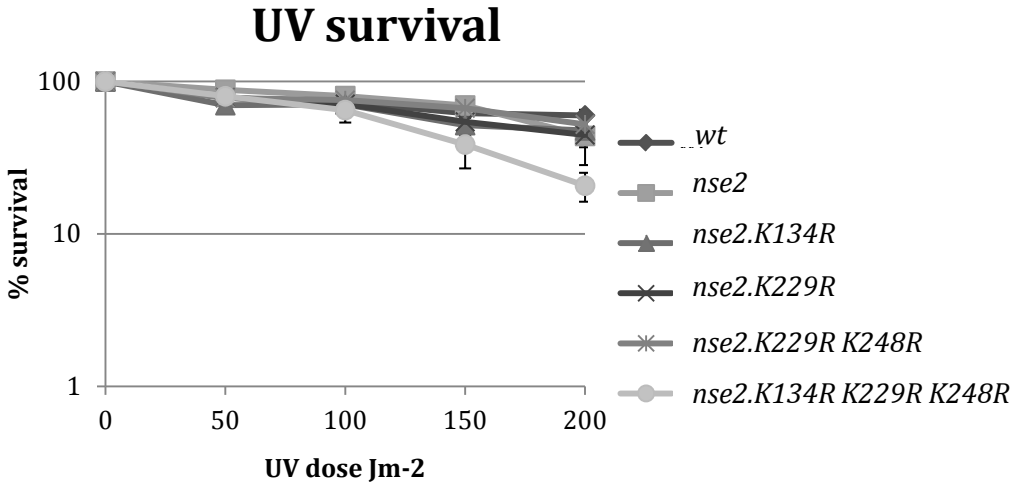

Figure 4.6. *nse2* lysine to arginine (K to R) mutants are not sensitive to UV or IR.

Survival curves were plotted following exposure to increasing doses of UV irradiation or ionising radiation. Single, double and triple *nse2* lysine mutants were not sensitive to ionising radiation The triple lysine mutant shows a very slight increase in sensitivity to UV irradiation.

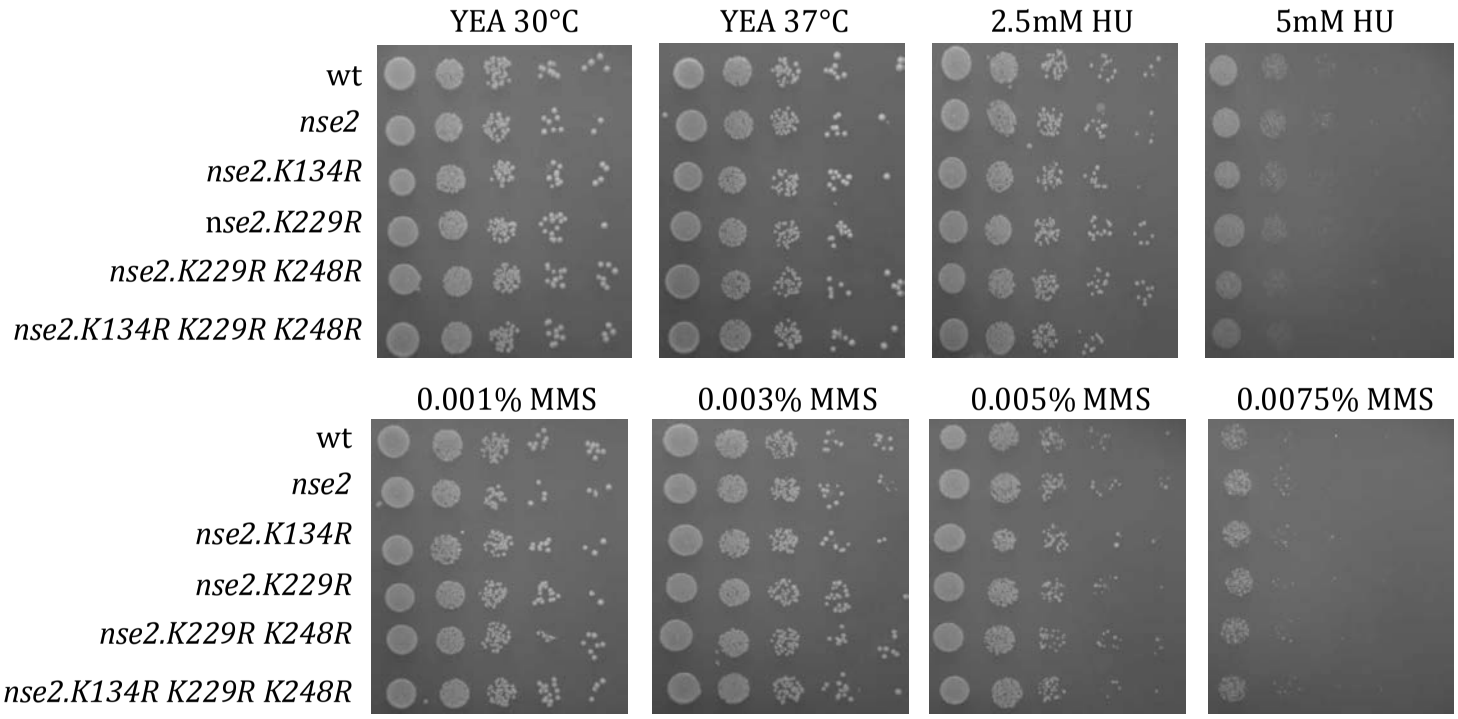

Figure 4.7. *nse2* K to R mutants have no mutant phenotype.

Lysine to arginine mutations were integrated into the genome in place of the wild type Nse2 ORF using the *nse2* base strain. 10 fold serial dilutions of each strain were spotted onto plates containing MMS or hydroxyurea. Neither the single, double or triple lysine mutants resulted in increased sensitivity to hydroxyurea or MMS.

4.6 Nse2 expression levels and global SUMOylation levels are unaffected in *nse2* K to R mutants

In order to investigate whether an inability to auto-SUMOylate Nse2 has an effect on global SUMOylation levels, total cell extracts were prepared from asynchronously growing *S. pombe* cells containing single, double and triple lysine to arginine mutants. Samples were analysed by western blot and probed with antibodies against SUMO to observe global SUMOylation levels in these cells (Figure 4.8). No significant change in SUMOylation levels could be observed compared to cells containing wild type Nse2 (Figure 4.8 A, lanes 2-5 compared with lane1). Samples were also probed with an Nse2 antibody in order to observe any changes in Nse2 protein expression levels in strains containing the lysine mutants. Again, no significant changes could be observed when compared to the wild type (Figure 4.8 B lanes 2-5 compared with lane1) or when comparing single and double lysine mutants (Figure 4.8 B lanes 2-5). Whilst the *nse2* base strain carrying wild type *nse2* appears to show an increase in SUMOylation levels (Figure 4.8 A lane 2) and Nse2 expression levels (Figure 4.8 B lane2), this can be attributed to loading error (Figure 4.8 C, lane 2) These results do not indicate an obvious role for auto-SUMOylation of Nse2 *in vivo*. It is possible that the role of Nse2 SUMOylation will only be revealed in combination with another genetic defect, for example when another pathway or protein is otherwise unavailable. Further genetic analysis would be required to investigate this. Additionally, SUMOylation of Nse2 needs to be confirmed *in vivo*. It is possible that the Nse2 SUMOylation observed *in vitro* is not biologically significant and may be an artefact of the reaction. These studies were not continued in favour of other projects.

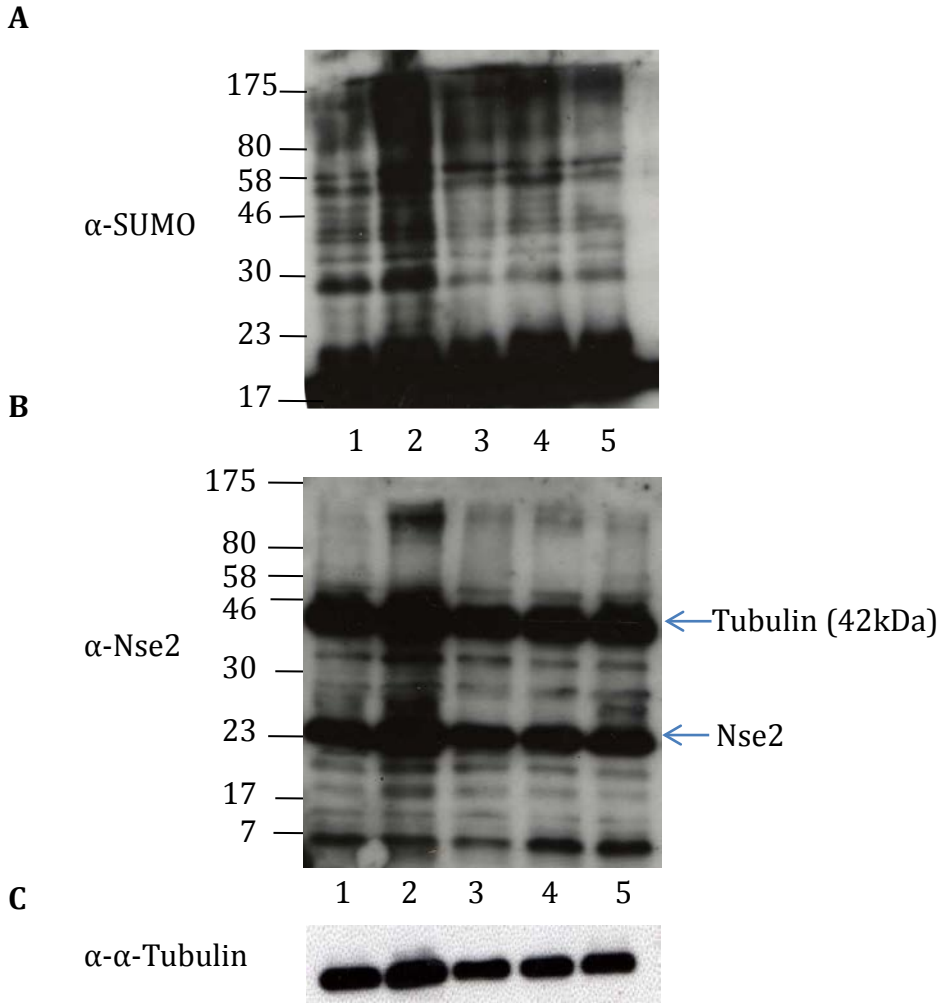

Figure 4.8 Nse2 K to R mutants are expressed at normal levels
Whole cell extracts from *S.pombe* cells containing *nse2* K to R mutants were probed with antibodies raised against SUMO and Nse2. (**A**) All of the K to R mutants tested have normal global SUMOylation levels. (**B**) All of the K to R mutants tested have normal expression levels of Nse2. Lane 1, wild type, lane2, n*se2*, lane3, n*se2.K134R*, Lane 4 n*se2.K229R,* lane 5 n*se2.K229R K248R*. (**C**) Tubulin loading control. Lane 2 (n*se2)* contains more protein than lanes 1, 3,4 and 5. SDS-PAGE gels 10%.

4.7 Modelling and integration of Nse2 patient mutations in *S. pombe*

The position of the mutations in nse2 found in patients with Nse2 defects can be mapped to the predicted structure for *S. pombe* Nse2 (Figure 4.9 A). Pymol software was used to manipulate the protein sequence, in order to predict the effect that the mutants might have on Nse2 protein structure (Figure 4.9 B-C). The *Nse2.T172A S223X* mutation results in the loss of 25 amino acids at the C terminus (Figure 4.9 B), which would likely de-stabilise the SP-RING finger domain and subsequently affect SUMO ligase activity. The effects of the S116fsX132 mutation are much more severe and would result in a loss of the whole catalytic domain of the protein (Figure 4.9 C).

The pAW8-*nse2* construct was used for site directed mutagenesis to create mutations mimicking those found in the DNA of two patients (See Figure 4.11 C, columns 1 and 2 for the equivalent mutations in *S. pombe*). A sequence alignment of the *S. pombe*, human and *S. cerevisiae* Nse2 (Mms21) sequences was used to map these mutations (Figure 4.10). Three of the mutations T172A, S223X and A234fsX236 are located within the SP-RING domain which is required for SUMO ligase activity. Of these, the threonine residue T172 is conserved in *S. pombe*. Site directed mutagenesis was used to create a point mutation in the pAW8-*nse2* construct, resulting in pAW8-*nse2.T172A*. The serine residue at position 223 in the human sequence is not conserved. In order to create a similar mutation, S226 was replaced with a stop codon. This is referred to as pAW8-*nse2.S226X*. pAW8-*nse2.T172A S226X* was also generated. Transformation of each of these constructs into the Nse2 base strain resulted in recombination between the LoxP and LoxM sites. As a result the wild type Nse2 ORF was replaced with the singly or doubly mutated sequences. The A234 residue is conserved in *S. pombe.* Mutagenesis was carried out in which the deletion of one nucleotide caused a frame shift. This resulted in a stop codon two nucleotides down-stream (A234fsX236). For simplicity, the construct is referred to as pAW8-*nse2.A234X*. The S116fsX132 frame-shift mutation was mimicked by mutating the equivalent residue at position 135 in the *S. pombe* sequence to a stop codon. This is referred to as pAW8-*nse2-K135X*. These

constructs were transformed into the *nse2* base strain to incorporate the mutant sequences into the genome in place of the wild type *nse2* sequence, under the control of the endogenous promoter. No colonies were formed following several attempts at transformation of the *nse2* base strain with pAW8-*nse2-K135X*. This suggests that this mutation is lethal in yeast.

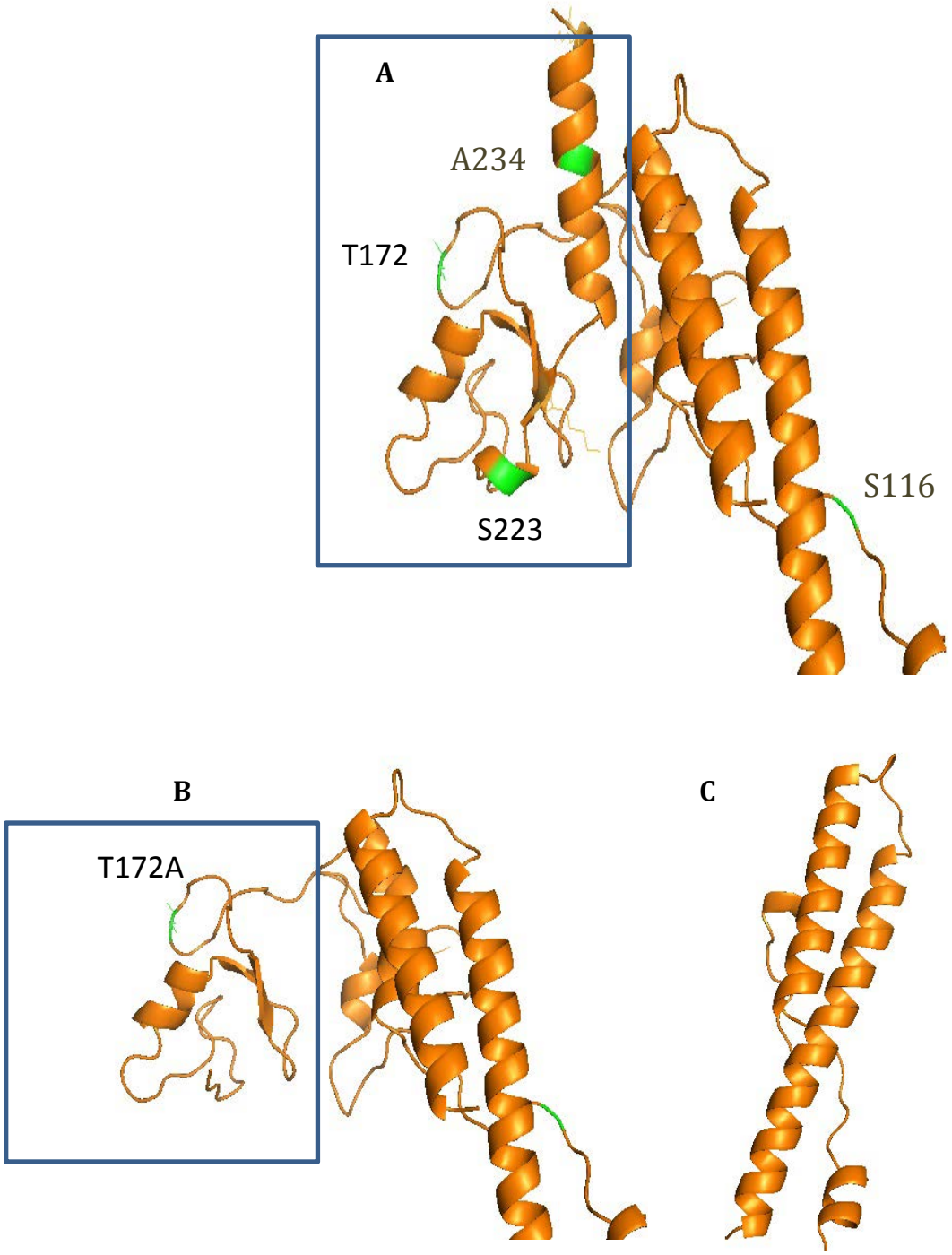

Figure 4.9. *Phyre2* predicted structures of *S.pombe* Nse2.
(**A**) The predicted structure of *S.pombe* Nse2 with the locations of human patient mutations highlighted in green. (**B**) The potential effects of the *nse2.T127A S223X* mutations on the structure of the *S.pombe* Nse2 protein. (**C**) The predicted effect of the *nse2.A234fsX236, S116fsX132* mutations on the *S.pombe* Nse2 protein structure. Here the entire C terminus including the RING domain required for SUMO ligase activity is abolished.

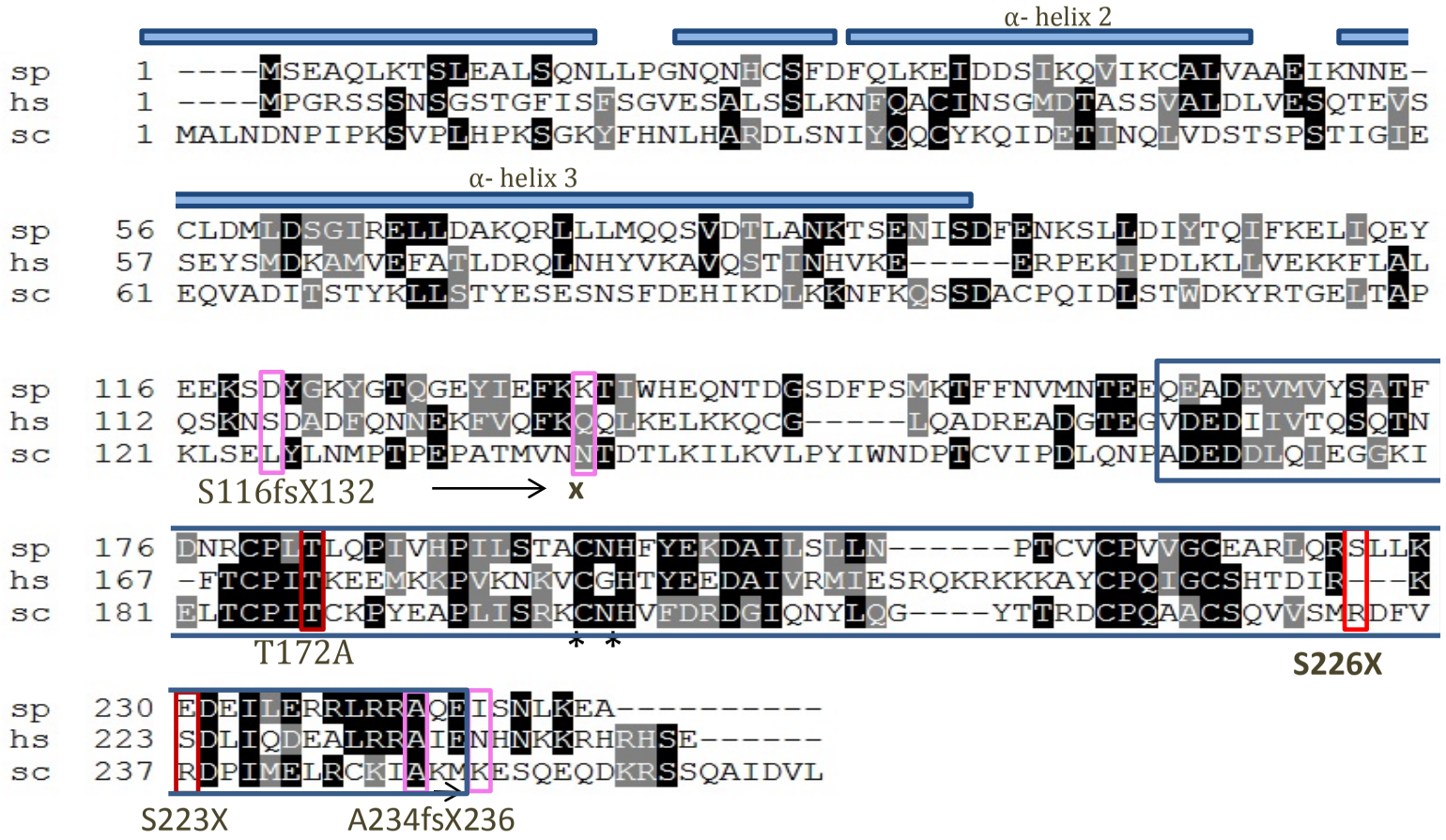

Figure 4.10. Sequence alignment of *S.pombe* Nse2 and human and *S.cerevisiae* Mms21 homologues.

Sequence alignment of *S.pombe* Nse2, *S.cerevisiae* and mammalian Mms21 amino acid sequences. Dark red boxes highlight two mutations found in one patient (T172A and S223X), pink boxes highlight two mutations found in a second patient (S116fsX132 and A234fsX236). Where residues are not conserved, equivalent or similar mutations were created. These are highlighted in bold. The SP-RING domain is highlighted with a blue box. Light blue boxes indicate four areas required for interaction with Smc5 in *S.cerevisiae* which include two α-helices and two N-terminal sequences (Duan, Sarangi et al. 2009). sp = *S.pombe*, hs = human, sc = *S.cerevisiae*

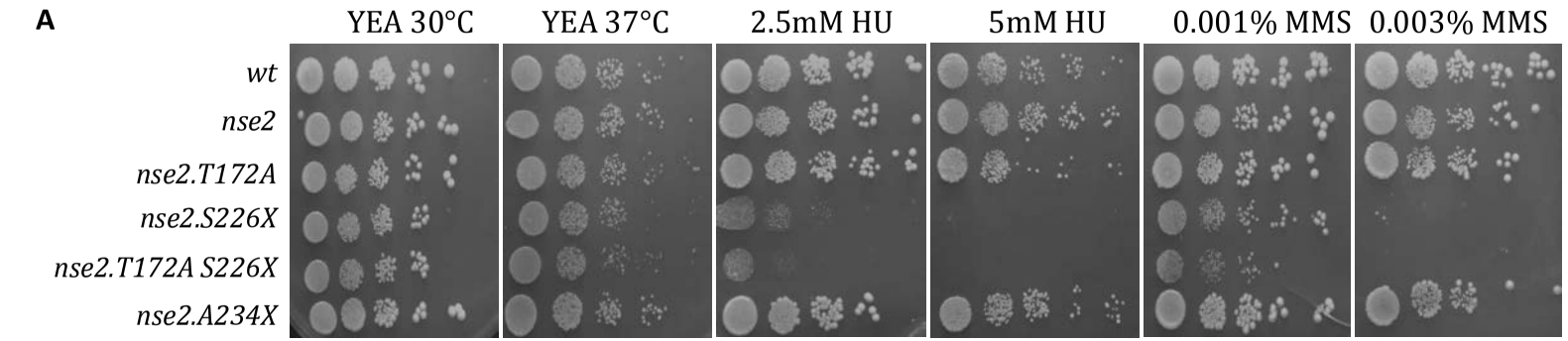
A
YEA 30°C
YEA 37°C
2.5mM HU
5mM HU
0.001% MMS
0.003% MMS
wt
nse2
nse2.T172A
nse2.S226X
nse2.T172A S226X
nse2.A234X

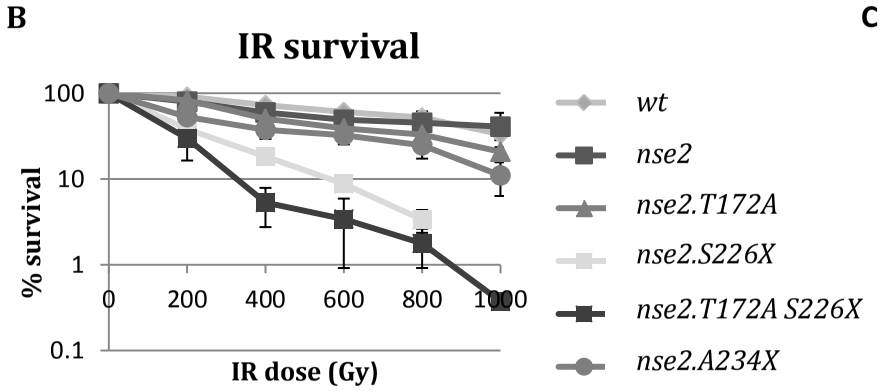
B
IR survival
% survival
100
10
1
0.1
0
200
400
600
800
1000
IR dose (Gy)
wt
nse2
nse2.T172A
nse2.S226X
nse2.T172A S226X
nse2.A234X

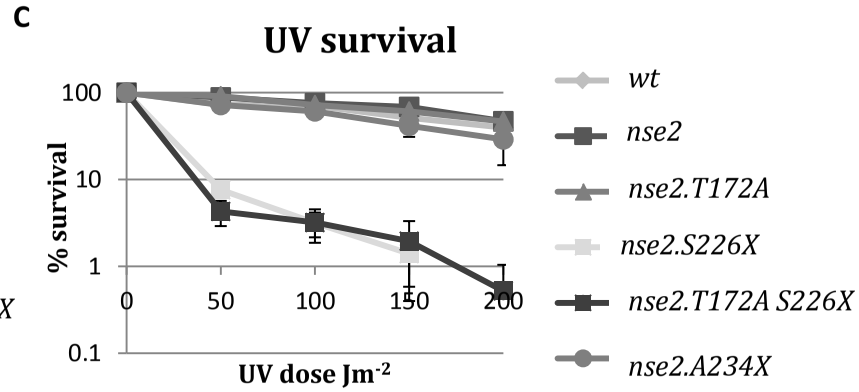
C
UV survival
% survival
100
10
1
0.1
0
50
100
150
200
UV dose Jm-2
wt
nse2
nse2.T172A
nse2.S226X
nse2.T172A S226X
nse2.A234X

D

Human mutation	***S.pombe* mutation**	**HU**	**MMS**	**IR**	**UV**
S223X	S226X	++	+++	++	+++
T172A	T172A	-	-	-	-
T172A S226X	T172A S226X	++	+++	+++	+++
S116fsX132	K135X	-(inviable)			
A234fsX236	A234fsX236 (A234X)	-	-	-	-

Figure 4.11 The *nse2* S226X mutant is sensitive to HU and DNA damaging agents.

(**A**) 10 fold serial dilutions of *nse2* mutant strains plated onto YEA plates containing 2.5mM HU, 5mM HU or a range of concentrations of MMS. Cell growth at 37°C indicates structural stability. (**B**) Survival curves following exposure to increasing concentrations of ionising radiation. (**C**) Survival curves following exposure of increasing concentrations of UV and IR irradiation. Only strains containing the *nse2*.S226X mutant show sensitivity to all DNA damaging agents tested. (**D**) Table of the *S.pombe* equivalents of human *mms21* mutations (column 1-2) summarising their sensitivity to HU, MMS, IR and UV.

4.8 Analysis of *nse2* mutants

Following integration of the mutant sequences into the genome, the resulting strains, *nse2.T172A, nse2.S226X, nse2.T172A S226X* and *nse2.A234fsX236* were tested for temperature sensitivity and sensitivity to hydroxyurea and MMS (Figure 4.10 A). All of the mutant strains grew at 37°C, suggesting that the Nse2 mutant proteins do not have a serious structural defect. Human cells containing the *nse2.S116fsX132* and n*se2.A234fsX236* mutations were noted to have a defect in recovery following exposure to hydroxyurea. The *S. pombe* single *nse2.A234X* mutant was not sensitive to up to 5mM concentrations of HU (Figure 4.10 A row 6). However due to the lethality of the *nse2-K135X* mutant, an *nse2.A234X K135X* mutant could not be characterised. Whilst the *nse2.T172A* mutant was not sensitive to hydroxyurea or MMS, the *nse2.S226X* mutant and the *nse2.T172A S226X* mutant had an increased sensitivity to both of these genotoxins (Figure 4.10 A row 5). Similarly, the *nse2.A234X* and *nse2.T172A* mutants were not dramatically sensitive to ionising radiation (Figure 4.10 B i) or UV irradiation (Figure 4.10 B ii). The *nse2.S226X* mutant and *nse2.T172A S226X* mutant showed a similar increase in sensitivity to UV radiation. Cells containing *nse2.T172A S226X* appear to be slightly more sensitive to ionising radiation compared to either single mutant.

Human cells containing *S116fsX132 A234fsX236* frame shift mutations in the *mms21 (nse2) coding sequence* have a severe defect in recovery following prolonged exposure to HU. In order to investigate whether the nse2 mutations resulted in a defect in chromosome segregation in *S. pombe*, mutant strains were blocked with 12mM HU for 3 hours. Samples were taken immediately and then again at one and two hours after release. Cells were stained with DAPI and calcofluor to visualise the DNA and septum (Ellen Petrovics, BSc final year project, university of Sussex 2013). The *nse2.A234X* and *nse2.T172A* mutants did not show a defect in chromosome segregation following HU treatment. The defects observed in human cells containing the *S116fsX132 A234fsX236* mutations are likely to be a result of the *S116fsX132* mutation, which appears to be inviable in *S. pombe*. The *nse2.S226X* mutant showed some aberrant cell

structures, and bi-nuclear cells could be observed following HU treatment, however these were not abundant.

4.9 Nse2 expression levels and global SUMOylation levels are unaffected in *nse2* mutants

Reduced SUMO ligase activity of the Nse2 protein was observed in human cells containing the S223X and T172A mutations. In order to investigate whether Nse2 expression levels or global SUMOylation levels were affected in mutant *S. pombe* strains, wholecell extracts were prepared and analysed by western blot (Figure 4.12). Samples were probed with α-SUMO and α-Nse2 antibodies. The *nse2.T172A* mutant appears to have a reduced level of global SUMOylation (Figure 4.12 A lane 3), however this is not observed for *nse2.T172A* S226X (Figure 4.12 A lane 4), suggesting a possible loading error. Levels of Nse2 protein were unaffected in all of the mutants analysed, compared to wild type (Figure 4.12 B). The truncated proteins resulting from the S226X and A234X mutations can be visualised in Figure 4.12 B lanes 4 and 5.

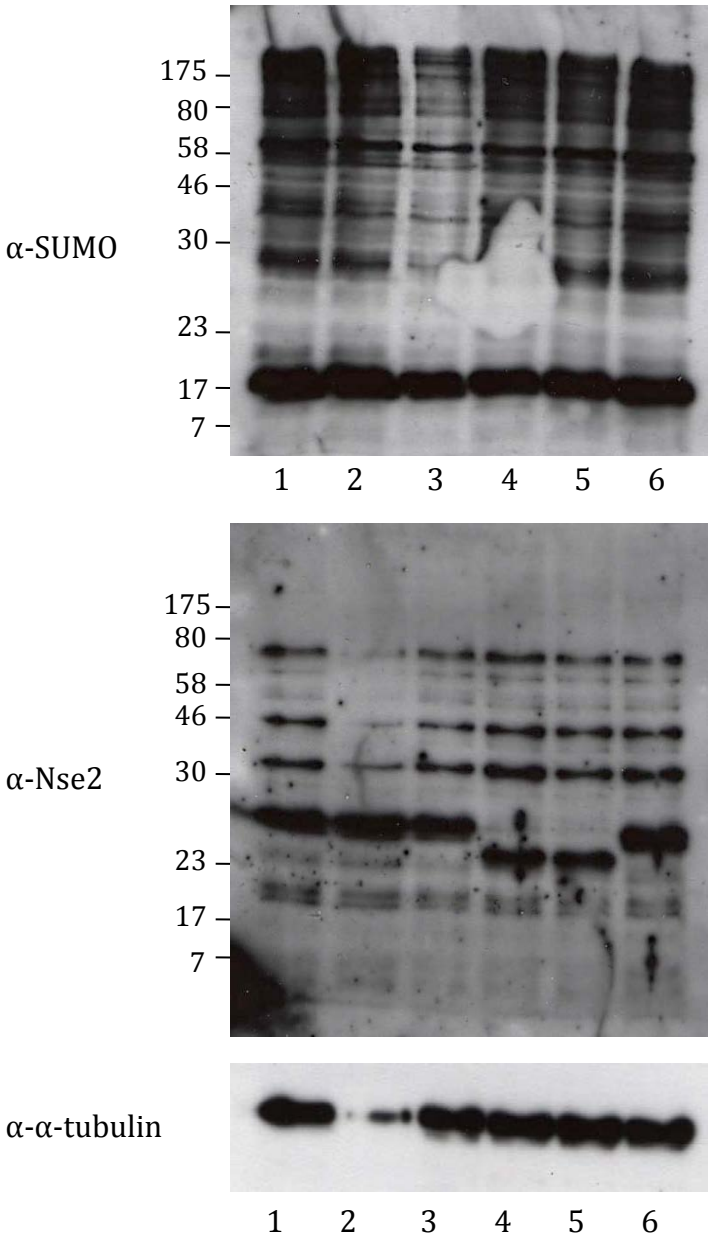

Figure 4.12. Global SUMOylation levels and expression levels in *nse2* mutants.

Whole cell extracts prepared from Nse2 mutant *S.pombe* strains probed with α-SUMO or α-Nse2 antibody as well as an α-tubulin loading control. Lane 1 wild type, lane2 *nse2* , lane 3 *nse2.T172A,* lane 4 *nse2.S226X,* lane 5 *nse2.T172A S226X*, lane 6 *nse2.A234X.*

4.10 Discussion

Three SUMO modified lysine residues in Nse2 (K134, K229 and K248) were identified by MS following *in vitro* SUMOylation assays (Figure 4.1- 4.2), two of which (K229 and K248.) have been identified from previous *in vitro* SUMOylation assays in this lab (Andrews, E, DPhil thesis, Univ. of Sussex). Previously, these lysine residues were mutated in the genome by integration. Subsequent analysis of these strains gave conflicting results. This work aimed to characterise non-SUMOylatable Nse2 mutants by integrating *nse2* K to R mutations into the genome in place of the wild type nse2 ORF, using the recombinase mediated cassette exchange system (Watson et al, 2008). A base strain was constructed in order to integrate Nse2 SUMOylation mutants into the genome in place of the wild type coding sequence (Figure 4.5). The single, double and triple lysine to arginine mutants were not sensitive to a range of DNA damaging agents (Figure 4.6-4.7). Nse2 expression levels and global SUMOylation levels were also unaffected in all of the *nse2* K to R mutants used in this study (Figure 4.8). As there was a slight increase in sensitivity of the triple mutant at high doses of ionising radiation, it is possible that Nse2 auto-SUMOylation plays a role in the repair of double strand breaks. If SUMOylation of Nse2 occurs *in vivo*, and only occurs on the lysine residues identified from the *in vitro* assay, the triple mutant should abolish Nse2 auto-SUMOylation completely. The lack of any obvious mutant phenotype suggests that Nse2 auto-SUMOylation on K134, K229 and K248 is dispensable for its roles in the repair of DNA damage in *S. pombe*. Auto-SUMOylation of Nse2 needs to be confirmed *in vivo* before further genetic analyses can be undertaken to reveal a biological role for SUMO modification at specific sites. This may only become apparent when a non-SUMOylatable Nse2 mutant is combined with other mutants.

Recently, two patients were identified with point mutations or frame shift mutations in Mms21/Nse2 (Professor Mark O'Driscoll, personal communication). Each patient was found to have two mutations, these were T172A with S223X and A234fsX236 with S116fsX132 respectively. A sequence alignment between *S. pombe*, *S. cerevisiae* and human Nse2 homologues showed that the threonine and alanine residues were highly conserved (Figure 4.10).

Whilst the serine residues were not conserved in *S. pombe*, stop codons were generated at the equivalent positions to mimic these mutations. Mutants were created and integrated into the genome to investigate their effects in *S. pombe*. Whilst the *nse2.T172A* and *nse2.A234fsX236* single mutants did not show a mutant phenotype, the *nse2.S226X* mutation resulted in sensitivity to several DNA damaging agents (Figure 4.11). The DNA damage sensitivity of this mutant is not surprising, as the mutation results in a loss of a large C terminal part of the Nse2 protein, and probable disruption of the catalytic RING domain required for SUMO ligase activity. A catalytic Nse2 mutant *Nse2-SA*, was previously shown to be deficient in the repair of double strand breaks (Andrews et al, 2005). Spot tests at 37°C and western blot analysis suggest that the *nse2.S226X* encoding protein is still structurally viable and expressed at normal levels (Figure 4.11 - 4.12). Some aberrant cell morphologies such as bi-nucleated cells could be observed following staining of the DNA and septum with DAPI and calcofluor after prolonged exposure to hydroxyurea, however these were not abundant. Loss of the C terminus could de-stabilise the interaction of Nse2 with Smc5. This could have an effect on the stability of the Smc5/6 complex, which is involved in chromosome segregation and homologous recombination (Murray & Carr, 2008). The *nse2.S116fsX132* mutant was lethal in *S. pombe* and results in a substantial truncation of the Nse2 protein, with a complete loss of the RING domain and the entire C terminus (Figure 4.9). Towards the end of the analysis of these mutants, the Sanger Centre withdrew two of the reported mutations, *nse2.S223X* and *nse2.T172A* due to sequencing errors. Additional analysis was thus discontinued.

5 *S. pombe* PCNA SUMOylation *in vitro* and *in vivo*

5.1 Introduction

PCNA is ubiquitinated in response to DNA damage in S phase in *S. cerevisiae.* Mono-ubiquitination mediated by ubiquitin E2 Rad6 and E3 Rad18 promotes error-prone TLS (Hoege et al, 2002), whilst polyubiquitination is mediated by Ubc13/Mms2 and Rad5 (Hoege et al, 2002; Ulrich & Jentsch, 2000). In *S. pombe*, mono-ubiquitination of PCNA is mediated by Rad6 and Rad18 homologues Rhp6 and Rhp18 and ubiquitin chains are extended by the ubiquitin E3 Rad5 homologue Rad8 with E2 heterodimer Mms2 and Ubc13 (Frampton et al, 2006). Ubiquitination of human PCNA has also been reported (Kannouche & Lehmann, 2004; Watanabe et al, 2004). Polyubiquitination is required for error free TLS which involves template switching (Hoege et al, 2002). PCNA is constitutively ubiquitinated during S phase in *S. pombe*. This modification is increased in response to DNA damage (Frampton et al, 2006). Modification of PCNA by SUMO has been observed in *S. cerevisiae*, Arabidopsis and humans. In *S. cerevisiae*, this modification occurs primarily on K164 and to a lesser extent on K127 (Armstrong et al, 2012; Hoege et al, 2002; Kolesar et al, 2012; Stelter & Ulrich, 2003). SUMOylation of human PCNA has been shown to occur on two lysine residues, K164 and K254, *in vitro* (Gali et al, 2012b). SUMOylation of *S. pombe* PCNA has not previously been observed.

This chapter identifies PCNA SUMOylation sites K13, K164, K172 and K253 *in vitro,* and uses 2D-gel analysis and pull-down experiments to demonstrate that *S. pombe* PCNA is SUMOylated at K164, K172 and K253 *in vivo*.

5.2 Aims

The aims of the work described in this chapter are firstly to utilise the *in vitro* SUMOylation system and mass spectrometry to identify SUMO modified lysine residues on *S. pombe* PCNA, and secondly to confirm that PCNA is SUMOylated *in vivo*.

5.3 *S. pombe* PCNA is SUMOylated *in vitro*

S. pombe PCNA had previously been cloned into the pET15b bacterial expression vector, resulting in the in-frame fusion of an N-terminal HIS tag. Expression of pET15b-HIS-PCNA was induced in *E. coli* BL21 cells and HIS-PCNA was purified using Ni^{2+} agarose beads (Figure 5.1 A). HIS-PCNA was used as a target protein in an *in vitro* assay using a HIS-tagged trypsin-cleavable SUMO (HIS-SUMO-tr) which was generated as described in chapter 3. The assay was carried out in either the presence or absence of the E3 SUMO ligase Pli1. Samples were analysed by western blot and probed with α-Pcn1 and α-HIS antibodies (Figure 5.1 B and C). Probing with α-HIS antibodies shows an increase in higher molecular weight bands in lanes containing HIS-SUMO, SUMO E1 and SUMO E2 proteins (Figure 5.1 C lane 3). The abundance of these species is increased by increasing the concentration of the E2 conjugating enzyme (Figure 5.1 C, lane 7) and further increased on addition of the E3 SUMO ligase (Figure 5.1 C, lane 8) , indicating that the *in vitro* SUMOylation reaction is efficient. Probing with α-Pcn1 antibody identifies unmodified PCNA at ~ 30kDa. Higher molecular weight species are observed in lanes 6 and 7 (Figure 5.1 B), which contain SUMO, E1, E2 and PCNA. Addition of the E3 ligase Pli1 (Figure 5.1 B, lane 8) resulted in an increase in high molecular weight species. In order to identify SUMOylation sites, several gel slices were cut from the stained gel and sent for LC-MS/MS (indicated by asterisks Figure 5.1 B). Asterisks indicate the bands that were analysed by mass spectrometry. Red asterisks indicate bands which contained SUMOylated PCNA as determined by MS.

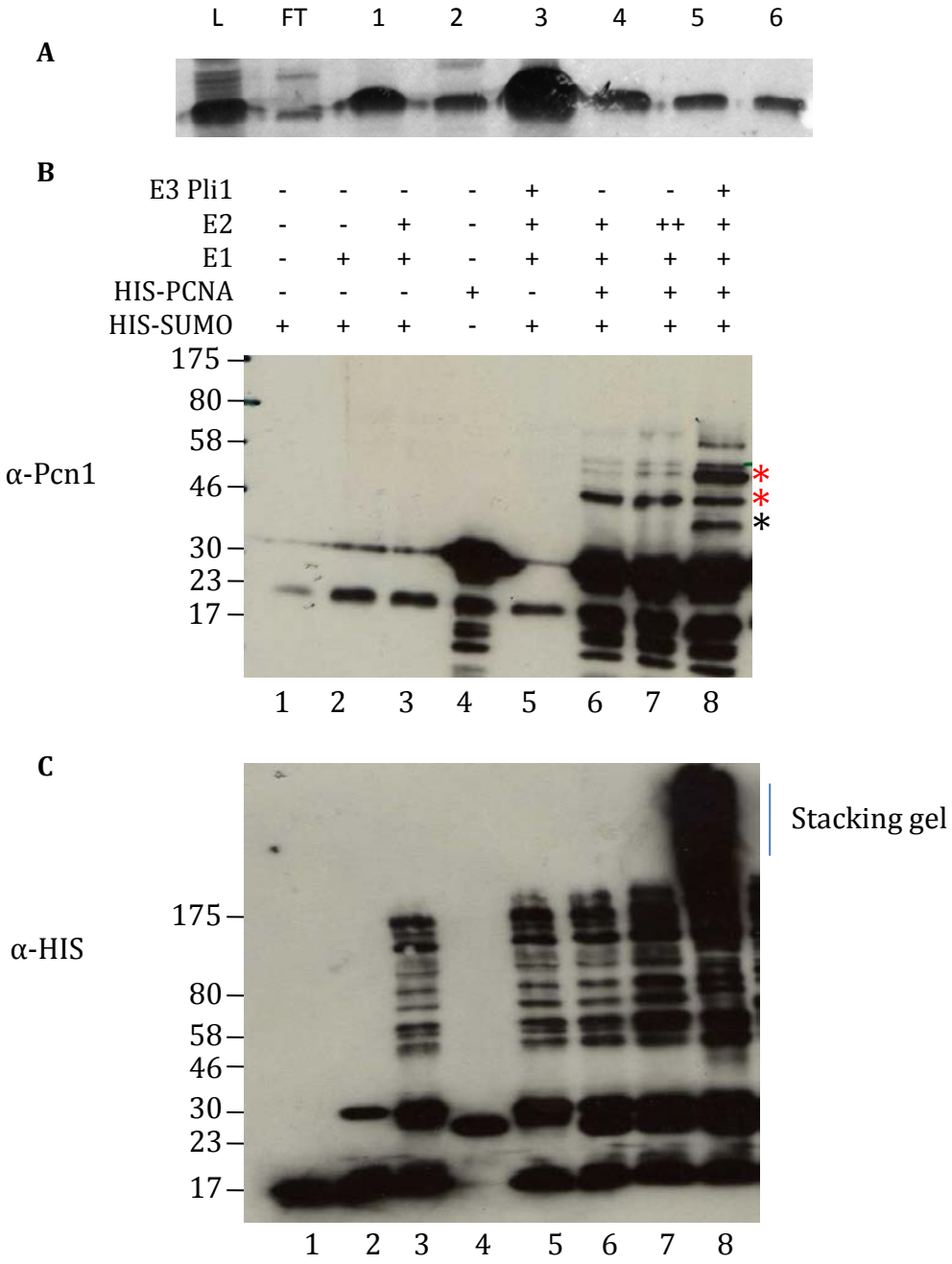

Figure 5.1. PCNA is SUMOylated *in vitro.*

(**A**) Recombinant HIS-PCNA purification from BL21 *E.coli* cells using Ni^{2+} agarose beads. L = cell lysate, FT = flow-through, 1-6 = elution fractions. (**B**) *In vitro* SUMOylation assay probed with α-Pcn1 **(B)** and α-HIS **(C)** antibodies. Higher molecular weight species can be detected in the presence of HIS-SUMO, SUMO E1, SUMO E2 and HIS-PCNA (**(B)** lanes 6 and 7) Where the SUMO E3 ligase Pli1 is added, some higher molecular weight species increase in intensity and additional bands can be seen (lane 8). Asterisks indicate bands cut from a coomassie stained gel and analysed by mass spectrometry. Red asterisks indicate bands which contained SUMOylated PCNA. Pcn1 = PCNA

Four lysine residues were identified by mass spectrometry as being modified by the SUMO diglycine motif following trypsin digest. These were K172, K164 (Figure 5.2 A), K253 and K13 (Figure 5.2 B). An alignment of *S. pombe*, *S. cerevisiae* and human PCNA coding sequences shows the high level of conservation between the species (Figure 5.3). The SUMO-modified lysine residues identified by mass spectrometry are highlighted in red boxes. K13, K164 and K253 are all conserved, whilst K172 is present only in the *S. pombe* protein. Protein structure modelling software 'Phyre2' was used to generate a predicted structure of *S. pombe* PCNA, based on previously published *S. cerevisiae (Krishna et al, 1994)* and human (Gulbis et al, 1996) crystal structures (Figure 5.4). K164, K172 and K253 are all located on the outer surface of the structure. K13 extends into the centre of the ring of the PCNA trimer which encircles DNA during replication.

A

K172

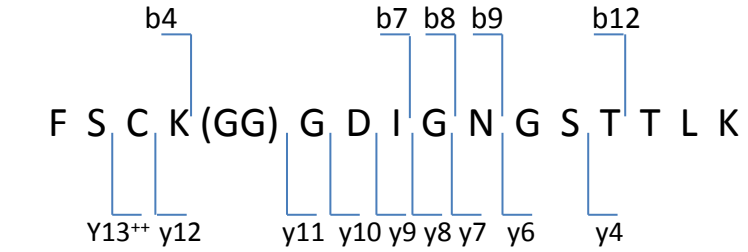
b4 b7 b8 b9 b12
F S C K (GG) G D I G N G S T T L K
Y13++ y12 y11 y10 y9 y8 y7 y6 y4

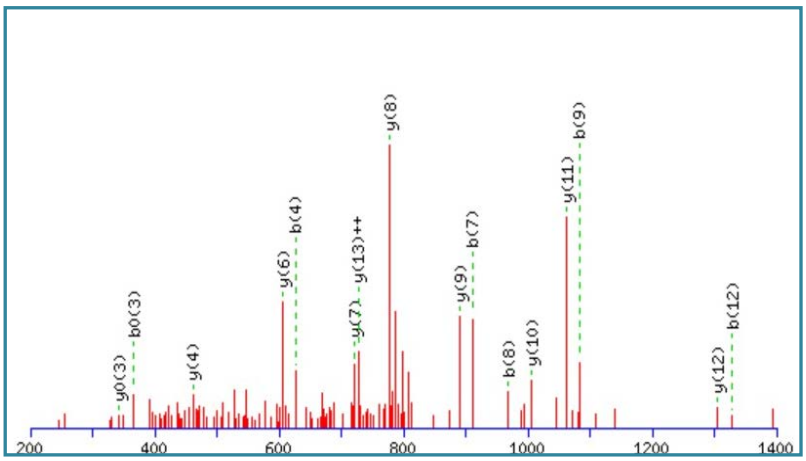
y(8)
b(9)
y(11)
b(4)
y(6)
y(13)++
b(7)
y(7)
y(9)
b(3)
y0(3)
y(4)
b(8)
y(10)
b(12)
y(12)
200
400
600
800
1000
1200
1400

K164

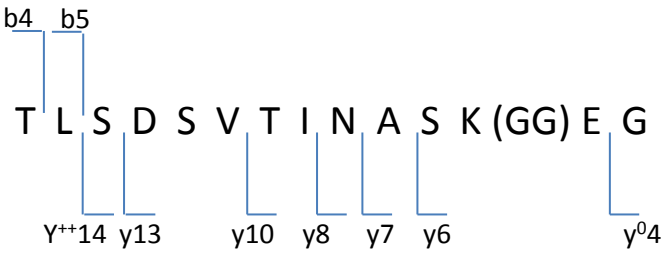
b4 b5
T L S D S V T I N A S K (GG) E G
Y++14 y13 y10 y8 y7 y6 y04

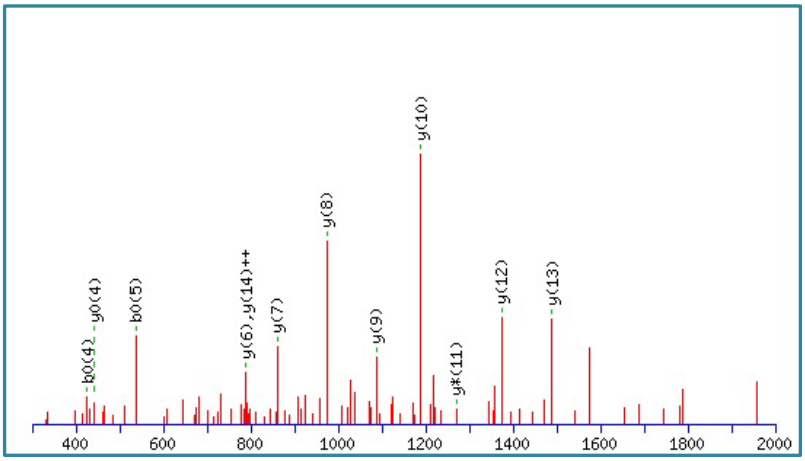
y(10)
y(8)
y(12)
y(13)
b0(5)
y0(4)
y(6),y(14)++
y(7)
y(9)
b0(4)
y*(11)
400
600
800
1000
1200
1400
1600
1800
2000

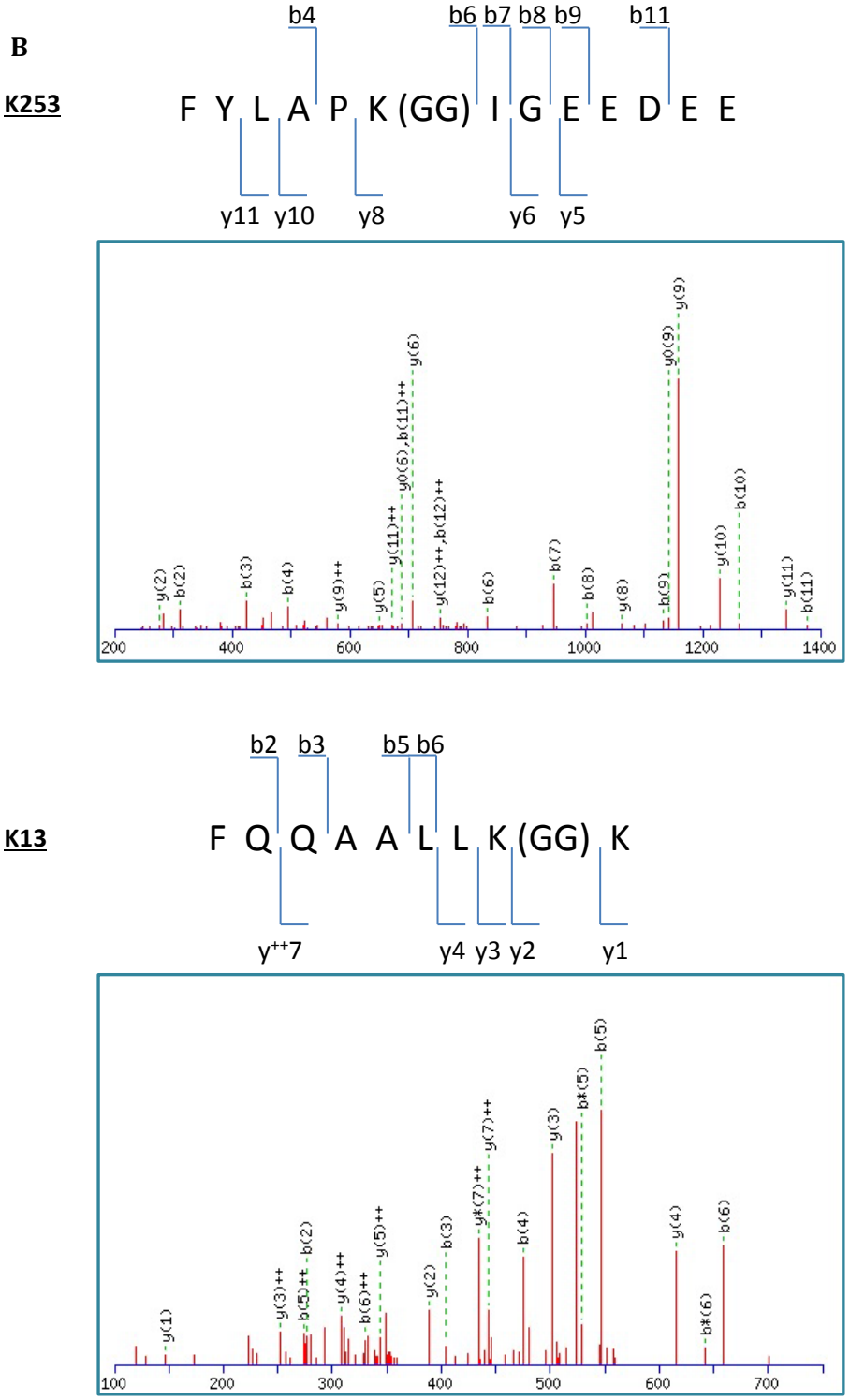

Figure 5.2. PCNA is SUMOylated on K172, K164, K253 and K13 *in vitro*.

(**A**) Mass spectrometry data identifying lysine residues at position 172 and 164 as modified by the SUMO diglycine moiety following trypsin cleavage of HIS-SUMO-tr. Peptide sequences are annotated with b and y ions shown in the graphs. (**B**) Mass spectrometry data identifying lysine residues 253 and 13.

Figure 5.3. PCNA sequence alignment.

Sequence alignment comparing *S.pombe*, human and *S.cerevisiae* PCNA amino acid sequences. The SUMO modified lysine residues identified by mass spectrometry following an *in vitro* SUMOylation assay are highlighted in red. K13, K164 and K253 are conserved between the three species.

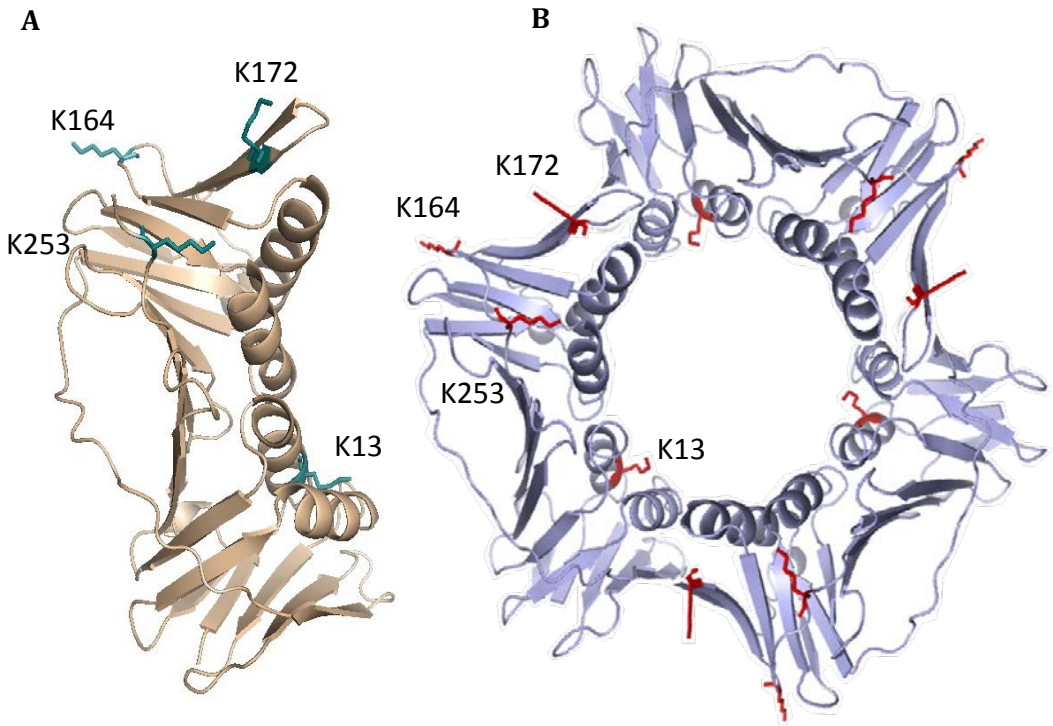

Figure 5.4. Predicted structure of *S.pombe* PCNA.
'Phyre2' generated predicted structure of *S.pombe* PCNA as a monomer (**A**) or homo-trimer (**B**). SUMO modified lysine residues identified *in vitro* are highlighted in aqua (**A**) and red (**B**).

5.4 PCNA modification *in vivo*

SUMOylation of *S. pombe* PCNA has not yet been observed *in vivo*. In order to confirm that SUMOylation of PCNA occurs *in vivo*, two approaches were taken. These were firstly, Ni^{2+} pull-downs of HIS-tagged SUMO from whole cell extracts and probing for PCNA, and secondly 2D gel analysis.

5.4.1 HA-tagged PCNA is modified by SUMO *in vivo*

Pull-down experiments were performed in order to determine if PCNA is SUMOylated *in vivo* and whether levels of SUMOylation are altered by DNA damaging agents. *S. pombe* cells were transformed with pREP medium strength *nmt* expression vectors containing HIS-SUMO (pREP42-HIS-SUMO (*LEU2*$^+$)) and HA-PCNA (pREP41-HA-PCNA (*ura4*$^+$)). Transformed *S. pombe* cells were grown to mid-log phase in the absence of thiamine to allow expression of HA-PCNA and HIS-SUMO. Expression of the tagged constructs was confirmed by probing total cell exacts with α-SUMO, α-Pcn1 and α-HA antibodies (Figure 5.5 A).

Denaturing pull-downs using Ni^{2+} agarose beads were performed and samples were analysed by SDS-PAGE and western blotting (Figure 5.5 B). A band of approximately 50kDa is detected in lane 4 (Figure 5.5 B, left panel) when probed with α-HA and α-Pcn1. This is the expected size for SUMOylated PCNA and confirms that *S. pombe* PCNA is SUMOylated *in vivo*.

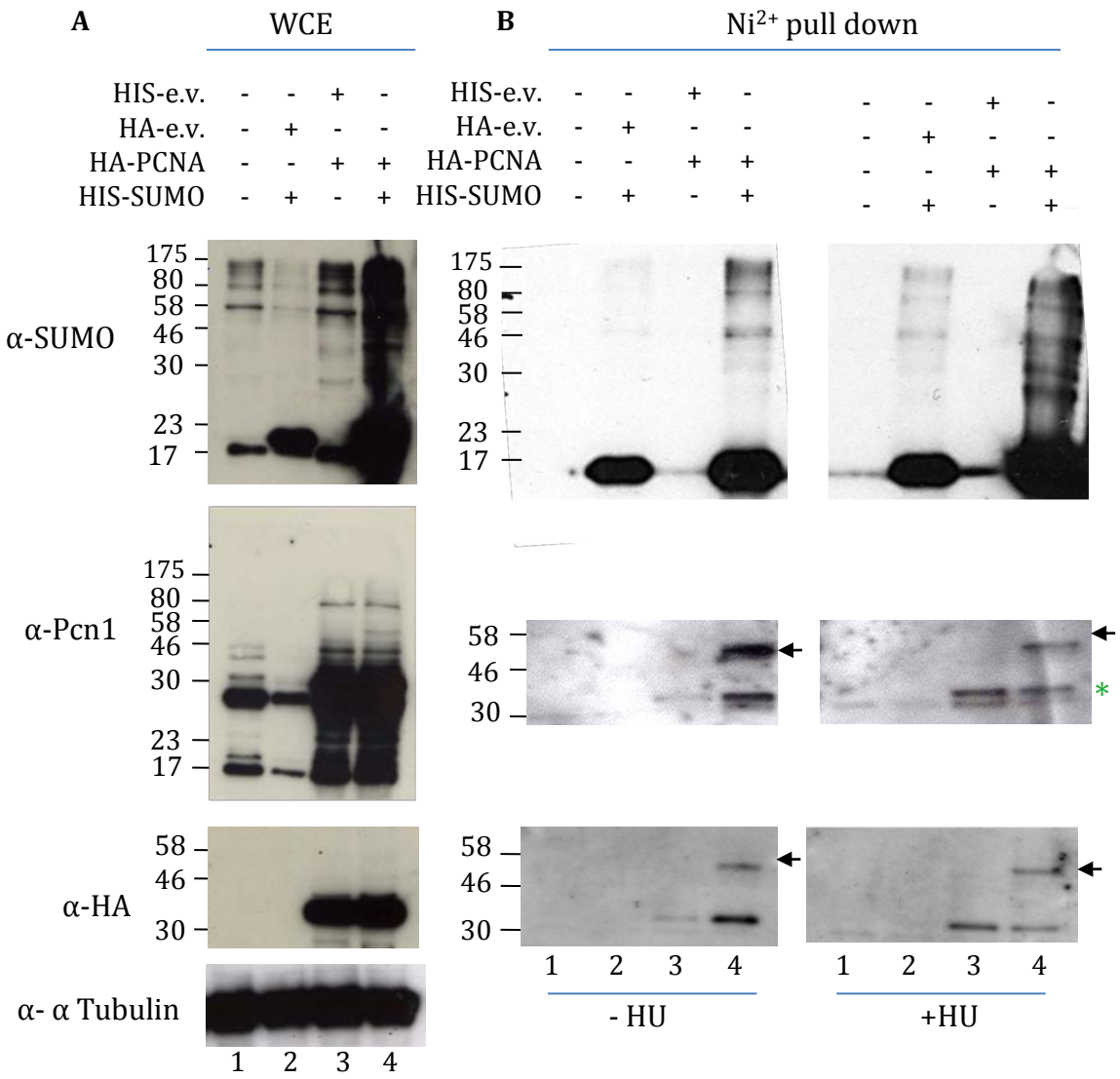

Figure 5.5. PCNA SUMOylation *in vivo*

(**A**) Whole cell extracts (WCE) from *S.pombe* cells. 1, wild type; 2, HIS-SUMO + HA-pREP41; 3, HA-PCNA + HIS-pREP42; 4, HIS-SUMO + HA-PCNA. Probed with α- SUMO, α- Pcn1 and α-HA to confirm expression of tagged constructs and α-α tubulin as a loading control. (**B**) Eluates following Ni^{2+} agarose bead purification for untreated cells (-HU, left panel) and cells treated with 12mM HU for two hours. 1-4 as in (**A**). Arrow indicates band shift at the expected size for SUMOylated HA-PCNA. e.v = empty vector, Pcn1 = PCNA. Green asterisk indicates double band corresponding to tagged and untagged PCNA

5.4.2 Effect of DNA damaging agents and HU on the SUMOylation of PCNA

In order to investigate the effect of DNA damage or replication stress on the SUMOylation of PCNA, Ni^{2+} pull-downs were performed as described in section 5.4.1 using *S. pombe* cells containing HIS-SUMO and HA-PCNA. Pull-downs were carried out under denaturing conditions following exposure of cells to UV and IR irradiation, MMS and hydroxyurea.

A band of approximately 50kDa is detected in both the untreated and HU treated samples when probed with α-HA and α-Pcn1 (Figure 5.5 B, lane 4 right panel). Pull-down experiments were repeated comparing untreated cells to cells exposed to 200 J/m^2 UV irradiation, 200 Gy ionising radiation (Figure 5.6 B) or 0.1% MMS (Figure 5.8 B). A higher molecular weight band was detected in cells containing both HIS-SUMO and HA-PCNA in the untreated samples and following exposure to IR and MMS, when probed with α-HA or α-Pcn1 antibodies (Figure 5.6 B lanes 3 and '3+IR' and Figure 5.8 B lane 4 +/- MMS). This was not observed following UV treatment (200 J/m^2) (Figure 5.6 B lane '3+UV'). A band at the size of unmodified PCNA (~30 kDa) can be detected in each of the pull-down experiments in all lanes where only HA-PCNA is being expressed in cells, as well as where HIS-SUMO and HA-PCNA are expressed together (Figure 5.5 B lanes 3 and 4, Figure 5.6 B lanes 1 and 3). This suggests that PCNA is 'sticky' and therefore is likely to be interacting with the Ni^{2+} agarose beads, which has been observed previously (Dr. Cath Green, University of Oxford, personal communication). In summary, these experiments show that *S. pombe* PCNA is SUMOylated in unchallenged cells, as well as in response to HU, MMS and IR. However SUMOylation of PCNA is not detected following exposure to UV irradiation. To avoid any potential false positive results resulting from PCNA binding to the Ni^{2+} agarose beads, a different approach was taken using 2D gel analysis.

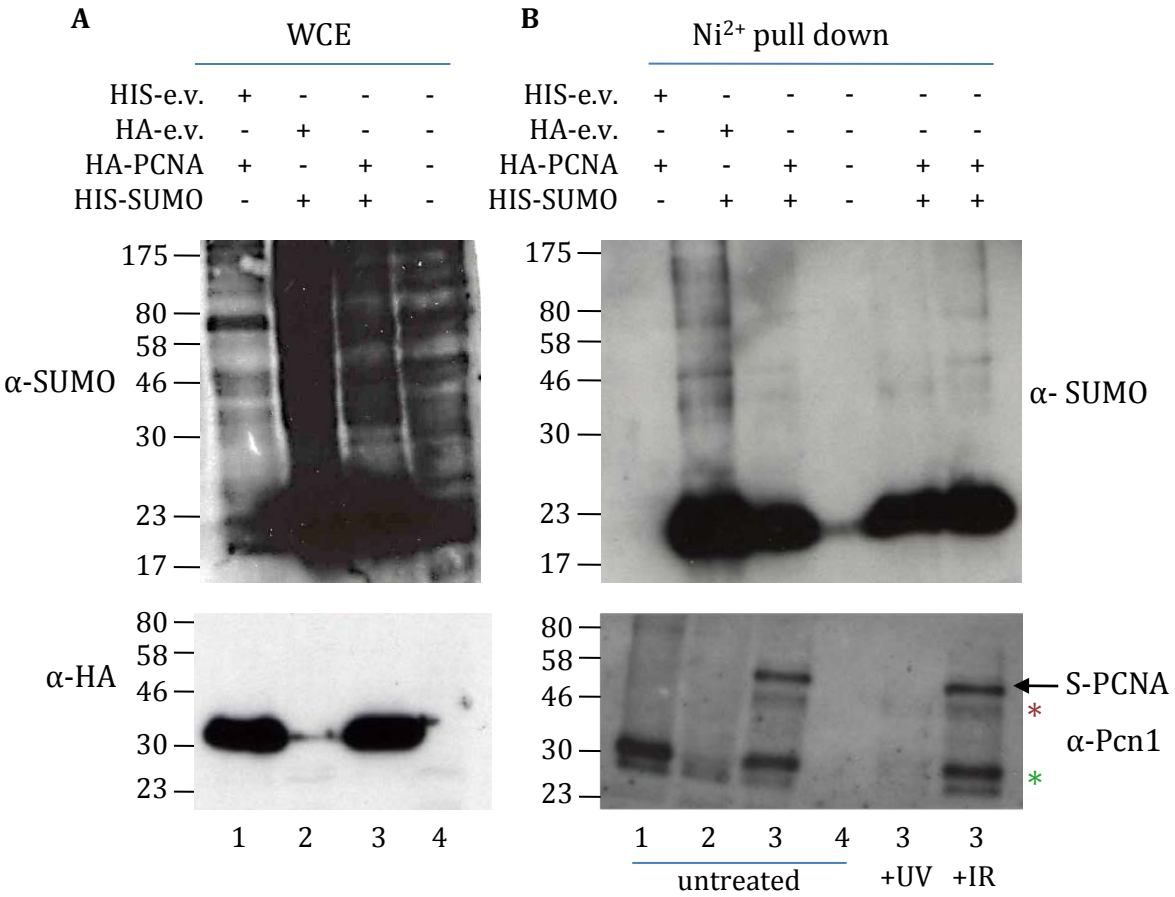

Figure 5.6. PCNA SUMOylation *in vivo* in response to UV and IR

(**A**) Whole cell extracts (WCE) from *S.pombe* cells transformed with tagged constructs Probed with α-SUMO and α-HA to confirm expression of tagged constructs : 1, HA-PCNA + HIS-pREP41; 2, HIS-SUMO + HA-pREP41; 3, HA-PCNA + HIS-SUMO; 4, wild type (**B**) Eluates following Ni^{2+} agarose bead purification. 1-4 as in (**A**). Cells were untreated or exposed to either 200Gy ionising radiation or 200J/m ^{2} UV irradiation (Lane 3+UV and 3+IR). Arrow indicates band shift corresponding to SUMOylated PCNA following 200Gy ionising radiation and in untreated cells. This is abolished in response to UV treatment. Pcn1 = PCNA. Green asterisk indicates a double band corresponding to tagged and untagged PCNA. Red asterisk indicates a double band corresponding to modified PCNA.

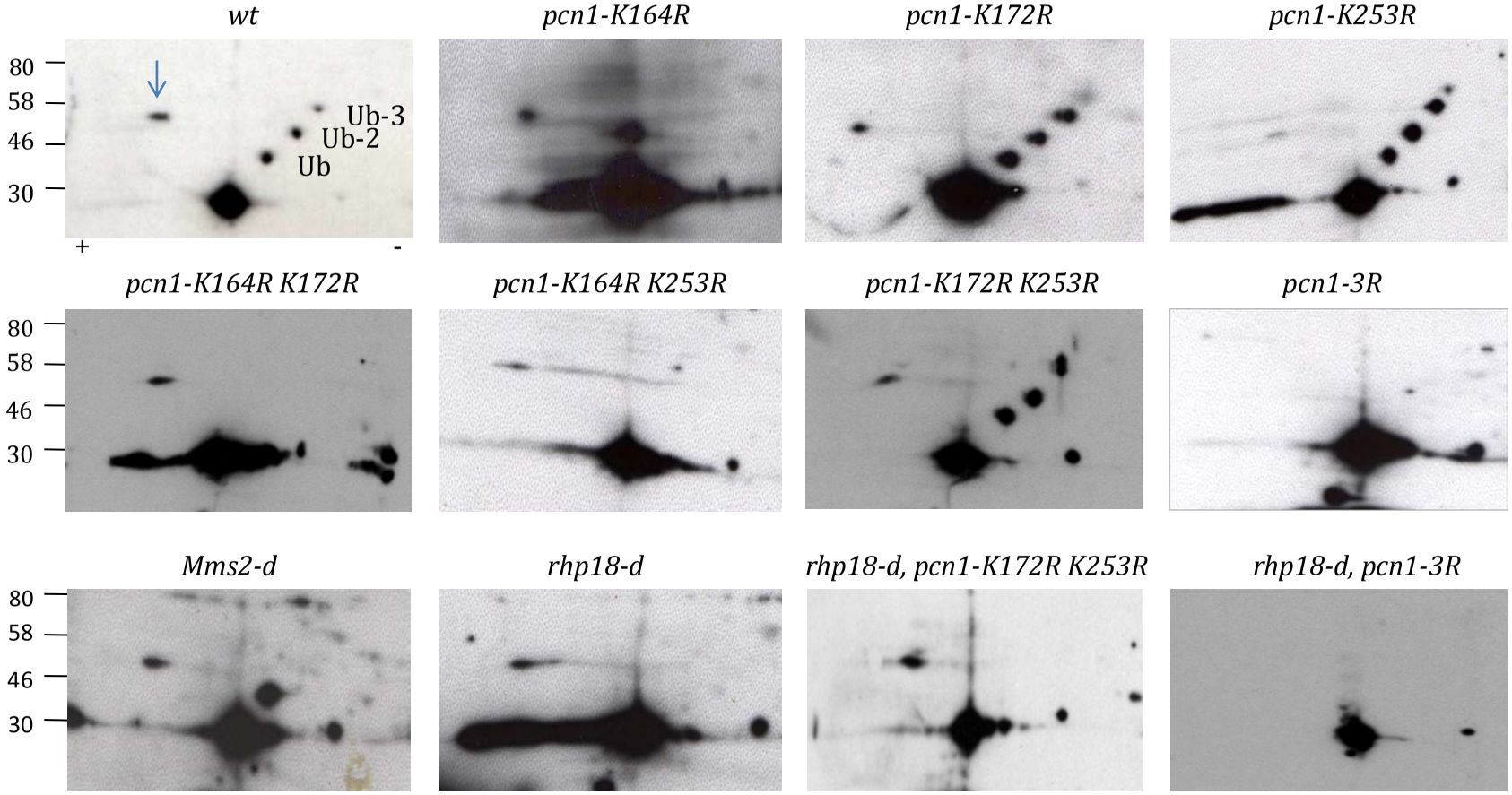

Figure 5.7 2D gel analysis of PCNA modification *in vivo*.

Proteins were extracted from asynchronous, exponentially growing *S. pombe* cultures and analysed by 2D gel. Proteins are separated by pH on the X axis and then by size on the Y axis orientation. All gels are probed with α-Pcn1 and in the same orientation, pH3 (+) to pH 6 (-). Three spots corresponding to mono, di and tri-ubiquitination on K164 can be observed (Marked with a Ub in the top left panel) as well as a spot corresponding to SUMOylated PCNA (highlighted with an arrow in the first panel). Isoelectric points (PI) of proteins are as follows: PCNA, PI = 4,27. Ubiquitin PI = 6.7, SUMO PI = 4.5

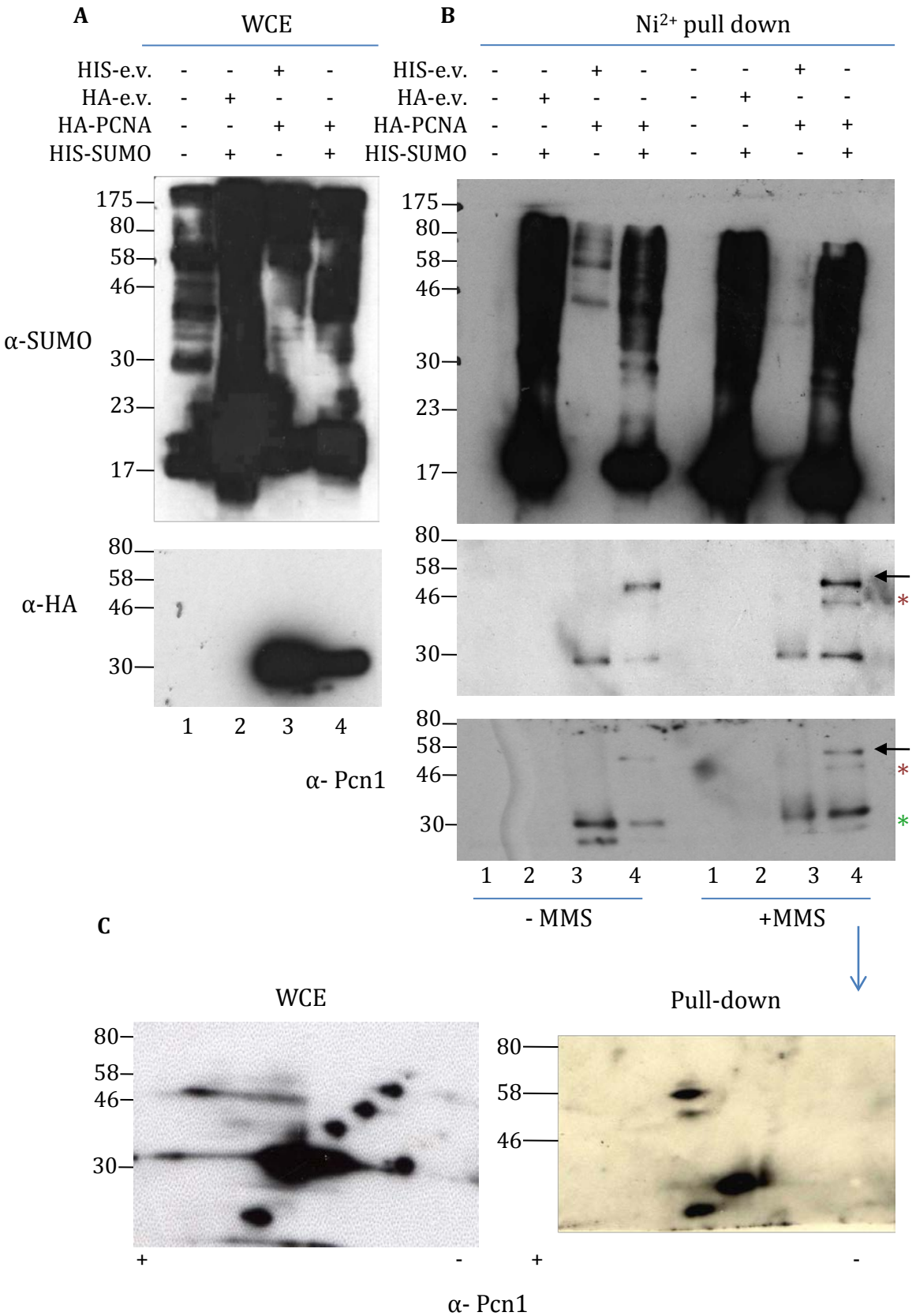
A
WCE
HIS-e.v. - - + -
HA-e.v. - + - -
HA-PCNA - - + +
HIS-SUMO - + - +
175
80
58
46
30
23
17
α-SUMO
80
58
46
30
α-HA
1 2 3 4
α- Pcn1
B
Ni2+ pull down
HIS-e.v. - - + - - - + -
HA-e.v. - + - - - + - -
HA-PCNA - - + + - - + +
HIS-SUMO - + - + - + - +
175
80
58
46
30
23
17
80
58
46
30
80
58
46
30
1 2 3 4 1 2 3 4
- MMS
+MMS
C
WCE
Pull-down
80
58
46
30
80
58
46
+ - + -
α- Pcn1

Figure 5.8 SUMOylation of PCNA *in vivo* in response to MMS

(A) Whole cell extracts (WCE) from *S. pombe* cells. 1, wild type; 2, HIS-SUMO + HA-pREP41; 3, HA-PCNA + HIS-pREP41; 4, HA-PCNA + HIS-SUMO. Probed with α-SUMO and α-HA to confirm expression of tagged constructs. (B) Eluates following Ni^{2+} agarose bead purification. 1-4 as in (A). Cells were either untreated (-MMS) or treated with 0.1% MMS. Arrow indicates band shift corresponding to SUMOylated PCNA in untreated cells which is increased in response to MMS treatment. (C) The MMS treated sample was analysed by 2D gel to compare to position of the modified species with previous 2D gels. The left panel shows total cell extract from wild type *S. pombe* cells. The right panel shows MMS treated cells containing HIS-SUMO and HA-PCNA following Ni^{2+} pull down. Green asterisk indicates a double band corresponding to tagged and untagged PCNA. Red asterisk indicates a double band corresponding to modified PCNA.

5.4.3 2D gel analysis of PCNA modification *in vivo*

As PCNA is also ubiquitinated, it was necessary to ensure that the species observed in the pull-down assays are in fact SUMOylated PCNA. In *S. cerevisiae*, ubiquitin and SUMO can modify the same lysine residue, and SUMOylated PCNA runs at approximately the same size as di-ubiquitinated PCNA. This can make differentiation between the two modifications problematic when using one-dimensional SDS-PAGE gels. 2D gel analysis was employed to address this issue. 2D gel analysis involves separating proteins firstly by their charge, and then by size. For the first dimension, proteins are applied to an IPG strip which has a pH gradient and separated by isoelectric focusing. When a current is applied, proteins migrate to a point where they have no net charge (their isoelectric point). The second dimension separates proteins according to their molecular weight using SDS-PAGE. This is a useful tool for differentiating between SUMO- and ubiquitin-modified PCNA. PCNA lysine to arginine (K to R) mutants analysed using this technique could also be used to indicate which lysine residues are modified *in vivo.*

5.4.3.1 Integration of PCNA lysine mutants into the genome

A base strain for PCNA (LoxP-PCNA-*ura4*$^+$-LoxM) and the pAW8-PCNA construct was created previously in the Carr lab, using methods described by (Watson et.al., 2008). Primers were designed for the construction of single, double and triple K to R mutants using site directed mutagenesis on pAW8-PCNA. K to R mutations were confirmed by sequencing before being transformed into the PCNA base strain, in parallel with pAW8-PCNA. This resulted in the integration

of wild type, single, double and triple K to R mutants into the *S. pombe* genome in place of the wild type PCNA coding sequence and *ura4*$^{+}$ marker. The identities of the resulting nine strains were confirmed by sequencing of genomic DNA. These strains are referred to by the appropriate lysine mutation as follows: *pcn1* (no mutation), *pcn1-K13R, pcn1-K164R*, *pcn1-K172R*, *pcn1-K253R*, *pcn1-K164R K172R*, *pcn1-K164R K253R, pcn1-K172R K253R* and *pcn1-3R* (K164R K172R K253R). The PCNA strain has no mutant phenotype, indicating that this method of integrating mutants is suitable for further analysis. Phenotypic analysis of the mutant strains is discussed in chapter 6.

5.4.3.2 2D gel analysis of PCNA lysine to arginine mutants

Whole cell extracts were prepared from asynchronous cultures of *S. pombe* strains containing wild type and mutant PCNA to analyse PCNA modification *in vivo* at endogenous levels (Figure 5.7). Three spots can be observed which correspond to mono, di- and tri-ubiquitinated forms of K164 (Figure 5.7 first panel). Rhp18 is the E3 ubiquitin ligase required for mono-ubiquitination of PCNA on K164. The ubiquitin spots are abolished in strains containing the K164R mutation, as well as in *rhp18-d* cells. Mms2 is part of the ubiquitin E2 heterodimer which is required for poly-ubiquitination of PCNA on K164. As expected, only mono-ubiquitination can be observed in *mms-d* cells, confirming that the spots identified as ubiquitinated PCNA are indeed ubiquitinated species. A spot at the expected size and pI for SUMOylated PCNA can be observed in all of the single and double K to R mutants (indicated by an arrow in the first panel). However there is no spot in the triple lysine mutant *(pcn1-3R)*. This suggests that *S. pombe* PCNA is SUMOylated on K164, K172 and K253 and not at any additional sites, e.g. K13.

5.4.3.3 2D gel analysis of pull-down samples

To further confirm that PCNA is SUMOylated, an additional pull-down assay was analysed by 2D PAGE and western blotting. Extracts of cells exposed to MMS were used to increase the chance of detection of the SUMOylated species, being as previous pull-down experiments using MMS treatment showed an increase in SUMOylated PCNA in response to MMS (Figure 5.8 B and unincluded data). Exposure of transformed *S. pombe* cells containing HIS-SUMO and HA-PCNA to

0.1% MMS results in the presence of a higher molecular weight species suggestive of SUMOylated PCNA, which is also observed in the untreated sample (Figure 5.8 B, lane 4 +/- MMS). The MMS treated sample was analysed by 2D gel in order to compare the position of the modified species in relation to those in the untreated 2D gel samples. When compared to a wild type total cell extract sample (Figure 5.8 C left panel), the putative SUMOylated spot from the MMS-treated pull-down sample was in a similar position on a 2D gel (Figure 5.8 C right panel). These experiments confirm that *S. pombe* PCNA is SUMOylated *in vivo*.

5.5 Discussion

At the start of this project SUMOylation of PCNA had been described in both *S. cerevisiae* and humans, and *S. pombe* PCNA had been demonstrated to be ubiquitinated. 2D gel analysis of wild type, K164R and *pli1-d* strains performed previously in the Watts lab indicated that *S. pombe* PCNA may be SUMOylated on K164 *in vivo,* and that this modification required the E3 SUMO ligase Pli1 (unpublished data). The work in this chapter demonstrates that *S. pombe* PCNA is SUMOylated. Specifically, four SUMOylated lysine residues were identified using an *in vitro* SUMOylation assay. These included K164, which is also ubiquitinated and SUMOylated in humans and *S. cerevisiae,* as well as K253, the equivalent of human PCNA K254, which has been identified as being SUMOylated *in vitro* (Gali et al, 2012b).

S. pombe cells over-expressing HIS-tagged SUMO and HA-tagged PCNA were used in pull-down experiments to confirm that PCNA is SUMOylated *in vivo*. A band at the expected size of SUMOylated PCNA was observed in untreated cells (Figure 5.5B, left panel). In order to observe any changes in SUMOylation of PCNA in response to DNA damage or replication fork stalling, pull-down experiments were carried out following exposure of cells to hydroxyurea (HU), UV, IR and MMS. A band corresponding to SUMOylated PCNA is visible following pull-downs using HIS-SUMO in untreated cells, as well as cells treated with HU, IR and MMS. These bands appear to be of similar intensities to the untreated sample following treatment with HU and IR, but are slightly increased following MMS treatment. Double bands at the size of unmodified PCNA (~30 kDa,

highlighted with a green asterisk) can be observed when probing with α-Pcn1 in both treated and untreated samples (Figure 5.5 B, Figure 5.6 B and Figure 5.8B). This indicates the presence of endogenous and HA-tagged PCNA. Double bands can also be observed at the size of SUMOylated PCNA (~50 kDa, highlighted with a red asterisk) in IR treated (Figure 5.6B) and MMS-treated samples (Fig 5.8B). These double bands could indicate two modifications at different residues on the same molecule, or di-SUMOylated species. Higher molecular weight bands are not visible following UV treatment. This could be due to the need for ubiquitination on K164 in order to carry out translesion synthesis, and possible suppression of PCNA SUMOylation on the other residues by unknown mechanisms. Whilst UV damage is bypassed by TLS and subsequently repaired by NER or UVER pathways, MMS induced alkylation damage is recognised and repaired by BER. PCNA is intimately linked with NER as well as BER as it is required to co-ordinate Ploζ or Pol ε - mediated gap filling. Several other BER factors interact with PCNA, including AP endonucleases (Tsuchimoto et al, 2001) FEN1 (S.p Rad2), (Dianova et al, 2001) and Polβ (Kedar et al, 2002) via PIP motifs. The increase in SUMOylation following MMS treatment could indicate that SUMOylated PCNA promotes BER-mediated repair of MMS-induced DNA damage, whilst the suppression of SUMOylation following UV treatment could direct repair via the NER pathway.

Bands corresponding to un-modified PCNA were also detected in each of the pull-down experiments. This can be explained by PCNA 'sticking' to the Ni^{2+} agarose beads and therefore being eluted even in the absence of HIS-SUMO. High doses of MMS cause thousands of DNA lesions, and processing by BER can result in the formation of closely spaced single strand DNA breaks (Ma et al, 2009). Subsequent processing can result in the formation of double strand breaks, which require recombinational repair (Ma et al, 2011; Ma et al, 2013). The relatively high doses of MMS and other DNA damaging agents in the pull-down assays could cause fragmentation of the DNA, to which PCNA remains bound. These chromatin fragments may remain following sample processing and could result in unmodified PCNA being present in the pull-down elution fractions. However, higher molecular weight bands are observed only in samples containing both HIS-SUMO and HA-PCNA, suggesting that they

correspond to modified PCNA and are not an artefact. To address this problem and avoid false-positive results, 2D gel analysis was undertaken. This is a useful tool for visualising PCNA species in *S. pombe* without using tagged constructs.

To confirm the presence of SUMOylated PCNA *in vivo*, 2D gel analysis was carried out using wild type *S. pombe* cells, and strains containing PCNA lysine to arginine mutants integrated into the genome. SUMO carries an opposite charge to ubiquitin and would therefore be expected to run closer towards the acidic (+) end of the gel. 2D gel analysis clearly shows mono, di and tri-ubiquitination of *S. pombe* PCNA. In addition to these species, a modified isoform of PCNA can be seen at the expected size and pH for a SUMOylated species. The spot remains in the *rhp18.d* strain which is unable to ubiquitinate PCNA. The absence of this species in the triple lysine mutant suggests that no additional residues are modified. It is not clear from 2D gel analysis which lysine residue, if any, is the predominant SUMOylation site, however the appearance of the spot in each of the double mutant combinations suggests that all three sites can be modified.

In conclusion, this chapter has provided evidence for PCNA SUMOylation *in vitro* and *in vivo* in *S. pombe*. The detection of a SUMOylated species of PCNA in asynchronous cells seen in both the 2D gels and in pull-down experiments suggests that PCNA SUMOylation occurs in G2, however synchronised cells would need to be analysed to confirm this. Further genetic analysis is required to uncover a role for PCNA SUMOylation in *S. pombe*, and this will be discussed in the following chapter.

6 Investigation into the role of PCNA SUMOylation in *S. pombe*

6.1 Introduction

Post-translational modification of PCNA by ubiquitin determines the route taken to overcome DNA damage or fork blocking lesions during replication, where mono-ubiquitination promotes error prone TLS, and poly-ubiquitination promotes error-free template switching. As is the case in *S. cerevisiae*, *S. pombe* PCNA is ubiquitinated in response to a range of cellular stresses including UV irradiation, HU and MMS treatment (Frampton et al, 2006; Hoege et al, 2002). However whilst in *S. cerevisiae* PCNA is SUMOylated during S phase (Hoege et al, 2002), in *S. pombe* PCNA is constituitively ubiquitinated during S phase. Ubiquitination occurs in unchallenged cells as well as in response to ionising radiation and DNA damage during G2. In line with these observations, the *S. pombe pcn1-K164R* mutant is sensitive to IR, and is epistatic with the ubiquitination mutants *rhp18-d, rad8-d, mms2-d and ubc13-d* following exposure to UV (Frampton et al, 2006). Ubiquitination of PCNA in *S. pombe* is not dependent on repair intermediates, as in the absence of Rad13 or Uve1 which are required for NER and UVER UV repair pathways respectively, ubiquitination of PCNA remains at a level similar to that in wild type cells. In the absence of PCNA ubiquitination in *S. pombe,* Rad51-mediated repair is required for UV-induced DNA damage (Frampton et al, 2006).

SUMOylation of PCNA in budding yeast and humans is required to suppress unscheduled recombination during S phase and to prevent the formation of DSBs following replication fork stalling. In *S. cerevisiae,* SUMOylation of PCNA on K164 and K127 recruits an anti-recombinogenic helicase Srs2 via its SIM (Armstrong et al, 2012; Hoege et al, 2002; Kolesar et al, 2012; Stelter & Ulrich, 2003). Srs2 acts during S phase (Pfander et al, 2005a) to inhibit unscheduled homologous recombination by disrupting Rad51 filament formation (Krejci et al, 2003; Veaute et al, 2003). In the absence of Rad6 and Rad18, *S. cerevisiae* cells are sensitive to DNA damage which requires the PRR pathway. Deletion of either the SUMO ligase Siz1 or the anti-recombinase Srs2 suppresses these DNA

repair defects, and this is dependent on the presence of genes required for HR, presumably allowing recombinational repair (Papouli et al, 2005; Pfander et al, 2005b; Schiestl et al, 1990; Stelter & Ulrich, 2003). SUMOylation of *S. cerevisiae* PCNA also recruits Rad18 via a SIM and this enhances its activity (Win et al, 2004).

SUMOylation of human PCNA has been shown to occur on several lysine residues, including K164 and K254, *in vitro,* and was demonstrated to decrease spontaneous recombination and double strand breaks *in vivo* (Gali et al, 2012b). SUMOylation of PCNA recruits PARI which was identified following a search for proteins containing a UvrD helicase domain, to identify potential Srs2 orthologues (Moldovan et al, 2012). UvrD domains are conserved domains found in helicase proteins, first characterised in the bacterial UvrD helicase protien (Chiolo et al, 2007). PARI was found to contain aUvrD like domain, a Rad51-binding domain similar to that identified in the C-terminus of Srs2 (Colavito et al, 2009) and PIP and SIM sequences, which are arranged similarly in Srs2. PARI recruitment is suggested to suppress HR by disrupting D-loop structures formed following strand invasion (Moldovan et al, 2012).

The role of PCNA SUMOylation in *S. pombe* has not yet been determined. Whilst an Srs2 homologue exists, it lacks a section of the C-terminus which includes the SIM that is required for recruitment to SUMOylated PCNA in *S. cerevisiae* (Frampton et al, 2006). This suggests that the SUMOylation of PCNA may play a less important role in suppressing homologous recombination in *S. pombe*. This chapter investigates the role for PCNA SUMOylation in *S. pombe*, using genetic analysis of un-SUMOylatable PCNA mutants in combination with mutants from a range of different repair pathways.

6.2 PCNA lysine to arginine mutants are sensitive to MMS.

Analysis of the role of SUMOylation is complicated by the fact that one of the SUMOylation sites (K164) is also used for ubiquitination. Thus, in order to demonstrate a role for SUMOylation, analysis of the *pcn1-K164R* mutant alone is insufficient. The phenotypes of the single, double and triple K to R mutants were therefore analysed. If K172 and K253 are SUMOylation sites, then cells

containing mutations in these residues might have phenotypes different to that of *pcn1-K164R.* The response of *S. pombe* PCNA (*pcn1*) K to R mutant strains (created as described in chapter 5) to a range of DNA damaging agents, starting with MMS and HU, was analysed (Figure 6.1). None of the single, double or triple K to R mutants showed an increase in sensitivity to hydroxyurea compared to wild type cells. This is consistent with previous reports that the ubiquitination of PCNA that promotes TLS is not required for the recovery of stalled replication forks caused by nucleotide depletion (Branzei et al, 2004; Frampton et al, 2006). Ubiquitination of K164 is known to be required for post-replicative repair and translesion synthesis. The *pcn1-K164R* mutant shows an increase in sensitivity to MMS (Figure 6.1 row 3) compared to wild type cells. The *pcn1-K172R*, *pcn1-K253R* and *pcn1-K13R* single mutants are not sensitive to MMS. However, when in combination with the K164R mutation, the K253 mutation results in increased sensitivity to MMS (Figure 6.1 rows 3, 8 and 10). This is not the case with the K172R mutation. This suggests that modification of K253 has a role in the repair of MMS-induced DNA damage. The single K13R mutation did not result in any mutant phenotypes. The location of K13 on the inner surface of PCNA which encircles DNA suggests that this is not a likely site for SUMOylation. Further, 2D gel analysis undertaken in chapter 5 (Figure 5.7) shows that SUMOylation of PCNA is abolished in the *pcn1-3R* mutant, where SUMOylation of K13 would be intact. Taken together, this suggests that the SUMOylation of PCNA on K13 is likely to be an artefact of the *in vitro* SUMOylation reaction.

UV and IR survival analysis shows that cells containing the *pcn1-K164R* mutation are highly sensitive to ionising radiation as well as UV-induced DNA damage (Figure 6.2 A and B). This sensitivity is not significantly increased in the *pcn1-3R* cells. In summary, SUMOylation of PCNA appears to be required for the response to DNA damage during S phase.

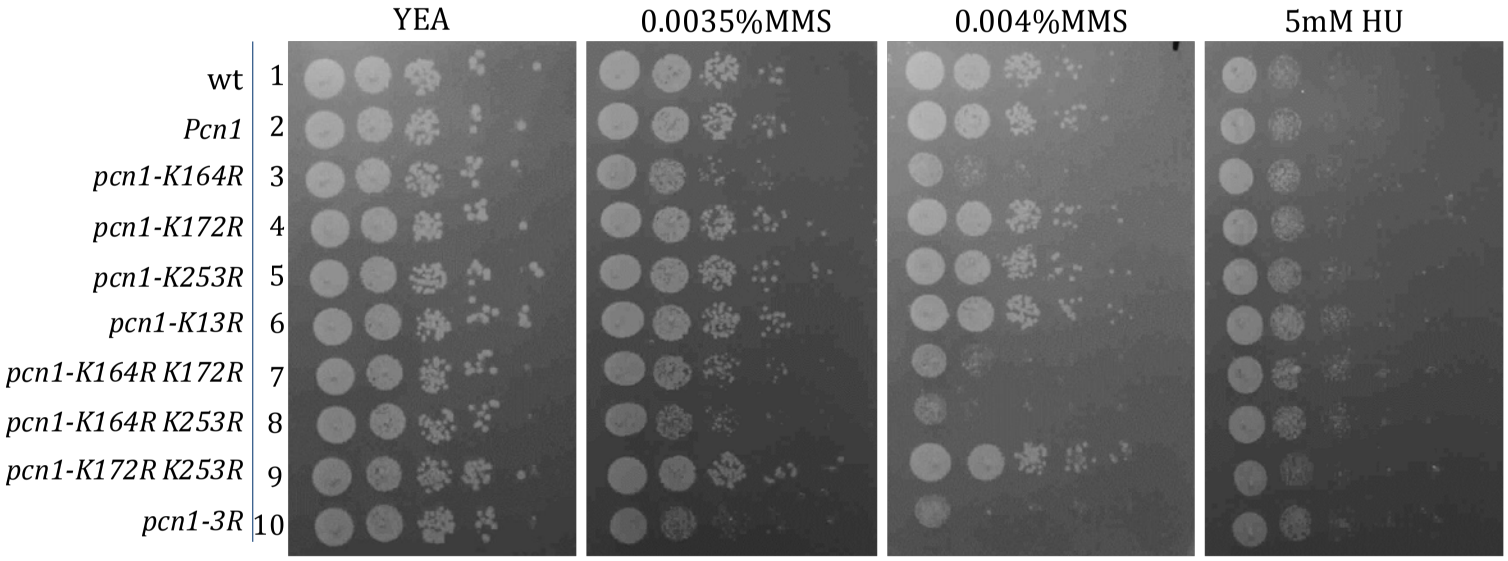

Figure 6.1 Analysis of *pcn1* lysine to arginine mutants in response to MMS and HU.

10 fold serial dilutions of exponentially growing *S. pombe* cells containing either wild type PCNA (*pcn1*) , or single, double or triple (*3R*) PCNA K to R mutants were plated onto YEA containing MMS or HU as indicated. The sensitivity of the *pcn1-K164R* mutant to MMS is increased in combination with K253R.

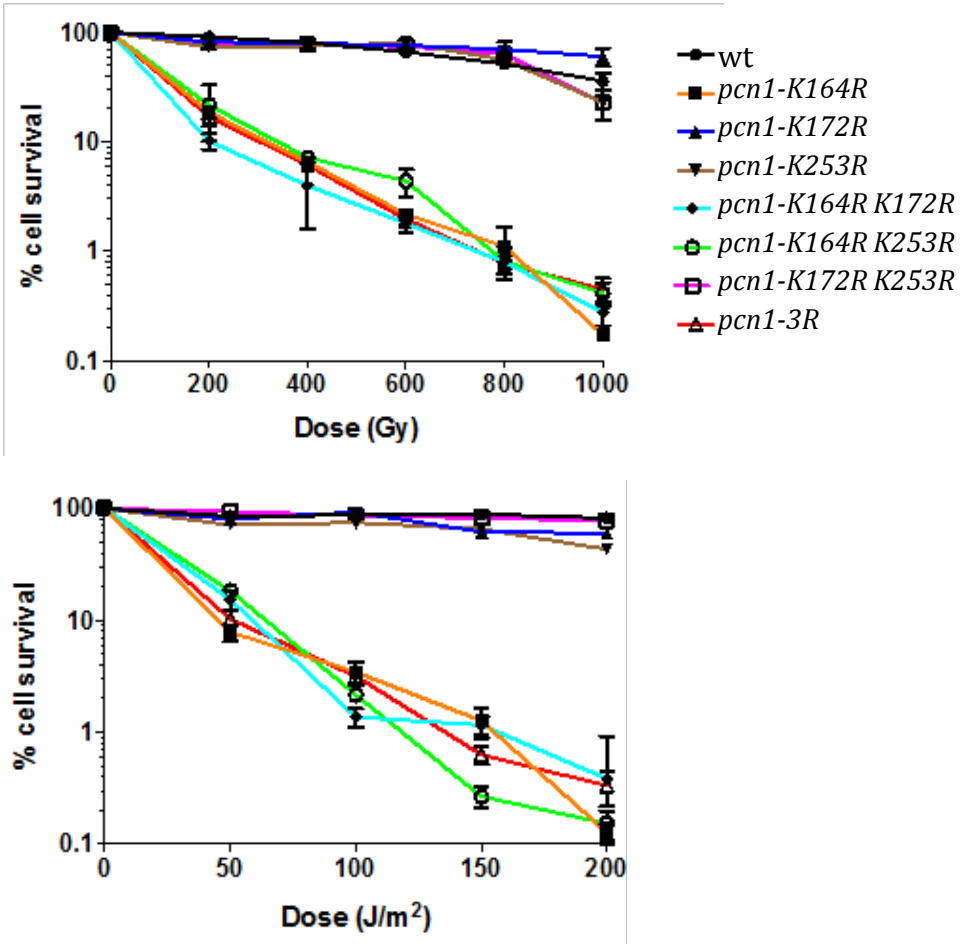

Figure 6.2 survival curves for *pcn1* lysine to arginine mutants in response to UV and IR irradiation.

Exponential cultures of *pcn1* K to R mutants were exposed to increasing doses of IR (A) or UV (B) irradiation. Cells from each sample were plated onto YEA plates and incubated at 30°C for 3 days. Cell viability was calculated by comparing the number of colonies formed with untreated controls. The viability of *pcn1*-3R is not increased compared to the *pcn1-K164R* .

6.3 Analysis of PCNA lysine to arginine mutants in combination with *pli1-d*

pcn1-K164R and *pcn1-3R* were integrated into strains lacking the E3 SUMO ligase Pli1 (*pli1-d*), resulting in *pli1-d, pcn1-K164R* and *pli1-d, pcn1-3R*. If Pli1 is the SUMO ligase responsible for SUMOylation of PCNA, the K to R mutations might be expected to be epistatic with the *pli1-d* mutation. None of the single or double mutants are sensitive to HU (Figure 6.3, right panel). The *pli1-d, pcn1-3R* double mutant is more sensitive to MMS than the *pcn1-3R* mutant (Figure 6.3 row 3 and row 6). The reason for this is unknown but may be due to the fact that Pli1 is required for SUMOylation of multiple proteins, including some required for HR, for example Rad22 (*S. pombe* homologue of Rad52) (Ho et al, 2001) which may be required in the absence of SUMOylation of PCNA .

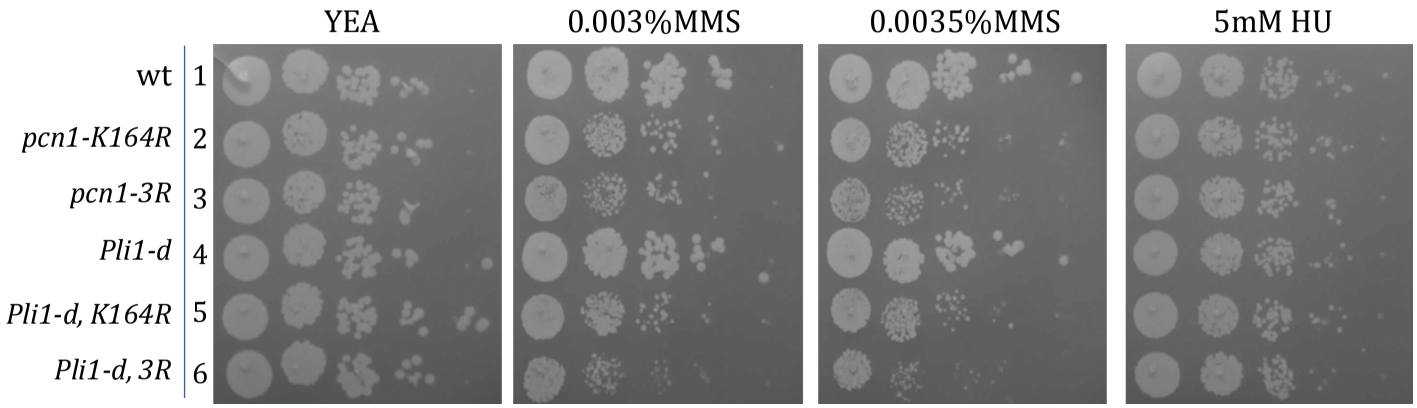

Figure 6.3 Analysis of *pcn1-K164R* and *pcn1-3R* in combination with *pli1-d*.
10 fold serial dilutions of exponentially growing *S. pombe* cultures containing single and double *pcn1* and pli1 mutants were plated onto YEA containing MMS or HU as indicated. Double mutants containing *pli1-d* and *pcn1-K164R* or *pli1-d* and *pcn1-3R* show an increase in sensitivity to MMS compared to single mutants.

6.4 Analysis of PCNA K to R mutants in combination with *nse2-SA*

The *nse2-SA* mutation results in a ligase-dead form of the only other E3 SUMO ligase identified in *S.pombe*, Nse2 (Andrews et al, 2005). PCNA K to R mutations were integrated into strains containing the *nse2-SA* mutation in order to investigate whether any epistasis could be observed, that would implicate Nse2 as the SUMO ligase required for PCNA SUMOylation *in vivo*. Double mutants containing *nse2-SA* and either *pcn-K164R*, or *pcn1-3R* do not show a notable increase in sensitivity to HU compared to the single *nse2-SA* mutant. *nse2-SA, pcn1-K164R* and *nse2-SA, pcn1-K3R* double mutants are significantly more sensitive to MMS compared to the single mutants (Figure 6.4 lanes 6 and 7). This is consistent with a loss of both the PRR pathway resulting from the inability to ubiquitinate K164 and loss of HR-mediated repair due to the *nse2-SA* mutation.

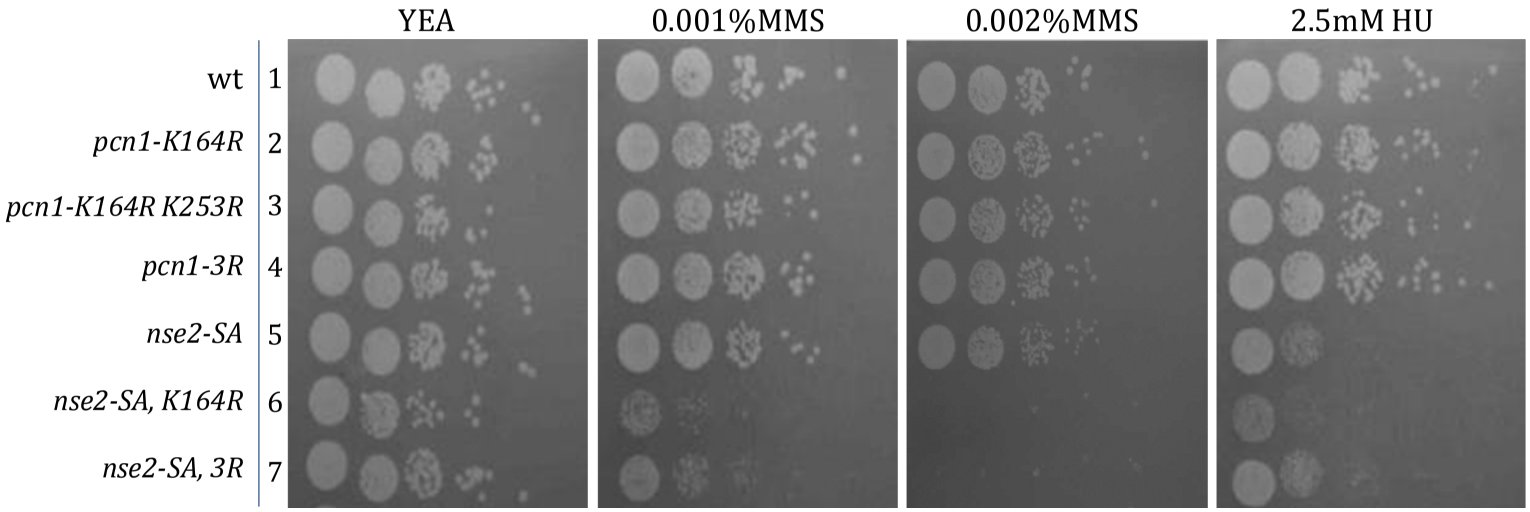

Figure 6.4 *nse2-SA* in combination with *pcn1-K164R* and *pcn1-3R* has increased sensitivity to MMS.
10 fold serial dilutions of exponentially growing *S. pombe* cultures containing single and double pcn1 and nse2 mutants were plated onto YEA containing MMS or HU as indicated. Double mutants *nse2-SA pcn1-K164* and *nse2-SA pcn1-3R* are highly sensitive to MMS. Double mutants do not show a notable increase in sensitivity to HU compared to the single *nse2-SA* mutant. Note that the apparent increase in sensitivity of *nse2-SA, pcn1-K164R* compared *nse2-SA, pcn1-3R* is due to there being less cells in the *nse2-SA, pcn1-K164R* sample (see YEA panel lane 6 compared to lane 7).

6.5 Analysis of PCNA lysine to arginine mutants in combination with *rhp18-d* and *mms2-d*

PCNA K to R mutants were integrated into cells lacking the genes required for the mono- and poly-ubiquitination of PCNA, *rhp18-d* and *mms2-d,* respectively, to investigate whether the phenotypes observed for cells containing the K164R mutation are due to a loss of ubiquitination or SUMOylation. Both mono- and poly-ubiquitination of PCNA are abolished in *rhp18-d* cells. The addition of the *pcn1-K164R* mutation does not increase sensitivity to MMS (Figure 6.5 rows 3, 10 and 11) and similarly double mutants *rhp18-d, pcn1-K164R K253R* and *rhp18-d pcn1-3R* do not show a notable increase in MMS sensitivity (Figure 6.5 rows 3, 10, 13 and 15).

mms2-d strains are defective in poly-ubiquitination of PCNA, but are still proficient in PCNA mono-ubiquitination and therefore error-prone TLS. In the presence of 0.003% MMS, *mms2-d, K164R* is slightly more sensitive compared to the single mutants (Figure 6.6 rows 3, 10 and 11), presumably due to the K164R mutation abolishing PCNA mono-ubiquitination and therefore both PRR pathways. The addition of the K253R mutation results in an increase in sensitivity at this concentration of MMS, which is further increased in the *mms2-d, pcn1-K3R* mutant (Figure 6.6 rows 11, 13 and 15). This again suggests a role for modification of PCNA on K253 in the repair of MMS-induced DNA damage, which does not involve Mms2. This would be consistent with SUMOylation on K253. The increase in sensitivity of *mms2-d, pcn1-K3R* compared to *mms2-d, pcn1-K164R K253* suggests that SUMOylation of PCNA on K172 could be utilised in the absence of other SUMOylation sites. Given that the *pcn1-3R* mutant shows an increased sensitivity to MMS in combination with the *mms2-d* mutant but not *rhp18-d*, it is possible that SUMOylation of PCNA plays a role in error prone TLS, or that Rhp18 has other roles that are as yet undefined. Mono-ubiquitination and thus TLS should be intact in the *mms2-d* strain. The loss of polyubiquitination means that damage must be repaired via a mechanism distinct from recombinational template switching. This could suggest that poly-ubiquitination may be important together with SUMOylation of K253 and possibly K172 in the response to MMS.

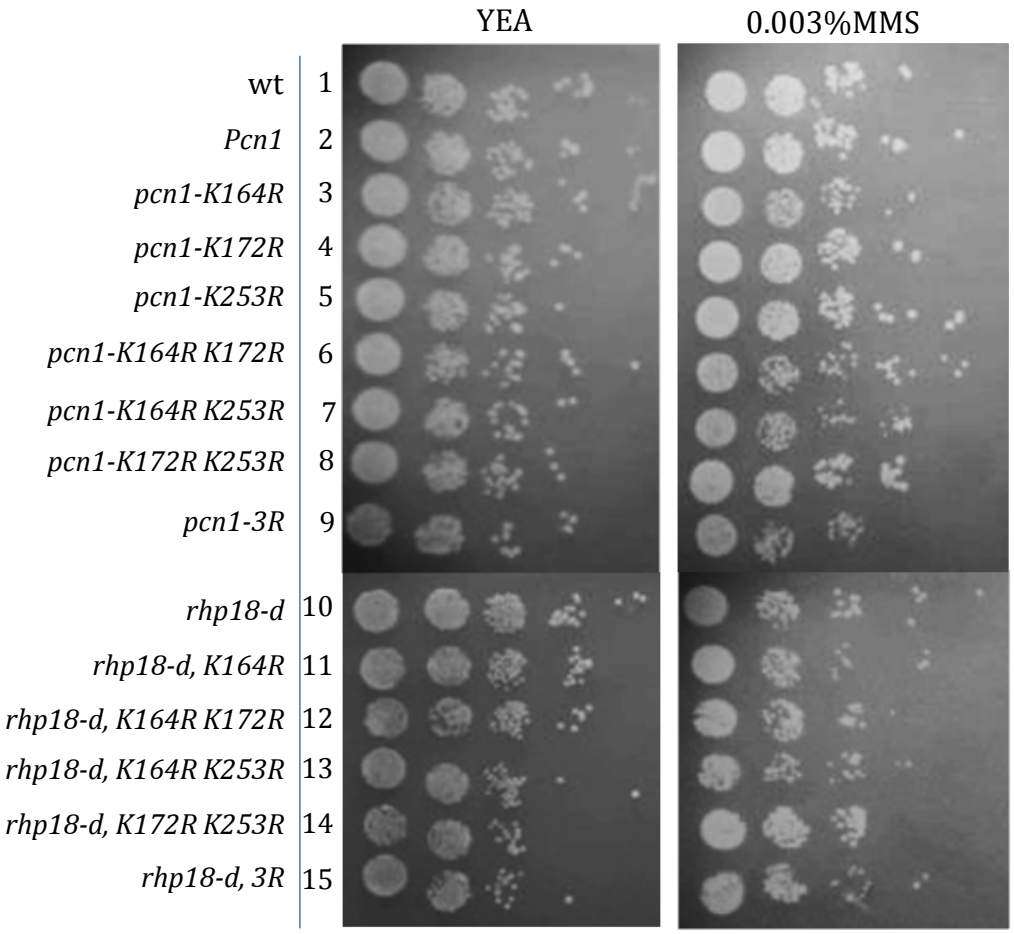

Figure 6.5 Analysis of *pcn1-K164R* and *pcn1-3R* in combination with *rhp18-d*.

10 fold serial dilutions of exponentially growing *S. pombe* cultures containing single and double *pcn1* and *rhp18* mutants were plated onto YEA containing 0.003% MMS. *rhp18-d* sensitivity to MMS no affected by the addition of *pcn1* lysine to arginine mutants.

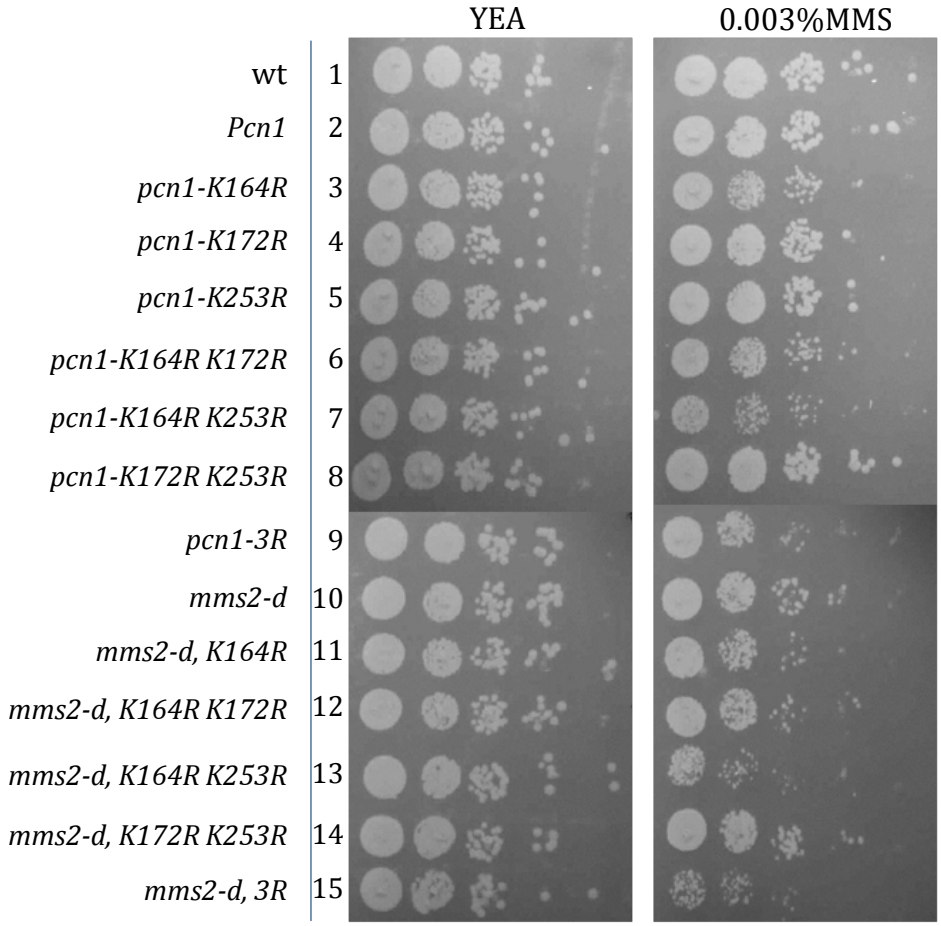

Figure 6.6 Analysis of *pcn1-K164R* and *pcn1-3R* in combination with *mms2-d.*

10 fold serial dilutions of exponentially growing *S. pombe* cultures containing single and double *pcn1* and *mms2-d* mutants were plated onto YEA containing 0.003% MMS. Double mutants containing *mms2-d* and *pcn1-3R* show a slight increase in sensitivity to MMS compared to single mutants.

6.6 SUMO modification of PCNA is not required for error-prone TLS

To address whether SUMOylation of *S. pombe* PCNA could be involved in the error-prone TLS pathway, PCNA K to R mutants were crossed with TLS polymerase mutants. Four polymerases are involved in TLS in *S. pombe,* Polκ (DinB), Polη, Polζ (Rev3-Rev7, of which Rev3 is the catalytic subunit) and Rev1 (Coulon et al, 2010). Evidence has suggested that Polη and Polκ are required for the bypass of CPD (cyclobutane pyrimidine dimers), whilst Polη Polζ and Rev1 are required for bypass of 6-4 photoproducts (Coulon et al, 2010). PCNA K to R mutants were integrated into strains lacking the Rev1, Rev3 or DinB polymerases (*rev1-d*, *rev3-d* and *dinB-d* respectively). For each of the three polymerase mutants, addition of the *pcn1-k164R* mutation results in a very slight increase in sensitivity to MMS (Figure 6.7 A, rows 3, 9 and 10, 15 and 16 and B rows 3, 9 and 10). This sensitivity is slightly further increased on addition of the K253R mutation for all three polymerase mutants (Figure 6.7 A, rows 6, 8, 9 12, 14, 15, 18 and 20 and B, rows 6, 8, 9, 12 and 14). This suggests a role for SUMOylation of PCNA that is not required for error-prone TLS in *S. pombe*.

A

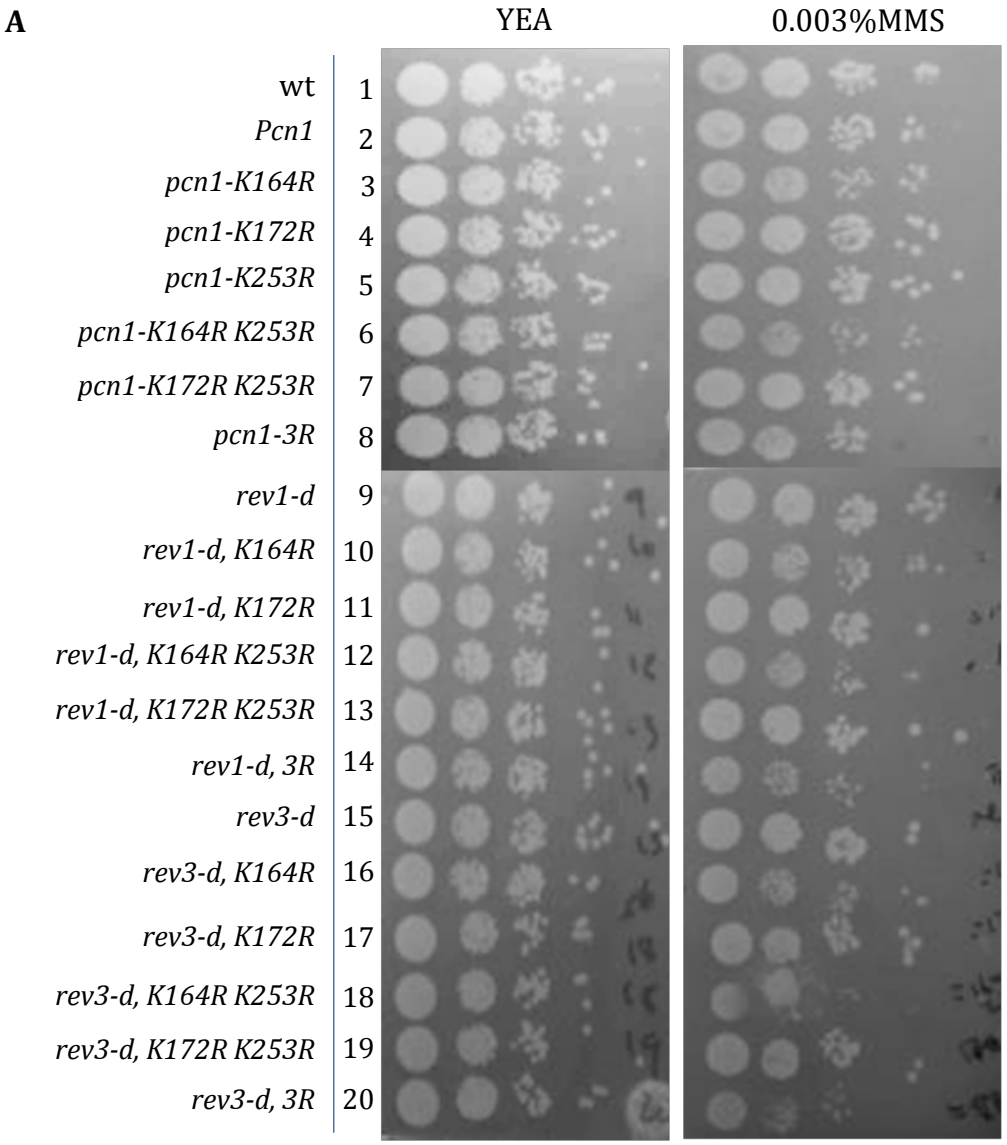
YEA
0.003%MMS
wt 1
Pcn1 2
pcn1-K164R 3
pcn1-K172R 4
pcn1-K253R 5
pcn1-K164R K253R 6
pcn1-K172R K253R 7
pcn1-3R 8
rev1-d 9
rev1-d, K164R 10
rev1-d, K172R 11
rev1-d, K164R K253R 12
rev1-d, K172R K253R 13
rev1-d, 3R 14
rev3-d 15
rev3-d, K164R 16
rev3-d, K172R 17
rev3-d, K164R K253R 18
rev3-d, K172R K253R 19
rev3-d, 3R 20

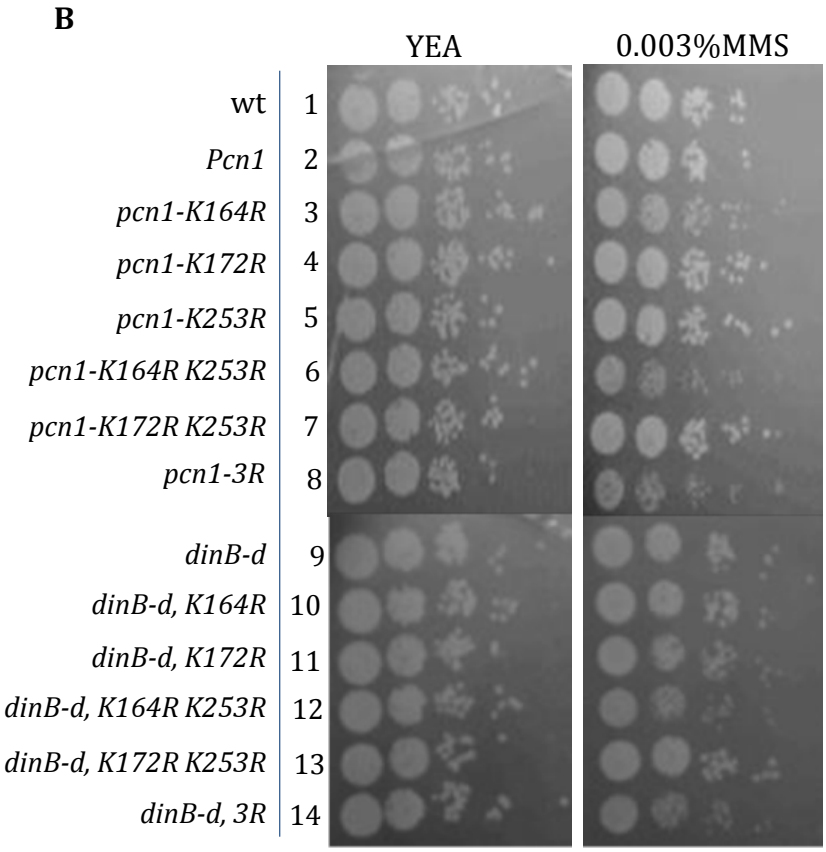

Figure 6.7 Analysis of *pcn1-K164R* and *pcn1-3R* in combination with TLS polymerase mutants *rev1-d , rev3-d and dinB-d.*

10 fold serial dilutions of exponentially growing S. pombe cultures containing single or double pcn1 mutants and either *rev1-d, rev3-d* (A) or *dinb-d* (B) were plated onto YEA containing 0.003% MMS.

rev1-d, rev3-d (A) and *dinB-d* (B) in combination with *pcn1-K164R*, *pcn1-K164R K253R* and *pcn1-3R* show a slight increase in sensitivity in response to MMS compared to single mutants.

6.7 SUMO modification of PCNA is not required for NER, BER or UVER repair pathways

PCNA K to R mutations were incorporated into *rad13-d*, *rad2-d* and *uve1-d* strains which are defective in the NER, BER and UVER repair pathways resepctively, in order to investigate whether any epistasis could be observed. Rad2 is a structure specific nuclease that is required for replication as well as several DNA repair pathways, including the processing of DNA overhangs which occur as a result of BER and NER (Alleva & Doetsch, 1998; Liu et al, 2004; Murray et al, 1994). Rad13 is the *S. pombe* homologue of mammalian XPG and is required for cleavage of damaged DNA in the NER pathway (Mu et al, 1996; O'Donovan et al, 1994). Uve1 is required for the alternative UV-damage excision pathway in *S. pombe* (Yonemasu et al, 1997).

Double mutants containing *rad13-d* and *pcn1-K164R* showed a significant increase in sensitivity to 0.003% MMS compared to either single mutant (Figure 6.8). This sensitivity is further increased in the *rad13-d pcn1-3R* double mutant. This additive effect suggests that modification of PCNA is important in the absence of a functional NER pathway for the repair of MMS-induced DNA damage, but is not directly involved in NER repair.

A similar increase in sensitivity can be observed for *rad2-d pcn1-K164R* compared to the single mutants (Figure 6.9 rows 2, 4 and 5). The *rad2-d pcn1-3R* double mutant strain is extremely sensitive to MMS (Figure 6.9 rows 3,4 and 6), suggesting an important role for K235 or K172 in the absence of Rad2 and in response to MMS treatment.

Double mutants containing *uve1-d* and *pcn1-K164R* also showed an additive effect for sensitivity to MMS (Figure 6.9 rows 2, 7 and 8), which is again strongly increased in the double mutant *uve1-d, pcn1-3R* (Figure 6.9 rows 3, 7 and 9). Single and double mutant cultures containing *rad2-d* and *pcn1-K164R* or *pcn1-3R* were treated with 0.1% MMS and cell survival assayed at 30 minute intervals for two hours following exposure (Figure 6.10). Cell viability is greatly reduced in cells containing the *rad2-d, pcn1-3R* double mutant compared to the single or *rad2-d, pcn1 K164R* double mutants. These experiments demonstrate that PCNA

modification of residues other than K164 is important for survival following MMS-induced DNA damage; however they are not required for the NER, BER or UVER repair pathways in *S. pombe*. Another possibility is that an inability to SUMOylate PCNA results in a specific type of damage that requires the HR pathway for viability.

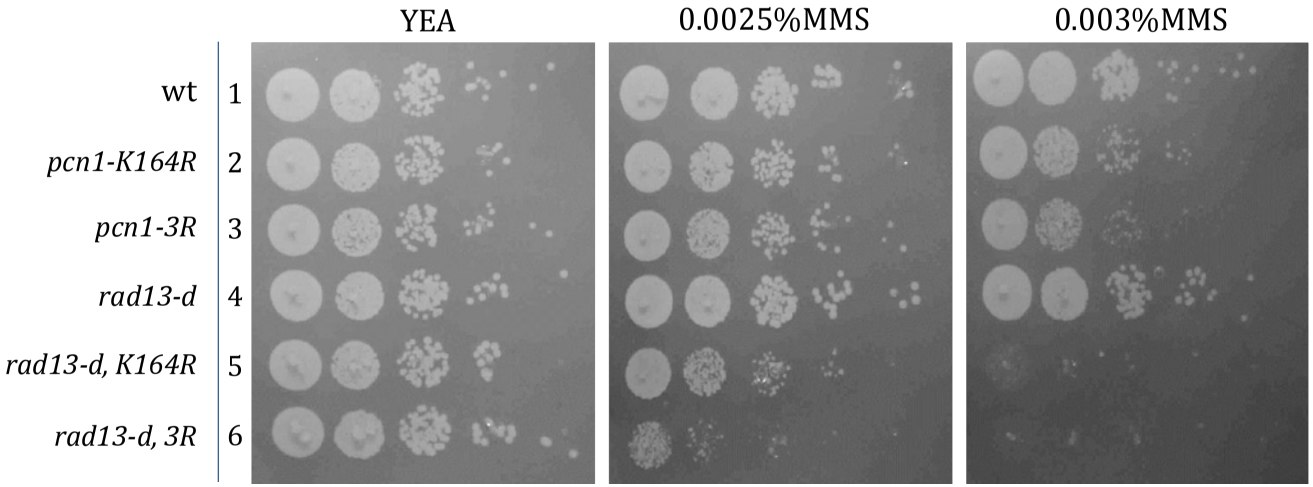

Figure 6.8 Analysis of *rad13-d* in combination with *pcn1-K164R* and *pcn1-3R.* 10 fold serial dilutions of exponentially growing *S. pombe* cultures containing single or double *pcn1* and *rad13-d* mutants were plated onto YEA plates containing 0.0025% and 0.003% MMS. *rad13-d, K164R* double mutants are significantly more sensitive to MMS than single mutants. This sensitivity is further increased in *rad13-d, pcn1-3R* double mutants.

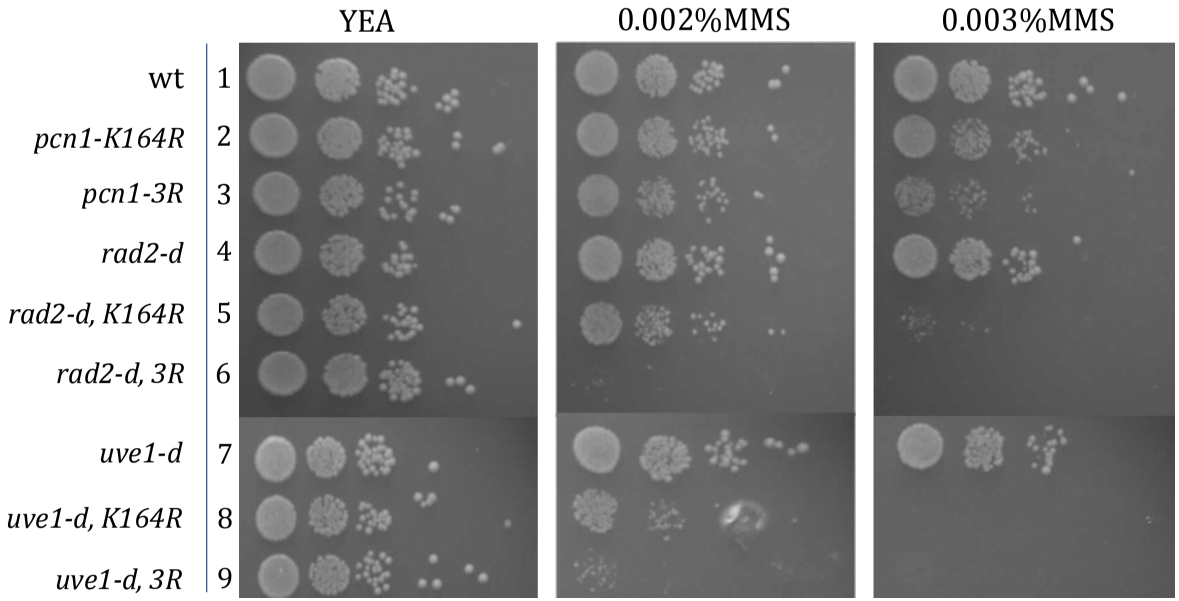

Figure 6.9 Analysis of rad2-*d* and *uve1-d* in combination with *pcn1-K164R* and *pcn1-3R*.

10 fold serial dilutions of exponentially growing *S. pombe* cultures containing single or double *pcn1* and either *rad2-d* or *uve1-d* mutants were plated onto YEA plates containing 0.002% and 0.003% MMS. *rad2-d, pcn1-K164R* and *uve1-d, pcn1-K164R* double mutants are more sensitive to MMS than single mutants. This sensitivity is further increased in *rad2-d, pcn1-3R* and *uve1-d, pcn1-3R* double mutants.

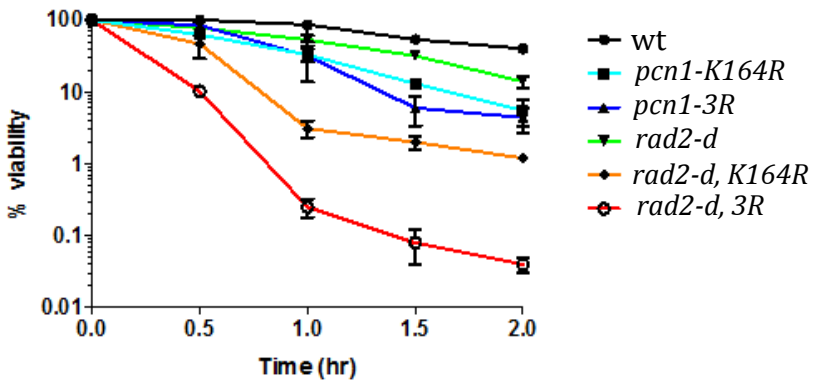

Figure 6.10 Survival curves of *rad2-d, pcn1-3R* in response to MMS.

Exponential cultures of single and double mutants were treated with 0.1% MMS. Samples were taken before MMS exposure (time 0) and at 0.5, 1 ,1.5 and 2 hours after addition of MMS. Cells from each sample were plated onto YEA plates and incubated at 30°C for 3 days. Cell viability was calculated by comparing the number of colonies formed with untreated controls. The viability of the *rad2-d, pcn1-3R* mutant is decreased compared to either single mutant and *rad2-d,pcn1-K164R*. (work completed in collaboration with Dr. Felicity Watts)

6.8 PCNA modification is required in the absence of Rad51, Rad55 and Sfr1

The results so far suggest that SUMOylation of PCNA is required for recovery from damage sustained during S phase. A major process required for this recovery is HR. In order to investigate epistasis between SUMOylation of PCNA and the HR pathway, PCNA K to R mutants were crossed with *rad51-d*, *rad55-d* and *sfr1-d* mutants. Rad51 is required to displace RPA on single-stranded DNA and form nucleofilaments which catalyse strand invasion in early HR (Kurokawa et al, 2008). Rad55 and Sfr1 form heterodimers with Rad57 and Swi5 respectively, both of which act in parallel to stabilise Rad51 filaments and promote D-loop formation (Akamatsu et al, 2007; Haruta et al, 2006). Several attempts at creating *rad51-d*, *pcn1-3R,* and *rad55-d, pcn1-3R* were unsuccessful, suggesting that the double mutants may not be viable. *rad51-d* and *rad55-d* mutants in *S. pombe* are very sick, and tetrad analysis was not performed, therefore lethality of the double mutants was not confirmed this way. *sfr1-d, pcn1-K164R* and *sfr1-d, pcn1-3R* double mutants were viable, however both are exquisitely sensitive to low doses of MMS (Figure 6.11.). A lower dose of MMS is required to establish whether the *sfr1-d, pcn1-K3R* double mutant is more sensitive than the *sfr1-d, pcn1-K164R* double mutant. These results suggest an important requirement for PCNA modification in the absence of an active Sfr1-Swi5 complex. Lethality of *rad55-d, pcn1-K3R* double mutants would suggest that the Rad55-dependant sub pathway is required for viability in the absence of PCNA SUMOylation.

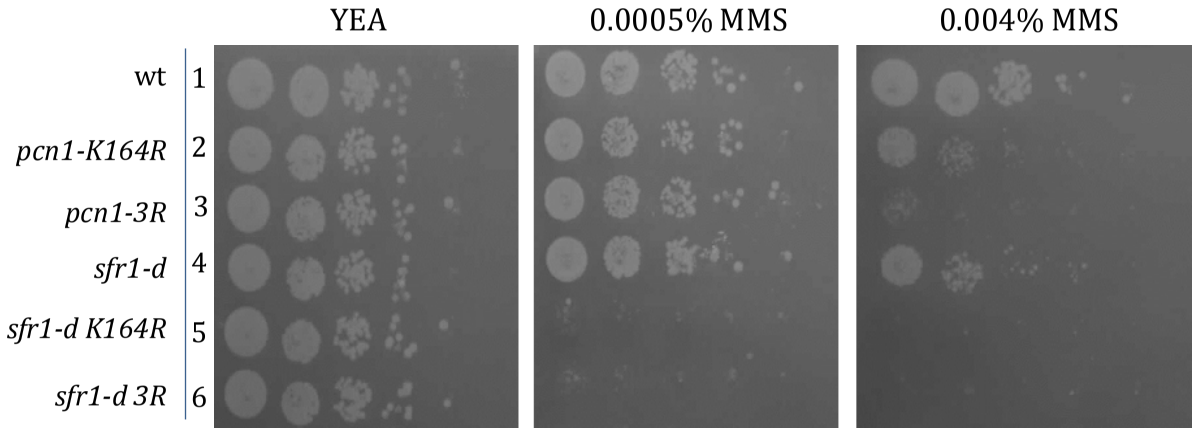

Figure 6.11 *pcn1-K164R* and *pcn1-3R* have an additive effect in combination with *sfr1-d*

10 fold serial dilutions of exponentially growing *S. pombe* cultures containing single or double pcn1 and *sfr1-d* mutants were plated onto YEA plates containing 0.0005% and 0.004% MMS. *Sfr1-d, pcn1-K164R and sfr1-d, pcn1-3R* double mutants are highly sensitive to MMS compared to single mutants.

6.9 PCNA lysine to arginine mutants rescue the MMS sensitivity of *mre11-d* mutants

Mre11 (formerly Rad32) is the *S. pombe* homologue of mammalian Mre11 and part of the MRN complex (Tavassoll et al, 1995; Wilson et al, 1998). The MRN complex is involved in several aspects of DNA damage repair, including the detection of DSBs, DNA end processing and checkpoint signalling (Williams et al, 2010). It has also been implicated in the removal of topoisomerase proteins from the DNA (Hartsuiker et al, 2009). The *mre11-d* strain is sensitive to low doses of MMS and HU (Figure 6.12 row 5). This sensitivity is reversed in *mre11-d pcn1-K164R* and *mre11-d rhp18-d* and *mre11-d pcn1-3R* double mutants to the same extent in all three double mutants in response to HU (Figure 6.12 rows 6 and 7). This suggests that ubiquitination of PCNA on K164 is detrimental in the absence of Mre11 in *S. pombe*. The *mre11-d pcn1-3R* double mutant rescues the MMS sensitivity of *mre11-d*, to a lesser extent than *mre11-d pcn1-K164R* and *mre11-d rhp18-d* (Figure 6.12 row 8 compared to rows 6 and 7). The reason for this is unknown, however it is possible that SUMOylation of PCNA may aid survival following MMS exposure in the absence of Mre11, and that this is only possible once ubiquitination is abolished. It is possible that SUMOylation of PCNA recruits another unknown exonuclease which promotes HR-mediated repair.

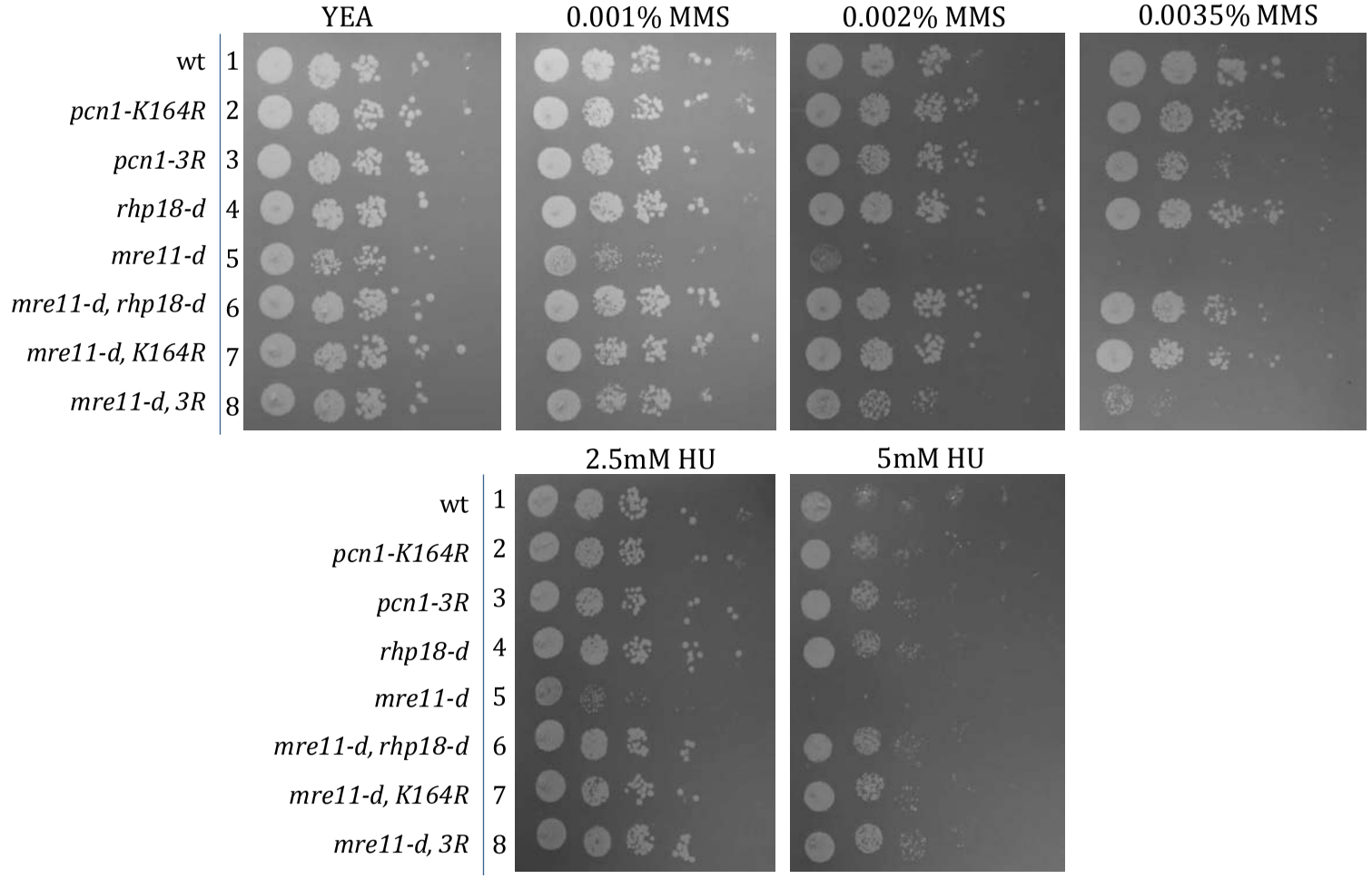

Figure 6.12 *pcn1-K164R*, *rhp18-d* and *pcn1-3R* rescue the MMS sensitivity of *mre11-d*

10 fold serial dilutions of exponentially growing *S. pombe* cultures containing single or double pcn1 and *mre11-d* mutants were plated onto YEA plates containing either MMS or HU at the concentrations indicated.
mre11-d, pcn1-K164R; mre11-d, rhp18-d and mre11-d, pcn1-3R double mutants rescue the MMS sensitivity of *mre11-d.*

6.10 SUMOylation of PCNA does not act in the same pathway as Cds1 or Chk1

Cds1 is the effector kinase which is phosphorylated by Rad3 following detection of DNA damage during S-phase. Cds1 activation results in phosphorylation of Cdc25 and the inhibition and subsequent slowing of S phase to allow for the repair of DNA damage and re-start of stalled replication forks. *cds1-d* strains were crossed with *pcn1-K164R* and *pcn1-3R* and single and double mutants used for spot tests on plates containing MMS and HU. *cds1-d, pcn1-K164R* mutants showed an increase in sensitivity to both MMS and HU when compared to single mutants (Figure 6.13 row 5). This sensitivity was further increased in the *cds1-d, pcn1-K3R* double mutants (Figure 6.13 row 6 compared to row 5). The additive effect of these double mutants does not implicate SUMOylation of PCNA in the Cds1 checkpoint signalling pathway, however it may be involved in a parallel pathway.

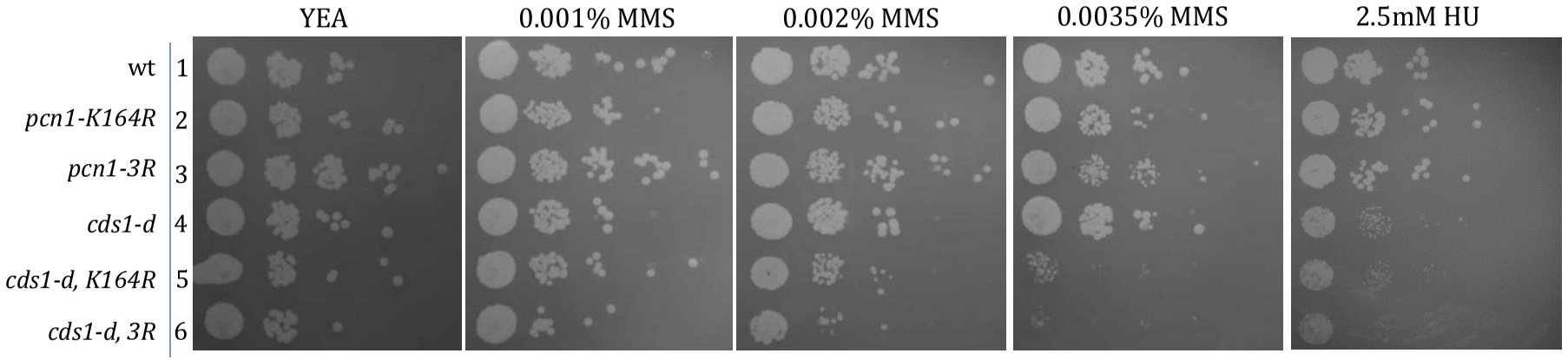

Figure 6.13 PCNA K to R mutants do not function in the same pathway as Cds1.

10 fold serial dilutions of exponentially growing *S. pombe* cultures containing single or double pcn1 and *cds1-d* mutants were plated onto YEA plates containing either MMS or HU at the concentrations indicated.
cds1-d pcn1-K164R and cds1-d, 3R double mutants are more sensitive to MMS than either single mutant.

Activation of the effector kinase Chk1 by Rad3 induces the G2/M phase checkpoint which prevents progression into mitosis in the presence of any DNA damage. In order to investigate whether the SUMOylation of PCNA acts in a Chk1-dependent pathway, double mutants were created containing *chk1-d* and either *pcn1-K164R* or *pcn1-3R* and spot tests carried out in plates containing either MMS or HU. The *chk1-d*, *pcn1-K164R* double mutant resulted in an increase in sensitivity to MMS and HU compared to either single mutant (Figure 6.14). *chk1-d*, *pcn1-K3R* double mutants showed a more dramatic increase in sensitivity specifically to MMS. Double mutants with *rad3-d* would have been analysed if time had permitted, although it is possible that such double mutants would be lethal.

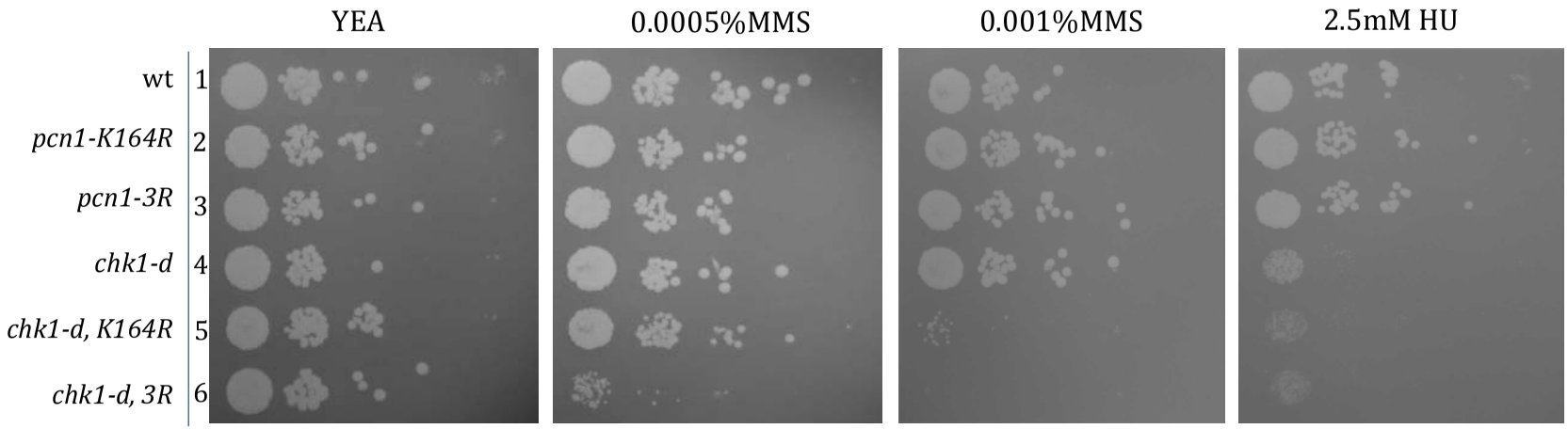

Figure 6.14 *pcn1* K to R mutants do not function in the same pathway as Chk1.

10 fold serial dilutions of exponentially growing *S. pombe* cultures containing single or double pcn1 and *chk1-d* mutants were plated onto YEA plates containing either MMS or HU at the concentrations indicated.
chk1-d pcn1-K164R and chk1-d, 3R double mutants are more sensitive to MMS than either single mutant.

6.11 PCNA K to R mutants activate the G2/M checkpoint

PCNA K to R mutants were integrated into a strain containing HA-tagged Chk1, in order to determine whether mutants could efficiently activate the G2/M checkpoint. Whole cell extracts were prepared from untreated samples, and samples were exposed to 200Gy of ionising radiation. No aberrant checkpoint activation was observed in untreated cells (Figure 6.15, lanes 4-6). A band shift correlating to activated Chk1 can be visualised following IR treatment in both the *pcn1-K164R* and *pcn1-K3R* mutants (Figure 6.15, lanes 7-9). It would be interesting to investigate whether Chk1 is activated in pcn1 K to R mutants following MMS treatment.

6.12 *pcn1-K164R* and *pcn1-K3R* mutants have reduced Cds1 phosphorylation in response to MMS.

A Phos-tag acrylamide gel was used in order to investigate whether Cds1 phosphorylation was affected in *pcn1-K164R* or *pcn1-3R* mutants. No aberrant Cds1 phosphorylation could be observed in untreated cells (Figure 6.16 lanes 3 – 5). HU treatment induced Cds1 phosphorylation in wild type, *pcn1-K164R* and *pcn1-3R* samples (Figure 6.16 lanes 2, 9 and 10). In contrast, following MMS treatment, *pcn1-K164R* and *pcn1-3R* showed decreased Cds1 phosphorylation compared to the wild type control (Figure 6.16 lanes 6-8) and phosphorylation could only be detected in longer exposures. This suggests that an inability to ubiquitinate and/or SUMOylate PCNA results in an inability to signal for S-phase arrest.

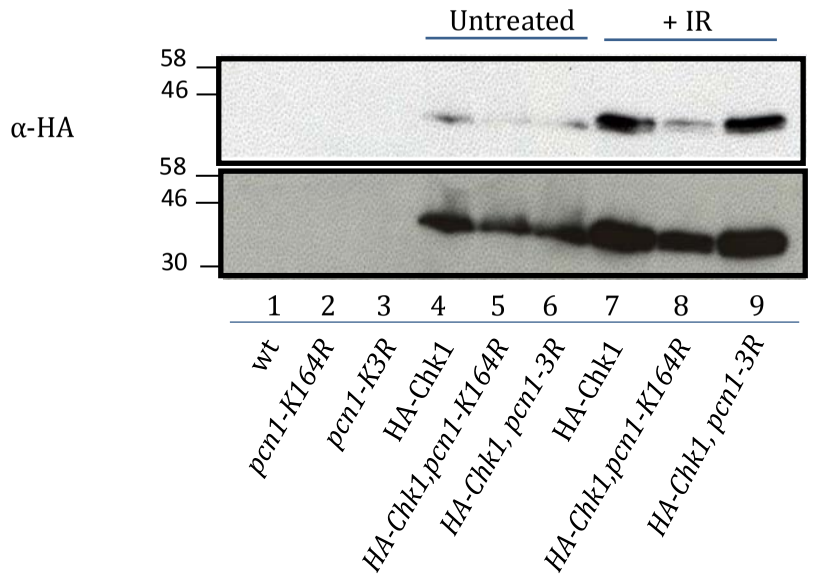

Figure 6.15 *pcn1-K164R* and *pcn1-3R* mutants are not defective in Chk1 phosphorylation following IR treatment.

Whole cell extracts from exponentially growing *S. pombe* strains as indicated were prepared and samples analysed by SDS-PAGE and probed with antibodies against the HA tag. HA-Chk1 phosphorylation can be observed in cells containing an integrated HA-tag following exposure to 100Gy IR (lane 7). Strains containing HA-Chk1 and either *pcn1-K164R* or *pcn1-3R* mutants do not appear have reduced Chk1 phosphorylation following IR treatment (lanes 8 and 9). (Note that lane 8 contains less sample compared to lanes 7 and 9). Bottom panel is a longer exposure of the same membrane.

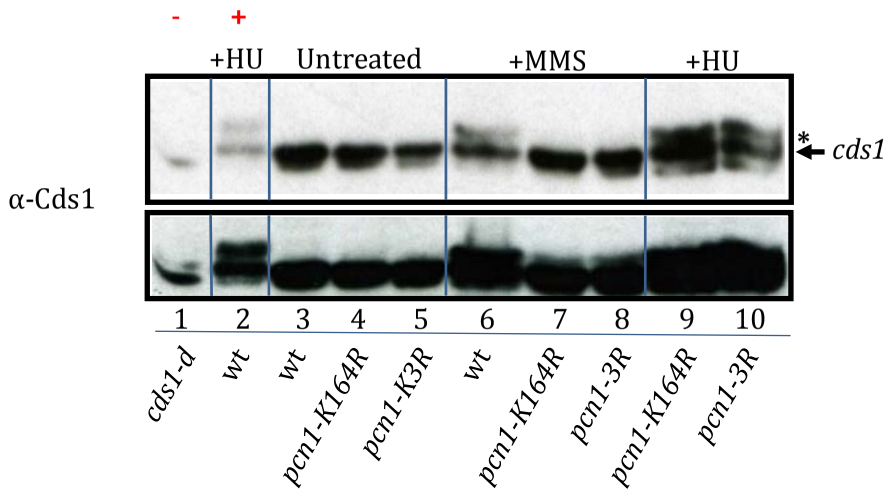

Figure 6.16 *pcn1-K164R* and *pcn1-3R* mutants do not activate the intra-S phase checkpoint as efficiently as wild type cells in the following MMS treatment.

Whole cell extracts were prepared from the strains indicated, which were either untreated (lanes 3-5), or treated with 0.05% MMS for 3 hours (lanes 6-8) or 12mM HU for 3 hours (lanes 2, 9 and 10). Samples were run on phosphate-affinity acrylamide gel and western blots probed with antibodies against Cds1. Red + and - indicate positive and negative controls (Lanes 1 and 2). Cds1 phosphorylation can be observed in wild type cells following exposure to either HU (lane 2) or MMS (lane 6) *pcn1-K164R* and *pcn1-3R* mutants have reduced Cds1 phosphorylation following MMS treatment (lanes 7 and 8). Arrow indicates band corresponding to unmodified Cds1, Asterisk indicates phosphorylated Cds1. Bottom panel is a longer exposure of the same membrane. 7.5% gels containing 20uM MnCl2 and 10uM phos-tag.

6.13 Discussion

Following the integration of *pcn1* K to R mutants into the *S. pombe* genome, spot tests showed a slight increase in sensitivity of the *pcn1-K164R K253R* mutant and *pcn1-3R* triple lysine mutant compared *pcn1-K164R* in response to MMS (Figure 6.1). Sensitivity to MMS is usually a sign of an inability to deal with to DNA damage during S phase. This could suggest a requirement of SUMOylated PCNA to either prevent or repair damage or specific structures such as stalled or collapsed replication forks during S phase, or a role for K253 SUMOylation in the repair of MMS-induced DNA damage. None of the single mutants except for *pcn1-K164R* conferred sensitivity to any other DNA damaging agents. As K13 is located on the inner surface of the PCNA trimer which encircles DNA, SUMOylation of the monomeric protein *in vitro* is likely to be an artefact of the reaction and not biologically relevant. The positively charged inner ring is approximately 35Å in diameter and a structure of mammalian PCNA encircling double stranded DNA has been published (Ivanov et al, 2006). It is unlikely that SUMO could occupy this space at the same time as DNA. SUMO modification at this position could potentially affect ring formation, however the absence of a mutant phenotype when K13 is mutated to arginine indicates that ring formation is unlikely to be adversely affected. Further evidence for K13 modification being an artefact of the *in vitro* reaction comes from 2D gel analysis of the *pcn1-K3R* mutant (Figure 5.7, bottom right panel). The spot corresponding to SUMOylated PCNA is abolished in this mutant, which would not be expected if K13 was also SUMOylated. For this reason the K13R mutant was not analysed further.

PCNA is mono-ubiquitinated by Rhp6 and Rhp18 to promote TLS, and is poly-ubiquitinated by Mms2-Ubc13 and Rad8 to promote template switching. PCNA is constituitively ubiquitinated in *S.pombe* in S-phase and ubiquitin levels are increased in response to DNA damage induced by HU, UV, IR and MMS in S-phase as well as in G2 (Frampton et al, 2006; Hoege et al, 2002). Whilst *pcn1-K164* mutants have previously been reported to be sensitive to UV- and IR-induced damage (Frampton et al, 2006), neither *pcn1-K164R K253R* nor *pcn1-3R* was observed to have a notable increase in sensitivity to either of these

damaging agents compared to *pcn1-K164R* (Figure 6.2), suggesting that SUMOylation of *S. pombe* PCNA on K253 or K172 is not required for the repair of UV- or IR-induced DNA damage. Extensive epistasis analysis was carried out, the results of which are summarised in Figure 6.17, and discussed in detail below.

It was reported previously (Frampton et al, 2006) that *pcn1-K164R* is epistatic with ubiquitin pathway mutants *rhp18-d, mms2-d* and *ubc13-d* in response to UV irradiation. Spot tests of double mutants on plates containing MMS demonstrate that *pcn1-K164R K253R* and *pcn1-3R* are epistatic *with rhp18-d*, but have an additive effect in combination with *mms2-d* (Figure 6.5-6.6). This implicates SUMOylation of PCNA in the error-prone TLS pathway. However, the *pcn1* K to R mutations displayed an additive effect on the MMS sensitivity of TLS polymerase mutants (Figure 6.7). As TLS is abolished in *pcn1-K164R*, the increase in sensitivity of double mutants supports another role for K164, presumably SUMOylation. It is possible that SUMOylation of PCNA is involved in an error-prone repair pathway that is independent of the TLS polymerases, or perhaps acts in a parallel pathway involving Rhp18 which is specific in response to MMS-induced DNA damage.

Epistasis analysis was carried out with cells deleted for the SUMO ligase Pli1, which enhanced the SUMOylation of PCNA *in vitro*. Cells lacking Pli1 are insensitive to a range of damaging agents, despite Pli1 having a range of target proteins involved in repair pathways (Xhemalce et al, 2004a). Double mutants *pli1-d pcn1-K164R* and *pli1-d pcn1-3R* display a slight increase in sensitivity to MMS compared to the single *pcn1-K164R* and *pcn1-3R* mutants, suggesting that Pli1 and SUMOylation of PCNA have some non-overlapping functions. For example, *pli1-d rad22-d* (*S.pombe* homologue of *rad52*) double mutants are lethal (Xhemalce et al, 2004a). *GFP-rad22 pcn1-3R* double mutants were generated, however there was no notable difference in foci formation compared to the single mutant in untreated or MMS treated samples (Dr. F. Z. Watts, data not included).

Strain	Function 192	Background		
		wt	*pcn1-K164R*	*pcn1-3R*
		-	+	++
mms2-d	ubiquitin E2 – poly-Ub	-	+	+(+)
rhp18-d	ubiquitin E3 – mono-Ub	-	-	(+)
rev1-d	TLS polymerase Rev1	-	(+)	+
rev3-d	TLS polymerase ζ subunit	-	(+)	+
dinB-d	TLS polymerase κ	-	(+)	+
pli1-d	SUMO E3 ligase	-	(+)	++
nse2-SA	SUMO E3 ligase	-	+++	+++
rad13-d	NER endonuclease (XPG)	-	++	+++
uve1-d	UV endonuclease	-	+++	++++
rad2-d	Flap endonuclease	-	+++	++++
rad51-d	Homologous recombination (HR)	nt	viable	lethal
rad55-d	HR	+++	+++	lethal
sfr1-d	HR	(+)	++++	++++
mre11-d	HR - MRN complex factor	+++	-	(+)
cds1-d	Replication/intra-S checkpoint	-	++	+++
chk1-d	G2/M checkpoint	-	++	++++

Figure 6.17 – Summary of epistasis analysis carried out in Chapter 6

MMS sensitivities of single and double mutant strains constructed in this study. - = not sensitive, (+) = slight increase in sensitivity, increasing + refers to relative increases in MMS sensitivity. + = exquisite sensitivity to MMS. nt = not tested in this study.

pcn1 K to R mutants were also combined with cells defective in the other SUMO ligase in *S.pombe*, Nse2. The significant increase in sensitivity of *nse2-SA pcn1-K164R* and n*se2-SA pcn1-3R* compared to single mutants can be explained by the elimination of both the TLS pathway (K164R) and Nse2-mediated recombinational repair. Whether SUMOylation of PCNA could be directing damage to Nse2-mediated repair is unknown.

Analysis of *pcn1* K to R mutants in combination with mutants from a range of repair pathways including BER (Figure 6.8), NER and UVDE (Figure 6.9) all resulted in additive phenotypes in response to MMS, which are increased on addition of the K253R mutation. This lends further evidence for a role of at least K253 modification in the repair of MMS-induced damage, or an accumulation of damage in unSUMOylatable mutants which requires another pathway, such as HR, for repair

Sfr1-Swi5 and Rad55-Rad57 are two mediator complexes which promote Rad51 filament stability and strand exchange during the early stages of recombination. Several attempts at creating double mutants containing *pcn1-3R* and either *rad51-d* or *rad55-d* were unsuccessful. Tetrad analysis would be required to confirm lethality of these double mutants, however previously *rad51-d, pcn1-K164R* and *rad55-d, pcn1-K164R* have been generated and shown to be very sick, having slow growth phenotypes and extreme sensitivity to DNA damaging agents (Frampton et al, 2006). More recently, double mutants containing *rad8-d* (which is defective in poly-ubiquitination of PCNA) with either *rad51-d* or *rad55-d* have been reported to show an increase in sensitivity to MMS, which is more extreme in the *rad51-d, rad8-d* mutant (Ding & Forsburg, 2014). It is clear that in the absence of Rad51 or when HR is impaired, PCNA ubiquitination is important for the response to DNA damage, particularly MMS-induced damage. If *rad51-d, pcn1-3R* and *rad55-d, pcn1-3R* double mutants are indeed inviable, then the apparent lethality of the *pcn1-3R* mutant in combination with *rhp51-d* and *rad55-d* is presumably due to a loss of HR repair (*rad51-d*) and both error-prone and error free damage avoidance (*pcn1-K164R*) and possibly another repair pathway involving SUMOylation of PCNA. *sfr1-d, pcn1-K164R* and *sfr1-d, pcn1-3R* double mutants are extremely sensitive to MMS, however it is not clear

from the MMS concentrations used whether the *sfr1-d, pcn1-K164R* is less sensitive than *sfr1-d, pcn1-3R* (Figure 6.11 lanes 5 and 6). The loss of both error-prone and error-free damage avoidance resulting from the *pcn1-K164R* mutation in combination with inefficient HR could be leading to the exquisite sensitivity of the double mutants to MMS. It is also likely that the Rad55-dependent HR pathway is essential in the absence of SUMOylation of PCNA. Interestingly, *pli1-d, rad51-d* double mutants are also lethal (Xhemalce et al, 2004a). It is possible that this lethality results from an inability to SUMOylate PCNA. It is interesting to note that *GFP-rad11, pcn1-3R* double mutants are lethal (confirmed by tetrad analysis). This implies that the Rad11 subunit of RPA plays an important role when SUMOylation of PCNA is impaired. It would be interesting to see whether *pli1-d* mutants are also lethal with *rad11.* Further analysis is required to understand the relationship between SUMOylation of PCNA, Pli1 and recombination mutants. *pli1-d, rhp18-d* double mutants are currently being generated, which will indicate whether the phenotype of *pli1-d, pcn1-3R* is mostly a result of an inability to ubiquitinate, or an inability to SUMOylate PCNA.

Mre11 binds to DNA ends and is involved in end processing and resection of the DNA at double strand breaks. The MRN complex is also involved in activation of the S phase checkpoint (Willis & Rhind, 2010). *mre11-d* cells are unable to efficiently repair DSBs and are sensitive to IR (Tavassoll et al, 1995). Spot tests using *mre11-d* strains in combination with *pcn1* K to R mutants and *rhp18-d* revealed that whilst the *mre11-d* single mutant is highly sensitive to MMS, this sensitivity is rescued when in combination with *rhp18-d* or *pcn1-K164R* (Figure 6.12 lanes 5, 6 and 7). This suggests that PCNA ubiquitination is detrimental to cell survival following DNA damage in the absence of Mre11. Interestingly (Ding & Forsburg, 2014) recently reported that *mre11-d* is epistatic with *rad8-d*, as a double mutant containing *rad8-d* and *mre11-d* was no more or less sensitive to either single mutant at low doses of MMS. Since *rad8* mutants are defective only in poly-ubiquitination, the results reported here suggest that the rescue of the *mre11-d* by *pcn1-K164* is due specifically to the absence of mono-ubiquitination and error-prone TLS. m*re11-d, pcn1-3R* double mutants also rescue the MMS sensitivity of *mre11-d* cells, to a lesser extent. This again implicates

SUMOylation of PCNA as being important in the repair of alkylation damage, in the absence of Mre11. One explanation for these results could be that in the absence of Mre11, recombinational repair is impaired and PCNA is heavily ubiquitinated, resulting in inhibition of SUMOylation and directing repair though the error-prone TLS pathways, resulting in genomic instability. Abolishing PCNA ubiquitination could allow for SUMOylation of PCNA to take place which could recruit an unknown endonuclease to resect the ends of DNA breaks in the absence of Mre11, in concert with Exo1. It has been shown recently using human proteins and in *Xenopus* extracts that PCNA enhances Exo1 activity (Chen et al, 2013). It is possible that this is also the case in *S. pombe*, or that SUMOylation of PCNA either recruits or enhances the activity of an alternative exonuclease. This would explain the less effective rescue of the *mre11-d, pcn1-3R* mutant compared to *mre11-d, pcn1-K164R.*

The additive effect observed for *pcn1-K164R* and *pcn1-3R* in combination with checkpoint kinase mutants *cds1-d* and *chk1-d* (Figure 6.13 and 6.14) suggests that SUMOylation of PCNA is not involved in the intra-S or G2/M checkpoint pathways, but is required in the response to specifically MMS-induced DNA damage in the absence of checkpoint activation. However, whilst Chk1 activation is unaffected in PCNA K to R mutants (Figure 6.15), phosphorylation of the intra S-phase checkpoint kinase Cds1 is reduced in both *pcn1-K164R* and *pcn1-3R* mutants (Figure 6.14). These results indicate that either ubiquitinated or SUMOylated of PCNA (or both) contribute to intra-S phase checkpoint activation in response to MMS. Analysis of a *rad3-d, pcn1-3R* double mutant is required to further investigate a role for the SUMOylation of PCNA in the checkpoint response, though it is likely that this double mutant is lethal.

Taken together, the results presented in this chapter strongly support a role for PCNA SUMOylation in *S. pombe*, particularly on K253, in response to MMS-induced damage. PCNA K to R mutants are exclusively sensitive to MMS and do not show an increase in sensitivity compared to *pcn1-K164R* to any of the other types of DNA damage tested, including CPT (data not included). The first of two possibilities is that SUMOylation of PCNA acts in a damage specific pathway required in response to MMS, which is important in the absence of other repair

pathways including NER, BER, UVER and HR. However data presented in this chapter does not provide evidence as to which pathway this modification might be implicated in. Perhaps SUMOylation of PCNA is only required in the absence of one or more repair pathways, and we have yet to identify any interacting proteins. Previous reports have implicated Swi1, Swi3 and Hsk1 to be involved in an alkylation specific repair pathway (Sommariva et al, 2005). It is possible that SUMOylation of PCNA plays a role in this or another parallel pathway. *pcn1-3R* mutants do not activate either the intra-S or G2/M phase checkpoint in the absence of DNA damage, which implies that there is not an accumulation of damage in untreated cells, as reported in *swi1*, *swi3* and *hsk1* mutants.

A second explanation for these results could be that an inability to SUMOylate PCNA causes a specific kind of damage or structure, for example replication fork collapse, which subsequently requires HR-mediated repair pathways for viability. Replication fork collapse could result from impaired Cds1 phosphorylation in *pcn1* K to R mutants, (Figure 6.16) affecting the intra-S phase checkpoint. Subsequent Chk1 phosphorylation and checkpoint signalling involving RPA could facilitate repair of collapsed forks by HR. This could explain the extreme sensitivity of *pcn1-3R* mutants with HR mutant *sfr1-d* and possible lethality with *rad51-d, rad55-d* and *GFP-rad11*. The stability of the PCNA protein and chromatin association of the *pcn1-3R* mutants is unaffected as tested in the presence and absence of MMS (data not included). Current work is being carried out to assess the stability of replication fork components in the *pcn1-3R* mutants.

Further analysis is required to find a role for the SUMOylation of PCNA in *S. pombe,* including investigation into recombination rates in *pcn1-K3R* mutants, as well as further genetic analysis, for example with Rad3, fork protection complex components Swi1 and Swi3, exonuclease Exo1 and helicase Rqh1, which is involved in the dissolution of recombination structures. It would also be interesting to analyse the phenotypes of pcn1 K to R mutants in combination with checkpoint signalling mutants including *rad9-d*, *rad17-d* and *cdc18-d* in order to identify a more specific role for SUMOylation of PCNA in *S.pombe*.

7 Discussion

SUMOylation is now known to be an important factor in the regulation of many cellular processes including transcription, translation, telomere maintenance and the DNA damage response. In recent years many proteins involved in DNA damage response pathways have been demonstrated to be SUMOylated, several as a result of high throughput screens. The work presented in this thesis was directed towards developing *in vitro* and *in vivo* assays for the efficient detection and identification of SUMO target proteins, and to specifically investigate the roles of SUMOylation of Smc5/6 complex-associated protein and SUMO ligase Nse2 and the replication-associated sliding clamp PCNA, in *S. pombe.* During this study, a trypsin cleavable SUMO was generated and purified for use in *in vitro* SUMOylation assays. has led to the isolation and identification of novel SUMO target proteins in *S.pombe*, including SUMO E2 conjugating enzyme Hus5 and PCNA. This system was successfully used for the identification of specific target lysine residues which can be utilised for *in vivo* study and molecular modelling. A HIS tagged, trypsin cleavable SUMO was successfully integrated into the genome in place of the wild type coding sequence. This strain was used in pull-down assays to visualise SUMO modified proteins *in vivo*. The HIS-SUMO-tr recombinant protein and strain are useful tools which can be utilised in future studies to identify and characterise known and novel SUMO target proteins at endogenous levels and in response to a wide range of cellular conditions,

In vitro SUMOylation studies identified four SUMOylation sites of *S.pombe* PCNA, K13, K164, K172 and K254. Pull-down and 2D gel analysis confirmed that S.pombe PCNA is SUMOylated *in vivo* at three of the four residues identified in vitro, K164, K172 and K253. SUMOylation was shown to increase following MMS treatment, and subsequent *in vivo* analysis of PCNA un-SUMOylatable mutants suggested a role for the SUMOylation of *S.pombe* PCNA in response to MMS-induced damage. Genetic analysis indicated that SUMOylation of PCNA functions upstream of Cds1 activation in the intra-S checkpoint, and upstream of Mre11 in response to MMS treatment (Figure 7.1). The successful integration of PCNA lysine to arginine mutants into the genome and this initial genetic analysis has confirmed for the first time that *S.pombe* PCNA is SUMOylated *in*

vivo and has hinted at roles in checkpoint signalling and the repair of alkylation damage, perhaps by promoting BER. Further analysis will contribute to the understanding of the differences in PCNA modification between *S.pombe*, *S.cerevisiae* and mammals. A complete understanding of the functions and regulation of PCNA in different organisms will ultimately contribute to cancer therapies, being as PCNA has a central role in the response to DNA damage,

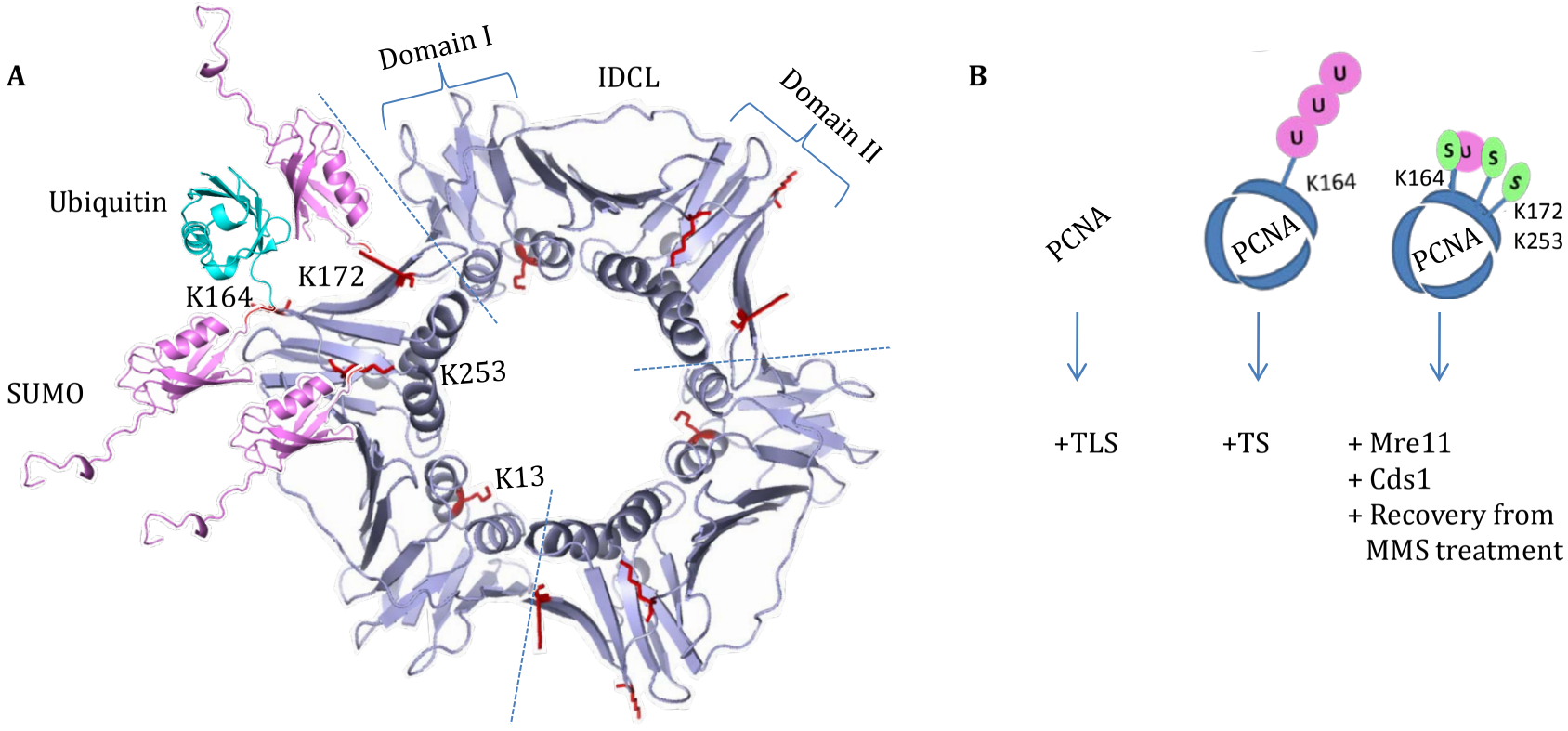

Figure 7.1 PCNA modifications in *S. pombe*

(**A**) Structural representation of the Domains and modification sites of *S. pombe* PCNA. Dashed lines separate three PCNA monomers. Each monomer contains two domains (domain I and domain II) and an inter-domain connecting loop (IDCL), where many PIP-box containing proteins interact with PCNA. *S.pombe* PCNA is ubiquitinated exclusively at K164 (ubiquitin highlighted in teal). This study identified three SUMOylation sites, K164, K172 and K253. SUMO is highlighted in purple. SUMOylated residues are highlighted in red. K13 was identified as SUMOylated *in vitro,* but was excluded as a real modification site following *in vivo* analysis. (**B**) Consequences of PCNA modification. Mono-ubiquitination promotes trans-lesion synthesis (TLS). Poly-ubiquitination promotes template switch-mediated repair (TS). SUMOylation and/or ubiquitination functions up-stream in Mre11 in the repair of MMS-induced damage and contributes to Cds1 phosphorylation following MMS. SUMOylation is important for repair or recovery in response to MMS-induced DNA damage.

7.1 Development of an efficient *in vitro* and *in vivo* SUMOylation system

An *in vitro* SUMOylation system was previously established in the Watts lab (Ho et al, 2001), whereby tagged SUMO pathway components were recombinantly expressed and purified from *E. coli.* At the beginning of this work, the baculovirus expression system was set up in an attempt to co-express and co-purify components of the SUMOylation pathway, including the E1 SUMO activating enzyme heterodimer Rad31-Fub2. The baculovirus system utilises insect cells which perform post-translational modifications that can improve protein folding and activity. In parallel to this, another member of the lab was optimising protein expression in *E. coli* and the baculovirus project was abandoned in favour of cheaper and more efficient bacterial protein expression.

Previously, the identification of specific lysine residues on SUMO target proteins involved mutating surface lysine residues one by one and assay the mutant proteins for SUMOylation *in vivo*. This method is frequently unproductive for two reasons. Firstly because of the time taken to mutate all of the lysine residues and secondly because SUMO has been observed to modify different lysine residues if the main SUMOylation site becomes unavailable. This could be particularly prevalent in *in vitro* conditions where there is an abundance of substrate and SUMO machinery. A limiting factor in mutating lysine residues *in vivo* is that other modifications which affect the same residue could also be abolished, resulting in a phenotype which is not necessarily due to an inability to SUMOylated.

In order to develop a reliable system for the identification of SUMO target residues, this study made use of mass spectrometry analysis which was available at the University of Sussex. Trypsin is regularly used as a protease to digest proteins into peptide fragments which can be analysed by mass spectrometry (MS). Trypsin cleaves at lysine and arginine residues. In *S.pombe* SUMO, the closest cleavage site is 23aa away from the diglycine motif which is covalently attached to target proteins. This means that MS analysis of modified proteins formed in an *in vitro* SUMOylation assay produces poor coverage of

peptides, as many modified fragments are too large for MS analysis. In order to overcome this problem, a leucine to arginine mutation was generated directly upstream of the diglycine residues in recombinant mature SUMO (HIS-SUMOGG). This was called HIS-SUMOGG.tr and was shown to efficiently SUMOylate proteins *in vitro* (Figure 3.2). Trypsin cleavage of modified proteins subsequently resulted in just two amino acids remaining attached to the target residue, which are recognised by a mass shift of the fragment containing the modification. This trypsin-cleavable SUMO was successfully used *in vitro* to identify SUMOylated target proteins including the E2 SUMO conjugating enzyme Hus5 (Figure 3.3) and E3 SUMO ligase Nse2 (Figure 4.1). This confirmed previous results from the lab which identified putative target residues for these two proteins.

Whilst *in vitro* assays are a useful tool in identifying potential SUMO target proteins and locating specific residues for molecular modelling, false positive results are inevitable and the SUMOylation of proteins identified in this way must be confirmed *in vivo*. The Hus5 SUMOylation site (K50) was confirmed as the sole SUMOylation site of *S. pombe* Hus5 *in vivo,* following pull-down assays using HIS-tagged SUMO and an HA-tagged Hus5 K50R mutant (Figure 3.5).

The trypsin cleavable SUMO coding sequence was incorporated in to the genome in place of the wild type gene sequence under the control of the endogenous SUMO promoter, with a view to identifying target proteins *in vivo*, at endogenous levels. This mutation, as well as the integration of a N-terminal HIS-tag did not result in any mutant phenotypes (Figure 3.8), making the strain suitable for use in *in vivo* pull-down experiments. To this end, Ni^{2+} agarose beads were used to pull-down HIS-SUMO.tr from asynchronously growing cultures, and the eluate was probed with antibodies raised against either Nse2 or PCNA (Figure 3.9). Modified species were detected for both proteins, although unmodified species were also detected, the reason for which is unknown. Their absence in wild type controls however, suggests that the modified bands are not non-specific artefacts.

In summary, a trypsin cleavage site was successfully integrated into the SUMO coding sequence and the recombinant protein was successfully used to identify

SUMOylated target proteins *in vitro*. Both the trypsin cleavage site and a HIS tag were successfully integrated into the genome with no resultant adverse phenotypes. SUMOylated species were successfully pulled down using this strain. The generation of this strain will enable large scale pull-down assays under a range of different conditions. Subsequent analysis by mass spectrometry could lead to the identification of known and novel SUMO target proteins *in vivo*, at endogenous levels under a range of different conditions.

7.2 Nse2 SUMOylation on K134, K228 and K248 is not important for cell survival in *S.pombe*

Nse2 is a SUMO ligase associated with the Smc5/6 complex (Andrews et al, 2005). Nse2 target proteins include telomere maintenance proteins Trf1 and Trf2, cohesin and Ku70 (Potts et al, 2006; Potts & Yu, 2007; Zhao & Blobel, 2005). Nse2 also SUMOylates members of the Smc5/6 complex including Smc6 and Nse2 its-self (Andrews et al, 2005). Previous *in vitro* studies identified Nse2 lysine residues K229 and K248 as being auto-SUMOylated, however subsequent analysis as to the role of Nse2 auto-SUMOylation *in vivo* was inconclusive. An *in vitro* SUMOylation assay using HIS-SUMOGG.tr and subsequent analysis by mass spectrometry identified three SUMO modified lysine residues, K134 and K229 and K248 (Figure 41- and 4.2). Molecular modelling revealed that K229 is located in the catalytic SP-RING domain which is required for SUMO ligase activity (Andrews et al, 2005), whilst K134 is located N-terminal to the SP-RING domain, and K248 at the extreme C-terminus of the protein (Figure 4.4). In order to investigate the function of Nse2 auto-SUMOylation *in vivo*, lysine to arginine mutants were integrated into the genome in place of the wild type *nse2* coding sequence. None of the single, double or triple *nse2* lysine to arginine mutants resulted in sensitivity to DNA damaging agents including UV or IR irradiation (Figure 4.6) and MMS, nor did they confer sensitivity to the replication inhibitor HU (Figure 4.7). Whole cell extracts from strains carrying lysine to arginine mutations did not show a decrease in Nse2 protein expression or Nse2 SUMO ligase activity (Figure 4.8). These results suggest that Nse2 auto-SUMOylation is not required for the response to DNA damage, replication stress or in undamaged, normally cycling cells. Whilst the pull-down experiment using

HIS-SUMO which was integrated into the genome suggests that Nse2 is SUMOylated *in vivo*, the SUMOylation sites identified *in vitro* by MS have not been confirmed *in vivo*, and therefore it is possible that auto-SUMOylation occurs at additional sites on Nse2.

During the course of these studies, mutations in the *nse2* gene were reported in two patients who presented with polymorphic dwarfism, resistance to insulin and a reduced activity of Nse2. In one patient these were S223X and T172A and in another S116fsX132 and A234fsX236. The equivalent mutations were integrated into the *S. pombe* genome using the Nse2 base strain which was constructed for use in Nse2 auto-SUMOylation studies. The *nse2.T172A* and *nse2.A234fsX236* mutants were not sensitive to a range of DNA damaging agents (Figure 4.11), and the presence of these mutations did not affect Nse2 protein stability, expression or activity (Figure 4.12). The *nse2.S116fsX132* mutation abolishes the SP-RING domains and a significant portion of the C-terminus of Nse2 (Figure 4.9). No cells containing this mutation could be isolated, suggesting that this mutation is lethal in *S. pombe*. Strains containing the *nse2.S226X* mutation (equivalent to the S223X mutation) were sensitive to HU, MMS and IR (Figure 4.11), and some aberrant cell structures were observed. However, this mutation was later withdrawn from the database by the Sanger centre following sequencing errors. As and the other *S.pombe* mutants did not display phenotypes similar to the human mutations, these studies were not taken further.

In summary of these findings, further studies are required to investigate a role for Nse2 auto-SUMOylation *in vivo* in *S. pombe*. SUMOylation of the residues observed *in vitro* needs to be confirmed *in vivo*. For example a large scale pull-down using HIS-SUMO or the integration of a HIS-tag into the Nse2 base strain could be used to isolate SUMOylated species of Nse2 *in vivo*. Subsequent analysis by mass spectrometry could identify additional target lysine residues which could be mutated to observe any resultant phenotypes *in vivo*. The Nse2 base strain could be utilised for future studies as it allows for the integration of any mutation of *nse2* into the genome.

7.3 *S.pombe* PCNA is SUMOylated *in vitro* and *in vivo*

PCNA is a hetero-trimeric sliding clamp protein which is essential for replication and interacts with a wide range of proteins involved in replication and the DNA damage response. It tethers replicative polymerases to the replication machinery and plays a central role in DNA damage avoidance, where replicative polymerases are switched for TLS polymerases which can accommodate damaged bases in their active site and insert bases opposite a lesion. This allows replication to continue past a potentially fork blocking lesion. Post translational modifications of PCNA determine the route taken to overcome DNA damage (Jentsch et al, 1987; Ulrich, 2005; Xiao et al, 1999). Ubiquitination of PCNA is highly conserved from yeast to mammals. Mono-ubiquitination of PCNA on K164 is facilitated by the E2 ubiquitin conjugating enzyme Rad6 and the E3 ubiquitin ligase Rad18 (Rhp6 and Rhp18 homologues in *S. pombe*) (Hoege et al, 2002). Mono-ubiquitination promotes error-prone TLS which is facilitated by polymerase switching (Haracska et al, 2004; Parker et al, 2007). Poly-ubiquitination extending from the same residue is facilitated by the E2 ubiquitin conjugating enzyme heterodimer Mms2-Ubc13 and E3 ubiquitin ligase Rad5. Poly-ubiquitination promotes an error-free pathway which involves template switching (Hoege et al, 2002; Parker & Ulrich, 2009). SUMOylation of PCNA has been observed in several organisms including *S. cerevisiae* (Hoege et al, 2002) *Xenopus* (Leach & Michael, 2005b), chicken DT40 cells (Arakawa et al, 2006) and humans (Gali et al, 2012a; Moldovan et al, 2012). SUMOylation of PCNA occurs during S phase in budding yeast on K164 and K172 (Hoege et al, 2002). It is facilitated by the E3 SUMO ligase Siz1 and inhibits homologous recombination through the recruitment of the anti-recombinase Srs2 (Papouli et al, 2005; Pfander et al, 2005b). Srs2 dismantles Rad51 filaments in the early stages of HR and this mechanism is thought to protect the genome from unscheduled recombination during replication which can lead to genome re-arrangements (Krejci et al, 2003; Veaute et al, 2003). A similar mechanism in mammalian cells has been observed where SUMOylation of PCNA on K164 and K254 recruits PARI, which acts to suppress recombination (Moldovan et al, 2012).

The modification of PCNA by two PTMs on the same residue presents a mechanism for switching between TLS and recombination-mediated repair. Whilst in *S. cerevisiae* and mammalian cells PCNA ubiquitination occurs in response to DNA damage during S phase (Hoege et al, 2002; Kannouche & Lehmann, 2004; Stelter & Ulrich, 2003), *S. pombe* PCNA is constitutively ubiquitinated during S phase and this is increased in response to damage. Ubiquitination of PCNA also occurs in G2 following DNA damage in *S. pombe* (Frampton et al, 2006). SUMOylation of *S. pombe* PCNA has not yet been reported and the Srs2 homologue lacks the section of the C-terminus which contains SUMO and PCNA interacting domains *S. cerevisiae* (Frampton et al, 2006). However, previous unpublished results from the Watts lab have suggested that *S. pombe* PCNA is SUMOylated *in vivo*.

In order to identify SUMOylated PCNA *in vitro*, an *in vitro* SUMOylation assay was carried out using recombinantly expressed HIS-tagged *S. pombe* PCNA as a target protein (Figure 5.1). Mass spectrometry analysis of higher molecular weight bands which appeared following the addition of E3 SUMO ligase Pli1 revealed four modified residues, K13, K164, K172 and K253 (Figure 5.2). The structure of PCNA is highly conserved between organisms and a model of *S. pombe* PCNA was generated using Phyre2, based on published structures of the *S. cerevisiae* and human homologues. K164, K172 and K253 all protrude from the outer surface of the protein, making them accessible for SUMO modification. K164 has been identified as a SUMOylation site in other organisms as well as K254 (same position as K253) on the human protein (Gali et al, 2012a). The location of K13 is such that it protrudes into the centre of the ring structure of a PCNA trimer. The passage of DNA through the PCNA ring during replication means that there would be insufficient space for SUMO modification in S phase (Figure 5.4).

2D gel analysis was undertaken in order to confirm PCNA SUMOylation *in vivo*. This method of analysis was chosen in order to distinguish between ubiquitination and SUMOylation, which can be masked when whole cell extracts are analysed by western blotting. Cells containing wild type *pcn1*, *pcn1* lysine to arginine mutants, *rhp18-d* and *mms2-d* were analysed. Spots corresponding to

ubiquitinated PCNA are clearly observed in wild type cells (Figure 5.7, top left panel). As expected, poly-ubiquitinated species were abolished in *mms-d* cells, and all ubiquitination was abolished in the *rhp18-d* mutant and any cells containing the *pcn1-K164R* mutation. A spot corresponding to SUMOylated PCNA can be observed in all samples except for *pcn1-3R* and *rhp18-d*, *3R*. This suggests that SUMOylation occurs only on the three lysine residues K164, K172 and K253 and supports the notion that K13 is not a true SUMOylation site on *S. pombe* PCNA.

Pull-down experiments using HIS-tagged SUMO and HA-tagged PCNA were carried out in order to observe PCNA SUMOylation *in vivo* in response to DNA damage. Bands corresponding to SUMOylated species were detected in untreated cells, as well as cells exposed to HU, IR and MMS (Figures 5.5-5.7). No higher molecular weight species were observed following UV treatment, which induces an increase in ubiquitination of PCNA in *S. pombe* (Frampton et al, 2006). In order to confirm that the species observed in 2D gels and the pull-down experiments was the same, the MMS-treated sample was analysed by 2D-PAGE. The higher molecular weight species observed from the pull-down experiments corresponded to the modified species observed by 2D gel.

Taken together, these results indicate that PCNA is SUMOylated on K164, K172 and K253 both *in vitro* and *in vivo* in *S. pombe*. *In vivo* analysis suggests that PCNA is SUMOylated in unchallenged cycling cells and in response to HU, IR and MMS treatment but is reduced following UV irradiation.

7.4 Un-SUMOylatable PCNA mutants are sensitive to MMS

Following the observation of PCNA SUMOylation both *in vitro* and *in vivo*, subsequent work set out to establish a role for the SUMOylation of PCNA in *S. pombe*.

PCNA K to R mutants were analysed for sensitivity to a range of DNA damaging agents. Whilst none of the single mutants except for *pcn1-K164R* conferred sensitivity to any of the damaging agents tested (HU, MMS, IR and UV), double mutants containing *pcn1-K164R K253R* were more sensitive to MMS than the single mutants, and *pcn1-3R* mutants, where SUMOylation is abolished, showed a further increased sensitivity to MMS (Figure 6.1). As MMS sensitivity can be an indicator of sensitivity to DNA damage during S phase, these results suggest that the SUMOylation of PCNA either helps to prevent DNA damage in S-phase, possibly by preventing replication fork collapse, or is involved specifically in the repair of MMS-induced DNA damage.

7.5 *pcn1* lysine to arginine mutants rescue the sensitivity of *mre11-d* cells

Cells containing an *mre11-d* mutation are impaired in DNA end processing which is required for HR, and are not able to efficiently repair DSBs (Tavassoll et al, 1995) (Willis & Rhind, 2010). *mre11-d* is epistatic with *rad8-d*, which is required for poly-ubiquitination of PCNA and error free repair (Ding & Forsburg, 2014), perhaps due to a requirement for Mre11 to process DNA ends for template switching. Interestingly, this study shows that both *mre11-d, pcn1-K164R; mre11-d, rhp18-d* and *mre11-d, pcn1-3R* double mutants rescue the MMS sensitivity of the *mre11-d* mutant, and that this rescue is less efficient in *mre11-d, pcn1-3R*. Taken together, this suggests the rescue of *mre11-d* in combination with *pcn1-K164R* is specifically due to inhibition of PCNA mono-ubiquitination and TLS. In *S. cerevisiae*, the MRX (MRN) complex has been suggested to a play a role in BER, during the gap filling process (Steininger et al, 2010), and very recently has also been implicated in PRR (Ball et al, 2014). If the same is true in *S. pombe*, PCNA modification could be involved in co-ordinating PRR and BER pathways. The fact that the *mre11-d, pcn1-3R* double mutant rescues the *mre11-*

d phenotype less efficiently suggests that this rescue is partially dependent on the SUMOylation of PCNA. If HR and Rad8-mediated repair is inhibited in *mre11-d* mutants, then ubiquitination of PCNA could be channelling repair through the error-prone TLS pathway, which could cause genomic instability. Activation of the TLS pathway could inhibit the SUMOylation of PCNA. When the TLS pathway is inactivated, as in the *pcn1-K164R* mutant, SUMOylation of PCNA could then either channel repair through a different pathway, or recruit or enhance another exonuclease to compensate for the loss of Mre11. Thus when SUMOylation of PCNA is inhibited in the *pcn1-3R* mutant, the rescue is less efficient. PCNA has recently been shown to enhance the activity of the exonuclease Exo1, which works in concert with Mre11 to resect DNA ends (Chen et al, 2013). It is possible that SUMOylation of PCNA in *S.pombe* promotes the activity of an exonuclease. Interestingly, there are several examples of Mre11 mutants being rescued by either over-expression of the endonuclease required for bulk resection, Exo1 in *S. cerevisiae* (Lee et al, 2002; Lewis et al, 2002) or by deletion of the Ku proteins, the rescue of which is dependent on a functional Exo1 in *S. pombe* (Williams et al, 2011). The rescue of MMS sensitivity of the *mre11-d* mutant in combination with *pcn1-K164* and *rhp18-d* suggests that PCNA modification on K164 is functionally upstream of Mre11 in the response to alkylation damage. The fact that the sensitivity of the *mre11-d pcn1-3R* double mutant is increased compared to the *mre11-d pcn1K164R* double mutant (Figure 6.12) suggests that SUMOylation of PCNA on either K172, K253 or both, could be contributing to an as yet unknown pathway that is required in the absence of Mre11 (Figure 7.2).

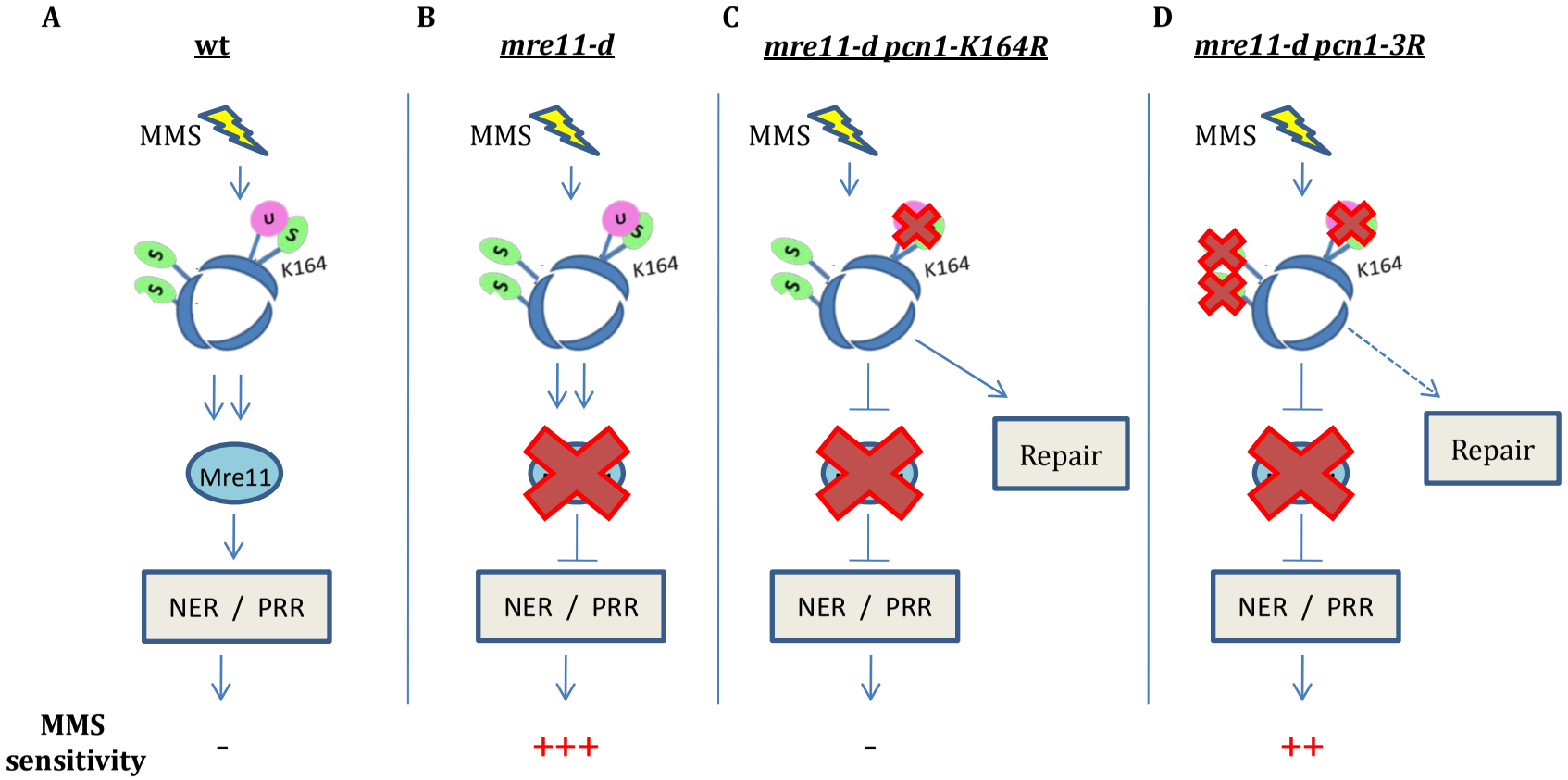

Figure 7.2 Working model for *pcn1 K164R* rescue of the MMS sensitivity of *mre11-d* mutants

(**A**) In wild type cells, modification of PCNA by ubiquitin and SUMO channel Mre11-mediated repair pathways, co-ordinating NER and PRR. (**B**) Deletion of Mre11 inhibits repair, leading to an increase in MMS sensitivity. (**C**) Abolishing PCNA modification on K164R rescues the MMS sensitivity of the *mre11-d* mutant, presumably allowing repair to be channelled through an unknown pathway. (**D**) *Mre11-d pcn1 3R* double mutants do not rescue as efficiently as *mre11-d pcn1 K164R*, suggesting that SUMOylation of PCNA on K172 and/or K253 contributes to survival via an unknown pathway. + indicates an increase in sensitivity to MMS

7.6 HR-mediated repair is required in the absence of SUMOylation of PCNA in *S. pombe*

Extensive epistasis analysis was undertaken using the *pcn1-K164R* and *pcn1-3R* mutants in combination with mutants which are defective in a range of DNA damage repair pathways, including BER, NER and HR. The outcome of these experiments indicates that HR is required for the recovery of S-phase damage in the absence of SUMOylation of PCNA.

In *S. cerevisiae* and human cells, SUMOylation of PCNA acts to inhibit unscheduled recombination events via the recruitment of Srs2 or PARI, respectively (Moldovan et al, 2012; Pfander et al, 2005b). The lack of C-terminal homology in the *S. pombe* Srs2 homologue suggests that HR is not inhibited by the same mechanism in *S. pombe*. *rad51-d, pcn1-3R* and *rad55-d, pcn1-3R* double mutants could not be generated, suggesting lethality, although this has not been confirmed by tetrad analysis. *sfr1-d*, *pcn1-K164R* and *sfr1-d, pcn1-3R* double mutants were viable, but were extremely sensitive to MMS at very low doses. Analysis of these two double mutants at lower doses of MMS is required to determine whether the *sfr1-d, pcn1-3R* mutant is more sensitive than the *sfr1-d, pcn1-K164R* mutant. The increased sensitivity of *sfr1-d, pcn1-K164R* mutants, as well as previously reported *rad51-d, pcn1-K164R* and *rad55-d, pcn1-K164R* double mutants (Frampton et al, 2006) can be explained by a loss of damage avoidance pathways in combination with impaired HR. However the potential lethality of *rad51-d, pcn1-3R* and *rad55-d, pcn1-3R* taken together with the fact that *pli1-d, rad51-d* mutants have been reported to be lethal (Xhemalce et al, 2004b), could highlight an absolute requirement for HR when SUMOylation of PCNA is impaired, specifically the Rad55-dependent HR pathway. It is unknown whether this requirement for HR-mediated repair is due to the presence of specific structures such as collapsed replication forks in the *pcn1-3R* mutant, or if abolishing SUMOylation of PCNA abolishes a damage-specific repair pathway which required following MMS-induced alkylation. The combination of *pcn1-K164R* and *pcn1-3R* with the *nse2-SA* mutant results in a significant increase in sensitivity to MMS and HU (Figure 6.4). This can be explained by the abolishment of the TLS and TS pathways, in combination with an impairment of

HR caused by *nse2.SA*. *pli1-d* mutants which are known to be insensitive to most damaging agents (Xhemalce et al, 2004a) show an increase in sensitivity to MMS in combination with *pcn1-K164R* which is further increased in combination with *pcn1-3R* (Figure 6.3). Whilst Pli1 enhanced the SUMOylation of PCNA *in vitro*, these results suggests some non-overlapping functions, which is not surprising given the wide range of Pli1 target proteins. Integration of the *pcn1-3R* mutant with GFP-tagged *rad22* strain did not result in a change in Rad22 foci formation in MMS treated cells, however *pli1-d, rad22-d* double mutants have proven to be inviable (Xhemalce et al, 2004a).

7.7 *pcn1* lysine to arginine mutants are defective in Cds1 phosphorylation.

Interestingly, Cds1 phosphorylation is reduced in both *pcn1-K164R* and *pcn1-3R* mutants, specifically in response to MMS (Figure 6.16), whereas Chk1 phosphorylation in response to IR is not (Figure 6.15). This indicates that PCNA modification by ubiquitin and/or SUMO contributes to phosphorylation of Cds1 and activation of the intra-S phase checkpoint. Analysis of an *rhp18-d* mutant which is defective in ubiquitination of PCNA but not SUMOylation would give insight into which modification is required for wild type levels of Cds1 phosphorylation. The generation of a *rad3-d* double mutant with both *pcn1* mutants would also be interesting to analyse. This has not been attempted due to time constraints but may result in lethality. S-phase checkpoint signalling results from an increase in ssDNA and involves RPA. The *pcn1-3R* mutants was crossed with GFP-tagged rad11 in order to investigate whether an inability to SUMOylate PCNA affects RPA foci. Interestingly, tetrad analysis demonstrated that these double mutants were not viable, suggesting that RPA function is essential in *pcn1-3R* cells. This data suggests that modification of PCNA contributes to Cds1 phosphorylation in a pathway that is specific to MMS-induced DNA damage, however further investigation is required in order uncover other components which may be involved or recruited following PCNA modification (Figure 7.3).

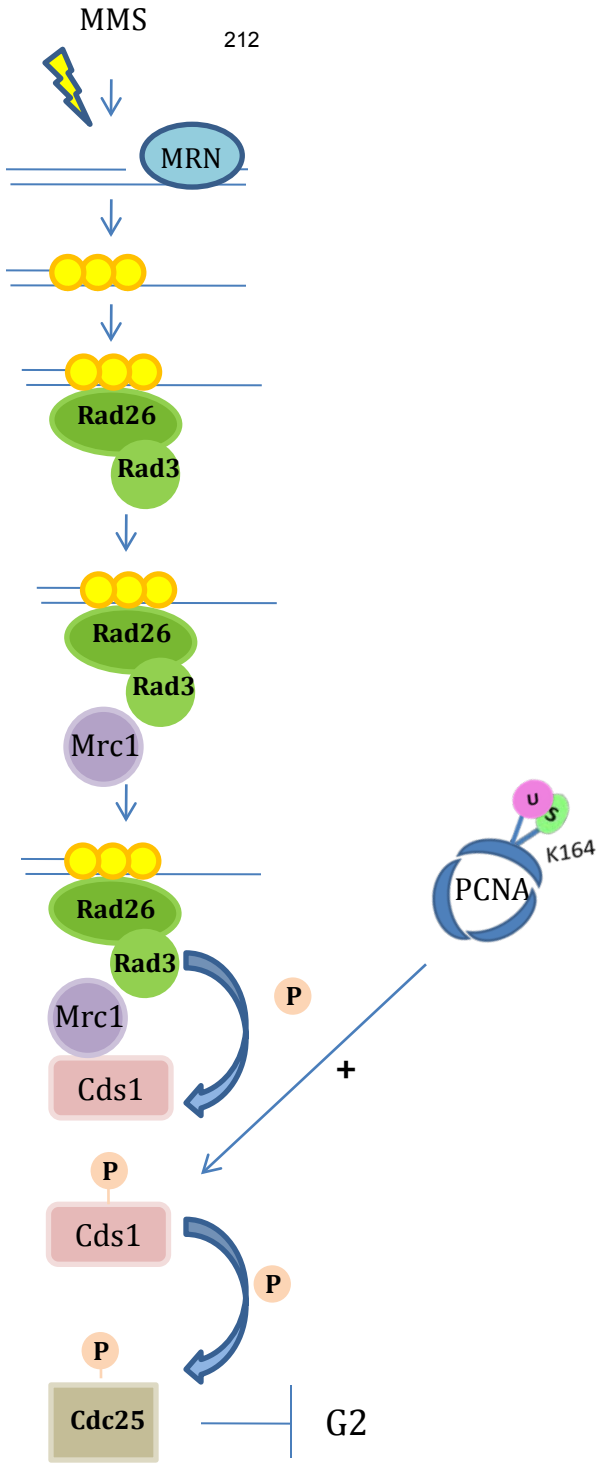

Figure 7.3. Modification of PCNA contributes to Cds1 phosphorylation in response to MMS

Processing of MMS-induced DNA damage involves resection of the DNA, possibly involving the MRN complex if closely apposed single strand breaks are converted to double strand breaks. Resected DNA is bound by RPA, which recruits Rad26 and Rad3. Rad3 recruits Mrc1, which in turn recruits Cds1, bringing it in close proximity to Rad3. Rad3 phosphorylates Cds1, which subsequently phosphorylates and inhibits Cdc25, leading to cell cycle arrest to allow time for the damage to be repaired. Cds1 phosphorylation was severely impaired in the *pcn1-K164R* and *pcn1-3R* mutants. This suggests that modification of PCNA contributes to Cds1 phosphorylation in an unknown pathway, which is specific in response to MMS induced DNA damage.

8 References

Ahmad F, Stewart E (2005) The N-terminal region of the Schizosaccharomyces pombe RecQ helicase, Rqh1p, physically interacts with Topoisomerase III and is required for Rqh1p function. *Molecular Genetics and Genomics* **273:** 102-114

Akamatsu Y, Tsutsui Y, Morishita T, Siddique MDSP, Kurokawa Y, Ikeguchi M, Yamao F, Arcangioli B, Iwasaki H (2007) *Fission yeast Swi5/Sfr1 and Rhp55/Rhp57 differentially regulate Rhp51-dependent recombination outcomes*, Vol. 26.

al-Khodairy F, Enoch T, Hagan I, Carr A (1995) The Schizosaccharomyces pombe hus5 gene encodes a ubiquitin conjugating enzyme required for normal mitosis. *J Cell Sci* **108:** 475-486

Alao JP, Sunnerhagen P (2008) Rad3 and Sty1 function in Schizosaccharomyces pombe: an integrated response to DNA damage and environmental stress? *Molecular Microbiology* **68:** 246-254

Albuquerque CP, Wang G, Lee NS, Kolodner RD, Putnam CD, Zhou H (2013) Distinct SUMO Ligases Cooperate with Esc2 and Slx5 to Suppress Duplication-Mediated Genome Rearrangements. *PLoS Genet* **9:** e1003670

Alkuraya FS, Saadi I, Lund JJ, Turbe-Doan A, Morton CC, Maas RL (2006) SUMO1 Haploinsufficiency Leads to Cleft Lip and Palate. *Science* **313:** 1751

Alleva JL, Doetsch PW (1998) Characterization of Schizosaccharomyces pombe Rad2 protein, a FEN-1 homolog. *Nucleic Acids Res* **26:** 3645-3650

Alleva JL, Zuo S, Hurwitz J, Doetsch PW (2000) In Vitro Reconstitution of the Schizosaccharomyces pombe Alternative Excision Repair Pathway†. *Biochemistry* **39:** 2659-2666

Ampatzidou E, Irmisch A, O'Connell MJ, Murray JM (2006) Smc5/6 Is Required for Repair at Collapsed Replication Forks. *Mol Cell Biol* **26:** 9387-9401

Andres SN, Vergnes A, Ristic D, Wyman C, Modesti M, Junop M (2012) A human XRCC4–XLF complex bridges DNA. *Nucleic Acids Research* **40:** 1868-1878

Andrews EA, Palecek J, Sergeant J, Taylor E, Lehmann AR, Watts FZ (2005) Nse2, a Component of the Smc5-6 Complex, Is a SUMO Ligase Required for the Response to DNA Damage. *Mol Cell Biol* **25:** 185-196

Arakawa H, Moldovan G-L, Saribasak H, Saribasak NN, Jentsch S, Buerstedde J-M (2006) A Role for PCNA Ubiquitination in Immunoglobulin Hypermutation. *PLoS Biol* **4:** e366

Armstrong AA, Mohideen F, Lima CD (2012) Recognition of SUMO-modified PCNA requires tandem receptor motifs in Srs2. *Nature* **483:** 59-63

Aspinwall R, Rothwell DG, Roldan-Arjona T, Anselmino C, Ward CJ, Cheadle JP, Sampson JR, Lindahl T, Harris PC, Hickson ID (1997) Cloning and characterization of a functional human homolog of Escherichia coli endonuclease III. *Proceedings of the National Academy of Sciences of the United States of America* **94:** 109-114

Atkinson J, McGlynn P (2009) Replication fork reversal and the maintenance of genome stability. *Nucleic Acids Research* **37:** 3475-3492

Ball LG, Hanna MD, Lambrecht AD, Mitchell BA, Ziola B, Cobb JA, Xiao W (2014) The Mre11-Rad50-Xrs2 Complex Is Required for Yeast DNA Postreplication Repair. *PLoS ONE* **9:** e109292

Bando M, Katou Y, Komata M, Tanaka H, Itoh T, Sutani T, Shirahige K (2009) Csm3, Tof1, and Mrc1 form a heterotrimeric mediator complex that associates with DNA replication forks. *J Biol Chem* **284:** 34355-34365

Barlow C, Hirotsune S, Paylor R, Liyanage M, Eckhaus M, Collins F, Shiloh Y, Crawley JN, Ried T, Tagle D, Wynshaw-Boris A (1996) Atm-Deficient Mice: A Paradigm of Ataxia Telangiectasia. *Cell* **86:** 159-171

Bartek J, Lukas J (2001) Mammalian G1- and S-phase checkpoints in response to DNA damage. *Current Opinion in Cell Biology* **13:** 738-747

Bass KL, Murray JM, O'Connell MJ (2012) Brc1-dependent recovery from replication stress. *Journal of Cell Science* **125:** 2753-2764

Batty DP, Wood RD (2000) Damage recognition in nucleotide excision repair of DNA. *Gene* **241:** 193-204

Baum B, Nishitani H, Yanow S, Nurse P (1998) *Cdc18 transcription and proteolysis couple S phase to passage through mitosis*, Vol. 17.

Bayer PA, Andreas; Metzger, Susanne; Mahajan, Rohit; Melchior, Frauke; Jaenicke, Rainer; Becker, Jörg (1998) Structure determination of the small ubiquitin-related modifier SUMO-1. *Journal of Molecular Biology* **280:** 275-286

Bencsath KP, Podgorski MS, Pagala VR, Slaughter CA, Schulman BA (2002) Identification of a Multifunctional Binding Site on Ubc9p Required for Smt3p Conjugation. *Journal of Biological Chemistry* **277:** 47938-47945

Benito J, Martín-Castellanos C, Moreno S (1998) *Regulation of the G1 phase of the cell cycle by periodic stabilization and degradation of the p25rum1 CDK inhibitor*, Vol. 17.

Bermudez VP, Lindsey-Boltz LA, Cesare AJ, Maniwa Y, Griffith JD, Hurwitz J, Sancar A (2003) Loading of the human 9-1-1 checkpoint complex onto DNA by the checkpoint clamp loader hRad17-replication factor C complex in vitro. *Proceedings of the National Academy of Sciences* **100:** 1633-1638

Beucher A, Birraux J, Tchouandong L, Barton O, Shibata A, Conrad S, Goodarzi AA, Krempler A, Jeggo PA, Lobrich M (2009) ATM and Artemis promote homologous recombination of radiation-induced DNA double-strand breaks in G2. *EMBO J* **28:** 3413-3427

Boddy MN, Furnari B, Mondesert O, Russell P (1998) Replication Checkpoint Enforced by Kinases Cds1 and Chk1. *Science* **280:** 909-912

Boddy MN, Shanahan P, McDonald WH, Lopez-Girona A, Noguchi E, Yates III JR, Russell P (2003) Replication Checkpoint Kinase Cds1 Regulates Recombinational Repair Protein Rad60. *Molecular and Cellular Biology* **23:** 5939-5946

Bowman GD, O'Donnell M, Kuriyan J (2004) Structural analysis of a eukaryotic sliding DNA clamp-clamp loader complex. *Nature* **429:** 724-730

Bowman KK, Sidik K, Smith CA, Taylor J-S, Doetsch PW, Freyer GA (1994) A new ATP-independent DNA endonuclease from Schizosaccharomyces pombe that recognizes cyclobutane pyrimidine dimers and 6–4 photoproducts. *Nucleic Acids Research* **22:** 3026-3032

Boyd LK, Mercer B, Thompson D, Main E, Watts FZ (2010) Characterisation of the SUMO-Like Domains of <italic>Schizosaccharomyces pombe</italic> Rad60. *PLoS ONE* **5:** e13009

Branzei D, Foiani M (2010) Maintaining genome stability at the replication fork. *Nat Rev Mol Cell Biol* **11:** 208-219

Branzei D, Seki M, Enomoto T (2004) Rad18/Rad5/Mms2-mediated polyubiquitination of PCNA is implicated in replication completion during replication stress. *Genes Cells* **9:** 1031-1042

Branzei D, Sollier J, Liberi G, Zhao X, Maeda D, Seki M, Enomoto T, Ohta K, Foiani M (2006) Ubc9- and Mms21-Mediated Sumoylation Counteracts Recombinogenic Events at Damaged Replication Forks. *Cell* **127:** 509-522

Brill SJ, Stillman B (1989) Yeast replication factor-A functions in the unwinding of the SV40 origin of DNA replication. *Nature* **342:** 92-95

Brizuela L, Draetta G, Beach D (1987) p13suc1 acts in the fission yeast cell division cycle as a component of the p34cdc2 protein kinase. *EMBO J* **6:** 3507-3514

Broach JR, Li Y-Y, Feldman J, Jayaram M, Abraham J, Nasmyth KA, Hicks JB (1983) Localization and Sequence Analysis of Yeast Origins of DNA Replication. *Cold Spring Harbor Symposia on Quantitative Biology* **47:** 1165-1173

Brondello J-M, Boddy MN, Furnari B, Russell P (1999) Basis for the Checkpoint Signal Specificity That Regulates Chk1 and Cds1 Protein Kinases. *Molecular and Cellular Biology* **19:** 4262-4269

Brooks CL, Gu W (2011) P53 regulation by ubiquitin. *FEBS Letters* **585:** 2803-2809

Bruning JB, Shamoo Y (2004) Structural and thermodynamic analysis of human PCNA with peptides derived from DNA polymerase-delta p66 subunit and flap endonuclease-1. *Structure* **12:** 2209-2219

Bryans M, Valenzano MC, Stamato TD (1999) Absence of DNA ligase IV protein in XR-1 cells: evidence for stabilization by XRCC4. *Mutation Research/DNA Repair* **433:** 53-58

Bustard DE, Menolfi D, Jeppsson K, Ball LG, Dewey SC, Shirahige K, Sjögren C, Branzei D, Cobb JA (2012) During Replication Stress, Non-Smc Element 5 (Nse5) Is Required for Smc5/6 Protein Complex Functionality at Stalled Forks. *Journal of Biological Chemistry* **287:** 11374-11383

Bylebyl GR, Belichenko I, Johnson ES (2003) The SUMO Isopeptidase Ulp2 Prevents Accumulation of SUMO Chains in Yeast. *Journal of Biological Chemistry* **278:** 44113-44120

Byun TS, Pacek M, Yee M-c, Walter JC, Cimprich KA (2005) Functional uncoupling of MCM helicase and DNA polymerase activities activates the ATR-dependent checkpoint. *Genes & Development* **19:** 1040-1052

Carr AM (1997) Control of cell cycle arrest by the Mec1sc/Rad3sp DNA structure checkpoint pathway. *Current Opinion in Genetics & Development* **7:** 93-98

Carr AM, Lambert S (2013) Replication Stress-Induced Genome Instability: The Dark Side of Replication Maintenance by Homologous Recombination. *Journal of Molecular Biology* **425:** 4733-4744

Carr AM, Paek AL, Weinert T (2011) DNA replication: Failures and inverted fusions. *Seminars in Cell & Developmental Biology* **22:** 866-874

Carr AM, Schmidt H, Kirchhoff S, Muriel WJ, Sheldrick KS, Griffiths DJ, Basmacioglu CN, Subramani S, Clegg M, Nasim A, et al. (1994) The rad16 gene of Schizosaccharomyces pombe: a homolog of the RAD1 gene of Saccharomyces cerevisiae. *Mol Cell Biol* **14:** 2029-2040

Caspari T, Dahlen M, Kanter-Smoler G, Lindsay HD, Hofmann K, Papadimitriou K, Sunnerhagen P, Carr AM (2000) Characterization of Schizosaccharomyces pombeHus1: a PCNA-Related Protein That Associates with Rad1 and Rad9. *Molecular and Cellular Biology* **20:** 1254-1262

Cavero S, Chahwan C, Russell P (2007) Xlf1 Is Required for DNA Repair by Nonhomologous End Joining in Schizosaccharomyces pombe. *Genetics* **175:** 963-967

Chau V, Tobias JW, Bachmair A, Marriott D, Ecker DJ, Gonda DK, Varshavsky A (1989) A multiubiquitin chain is confined to specific lysine in a targeted short-lived protein. *Science* **243:** 1576-1583

Chavez A, George V, Agrawal V, Johnson FB (2010) Sumoylation and the Structural Maintenance of Chromosomes (Smc) 5/6 Complex Slow Senescence through Recombination Intermediate Resolution. *Journal of Biological Chemistry* **285:** 11922-11930

Chen X, Paudyal SC, Chin RI, You Z (2013) PCNA promotes processive DNA end resection by Exo1. *Nucleic Acids Res* **41:** 9325-9338

Chiolo I, Saponaro M, Baryshnikova A, Kim J-H, Seo Y-S, Liberi G (2007) The Human F-Box DNA Helicase FBH1 Faces Saccharomyces cerevisiae Srs2 and Postreplication Repair Pathway Roles. *Molecular and Cellular Biology* **27:** 7439-7450

Christensen PU, Bentley NJ, Martinho RG, Nielsen O, Carr AM (2000) Mik1 levels accumulate in S phase and may mediate an intrinsic link between S phase and mitosis. *Proceedings of the National Academy of Sciences* **97:** 2579-2584

Claire Chappell LAH, Feridoun Karimi-Busheri, Michael Weinfeld, Stephen C. West (2002) *Involvement of human polynucleotide kinase in double-strand break repair by non-homologous end joining*, Vol. 21.

Cliby WA, Roberts CJ, Cimprich KA, Stringer CM, Lamb JR, Schreiber SL, Friend SH (1998) Overexpression of a kinase-inactive ATR protein causes sensitivity to DNA-damaging agents and defects in cell cycle checkpoints. *EMBO J* **17:** 159-169

Colavito S, Macris-Kiss M, Seong C, Gleeson O, Greene EC, Klein HL, Krejci L, Sung P (2009) Functional significance of the Rad51-Srs2 complex in Rad51 presynaptic filament disruption. *Nucleic Acids Research* **37:** 6754-6764

Correa-Bordes J, Gulli MP, Nurse P (1997) *p25rum1 promotes proteolysis of the mitotic B-cyclin p56cdc13 during G1 of the fission yeast cell cycle*, Vol. 16.

Coulon S, Gaillard PH, Chahwan C, McDonald WH, Yates JR, 3rd, Russell P (2004) Slx1-Slx4 are subunits of a structure-specific endonuclease that maintains ribosomal DNA in fission yeast. *Mol Biol Cell* **15:** 71-80

Coulon S, Ramasubramanyan S, Alies C, Philippin G, Lehmann A, Fuchs RP (2010) Rad8Rad5/Mms2-Ubc13 ubiquitin ligase complex controls translesion synthesis in fission yeast. *EMBO J* **29:** 2048-2058

Cremona Catherine A, Sarangi P, Yang Y, Hang Lisa E, Rahman S, Zhao X (2012) Extensive DNA Damage-Induced Sumoylation Contributes to Replication and Repair and Acts in Addition to the Mec1 Checkpoint. *Molecular Cell* **45:** 422-432

Datta AB, Hura GL, Wolberger C (2009) The Structure and Conformation of Lys63-Linked Tetraubiquitin. *Journal of Molecular Biology* **392:** 1117-1124

de Klein A, Muijtjens M, van Os R, Verhoeven Y, Smit B, Carr AM, Lehmann AR, Hoeijmakers JHJ (2000) Targeted disruption of the cell-cycle checkpoint gene ATR leads to early embryonic lethality in mice. *Current Biology* **10:** 479-482

de Laat WL, Jaspers NGJ, Hoeijmakers JHJ (1999) Molecular mechanism of nucleotide excision repair. *Genes & Development* **13:** 768-785

De Piccoli G, Cortes-Ledesma F, Ira G, Torres-Rosell J, Uhle S, Farmer S, Hwang J-Y, Machin F, Ceschia A, McAleenan A, Cordon-Preciado V, Clemente-Blanco A, Vilella-Mitjana F, Ullal P, Jarmuz A, Leitao B, Bressan D, Dotiwala F, Papusha A, Zhao X, Myung K, Haber JE, Aguilera A, Aragon L (2006) Smc5-Smc6 mediate DNA double-strand-break repair by promoting sister-chromatid recombination. *Nat Cell Biol* **8:** 1032-1034

Deshaies RJ, Joazeiro CAP (2009) RING Domain E3 Ubiquitin Ligases. *Annual Review of Biochemistry* **78:** 399-434

Desterro JMP, Rodriguez MS, Hay RT (1998) SUMO-1 Modification of IκBα Inhibits NF-κB Activation. *Molecular Cell* **2:** 233-239

Desterro JMPT, Jill; Hay, Ronald T (1997) Ubch9 conjugates SUMO but not ubiquitin. *FEBS Letters* **417:** 297-300

Dianova II, Bohr VA, Dianov GL (2001) Interaction of Human AP Endonuclease 1 with Flap Endonuclease 1 and Proliferating Cell Nuclear Antigen Involved in Long-Patch Base Excision Repair. *Biochemistry* **40:** 12639-12644

Diffley JFX (2004) Regulation of Early Events in Chromosome Replication. *Current Biology* **14:** R778-R786

Ding L, Forsburg SL (2014) Essential Domains of Schizosaccharomyces pombe Rad8 Required for DNA Damage Response. *G3 (Bethesda)*

Dou H, Huang C, Singh M, Carpenter PB, Yeh ETH (2010) Regulation of DNA Repair through DeSUMOylation and SUMOylation of Replication Protein A Complex. *Molecular Cell* **39:** 333-345

Doyle JM, Gao J, Wang J, Yang M, Potts PR (2010) MAGE-RING Protein Complexes Comprise a Family of E3 Ubiquitin Ligases. *Molecular Cell* **39:** 963-974

Duan X, Sarangi P, Liu X, Rangi GK, Zhao X, Ye H (2009a) Structural and Functional Insights into the Roles of the Mms21 Subunit of the Smc5/6 Complex. *Molecular Cell* **35:** 657-668

Duan X, Yang Y, Chen Y-H, Arenz J, Rangi GK, Zhao X, Ye H (2009b) Architecture of the Smc5/6 Complex of Saccharomyces cerevisiae Reveals a Unique Interaction between the Nse5-6 Subcomplex and the Hinge Regions of Smc5 and Smc6. *Journal of Biological Chemistry* **284:** 8507-8515

Duda DM, van Waardenburg RCAM, Borg LA, McGarity S, Nourse A, Waddell MB, Bjornsti M-A, Schulman BA (2007) Structure of a SUMO-binding-motif Mimic Bound to Smt3p–Ubc9p: Conservation of a Non-covalent Ubiquitin-like Protein–E2 Complex as a Platform for Selective Interactions within a SUMO Pathway. *Journal of Molecular Biology* **369:** 619-630

Dunphy WG, Kumagai A (1991) The cdc25 protein contains an intrinsic phosphatase activity. *Cell* **67:** 189-196

Eddins MJ, Varadan R, Fushman D, Pickart CM, Wolberger C (2007) Crystal Structure and Solution NMR Studies of Lys48-linked Tetraubiquitin at Neutral pH. *Journal of Molecular Biology* **367:** 204-211

Edwards RJ, Bentley NJ, Carr AM (1999) A Rad3-Rad26 complex responds to DNA damage independently of other. *nat Cell Biol* **1:** 393-398

Erdile LF, Heyer WD, Kolodner R, Kelly TJ (1991) Characterization of a cDNA encoding the 70-kDa single-stranded DNA-binding subunit of human replication protein A and the role of the protein in DNA replication. *J Biol Chem* **266:** 12090-12098

Errico A, Cosentino C, Rivera T, Losada A, Schwob E, Hunt T, Costanzo V (2009) Tipin/Tim1/And1 protein complex promotes Pol alpha chromatin binding and sister chromatid cohesion. *EMBO J* **28:** 3681-3692

Evans T, Rosenthal ET, Youngblom J, Distel D, Hunt T (1983) Cyclin: A protein specified by maternal mRNA in sea urchin eggs that is destroyed at each cleavage division. *Cell* **33:** 389-396

Ferguson DO, Holloman WK (1996) Recombinational repair of gaps in DNA is asymmetric in Ustilago maydis and can be explained by a migrating D-loop model. *Proceedings of the National Academy of Sciences of the United States of America* **93:** 5419-5424

Fortini P, Dogliotti E (2007) Base damage and single-strand break repair: Mechanisms and functional significance of short- and long-patch repair subpathways. *DNA repair* **6:** 398-409

Frampton J, Irmisch A, Green CM, Neiss A, Trickey M, Ulrich HD, Furuya K, Watts FZ, Carr AM, Lehmann AR (2006) Postreplication Repair and PCNA Modification in Schizosaccharomyces pombe. *Molecular Biology of the Cell* **17:** 2976-2985

Freudenthal BD, Brogie JE, Gakhar L, Kondratick CM, Washington MT (2011) Crystal Structure of SUMO-Modified Proliferating Cell Nuclear Antigen. *Journal of Molecular Biology* **406:** 9-17

Friedberg EC (2005) Suffering in silence: the tolerance of DNA damage. *Nat Rev Mol Cell Biol* **6:** 943-953

Furuya K, Carr AM (2003) DNA checkpoints in fission yeast. *Journal of Cell Science* **116:** 3847-3848

Furuya K, Poitelea M, Guo L, Caspari T, Carr AM (2004) Chk1 activation requires Rad9 S/TQ-site phosphorylation to promote association with C-terminal BRCT domains of Rad4TOPBP1. *Genes Dev* **18:** 1154-1164

Galanty Y, Belotserkovskaya R, Coates J, Polo S, Miller KM, Jackson SP (2009) Mammalian SUMO E3-ligases PIAS1 and PIAS4 promote responses to DNA double-strand breaks. *nature* **462:** 935-939

Gali H, Juhasz S, Morocz M, Hajdu I, Fatyol K, Szukacsov V, Burkovics P, Haracska L (2012a) Role of SUMO modification of human PCNA at stalled replication fork. *Nucleic Acids Research*

Gali H, Juhasz S, Morocz M, Hajdu I, Fatyol K, Szukacsov V, Burkovics P, Haracska L (2012b) Role of SUMO modification of human PCNA at stalled replication fork. *Nucleic Acids Research* **40:** 6049-6059

Garcia V, Phelps SEL, Gray S, Neale MJ (2011) Bidirectional resection of DNA double-strand breaks by Mre11 and Exo1. *Nature* **479:** 241-244

Gary R, Ludwig DL, Cornelius HL, MacInnes MA, Park MS (1997) The DNA repair endonuclease XPG binds to proliferating cell nuclear antigen (PCNA) and shares sequence elements with the PCNA-binding regions of FEN-1 and cyclin-dependent kinase inhibitor p21. *J Biol Chem* **272:** 24522-24529

Goodarzi AA, Jeggo PA (2013) Chapter One - The Repair and Signaling Responses to DNA Double-Strand Breaks. In *Advances in Genetics*, Theodore Friedmann JCD, Stephen FG (eds), Vol. Volume 82, pp 1-45. Academic Press

Goulian M, Richards SH, Heard CJ, Bigsby BM (1990) Discontinuous DNA synthesis by purified mammalian proteins. *Journal of Biological Chemistry* **265:** 18461-18471

Groth P, Ausländer S, Majumder MM, Schultz N, Johansson F, Petermann E, Helleday T (2010) Methylated DNA Causes a Physical Block to Replication Forks Independently of Damage Signalling, O6-Methylguanine or DNA Single-Strand Breaks and Results in DNA Damage. *Journal of Molecular Biology* **402:** 70-82

Guerineau M, Kriz Z, Kozakova L, Bednarova K, Janos P, Palecek J (2012) Analysis of the Nse3/MAGE-Binding Domain of the Nse4/EID Family Proteins. *PLoS ONE* **7:** e35813

Gulbis JM, Kelman Z, Hurwitz J, O'Donnell M, Kuriyan J (1996) Structure of the C-Terminal Region of p21WAF1/CIP1 Complexed with Human PCNA. *Cell* **87:** 297-306

Guo DL, Manyu; Zhang, Yan; Yang, Ping; Eckenrode, Sarah; Hopkins, Diane; Zheng, Weipeng; Purohit, Sharad; Podolsky, Robert H; Muir, Andrew; Wang, Jinzhao; Dong, Zheng; Brusko, Todd; Atkinson, Mark; Pozzilli, Paolo; Zeidler, Adina; Raffel, Leslie J; Jacob, Chaim O; Park, Yongsoo; Serrano-Rios, Manuel; Larrad, Maria T Martinez; Zhang, Zixin; Garchon, Henri-Jean; Bach, Jean-Francois; Rotter, Jerome I; She, Jin-Xiong; Wang, Cong-Yi (2004) A functional variant of SUMO4, a new I[kappa]B[alpha] modifier, is associated with type 1 diabetes. *Nature Genetics* **36:** 837-841

Haas AL, Rose IA (1982) The mechanism of ubiquitin activating enzyme. A kinetic and equilibrium analysis. *Journal of Biological Chemistry* **257:** 10329-10337

Hannich JT, Lewis A, Kroetz MB, Li SJ, Heide H, Emili A, Hochstrasser M (2005) Defining the SUMO-modified proteome by multiple approaches in Saccharomyces cerevisiae. *J Biol Chem* **280:** 4102-4110

Haracska L, Torres-Ramos CA, Johnson RE, Prakash S, Prakash L (2004) Opposing Effects of Ubiquitin Conjugation and SUMO Modification of PCNA on Replicational Bypass of DNA Lesions in Saccharomyces cerevisiae. *Molecular and Cellular Biology* **24:** 4267-4274

Hardeland U, Steinacher R, Jiricny J, Schär P (2002) *Modification of the human thymine-DNA glycosylase by ubiquitin-like proteins facilitates enzymatic turnover*, Vol. 21.

Hari KL, Cook KR, Karpen GH (2001) The Drosophila Su(var)2-10 locus regulates chromosome structure and function and encodes a member of the PIAS protein family. *Genes Dev* **15:** 1334-1348

Harper JW (2001) Protein destruction: Adapting roles for Cks proteins. *Current Biology* **11:** R431-R435

Hartsuiker E, Neale MJ, Carr AM (2009) Distinct requirements for the Rad32(Mre11) nuclease and Ctp1(CtIP) in the removal of covalently bound topoisomerase I and II from DNA. *Mol Cell* **33:** 117-123

Haruta N, Kurokawa Y, Murayama Y, Akamatsu Y, Unzai S, Tsutsui Y, Iwasaki H (2006) The Swi5-Sfr1 complex stimulates Rhp51/Rad51- and Dmc1-mediated DNA strand exchange in vitro. *Nat Struct Mol Biol* **13:** 823-830

Harvey S, Krien M, O'Connell M (2002) Structural maintenance of chromosomes (SMC) proteins, a family of conserved ATPases. *Genome Biology* **3:** reviews3003.3001 - reviews3003.3005

Hay RT (2005) SUMO: A History of Modification. *Molecular Cell* **18:** 1-12

Hay RT (2007) SUMO-specific proteases: a twist in the tail. *Trends in Cell Biology* **17:** 370-376

Hayden MS, Ghosh S (2008) Shared Principles in NF-κB Signaling. *Cell* **132:** 344-362

He F MY, Inoue M, Kigawa T, Shirouzu M, Tarada T, Yokoyama S. (2007) Solution structure of the sp-ring domain in non-smc element 2 homolog (Mms21, s. cerevisiae).
http://www.ncbi.nlm.nih.gov/Structure/mmdb/mmdbsrv.cgi?uid=59915.

Heideker J, Prudden J, Perry JJP, Tainer JA, Boddy MN (2011) SUMO-Targeted Ubiquitin Ligase, Rad60, and Nse2 SUMO Ligase Suppress Spontaneous Top1–Mediated DNA Damage and Genome Instability. *PLoS Genet* **7:** e1001320

Hirano T, Kobayashi R, Hirano M (1997) Condensins, Chromosome Condensation Protein Complexes Containing XCAP-C, XCAP-E and a Xenopus Homolog of the Drosophila Barren Protein. *Cell* **89:** 511-521

Ho C-W, Chen H-T, Hwang J (2011) UBC9 Autosumoylation Negatively Regulates Sumoylation of Septins in Saccharomyces cerevisiae. *Journal of Biological Chemistry* **286:** 21826-21834

Ho JCY, Warr NJ, Shimizu H, Watts FZ (2001) SUMO modification of Rad22, the Schizosaccharomyces pombe homologue of the recombination protein Rad52. *Nucleic Acids Research* **29:** 4179-4186

Hochstrasser M (2001) SP-RING for SUMO: New Functions Bloom for a Ubiquitin-like Protein. *Cell* **107:** 5-8

Hock AK, Vigneron AM, Carter S, Ludwig RL, Vousden KH (2011) *Regulation of p53 stability and function by the deubiquitinating enzyme USP42*, Vol. 30.

Hoege C, Pfander B, Moldovan G-L, Pyrowolakis G, Jentsch S (2002) RAD6-dependent DNA repair is linked to modification of PCNA by ubiquitin and SUMO. *Nature* **419:** 135-141

Holmes AM, Haber JE (1999) Double-strand break repair in yeast requires both leading and lagging strand DNA polymerases. *Cell* **96:** 415-424

Hope JC, Cruzata LD, Duvshani A, Mitsumoto J, Maftahi M, Freyer GA (2007) Mus81-Eme1-Dependent and -Independent Crossovers Form in Mitotic Cells during Double-Strand Break Repair in Schizosaccharomyces pombe. *Molecular and Cellular Biology* **27:** 3828-3838

Huang JC, Svoboda DL, Reardon JT, Sancar A (1992) Human nucleotide excision nuclease removes thymine dimers from DNA by incising the 22nd phosphodiester bond 5' and the 6th phosphodiester bond 3' to the photodimer. *Proceedings of the National Academy of Sciences* **89:** 3664-3668

Hudson JJR, Bednarova K, Kozakova L, Liao C, Guerineau M, Colnaghi R, Vidot S, Marek J, Bathula SR, Lehmann AR, Palecek J (2011) Interactions between the Nse3 and Nse4 Components of the SMC5-6 Complex Identify Evolutionarily Conserved Interactions between MAGE and EID Families. *PLoS ONE* **6:** e17270

Ip SC, Rass U, Blanco MG, Flynn HR, Skehel JM, West SC (2008) Identification of Holliday junction resolvases from humans and yeast. *Nature* **456:** 357-361

Iraqui I, Chekkal Y, Jmari N, Pietrobon V, Fréon K, Costes A, Lambert SAE (2012) Recovery of Arrested Replication Forks by Homologous Recombination Is Error-Prone. *PLoS Genet* **8:** e1002976

Irmisch A, Ampatzidou E, Mizuno Ki, O'Connell MJ, Murray JM (2009) Smc5/6 maintains stalled replication forks in a recombination-competent conformation. *EMBO J* **28:** 144-155

Ivanov I, Chapados BR, McCammon JA, Tainer JA (2006) Proliferating cell nuclear antigen loaded onto double-stranded DNA: dynamics, minor groove interactions and functional implications. *Nucleic Acids Research* **34:** 6023-6033

Iwai K (2014) Diverse roles of the ubiquitin system in NF-κB activation. *Biochimica et Biophysica Acta (BBA) - Molecular Cell Research* **1843:** 129-136

Iyama T, Wilson Iii DM (2013) DNA repair mechanisms in dividing and non-dividing cells. *DNA repair* **12:** 620-636

Jentsch S, McGrath JP, Varshavsky A (1987) The yeast DNA repair gene RAD6 encodes a ubiquitin-conjugating enzyme. *Nature* **329:** 131-134

Jin L, Williamson A, Banerjee S, Philipp I, Rape M (2008) Mechanism of Ubiquitin-Chain Formation by the Human Anaphase-Promoting Complex. *Cell* **133:** 653-665

Johnson ES (2004) PROTEIN MODIFICATION BY SUMO. *Annual Review of Biochemistry* **73:** 355-382

Johnson ES, Blobel G (1997) Ubc9p Is the Conjugating Enzyme for the Ubiquitin-like Protein Smt3p. *Journal of Biological Chemistry* **272:** 26799-26802

Johnson ES, Schwienhorst I, Dohmen RJ, Blobel G (1997) *The ubiquitin-like protein Smt3p is activated for conjugation to other proteins by an Aos1p/Uba2p heterodimer*, Vol. 16.

Jonsson ZO, Hindges R, Hubscher U (1998) Regulation of DNA replication and repair proteins through interaction with the front side of proliferating cell nuclear antigen. *EMBO J* **17:** 2412-2425

Kagey MH, Melhuish TA, Wotton D (2003) The polycomb protein Pc2 is a SUMO E3. *Cell* **113:** 127-137

Kannouche PL, Lehmann AR (2004) Ubiquitination of PCNA and the Polymerase Switch in Human Cells. *Cell Cycle* **3:** 1009-1011

Katou Y, Kanoh Y, Bando M, Noguchi H, Tanaka H, Ashikari T, Sugimoto K, Shirahige K (2003) S-phase checkpoint proteins Tof1 and Mrc1 form a stable replication-pausing complex. *Nature* **424:** 1078-1083

Kearsey SE, Montgomery S, Labib K, Lindner K (2000) *Chromatin binding of the fission yeast replication factor mcm4 occurs during anaphase and requires ORC and cdc18*, Vol. 19.

Kedar PS, Kim S-J, Robertson A, Hou E, Prasad R, Horton JK, Wilson SH (2002) Direct Interaction between Mammalian DNA Polymerase β and Proliferating Cell Nuclear Antigen. *Journal of Biological Chemistry* **277:** 31115-31123

Kegel A, Sjögren C (2010) The Smc5/6 Complex: More Than Repair? *Cold Spring Harbor Symposia on Quantitative Biology* **75:** 179-187

Kelley LA, Sternberg MJ (2009) Protein structure prediction on the Web: a case study using the Phyre server. *Nature protocols* **4:** 363-371

Kirkpatrick DS, Hathaway NA, Hanna J, Elsasser S, Rush J, Finley D, King RW, Gygi SP (2006) Quantitative analysis of in vitro ubiquitinated cyclin B1 reveals complex chain topology. *Nat Cell Biol* **8:** 700-710

Klug H, Xaver M, Chaugule Viduth K, Koidl S, Mittler G, Klein F, Pichler A (2013) Ubc9 Sumoylation Controls SUMO Chain Formation and Meiotic Synapsis in Saccharomyces cerevisiae. *Molecular Cell*

Knipscheer P, Flotho A, Klug H, Olsen JV, van Dijk WJ, Fish A, Johnson ES, Mann M, Sixma TK, Pichler A (2008) Ubc9 Sumoylation Regulates SUMO Target Discrimination. *Molecular Cell* **31:** 371-382

Kolesar P, Sarangi P, Altmannova V, Zhao X, Krejci L (2012) Dual roles of the SUMO-interacting motif in the regulation of Srs2 sumoylation. *Nucleic Acids Research*

Komander D (2009) The emerging complexity of protein ubiquitination. *Biochem Soc Trans* **37:** 937-953

Komander D, Rape M (2012) The Ubiquitin Code. *Annual Review of Biochemistry* **81:** 203-229

Komander D, Reyes-Turcu F, Licchesi JD, Odenwaelder P, Wilkinson KD, Barford D (2009) Molecular discrimination of structurally equivalent Lys 63-linked and linear polyubiquitin chains. *EMBO Rep* **10:** 466-473

Kranz A-L, Jiao C-Y, Winterkorn L, Albritton S, Kramer M, Ercan S (2013) Genome-wide analysis of condensin binding in Caenorhabditis elegans. *Genome Biology* **14:** R112

Krejci L, Altmannova V, Spirek M, Zhao X (2012) Homologous recombination and its regulation. *Nucleic Acids Res* **40:** 5795-5818

Krejci L, Van Komen S, Li Y, Villemain J, Reddy MS, Klein H, Ellenberger T, Sung P (2003) DNA helicase Srs2 disrupts the Rad51 presynaptic filament. *Nature* **423:** 305-309

Krishna TSR, Kong X-P, Gary S, Burgers PM, Kuriyan J (1994) Crystal structure of the eukaryotic DNA polymerase processivity factor PCNA. *Cell* **79:** 1233-1243

Kubota T, Nishimura K, Kanemaki MT, Donaldson AD (2013) The Elg1 replication factor C-like complex functions in PCNA unloading during DNA replication. *Mol Cell* **50:** 273-280

Kumagai A, Dunphy WG (1991) The cdc25 protein controls tyrosine dephosphorylation of the cdc2 protein in a cell-free system. *Cell* **64:** 903-914

Kunz C, Fleck O (2001) Role of the DNA repair nucleases rad13, rad2 and uve1 of Schizosaccharomyces pombe in mismatch correction. *Journal of Molecular Biology* **313:** 241-253

Kurepa J, Walker JM, Smalle J, Gosink MM, Davis SJ, Durham TL, Sung D-Y, Vierstra RD (2003) The Small Ubiquitin-like Modifier (SUMO) Protein Modification System in Arabidopsis : ACCUMULATION OF SUMO1 AND -2 CONJUGATES IS INCREASED BY STRESS. *Journal of Biological Chemistry* **278:** 6862-6872

Kurokawa Y, Murayama Y, Haruta-Takahashi N, Urabe I, Iwasaki H (2008) Reconstitution of DNA strand exchange mediated by Rhp51 recombinase and two mediators. *PLoS Biol* **6:** e88

Kurosawa A, Adachi N (2010) Functions and Regulation of Artemis: A Goddess in the Maintenance of Genome Integrity. *Journal of Radiation Research* **51:** 503-509

Labib K, Tercero JA, Diffley JFX (2000) Uninterrupted MCM2-7 Function Required for DNA Replication Fork Progression. *Science* **288:** 1643-1647

Lambert S, Carr A (2013) Impediments to replication fork movement: stabilisation, reactivation and genome instability. *Chromosoma* **122:** 33-45

Lambert S, Mizuno Ki, Blaisonneau J, Martineau S, Chanet R, Fréon K, Murray JM, Carr AM, Baldacci G (2010) Homologous Recombination Restarts Blocked Replication Forks at the Expense of Genome Rearrangements by Template Exchange. *Molecular Cell* **39:** 346-359

Lambert S, Watson A, Sheedy DM, Martin B, Carr AM (2005) Gross Chromosomal Rearrangements and Elevated Recombination at an Inducible Site-Specific Replication Fork Barrier. *Cell* **121:** 689-702

Larsen CN, Krantz BA, Wilkinson KD (1998) Substrate Specificity of Deubiquitinating Enzymes: Ubiquitin C-Terminal Hydrolases†. *Biochemistry* **37:** 3358-3368

Lavin MF, Shiloh Y (1997) THE GENETIC DEFECT IN ATAXIA-TELANGIECTASIA. *Annual Review of Immunology* **15:** 177-202

Leach CA, Michael WM (2005a) Ubiquitin/SUMO modification of PCNA promotes replication fork progression in Xenopus laevis egg extracts. *The Journal of Cell Biology* **171:** 947-954

Leach CA, Michael WM (2005b) Ubiquitin/SUMO modification of PCNA promotes replication fork progression in Xenopus laevis egg extracts. *J Cell Biol* **171:** 947-954

Lee SE, Bressan DA, Petrini JH, Haber JE (2002) Complementation between N-terminal Saccharomyces cerevisiae mre11 alleles in DNA repair and telomere length maintenance. *DNA repair* **1:** 27-40

Lehmann A, Walicka M, Griffiths D, Murray J, Watts F, McCready S, Carr A (1995) The rad18 gene of Schizosaccharomyces pombe defines a new subgroup of the SMC superfamily involved in DNA repair. *Mol Cell Biol* **15:** 7067-7080

Lehmann AR (2003) DNA repair-deficient diseases, xeroderma pigmentosum, Cockayne syndrome and trichothiodystrophy. *Biochimie* **85:** 1101-1111

Lei M, Tye BK (2001) Initiating DNA synthesis: from recruiting to activating the MCM complex. *Journal of Cell Science* **114:** 1447-1454

Leman A, Noguchi E (2013) The Replication Fork: Understanding the Eukaryotic Replication Machinery and the Challenges to Genome Duplication. *Genes* **4:** 1-32

Lewis LK, Karthikeyan G, Westmoreland JW, Resnick MA (2002) Differential suppression of DNA repair deficiencies of Yeast rad50, mre11 and xrs2 mutants by EXO1 and TLC1 (the RNA component of telomerase). *Genetics* **160:** 49-62

Li J-j, Schnick J, Hayles J, MacNeill SA (2011) Purification and functional inactivation of the fission yeast MCMMCM–BP complex. *FEBS Letters* **585:** 3850-3855

Li J, Coïc E, Lee K, Lee C-S, Kim J-A, Wu Q, Haber JE (2012) Regulation of Budding Yeast Mating-Type Switching Donor Preference by the FHA Domain of Fkh1. *PLoS Genet* **8:** e1002630

Li S-JH, Mark (1999) A new protease required for cell-cycle progression in yeast. *Nature* **398:** 246-251

Li X, Heyer W-D (2008) Homologous recombination in DNA repair and DNA damage tolerance. *Nature* **18**

Lin X, Sun B, Liang M, Liang YY, Gast A, Hildebrand J, Brunicardi FC, Melchior F, Feng XH (2003) Opposed regulation of corepressor CtBP by SUMOylation and PDZ binding. *Molecular Cell* **11:** 1389-1396

Lindroos HB, Ström L, Itoh T, Katou Y, Shirahige K, Sjögren C (2006) Chromosomal Association of the Smc5/6 Complex Reveals that It Functions in Differently Regulated Pathways. *Molecular Cell* **22:** 755-767

Lindsay HD, Griffiths DJF, Edwards RJ, Christensen PU, Murray JM, Osman F, Walworth N, Carr AM (1998) S-phase-specific activation of Cds1 kinase defines a subpathway of the checkpoint response in Schizosaccharomyces pombe. *Genes & Development* **12:** 382-395

Liu Y, Kao HI, Bambara RA (2004) Flap endonuclease 1: a central component of DNA metabolism. *Annu Rev Biochem* **73:** 589-615

Lois LM, Lima CD, Chua N-H (2003) Small Ubiquitin-Like Modifier Modulates Abscisic Acid Signaling in Arabidopsis. *The Plant Cell Online* **15:** 1347-1359

Lopez-Girona A, Furnari B, Mondesert O, Russell P (1999) Nuclear localization of Cdc25 is regulated by DNA damage and a 14-3-3 protein. *Nature* **397:** 172-175

Lygerou Z, Nurse P (1999) The fission yeast origin recognition complex is constitutively associated with chromatin and is differentially modified through the cell cycle. *Journal of Cell Science* **112:** 3703-3712

M J Matunis EC, and G Blobel (1996) A novel ubiquitin-like modification modulates the partitioning of the Ran-GTPase-activating protein RanGAP1 between the cytosol and the nuclear pore complex. . *J Cell Biol* **135:** 1457-1470

Ma W, Panduri V, Sterling JF, Van Houten B, Gordenin DA, Resnick MA (2009) The Transition of Closely Opposed Lesions to Double-Strand Breaks during Long-Patch Base Excision Repair Is Prevented by the Coordinated Action of DNA Polymerase δ and Rad27/Fen1. *Molecular and Cellular Biology* **29:** 1212-1221

Ma W, Westmoreland JW, Gordenin DA, Resnick MA (2011) Alkylation Base Damage Is Converted into Repairable Double-Strand Breaks and Complex Intermediates in G2 Cells Lacking AP Endonuclease. *PLoS Genet* **7:** e1002059

Ma W, Westmoreland JW, Resnick MA (2013) Homologous recombination rescues ssDNA gaps generated by nucleotide excision repair and reduced translesion DNA synthesis in yeast G2 cells. *Proceedings of the National Academy of Sciences of the United States of America* **110:** E2895-2904

Mahajan R, Delphin C, Guan T, Gerace L, Melchior F (1997) A Small Ubiquitin-Related Polypeptide Involved in Targeting RanGAP1 to Nuclear Pore Complex Protein RanBP2. *Cell* **88:** 97-107

Matic I, van Hagen M, Schimmel J, Macek B, Ogg SC, Tatham MH, Hay RT, Lamond AI, Mann M, Vertegaal ACO (2008) In Vivo Identification of Human Small Ubiquitin-like Modifier Polymerization Sites by High Accuracy Mass Spectrometry and an in Vitro to in Vivo Strategy. *Molecular & Cellular Proteomics* **7:** 132-144

Matsumoto M, Wickliffe K, Dong K, Yu C, Bosanac I, Bustos D, Phu L, Kirkpatrick D, Hymowitz S, Rape M, Kelley R, Dixit V (2010a) K11-linked polyubiquitination in cell cycle control revealed by a K11 linkage-specific antibody. *Molecular Cell* **39:** 477-484

Matsumoto ML, Wickliffe KE, Dong KC, Yu C, Bosanac I, Bustos D, Phu L, Kirkpatrick DS, Hymowitz SG, Rape M, Kelley RF, Dixit VM (2010b) K11-linked polyubiquitination in cell cycle control revealed by a K11 linkage-specific antibody. *Mol Cell* **39:** 477-484

McCready S, Carr AM, Lehmann AR (1993) Repair of cyclobutane pyrimidine dimers and 6-4 photoproducts in the fission yeast Schizosaccharomyces pombe. *Molecular Microbiology* **10:** 885-890

McCready SJ, Osman F, Yasui A (2000) Repair of UV damage in the fission yeast Schizosaccharomyces pombe. *Mutation Research/Fundamental and Molecular Mechanisms of Mutagenesis* **451:** 197-210

McDonald WH, Pavlova Y, Yates JR, Boddy MN (2003) Novel Essential DNA Repair Proteins Nse1 and Nse2 Are Subunits of the Fission Yeast Smc5-Smc6 Complex. *Journal of Biological Chemistry* **278:** 45460-45467

Meierhofer D, Wang X, Huang L, Kaiser P (2008) Quantitative Analysis of global Ubiquitination in HeLa Cells by Mass Spectrometry. *Journal of Proteome Research* **7:** 4566-4576

Meister P, Taddei A, Ponti A, Baldacci G, Gasser SM (2007) *Replication foci dynamics: replication patterns are modulated by S-phase checkpoint kinases in fission yeast*, Vol. 26.

Melchior F (2000) SUMO-NONCLASSICAL UBIQUITIN. *Annual Review of Cell and Developmental Biology* **16:** 591-626

Meluh PB, Koshland D (1995) Evidence that the MIF2 gene of Saccharomyces cerevisiae encodes a centromere protein with homology to the mammalian centromere protein CENP-C. *Molecular Biology of the Cell* **6:** 793-807

Memisoglu A, Samson L (2000) Base excision repair in yeast and mammals. *Mutation Research/Fundamental and Molecular Mechanisms of Mutagenesis* **451:** 39-51

Minty A, Dumont X, Kaghad M, Caput D (2000) Covalent modification of p73alpha by SUMO-1. Two-hybrid screening with p73 identifies novel SUMO-1-interacting proteins and a SUMO-1 interaction motif. *J Biol Chem* **275:** 36316-36323

Mirkin EV, Mirkin SM (2007) Replication Fork Stalling at Natural Impediments. *Microbiology and Molecular Biology Reviews* **71:** 13-35

Miyabe I, Morishita T, Shinagawa H, Carr AM (2009) Schizosaccharomyces pombe Cds1Chk2 regulates homologous recombination at stalled replication forks through the phosphorylation of recombination protein Rad60. *Journal of Cell Science* **122:** 3638-3643

Miyachi K, Fritzler MJ, Tan EM (1978) Autoantibody to a Nuclear Antigen in Proliferating Cells. *The Journal of Immunology* **121:** 2228-2234

Moldovan G-L, Dejsuphong D, Petalcorin Mark IR, Hofmann K, Takeda S, Boulton Simon J, D'Andrea Alan D (2012) Inhibition of Homologous Recombination by the PCNA-Interacting Protein PARI. *Molecular Cell* **45:** 75-86

Moldovan G-L, Pfander B, Jentsch S (2006) PCNA Controls Establishment of Sister Chromatid Cohesion during S Phase. *Molecular Cell* **23:** 723-732

Moldovan G-L, Pfander B, Jentsch S (2007) PCNA, the Maestro of the Replication Fork. *Cell* **129:** 665-679

Moon K-Y, Kong D, Lee J-K, Raychaudhuri S, Hurwitz J (1999) Identification and reconstitution of the origin recognition complex from Schizosaccharomyces pombe. *Proceedings of the National Academy of Sciences* **96:** 12367-12372

Morgan DO (1997) CYCLIN-DEPENDENT KINASES: Engines, Clocks, and Microprocessors. *Annual Review of Cell and Developmental Biology* **13:** 261-291

Morishita T, Tsutsui Y, Iwasaki H, Shinagawa H (2002) The Schizosaccharomyces pombe rad60 Gene Is Essential for Repairing Double-Strand DNA Breaks Spontaneously Occurring during Replication and Induced by DNA-Damaging Agents. *Mol Cell Biol* **22:** 3537-3548

Morris JR, Boutell C, Keppler M, Densham R, Weekes D, Alamshah A, Butler L, Galanty Y, Pangon L, Kiuchi T (2009) The SUMO modification pathway is involved in the BRCA1 response to genotoxic stress. *Nature* **462:** 886-890

Moyer SE, Lewis PW, Botchan MR (2006) Isolation of the Cdc45/Mcm2–7/GINS (CMG) complex, a candidate for the eukaryotic DNA replication fork helicase. *Proceedings of the National Academy of Sciences* **103:** 10236-10241

Mu D, Hsu DS, Sancar A (1996) Reaction mechanism of human DNA repair excision nuclease. *Journal of Biological Chemistry* **271:** 8285-8294

Murray JM, Carr AM (2008) Smc5/6: a link between DNA repair and unidirectional replication? *Nat Rev Mol Cell Biol* **9:** 177-182

Murray JM, Tavassoli M, al-Harithy R, Sheldrick KS, Lehmann AR, Carr AM, Watts FZ (1994) Structural and functional conservation of the human homolog of the Schizosaccharomyces pombe rad2 gene, which is required for chromosome segregation and recovery from DNA damage. *Mol Cell Biol* **14:** 4878-4888

N J Bentley, D A Holtzman, G Flaggs, K S Keegan, A DeMaggio, J C Ford, M Hoekstra, Carr AM (1996) The Schizosaccharomyces pombe rad3 checkpoint gene. *EMBO J* **15:** 6641-6651

Nacerddine KL, François; Bhaumik, Mantu; Artus, Jérôme; Cohen-Tannoudji, Michel; Babinet, Charles; Pandolfi, Pier Paolo; Dejean, Anne (2005) The SUMO Pathway Is Essential for Nuclear Integrity and Chromosome Segregation in Mice. *Developmental Cell* **9:** 769-779

Nash HM, Lu R, Lane WS, Verdine GL (1997) The critical active-site amine of the human 8-oxoguanine DNA glycosylase, hOgg1: direct identification, ablation and chemical reconstitution. *Chem Biol* **4:** 693-702

Nasmyth K, Haering CH (2005) THE STRUCTURE AND FUNCTION OF SMC AND KLEISIN COMPLEXES. *Annual Review of Biochemistry* **74:** 595-648

Nassif N, Penney J, Pal S, Engels WR, Gloor GB (1994) Efficient copying of nonhomologous sequences from ectopic sites via P-element-induced gap repair. *Molecular and Cellular Biology* **14:** 1613-1625

Neuwald AF, Aravind L, Spouge JL, Koonin EV (1999) AAA+: A Class of Chaperone-Like ATPases Associated with the Assembly, Operation, and Disassembly of Protein Complexes. *Genome Research* **9:** 27-43

Neuwald AF, Hirano T (2000) HEAT Repeats Associated with Condensins, Cohesins, and Other Complexes Involved in Chromosome-Related Functions. *Genome Research* **10:** 1445-1452

Newlon CS, Theis JF (1993) The structure and function of yeast ARS elements. *Current Opinion in Genetics & Development* **3:** 752-758

Nishitani H, Lygerou Z, Nishimoto T, Nurse P (2000) The Cdt1 protein is required to license DNA for replication in fission. *Nature* **204**

Noguchi E, Noguchi C, McDonald WH, Yates JR, Russell P (2004) Swi1 and Swi3 Are Components of a Replication Fork Protection Complex in Fission Yeast. *Molecular and Cellular Biology* **24:** 8342-8355

Novatchkova M, Bachmair A, Eisenhaber B, Eisenhaber F (2005) Proteins with two SUMO-like domains in chromatin-associated complexes: the RENi (Rad60-Esc2-NIP45) family. *BMC Bioinformatics* **6:** 22

Nurse P, Bissett Y (1981) Gene required in G1 for commitment to cell cycle and in G2 for control of mitosis in fission yeast. *Nature* **6:** 550-560

Nurse P, Thuriaux P, Nasmyth K (1976) Genetic control of the cell division cycle in the fission yeast Schizosaccharomyces pombe. *Molecular and General Genetics MGG* **146:** 167-178

O'Donovan A, Davies AA, Moggs JG, West SC, Wood RD (1994) XPG endonuclease makes the 3[prime] incision in human DNA nucleotide excision repair. *Nature* **371:** 432-435

Ogawa Y, Takahashi T, Masukata H (1999) Association of Fission Yeast Orp1 and Mcm6 Proteins with Chromosomal Replication Origins. *Molecular and Cellular Biology* **19:** 7228-7236

Okazaki R, Okazaki T, Sakabe K, K. S (1967) Mechanism of DNA replication possible discontinuity of DNA chain growth. *Jpn J Med Sci Biol* **20:** 255-260

Olsen SK, Capili AD, Lu X, Tan DS, Lima CD (2010) Active site remodelling accompanies thioester bond formation in the SUMO E1. *Nature* **463:** 906-912

Palecek J, Vidot S, Feng M, Doherty AJ, Lehmann AR (2006a) The Smc5-Smc6 DNA repair complex. bridging of the Smc5-Smc6 heads by the KLEISIN, Nse4, and non-Kleisin subunits. *J Biol Chem* **281:** 36952-36959

Palecek J, Vidot S, Feng M, Doherty AJ, Lehmann AR (2006b) The Smc5-Smc6 DNA Repair Complex: BRIDGING OF THE Smc5-Smc6 HEADS BY THE KLEISIN, Nse4, AND NON-KLEISIN SUBUNITS. *Journal of Biological Chemistry* **281:** 36952-36959

Papouli E, Chen S, Davies AA, Huttner D, Krejci L, Sung P, Ulrich HD (2005) Crosstalk between SUMO and Ubiquitin on PCNA Is Mediated by Recruitment of the Helicase Srs2p. *Molecular Cell* **19:** 123-133

Parker AE, Clyne RK, Carr AM, Kelly TJ (1997) The Schizosaccharomyces pombe rad11+ gene encodes the large subunit of replication protein A. *Mol Cell Biol* **17:** 2381-2390

Parker JL, Bielen AB, Dikic I, Ulrich HD (2007) Contributions of ubiquitin- and PCNA-binding domains to the activity of Polymerase η in Saccharomyces cerevisiae. *Nucleic Acids Research* **35:** 881-889

Parker JL, Ulrich HD (2009) Mechanistic analysis of PCNA poly-ubiquitylation by the ubiquitin protein ligases Rad18 and Rad5. *EMBO J* **28:** 3657-3666

Parnas O, Zipin-Roitman A, Pfander B, Liefshitz B, Mazor Y, Ben-Aroya S, Jentsch S, Kupiec M (2010) Elg1, an alternative subunit of the RFC clamp loader, preferentially interacts with SUMOylated PCNA. *EMBO J* **29:** 2611-2622

Pebernard S, Perry JJP, Tainer JA, Boddy MN (2008) Nse1 RING-like Domain Supports Functions of the Smc5-Smc6 Holocomplex in Genome Stability. *Molecular Biology of the Cell* **19:** 4099-4109

Pebernard S, Wohlschlegel J, McDonald WH, Yates JR, Boddy MN (2006) The Nse5-Nse6 Dimer Mediates DNA Repair Roles of the Smc5-Smc6 Complex. *Molecular and Cellular Biology* **26:** 1617-1630

Peng J, Schwartz D, Elias JE, Thoreen CC, Cheng D, Marsischky G, Roelofs J, Finley D, Gygi SP (2003) A proteomics approach to understanding protein ubiquitination. *Nature Biotechnology* **21:** 921-926

Pfander B, Moldovan G-L, Sacher M, Hoege C, Jentsch S (2005a) SUMO-modified PCNA recruits Srs2 to prevent recombination during S phase. *Nature* **436:** 428 - 433

Pfander B, Moldovan GL, Sacher M, Hoege C, Jentsch S (2005b) SUMO-modified PCNA recruits Srs2 to prevent recombination during S phase. *Nature* **436:** 428-433

Pichler A, Gast A, Seeler JS, Dejean A, Melchior F (2002) The Nucleoporin RanBP2 Has SUMO1 E3 Ligase Activity. *Cell* **108:** 109-120

Pluciennik A, Dzantiev L, Iyer RR, Constantin N, Kadyrov FA, Modrich P (2010) PCNA function in the activation and strand direction of MutLα endonuclease in mismatch repair. *Proceedings of the National Academy of Sciences* **107:** 16066-16071

Podlutsky AJ, Dianova, II, Podust VN, Bohr VA, Dianov GL (2001) Human DNA polymerase beta initiates DNA synthesis during long-patch repair of reduced AP sites in DNA. *EMBO J* **20:** 1477-1482

Potts PR, Porteus MH, Yu H (2006) *Human SMC5/6 complex promotes sister chromatid homologous recombination by recruiting the SMC1/3 cohesin complex to double-strand breaks*, Vol. 25.

Potts PR, Yu H (2005) Human MMS21/NSE2 is a SUMO ligase required for DNA repair. *Mol Cell Biol* **25:** 7021-7032

Potts PR, Yu H (2007) The SMC5/6 complex maintains telomere length in ALT cancer cells through SUMOylation of telomere-binding proteins. *Nat Struct Mol Biol* **14:** 581-590

Prakash L, Prakash S (1977) ISOLATION AND CHARACTERIZATION OF MMS-SENSITIVE MUTANTS OF SACCHAROMYCES CEREVISIAE. *Genetics* **86:** 33-55

Prudden J, Pebernard S, Raffa G, Slavin DA, Perry JJP, Tainer JA, McGowan CH, Boddy MN (2007) *SUMO-targeted ubiquitin ligases in genome stability*, Vol. 26.

Prudden J, Perry JJP, Arvai AS, Tainer JA, Boddy MN (2009) Molecular mimicry of SUMO promotes DNA repair. *Nat Struct Mol Biol* **16:** 509-516

Prudden J, Perry JJP, Nie M, Vashisht AA, Arvai AS, Hitomi C, Guenther G, Wohlschlegel JA, Tainer JA, Boddy MN (2011) DNA Repair and Global Sumoylation are Regulated by Distinct Ubc9 Non-covalent Complexes. *Mol Cell Biol***:** MCB.05188-05111

Qu M, Rappas M, Wardlaw Christopher P, Garcia V, Ren J-Y, Day M, Carr Antony M, Oliver Antony W, Du L-L, Pearl Laurence H (2013) Phosphorylation-Dependent Assembly and Coordination of the DNA Damage Checkpoint Apparatus by Rad4TopBP1. *Molecular Cell* **51:** 723-736

Raffa GD, Wohlschlegel J, Yates JR, 3rd, Boddy MN (2006) SUMO-binding motifs mediate the Rad60-dependent response to replicative stress and self-association. *J Biol Chem* **281:** 27973-27981

Ragland RL, Patel S, Rivard RS, Smith K, Peters AA, Bielinsky A-K, Brown EJ (2013) RNF4 and PLK1 are required for replication fork collapse in ATR-deficient cells. *Genes & Development* **27:** 2259-2273

Raji H, Hartsuiker E (2006) Double-strand break repair and homologous recombination in Schizosaccharomyces pombe. *Yeast* **23:** 963-976

Raleigh JM, O'Connell MJ (2000) The G(2) DNA damage checkpoint targets both Wee1 and Cdc25. *Journal of Cell Science* **113:** 1727-1736

Reverter D, Lima CD (2005) Insights into E3 ligase activity revealed by a SUMO-RanGAP1-Ubc9-Nup358 complex. *Nature* **435:** 687-692

Riballo E, Woodbine L, Stiff T, Walker SA, Goodarzi AA, Jeggo PA (2009) XLF-Cernunnos promotes DNA ligase IV–XRCC4 re-adenylation following ligation. *Nucleic Acids Research* **37:** 482-492

Robertson AB, Klungland A, Rognes T, Leiros I (2009) DNA Repair in Mammalian Cells. *Cellular and Molecular Life Sciences* **66:** 981-993

Rodel C, Jupitz T, Schmidt H (1997) Complementation of the DNA repair-deficient swi10 mutant of fission yeast by the human ERCC1 gene. *Nucleic Acids Res* **25:** 2823-2827

Rodriguez MS, Dargemont C, Hay RT (2001) SUMO-1 Conjugation in Vivo Requires Both a Consensus Modification Motif and Nuclear Targeting. *Journal of Biological Chemistry* **276:** 12654-12659

Rudolph C, Kunz C, Parisi S, Lehmann E, Hartsuiker E, Fartmann B, Kramer W, Kohli J, Fleck O (1999) The msh2 Gene ofSchizosaccharomyces pombe Is Involved in Mismatch Repair, Mating-Type Switching, and Meiotic Chromosome Organization. *Molecular and Cellular Biology* **19:** 241-250

Rupeš I (2002) Checking cell size in yeast. *Trends in Genetics* **18:** 479-485

Russell P, Nurse P (1986) cdc25+ functions as an inducer in the mitotic control of fission yeast. *Cell* **45:** 145-153

Rytinki M, Kaikkonen S, Pehkonen P, Jääskeläinen T, Palvimo J (2009) PIAS proteins: pleiotropic interactors associated with SUMO. *Cellular and Molecular Life Sciences* **66:** 3029-3041

Saitoh H, Hinchey J (2000) Functional heterogeneity of small ubiquitin-related protein modifiers SUMO-1 versus SUMO-2/3. *J Biol Chem* **275:** 6252-6258

Saka Y, Esashi F, Matsusaka T, Mochida S, Yanagida M (1997) Damage and replication checkpoint control in fission yeast is ensured by interactions of Crb2, a protein with BRCT motif, with Cut5 and Chk1. *Genes Dev* **11:** 3387-3400

Sakurai S, Kitano K, Yamaguchi H, Hamada K, Okada K, Fukuda K, Uchida M, Ohtsuka E, Morioka H, Hakoshima T (2005) *Structural basis for recruitment of human flap endonuclease 1 to PCNA*, Vol. 24.

Sale JE, Lehmann AR, Woodgate R (2012) Y-family DNA polymerases and their role in tolerance of cellular DNA damage. *Nat Rev Mol Cell Biol* **13:** 141-152

Sartori AA, Lukas C, Coates J, Mistrik M, Fu S, Bartek J, Baer R, Lukas J, Jackson SP (2007) Human CtIP promotes DNA end resection. *Nature* **450:** 509-U506

Schär P, Baur M, Schneider C, Kohli J (1997) Mismatch Repair in Schizosacchromyces pombe Requires the mutL Homologous Gene pms1: Molecular Cloning and Functional Analysis. *Genetics* **146:** 1275-1286

Schärer OD (2013) Nucleotide Excision Repair in Eukaryotes. *Cold Spring Harbor Perspectives in Biology* **5**

Schiestl RH, Prakash S, Prakash L (1990) The SRS2 suppressor of rad6 mutations of Saccharomyces cerevisiae acts by channeling DNA lesions into the RAD52 DNA repair pathway. *Genetics* **124:** 817-831

Schulman BA, Wade Harper J (2009) Ubiquitin-like protein activation by E1 enzymes: the apex for downstream signalling pathways. *Nat Rev Mol Cell Biol* **10:** 319-331

Schwarz SE, Matuschewski K, Liakopoulos D, Scheffner M, Jentsch S (1998) The ubiquitin-like proteins SMT3 and SUMO-1 are conjugated by the UBC9 E2 enzyme. *Proceedings of the National Academy of Sciences* **95:** 560-564

Segurado M, de Luis A, Antequera F (2003) *Genome-wide distribution of DNA replication origins at A+T-rich islands in Schizosaccharomyces pombe*, Vol. 4.

Sergeant Jea (2005) Composition and architecture of the Zchizosaccharomyces pombe Rad18 (Smc5-6) complex. *Molecular and cell biology* **25:** 172-184

Shaheen M, Schanmugam I, Hromas R (2010) The role of PCNA posttranslational modifications in translesion synthesis. *Journal of Nucleic Acids* **2010:** 1-8

Shayeghi M, Doe CL, Tavassoli M, Watts FZ (1997) Characterisation of Schizosaccharomyces Pombe Rad31, a UBA-related Gene Required for DNA Damage Tolerance. *Nucleic Acids Research* **25:** 1162-1169

Sheedy DM, Dimitrova D, Rankin JK, Bass KL, Lee KM, Tapia-Alveal C, Harvey SH, Murray JM, O'Connell MJ (2005) Brc1-Mediated DNA Repair and Damage Tolerance. *Genetics* **171:** 457-468

Skilton A, Ho JCY, Mercer B, Outwin E, Watts FZ (2009) SUMO Chain Formation Is Required for Response to Replication Arrest in <italic>S. pombe</italic>. *PLoS ONE* **4:** e6750

Sogo JM, Lopes M, Foiani M (2002) Fork Reversal and ssDNA Accumulation at Stalled Replication Forks Owing to Checkpoint Defects. *Science* **297:** 599-602

Sommariva E, Pellny TK, Karahan N, Kumar S, Huberman JA, Dalgaard JZ (2005) Schizosaccharomyces pombe Swi1, Swi3, and Hsk1 are components of a novel S-phase response pathway to alkylation damage. *Mol Cell Biol* **25:** 2770-2784

Song J, Durrin LK, Wilkinson TA, Krontiris TG, Chen Y (2004) Identification of a SUMO-binding motif that recognizes SUMO-modified proteins. *Proceedings of the National Academy of Sciences of the United States of America* **101:** 14373-14378

Srikumar T, Lewicki MC, Costanzo M, Tkach JM, van Bakel H, Tsui K, Johnson ES, Brown GW, Andrews BJ, Boone C, Giaever G, Nislow C, Raught B (2013) Global analysis of SUMO chain function reveals multiple roles in chromatin regulation. *The Journal of Cell Biology* **201:** 145-163

Sriramachandran AM, Dohmen RJ (2014) SUMO-targeted ubiquitin ligases. *Biochimica et Biophysica Acta (BBA) - Molecular Cell Research* **1843:** 75-85

Steinacher R, Osman F, Lorenz A, Bryer C, Whitby MC (2013) Slx8 Removes Pli1-Dependent Protein-SUMO Conjugates Including SUMOylated Topoisomerase I to Promote Genome Stability. *PLoS ONE* **8:** e71960

Steininger S, Ahne F, Winkler K, Kleinschmidt A, Eckardt-Schupp F, Moertl S (2010) A novel function for the Mre11-Rad50-Xrs2 complex in base excision repair. *Nucleic Acids Res* **38:** 1853-1865

Stelter P, Ulrich HD (2003) Control of spontaneous and damage-induced mutagenesis by SUMO and ubiquitin conjugation. *Nature* **425:** 188-191

Stephan AK, Kliszczak M, Morrison CG The Nse2/Mms21 SUMO ligase of the Smc5/6 complex in the maintenance of genome stability. *FEBS Letters* **In Press, Corrected Proof**

Strunnikov AV, Aravind L, Koonin EV (2001) Saccharomyces cerevisiae SMT4 encodes an evolutionarily conserved protease with a role in chromosome condensation regulation. *Genetics* **158:** 95-107

Strzalka W, Ziemienowicz A (2011) Proliferating cell nuclear antigen (PCNA): a key factor in DNA replication and cell cycle regulation. *Annals of Botany* **107:** 1127-1140

Su HL, Li SS (2002) Molecular features of human ubiquitin-like SUMO genes and their encoded proteins. *Gene* **296:** 65-73

Sun B, Latham KA, Dodson ML, Lloyd RS (1995) Studies on the catalytic mechanism of five DNA glycosylases. Probing for enzyme-DNA imino intermediates. *J Biol Chem* **270:** 19501-19508

Sun H, Leverson JD, Hunter T (2007) *Conserved function of RNF4 family proteins in eukaryotes: targeting a ubiquitin ligase to SUMOylated proteins*, Vol. 26.

Sung P (1994) Catalysis of ATP-dependent homologous DNA pairing and strand exchange by yeast RAD51 protein. *Science* **265:** 1241-1243

Svendsen JM, Harper JW (2010) GEN1/Yen1 and the SLX4 complex: solutions to the problem of Holliday junction resolution. *Genes & Development* **24:** 521-536

Takeda T, Ogino K, Matsui E, Cho MK, Kumagai H, Miyake T, Arai K-i, Masai H (1999) A Fission Yeast Gene,him1+/dfp1+ , Encoding a Regulatory Subunit for Hsk1 Kinase, Plays Essential Roles in S-Phase Initiation as Well as in S-Phase Checkpoint Control and Recovery from DNA Damage. *Molecular and Cellular Biology* **19:** 5535-5547

Tanaka K, Nishide J, Okazaki K, Kato H, Niwa O, Nakagawa T, Matsuda H, Kawamukai M, Murakami Y (1999) Characterization of a Fission Yeast SUMO-1 Homologue, Pmt3p, Required for Multiple Nuclear Events, Including the Control of Telomere Length and Chromosome Segregation. *Molecular and Cellular Biology* **19:** 8660-8672

Tatham MH, Geoffroy M-C, Shen L, Plechanovova A, Hattersley N, Jaffray EG, Palvimo JJ, Hay RT (2008) RNF4 is a poly-SUMO-specific E3 ubiquitin ligase required for arsenic-induced PML degradation. *Nat Cell Biol* **10:** 538-546

Tatham MH, Jaffray E, Vaughan OA, Desterro JMP, Botting CH, Naismith JH, Hay RT (2001) Polymeric Chains of SUMO-2 and SUMO-3 Are Conjugated to Protein Substrates by SAE1/SAE2 and Ubc9. *Journal of Biological Chemistry* **276:** 35368-35374

Tatham MH, Kim S, Jaffray E, Song J, Chen Y, Hay RT (2005) Unique binding interactions among Ubc9, SUMO and RanBP2 reveal a mechanism for SUMO paralog selection. *Nat Struct Mol Biol* **12:** 67-74

Tavassoll M, Shayeghl M, Nasim A, Watts FZ (1995) Cloning and characterisation of the Schizosaccharomyces pombe rad32 gene: a gene required for repair of double strand breaks and recombination. *Nucleic Acids Research* **23:** 383-388

Taylor DL, Ho JCY, Oliver A, Watts FZ (2002) Cell-cycle-dependent localisation of Ulp1, a Schizosaccharomyces pombe Pmt3 (SUMO)-specific protease. *J Cell Sci* **115:** 1113-1122

Tenno T, Fujiwara K, Tochio H, Iwai K, Morita EH, Hayashi H, Murata S, Hiroaki H, Sato M, Tanaka K, Shirakawa M (2004) Structural basis for distinct roles of Lys63- and Lys48-linked polyubiquitin chains. *Genes to Cells* **9:** 865-875

Thelen MP, Venclovas C, Fidelis K (1999) A sliding clamp model for the Rad1 family of cell cycle checkpoint proteins. *Cell* **96:** 769-770

Thrower JS, Hoffman L, Rechsteiner M, Pickart CM (2000) Recognition of the polyubiquitin proteolytic signal. *EMBO J* **19:** 94-102

Tomita K, Matsuura A, Caspari T, Carr AM, Akamatsu Y, Iwasaki H, Mizuno K, Ohta K, Uritani M, Ushimaru T, Yoshinaga K, Ueno M (2003) Competition between the Rad50 complex and the Ku heterodimer reveals a role for Exo1 in processing double-strand breaks but not telomeres. *Mol Cell Biol* **23:** 5186-5197

Tornier C, Bessone S, Varlet I, Rudolph C, Darmon M, Fleck O (2001) Requirement for Msh6, but Not for Swi4 (Msh3), in Msh2-Dependent Repair of Base-Base Mismatches and Mononucleotide Loops in Schizosaccharomyces pombe. *Genetics* **158:** 65-75

Tsuchimoto D, Sakai Y, Sakumi K, Nishioka K, Sasaki M, Fujiwara T, Nakabeppu Y (2001) Human APE2 protein is mostly localized in the nuclei and to some extent in the mitochondria, while nuclear APE2 is partly associated with proliferating cell nuclear antigen. *Nucleic Acids Research* **29:** 2349-2360

Tyson JJ, Csikasz-Nagy A, Novak B (2002) The dynamics of cell cycle regulation. *BioEssays* **24:** 1095-1109

Ulrich HD (2005) The RAD6 Pathway: Control of DNA Damage Bypass and Mutagenesis by Ubiquitin and SUMO. *ChemBioChem* **6:** 1735-1743

Ulrich HD (2008) The Fast-Growing Business of SUMO Chains. *Molecular Cell* **32:** 301-305

Ulrich HD (2013) New Insights into Replication Clamp Unloading. *Journal of Molecular Biology* **425:** 4727-4732

Ulrich HD, Jentsch S (2000) *Two RING finger proteins mediate cooperation between ubiquitin-conjugating enzymes in DNA repair*, Vol. 19.

Varadan R, Walker O, Pickart C, Fushman D (2002) Structural properties of polyubiquitin chains in solution. *Journal of Molecular Biology* **324:** 637-647

Veaute X, Jeusset J, Soustelle C, Kowalczykowski SC, Le Cam E, Fabre F (2003) The Srs2 helicase prevents recombination by disrupting Rad51 nucleoprotein filaments. *Nature* **423:** 309-312

Verkade HM, Bugg SJ, Lindsay HD, Carr AM, O'Connell MJ (1999) Rad18 is required for DNA repair and checkpoint responses in fission yeast. *Mol Biol Cell* **10:** 2905-2918

Vertegaal AC, Andersen JS, Ogg SC, Hay RT, Mann M, Lamond AI (2006a) Distinct and overlapping sets of SUMO-1 and SUMO-2 target proteins revealed by quantitative proteomics. *Mol Cell Proteomics* **5:** 2298-2310

Vertegaal ACO, Andersen JS, Ogg SC, Hay RT, Mann M, Lamond AI (2006b) Distinct and Overlapping Sets of SUMO-1 and SUMO-2 Target Proteins Revealed by Quantitative Proteomics. *Molecular & Cellular Proteomics* **5:** 2298-2310

Vijay-Kumar S, Bugg CE, Cook WJ (1987) Structure of ubiquitin refined at 1.8Åresolution. *Journal of Molecular Biology* **194:** 531-544

Walker JR, Corpina RA, Goldberg J (2001) Structure of the Ku heterodimer bound to DNA and its implications for double-strand break repair. *Nature* **412:** 607-614

Wallace SS (2013) DNA glycosylases search for and remove oxidized DNA bases. *Environmental and Molecular Mutagenesis* **54:** 691-704

Wang J, Hu W, Cai S, Lee B, Song J, Chen Y (2007) The Intrinsic Affinity between E2 and the Cys Domain of E1 in Ubiquitin-like Modifications. *Molecular Cell* **27:** 228-237

Watanabe K, Tateishi S, Kawasuji M, Tsurimoto T, Inoue H, Yamaizumi M (2004) *Rad18 guides polη to replication stalling sites through physical interaction and PCNA monoubiquitination*, Vol. 23.

Watson AT, Garcia V, Bone N, Carr AM, Armstrong J (2008) Gene tagging and gene replacement using recombinase-mediated cassette exchange in Schizosaccharomyces pombe. *Gene* **407:** 63-74

Watts FZ, Skilton A, Ho JC-Y, Boyd LK, Trickey MAM, Gardner L, Ogi F-X, Outwin EA (2007) The role of Schizosaccharomyces pombe SUMO ligases in genome stability. *Biochemical Society Transactions* **035:** 1379-1384

Weeks SD, Grasty KC, Hernandez-Cuebas L, Loll PJ (2009) Crystal structures of Lys-63-linked tri- and di-ubiquitin reveal a highly extended chain architecture. *Proteins* **77:** 753-759

Williams GJ, Lees-Miller SP, Tainer JA (2010) Mre11–Rad50–Nbs1 conformations and the control of sensing, signaling, and effector responses at DNA double-strand breaks. *DNA repair* **9:** 1299-1306

Williams GJ, Williams RS, Williams JS, Moncalian G, Arvai AS, Limbo O, Guenther G, SilDas S, Hammel M, Russell P, Tainer JA (2011) ABC ATPase signature helices in Rad50 link nucleotide state to Mre11 interface for DNA repair. *Nat Struct Mol Biol* **18:** 423-431

Willis N, Rhind N (2010) The fission yeast Rad32(Mre11)-Rad50-Nbs1 complex acts both upstream and downstream of checkpoint signaling in the S-phase DNA damage checkpoint. *Genetics* **184:** 887-897

Wilson S, Tavassoli M, Watts FZ (1998) Schizosaccharomyces pombe Rad32 protein: a phosphoprotein with an essential phosphoesterase motif required for repair of DNA double strand breaks. *Nucleic Acids Research* **26:** 5261-5269

Win TZ, Goodwin A, Hickson ID, Norbury CJ, Wang S-W (2004) Requirement for Schizosaccharomyces pombe Top3 in the maintenance of chromosome integrity. *Journal of Cell Science* **117:** 4769-4778

Wood RD, Shivji MK (1997) Which DNA polymerases are used for DNA-repair in eukaryotes? *Carcinogenesis* **18:** 605-610

Wright JA, Keegan KS, Herendeen DR, Bentley NJ, Carr AM, Hoekstra MF, Concannon P (1998) Protein kinase mutants of human ATR increase sensitivity to UV and ionizing radiation and abrogate cell cycle checkpoint control. *Proceedings of the National Academy of Sciences* **95:** 7445-7450

Wu L, Hickson ID (2003) The Bloom's syndrome helicase suppresses crossing over during homologous recombination. *Nature* **426**

Xhemalce B, Seeler J-S, Thon G, Dejean A, Arcangioli B (2004a) Role of the fission yeast SUMO E3 ligase Pli1p in centromere and telomere maintenance. *EMBO J* **23:** 3844-3853

Xhemalce B, Seeler JS, Thon G, Dejean A, Arcangioli B (2004b) *Role of the fission yeast SUMO E3 ligase Pli1p in centromere and telomere maintenance*, Vol. 23.

Xiao W, Chow BL, Fontanie T, Ma L, Bacchetti S, Hryciw T, Broomfield S (1999) Genetic interactions between error-prone and error-free postreplication repair pathways in Saccharomyces cerevisiae. *Mutat Res* **435:** 1-11

Xu H, Zhang P, Liu L, Lee MYWT (2001) A Novel PCNA-Binding Motif Identified by the Panning of a Random Peptide Display Library†. *Biochemistry* **40:** 4512-4520

Yang S-H, Jaffray E, Senthinathan B, Hay RT, Sharrocks AD (2003) SUMO and Transcriptional Repression: Dynamic Interactions Between the MAP Kinase and SUMO Pathways. *Cell Cycle* **2:** 528-530

Yanow SK, Lygerou Z, Nurse P (2001) Expression of Cdc18/Cdc6 and Cdt1 during G2 phase induces initiation of DNA replication. *EMBO J* **20:** 4648-4656

Yonemasu R, McCready SJ, Murray JM, Osman F, Takao M, Yamamoto K, Lehmann AR, Yasui A (1997) Characterization of the Alternative Excision Repair Pathway of UV-Damaged DNA in Schizosaccharomyces Pombe. *Nucleic Acids Research* **25:** 1553-1558

Yoo S, Dynan WS (1999) Geometry of a complex formed by double strand break repair proteins at a single DNA end: Recruitment of DNA-PKcs induces inward translocation of Ku protein. *Nucleic Acids Research* **27:** 4679-4686

Yuan J, Luo K, Zhang L, Cheville JC, Lou Z (2010) USP10 Regulates p53 Localization and Stability by Deubiquitinating p53. *Cell* **140:** 384-396

Zegerman P, Diffley JFX (2009) DNA replication as a target of the DNA damage checkpoint. *DNA repair* **8:** 1077-1088

Zeman MK, Cimprich KA (2012) Finally, polyubiquitinated PCNA gets recognized. *Mol Cell* **47:** 333-334

Zeman MK, Cimprich KA (2014) Causes and consequences of replication stress. *Nat Cell Biol* **16:** 2-9

Zhao X, Blobel G (2005) A SUMO ligase is part of a nuclear multiprotein complex that affects DNA repair and chromosomal organization. *Proceedings of the National Academy of Sciences of the United States of America* **102:** 4777-4782

Zou L, Elledge SJ (2003) Sensing DNA Damage Through ATRIP Recognition of RPA-ssDNA Complexes. *Science* **300:** 1542-1548